

DEVELOPMENT OF BIO-BASED FILMS USING PEA PROTEIN
AND HASKAP LEAF (*LONICERA CAERULEA*) EXTRACTS
FROM AQUEOUS TWO-PHASE SYSTEMS

by

Kar Yeen Chong

Submitted in partial fulfilment of the requirements
for the degree of Doctor of Philosophy

at

Dalhousie University
Halifax, Nova Scotia
April 2021

© Copyright by Kar Yeen Chong, 2021

DEDICATION

To those whom our paths have crossed,
to those who have inspired me,
the dreamweavers.

Like all infinite games,
in the game of life,
the goal is not to win,
it is to perpetuate the game.
- Simon Sinek

TABLE OF CONTENTS

LIST OF TABLES	viii
LIST OF FIGURES	x
ABSTRACT	xii
LIST OF ABBREVIATIONS AND SYMBOLS USED	xiii
ACKNOWLEDGEMENTS	xvi
Chapter 1 : General Introduction	1
Chapter 2 : Literature Review	7
2.1 Haskap Plants	7
2.2 Bioactive Compounds in Berry Leaves	8
2.3 Extraction of Bioactive Compounds	13
2.3.1 Aqueous Two-Phase Systems (ATPS).....	13
2.3.2 Aqueous Two-Phase Extraction (ATPE)	20
2.3.2.1 Effect of Type of Salt.....	21
2.3.2.2 Effect of ATPS Composition	22
2.3.2.3 Effect of pH.....	23
2.3.2.4 Effect of Temperature	23
2.3.2.5 Effect of Sample Loading	24
2.3.2.6 Recycling ATPS Phase-Forming Components	24
2.3.3 Aqueous Two-Phase Extraction with Flotation (ATPF).....	25
2.3.3.1 Effect of Air Flow Rate.....	26
2.3.3.2 Effect of Flotation Time.....	27
2.4 Bio-Based Films.....	27
2.4.1 Introduction.....	27
2.4.2 Formulating Biobased Films	30
2.4.2.1 Binding Agents	30
2.4.2.2 Plasticizers	31
2.4.2.3 Cross-linkers	32
2.4.3 Functional Biobased Films	33
2.4.4.1 Degassing	35
2.4.4.2 Casting	35

2.4.4.3 Dipping	36
2.4.4.4 Spraying	36
2.4.4.5 Extrusion	37
2.4.5 Assessment of Biobased Film Properties	37
2.4.5.1 Film Thickness	37
2.4.5.2 Moisture Content	38
2.4.5.3 Light Transmission and Film Transparency	39
2.4.5.4 Film Colour	40
2.4.5.5 Microstructure	40
2.4.5.6 Tensile Strength and Elongation at Break	41
2.4.5.7 Water Vapor Permeability	43
2.4.5.8 Thermal Properties	44
2.4.5.9 Antioxidant Properties	45
2.5 Summary	46
Connecting Statement 1	47
Chapter 3 : Aqueous Two-Phase Extraction of Bioactive Compounds from Haskap Leaves (<i>Lonicera caerulea</i>): Comparison of Salt/Ethanol and Sugar/Propanol Systems	48
3.1 Abstract	48
3.2 Introduction	49
3.3 Materials and Methods	51
3.3.1 Materials	51
3.3.2 Methods	52
3.3.2.1 Aqueous Two-Phase Extraction (ATPE) and Conventional Extraction ...	52
3.3.2.2 UV-Vis Spectrophotometric Analysis of Bioactive Compounds	55
Chlorogenic Acid	56
Flavonoid Content	56
Total Phenolic Content (TPC)	56
3.3.2.3 Performance Indicators	56
3.3.2.4 Design of Experiment, Optimization, and Statistical Analysis	57
3.3.2.5 High Performance Liquid Chromatography (HPLC) and Nuclear Magnetic Resonance (NMR) Analysis for Optimized Conditions	60
3.4 Results and Discussion	61

3.4.1 Phase Diagram	61
3.4.2 Response Surface Regression	62
3.4.3 Optimization of ATPE and Comparison between Systems	66
3.4.4 HPLC and NMR Analysis	72
3.5 Conclusion	76
Connecting Statement 2	78
Chapter 4 : Effects of Recycling on the Aqueous Two-Phase Extraction of Bioactives from Haskap Leaves	79
4.1 Abstract	79
4.2 Introduction.....	79
4.3 Materials and Methods.....	81
4.3.1 Materials	81
4.3.2 Methods.....	82
4.3.2.1 Aqueous Two-Phase Extraction (ATPE) and Recycling	82
4.3.2.2 UV-Vis Spectrophotometric Analysis of Bioactive Compounds	87
4.3.2.3 Performance Indicators and Statistical Analysis.....	87
4.4 Results and Discussion	87
4.4.1 Comparison of Partition Coefficients with Previous Optimization Study	87
4.4.2 Effects of Recycling on ATPE Partition Coefficient and Extraction Efficiency	88
4.4.3 Effects of Recycling on ATPE Extraction Yields.....	92
4.5 Conclusion and Future Work	95
Connecting Statement 3	96
Chapter 5 : Extraction of Bioactive Compounds from Haskap Leaves (<i>Lonicera caerulea</i>) using Salt/Ethanol Aqueous Two-Phase Flotation	97
5.1 Abstract	97
5.2 Introduction.....	97
5.3 Materials and Methods.....	100
5.3.1 Materials	100
5.3.2 Methods.....	101
5.3.2.1 Extraction	101
Conventional Extraction	101
Aqueous Two-Phase Flotation (ATPF)	101

Aqueous Two-Phase Extraction (ATPE)	103
Water Extraction	103
5.3.2.2 UV-Vis Spectrophotometric Analysis of Bioactive Compounds	105
5.3.2.3 Performance Indicators	105
5.3.2.4 Design of Experiment, Optimization, and Statistical Analysis.....	105
5.3.2.5 High Performance Liquid Chromatography (HPLC) Analysis for Optimized Conditions	106
5.4 Results and Discussion	107
5.4.1 Response Surface Regression	107
5.4.2 Optimization of ATPF	110
5.4.3 Comparison of Optimized Parameters with Aqueous Two-Phase Extraction	111
5.4.4 HPLC Analysis	116
5.5 Conclusion	120
Connecting Statement 4	121
Chapter 6 : Development of pea protein films with haskap (<i>Lonicera caerulea</i>) leaf extracts from aqueous two-phase systems	122
6.1 Abstract	122
6.2 Introduction.....	122
6.3 Materials and Methods.....	124
6.3.1 Materials	124
6.3.2 Methods.....	125
6.3.2.1 Extraction of Haskap Leaves	125
6.3.2.2 Film Preparation.....	125
6.3.2.3 Analysis of Films	126
Thickness	126
Moisture Content	127
Mechanical Properties.....	128
Optical Properties.....	128
Water Vapor Permeability (WVP).....	128
Thermal Properties	129
Migration and Antioxidant Tests	129
Statistical Analysis.....	130

6.4 Results and Discussion	130
6.4.1 Characterization of Haskap Leaf Extracts from ATPE and ATPF	130
6.4.2 Film Thickness	132
6.4.3 Moisture Content	133
6.4.4 Tensile Strength and Elongation at Break	135
6.4.5 Transparency and Light Transmission	137
6.4.6 Water Vapor Permeability (WVP)	139
6.4.7 Thermal Analysis	140
6.4.8 Migration and Antioxidant Tests	143
6.5 Conclusion	147
Chapter 7 : Conclusions	149
7.1 Summary and Conclusions	149
7.2 Contributions to Knowledge	151
7.3 Recommendations for Future Work	152
REFERENCES	155
APPENDIX A: Supplementary Figures	196
APPENDIX B: Supplementary Tables	202
APPENDIX C: Copyright Permission Letters	205

LIST OF TABLES

Table 2.1	Average concentration of chlorogenic acid, flavonoids, and total phenolic content in berry leaves	12
Table 2.2	Applications of aqueous two-phase systems (ATPS) to recover non-proteinaceous compounds using ATPE.....	16
Table 2.3	Applications of aqueous two-phase systems (ATPS) to recover non-proteinaceous compounds using ATPF	17
Table 2.4	Films, nanofibre mats, and bioplastics containing pea protein.....	29
Table 2.5	Chemical composition of pea products (Tömösközi et al., 2001)	30
Table 2.6	Extracts incorporated into protein films	34
Table 3.1	Tie line length and their respective compositions.....	55
Table 3.2	Design of experiment in uncoded units	59
Table 3.3	pH values of different ATPS studied.....	62
Table 3.4	Regression coefficients of quadratic polynomial model.....	64
Table 3.5	Optimization of ATPE based on maximum CGA yield ($\mu\text{g}/\text{mg}$), flavonoids yield ($\text{mg RE}/\text{mg}$), and TPC yield ($\text{mg GAE}/\text{mg}$).....	69
Table 4.1	Aqueous two-phase extraction optimized parameters (Chong et al., 2020).....	83
Table 4.2	Comparison of partition coefficient obtained from previous work and this study.....	88
Table 4.3	Effect of extraction and recycling on TPC yield ($\text{mg GAE}/\text{mg}$), flavonoids yield ($\text{mg RE}/\text{mg}$), and CGA yield ($\mu\text{g CGA}/\text{mg}$)	94
Table 5.1	Box Behnken experimental design matrix and yields (mg/mg leaves) from two independent experiments	104
Table 5.2	Regression coefficients for yields obtained from ATPF	108
Table 5.3	Optimized parameters of ATPF, desirability, and validation results for CGA yield (mg/mg leaves), flavonoids yield ($\text{mg RE}/\text{mg}$ leaves), and TPC yield ($\text{mg GAE}/\text{mg}$ leaves)	110

Table 5.4	Comparison of partition coefficient, k, and extraction efficiency, EE (%), of ATPF and ATPE for ammonium sulphate/ethanol and sodium phosphate/ethanol systems	115
Table 5.5	Wavelength, retention time, and content of selected bioactive compounds from HPLC.....	118
Table 6.1	Composition of pea protein films.....	127
Table 6.2	Concentration of bioactive compounds in pooled haskap leaf extracts ..	131
Table 6.3	Thickness of pea protein films	132
Table 6.4	Moisture content of pea protein films	134
Table 6.5	Mechanical properties of pea protein films.....	136
Table 6.6	Transparency and light transmission of pea protein films	137
Table 6.7	Water vapor permeability (WVP) of pea protein films.....	140
Table 6.8	Thermal properties of pea protein flours and films.....	141
Table 6.9	Total phenolic content and radical scavenging activity of PPI and PPC films in 10% ethanol.....	144

LIST OF FIGURES

Figure 2.1	Chemical structure of quercetin-3-rutinoside (ChemAxon, 2019).....	9
Figure 2.2	Chemical structure of chlorogenic acid (ChemAxon, 2019).....	10
Figure 2.3	Chemical structure of gallic acid (ChemAxon, 2019).....	11
Figure 2.4	ATPS phase diagram of ethanol and ammonium sulphate at 25°C (Chong et al., 2020).....	14
Figure 2.5	Concept of aqueous two-phase extraction with an alcohol and salt/sugar combination with leaves as the raw material (Chong et al., 2020).....	21
Figure 2.6	Experimental set-up of aqueous two-phase flotation (ATPF) (Chong et al., 2020b).....	26
Figure 3.1	ATPS phase diagrams for (a) (NH ₄) ₂ SO ₄ /ethanol, (b) NaH ₂ PO ₄ /ethanol, (c) glucose/1-propanol/, and (d) maltose/1-propanol at 25°C	61
Figure 3.2	Interaction effects of sample loading and time on CGA yield, flavonoid yield, and TPC yield for (a) (NH ₄) ₂ SO ₄ /ethanol ATPE at High TLL, (b) NaH ₂ PO ₄ /ethanol ATPE at Low TLL, (c) glucose/1- propanol ATPE at High TLL, and (d) maltose/1-propanol ATPE at Medium TLL	66
Figure 3.3	Yield comparison of ATPE and conventional Soxhlet extraction using Batch A leaves.....	68
Figure 3.4	Comparison of partition coefficient (k) and extraction efficiency (EE) between four ATPE systems for (a) chlorogenic acid, (b) flavonoids, and (c) total phenolic content using Batch B leaves	71
Figure 3.5	Bioactive compounds yield in conventional extract and top phase ATPE extract as determined by HPLC.....	73
Figure 3.6	HPLC chromatograms of (a) conventional extracts and (b) NaH ₂ PO ₄ /ethanol extract using Batch A leaves	75
Figure 3.7	¹ H-NMR spectra for NaH ₂ PO ₄ /ethanol extract and conventional extract using Batch A leaves	76
Figure 4.1	Flowchart of experimental work	84

Figure 4.2	Partition coefficient and extraction efficiency of (a) $(\text{NH}_4)_2\text{SO}_4$ /ethanol, (b) NaH_2PO_4 /ethanol, (c) glucose/1-propanol, and (d) maltose/1-propanol ATPE for the first extraction and subsequent two recycling stages	90
Figure 5.1	Experimental set-up of ATPF.....	102
Figure 5.2	Interaction effects on (a) CGA yield from sodium phosphate/ethanol ATPF; and (b) flavonoids yield, and (c) TPC yield from ammonium sulphate/ethanol ATPF	109
Figure 5.3	Yield comparison between conventional extraction, ATPF and ATPE using ammonium sulphate/ethanol, water extraction with flotation, and water extraction without flotation.....	113
Figure 5.4	Yield comparison between conventional extraction, ATPF and ATPE using sodium phosphate/ethanol, water extraction with flotation, and water extraction without flotation	114
Figure 5.5	Yield comparison of chlorogenic acid, rutin, luteolin-7- <i>O</i> -glucoside, and diosmin as detected by HPLC.	117
Figure 6.1	Light transmittance of selected films in the UV/visible spectrum	138
Figure 6.2	Differential scanning calorimetry thermograms for (a) pea protein flours and (b) pea protein films	142

ABSTRACT

Haskap leaves (*Lonicera caerulea*) are an agricultural residue from haskap plants and are expected to become more abundant as interest grows in haskap berries as a commercial crop in Canada. Although haskap berries are mainly associated with health-promoting benefits, haskap leaves are also a source of bioactive compounds, such as chlorogenic acid (CGA) and flavonoids. The conventional extraction techniques used with biological materials present certain drawbacks such as the use of toxic solvents, high temperatures, and long extraction times. This thesis investigates aqueous two-phase systems (ATPS) for the recovery of bioactive compounds from haskap leaves and the development of novel biobased pea protein films. In view of possible food and health product applications, different ATPS comprised of generally recognized as safe (GRAS) components were studied: ammonium sulphate/ethanol, sodium dihydrogen sulphate/ethanol, glucose/1-propanol, and maltose/1-propanol. The results showed that salt/ethanol aqueous two-phase extraction (ATPE) had higher extraction efficiencies than sugar/propanol ATPE. Sodium dihydrogen phosphate/ethanol ATPE had maximum extraction efficiency at 93.9% for CGA, 96.8% for flavonoids, and 97.8% for total phenolic content (TPC). Recycling of the ATPE phase-forming components was also examined to increase the overall process sustainability and economics. With two recycling stages, the extraction efficiency of the ATPE systems were maintained. Aqueous two-phase flotation (ATPF) was then investigated with salt/alcohol systems by integrating air bubbles and ATPE. Ammonium sulphate/ethanol ATPF increased the partition coefficient from 9.6 to 29.6 for CGA, 23.1 to 62.4 for flavonoids, and 161.6 to 231.4 for TPC. Haskap leaf extracts obtained from ATPE and ATPF consisting of bioactive compounds, ethanol, water, and residual salt were then directly incorporated into pea protein films. Some film formulations with haskap leaf extracts showed improved water vapour permeability and flexibility. Pea protein isolate (PPI) films with sodium phosphate extracts showed the best potential for development as a packaging material for alcoholic and aqueous food products.

LIST OF ABBREVIATIONS AND SYMBOLS USED

ANOVA	Analysis of variance
AS	Ammonium sulphate
ATPE	Aqueous two-phase extraction
ATPF	Aqueous two-phase flotation
ATPS	Aqueous two-phase system
CA	Citric acid
C_B	Concentration of bioactive compounds at bottom phase
CGA	Chlorogenic acid
C_T	Concentration of bioactive compounds at top phase
D	Overall desirability
d	Individual desirability
DPPH	2,2-diphenyl-1-picrylhydrazyl
DSC	Differential scanning calorimetry
DW	Dry weight
EAB	Elongation at break
EE	Extraction efficiency
FW	Fresh weight
GAE	Gallic acid equivalents
GRAS	Generally recognized as safe
H/D	Height-to-diameter ratio
HPLC	High-performance liquid chromatography

k	Partition coefficient
LLE	Liquid-liquid equilibrium
MA	Malic acid
M_{bottom}	Mass of target compounds at bottom phase
M_{top}	Mass of target compounds at top phase
M_{total}	Total mass of target compounds in both top and bottom phases
NMR	Nuclear magnetic resonance
pKa	Negative log of the acid dissociation constant
PPC	Pea protein concentrate
PPI	Pea protein isolate
R^2	Regression coefficient
RE	Rutin equivalents
RH	Relative humidity
RSA	Radical scavenging activity
RSM	Response surface methodology
R_v	Volume ratio
SEM	Standard error of mean
SP	Sodium dihydrogen phosphate
SPE	Solid phase extraction
T_d	Denaturation temperature
T_g	Glass transition temperature
TLL	Tie line length
T_m	Melting temperature

TPC	Total phenolic content
TS	Tensile strength
UV	Ultraviolet
V_B	Volume of bottom phase
V_T	Volume of top phase
WVP	Water vapour permeability
WVTR	Water vapour transmission rate
X_B	Weight fraction of salt or sugar at the bottom phase
X_T	Weight fraction of salt or sugar at the top phase
Y_B	Weight fraction of alcohol at the bottom phase
Y_T	Weight fraction of alcohol at the top phase
ΔH_d	Enthalpy of denaturation
ΔH_m	Enthalpy of melting

ACKNOWLEDGEMENTS

I would like to thank my supervisor, Dr. Su-Ling Brooks, for her guidance, support, and dedication during the course of my PhD program. Due to the pandemic, she has made the transitions as smooth as possible to get us back into the laboratory space. Furthermore, I acknowledge the Natural Sciences and Engineering Research Council for the financial support of my graduate studies and this project. I would also like to thank my supervisory committee, Dr. Azadeh Kermanshahi-pour and Dr. Junzeng Zhang, who provided advice and guidance in the research project. I am also thankful to Roumiana Stefanova who gave me helpful guidance on HPLC, NMR, and SPE.

I am also grateful to Dr. Evie Kemp, Cynthia Swinimer, and volunteers who have assisted in collecting the haskap leaves. I have always looked forward to the idyllic countryside field trips. I would like to also thank our departmental technicians John Pyke, Dean Grijm, and Scott MacKinnon who are always ready to help, be it some equipment that needs a quick fix or retrofitting them. Not forgetting our graduate coordinator Dr. Suzanne Budge and PEAS administrative team Julie O'Grady and Paula Colicchio who make the overall journey a smoother one. I would also like to thank our collaborators at Cape Breton University who helped with some analysis when we had limited access to facilities during the pandemic.

Finally, I want to thank my parents, family, and friends both near and far for their support, encouragement, and for keeping yourselves safe during these times.

Chapter 1 : General Introduction

Haskap plants (*Lonicera caerulea*) are grown commercially for their berries which are considered “superfruits” as they are rich in antioxidants and have higher anthocyanin and ascorbic acid content than blueberries (Celli et al., 2014). Native to northern boreal forests in Asia, Europe, and North America (Bors, 2009), haskap plants thrive in North America as they can withstand severe cold climates and are resistant to temperatures below -40°C (Ochmian et al., 2008). The haskap industry is expanding rapidly in Atlantic Canada and it has been estimated that this business could fetch \$500 million annually in the next five years (O’Connor, 2018). The commonly grown varieties in Nova Scotia, Canada, are Indigo Gem, Berry Blue, and Tundra (Iheshiulo, 2018) and it is expected that berry yields of 2 to 5 kg per plant can be obtained after 8 to 15 years of growth (Dawson, 2017). While berries are the primary crop, haskap leaves could provide a potential source of revenue as they are currently an underutilized resource.

Commercially harvested berries such as haskap, blueberries, blackberries and raspberries (Häkkinen et al., 1999; Hummer et al., 2012; Pimpão et al., 2013) are rich in bioactive compounds such as anthocyanins, phenolic acids, flavonols, flavonoids, and iridoids (Kucharska et al., 2017; Oszmiański et al., 2011; Tian et al., 2018). Many of these bioactive compounds have positive effects on human health and demonstrate antioxidant, antibacterial, anti-obesity, anti-diabetic, and anti-inflammatory properties (Kowalska & Olejnik, 2016; Nile & Park, 2014; Pereira et al., 2016; Shi et al., 2017). Similarly, research has shown that leaves from berry-producing plants such as haskap, blueberry, blackberry and raspberry contain various bioactive compounds such as hydroxycinnamic acids, flavonoids, flavonols, proanthocyanidins, tannins and triterpenes (Ferlemi & Lamari, 2016; Oszmiański et al., 2011) and some studies have reported that the leaves can have significantly higher levels of bioactive compounds compared to the berries (Ehlenfeldt & Prior, 2001; López de Dicastillo et al., 2017). The high concentration of bioactive compounds in the leaves has been attributed to protection against herbivores and pathogens, whereas the lower concentrations present in mature berries are to attract animals to consume and disseminate the seeds (Dawson, 2017). Although mulberry leaves have been

used as a traditional Chinese medicinal tea (Kobayashi et al., 2010; Wilson & Islam, 2015), the leaves from berry plants are generally perceived as by-products or agricultural residues (Bujor et al., 2019; Zhu et al., 2013). For example, haskap leaves are typically left under the plants as mulch after shedding their leaves every autumn (C. Swinimer, personal communication, May 4, 2018). As studies have indicated that haskap leaves are rich in bioactive compounds such as chlorogenic acid, loganin, secologanin, quercetin-3-sambubioside, quercetin-3-rutinoside, and quercetin-3-glucoside (Bonarska-Kujawa et al., 2014; Dawson, 2017; Oszmiański et al., 2011), there is the potential to extract these valuable compounds from this underutilized agricultural resource.

Conventional extraction methods such as Soxhlet extraction (Szakiel et al., 2012) and maceration (Raudsepp et al., 2010), and assisted extractions such as ultrasonication and microwave (Routray & Orsat, 2014) have been used to extract bioactive compounds from berry leaves. The drawbacks of these techniques are the use of toxic solvents such as methanol and hexane (Tabera et al., 2004), high extraction temperatures, lengthy extraction times (Luque de Castro & Priego-Capote, 2010), and the need of specialized parts such as ultrasound transducer and magnetron (Routray, 2014). In recent years, the importance of designing processes in accordance with the Principles of Green Engineering has been recognized (Anastas & Zimmerman, 2003), and there is a need to find alternative extraction processes that are more sustainable. For example, extraction techniques using an aqueous two-phase system (ATPS) provide a more environmentally friendly alternative and involves a simpler set-up than other methods. An ATPS is formed with two aqueous components such as polymer/polymer, polymer/salt, ionic liquid/salt, or alcohol/salt (Hatti-Kaul, 2000), forming two phases (top and bottom) once equilibrium has been reached. In keeping with the Principles of Green Engineering (Anastas & Zimmerman, 2003), ATPS phase-forming components can be selected to be less toxic and generally recognized as safe (GRAS). Aqueous two-phase extraction (ATPE) occurs when leaves are added and the target compounds selectively partition to either phase in the ATPS. This technique integrates equilibration, phase separation, and concentration of solutes in a single step (Hatti-Kaul, 2000). ATPE can achieve phase separation at a rapid rate and it can occur at low temperatures (Hou et al., 2018; Leong, Ooi, Law, Julkifle, & Show, 2018). In

comparison to the conventional Soxhlet extraction, ATPE does not require long extraction time and is effective at relatively lower extraction temperatures. These features align with the Principles of Green Engineering where processes should be designed to maximize energy and time efficiency (Anastas & Zimmerman, 2003). ATPE also allows the use of less toxic components where this corresponds with the Principles of Green Chemistry where the use of safer solvents are recommended (Tang et al., 2005). The ATPE process features low interfacial tension and high water content which create a gentle aqueous environment to preserve the properties of the biomolecules (Grilo et al., 2016). Studies have shown that ATPE achieved a higher purity (Zhang et al., 2013) and yield (Fu et al., 2019; He et al., 2016) of bioactive compounds when compared to conventional extraction methods.

Scaling up ATPE has some associated drawbacks which include the high salt concentrations involved (Rosa et al., 2009) and post-use handling of the phase-forming components (Soares et al., 2015). In view of these issues, researchers have explored the effect of recycling the phase-forming components from ATPE on extraction efficiencies (Tan et al., 2014) and extraction yields (Cheng et al., 2016). In addition, aqueous-two phase flotation (ATPF) is another approach that can be used to increase extraction efficiency and to aid in scaling up the process. This bubble-assisted method involves the addition of an ATPS into a flotation column and the introduction of air at the bottom of the column (Leong, Ooi, Law, Julkifle, Ling, et al., 2018; Pakhale et al., 2013). The surface-active biomolecules selectively adsorb onto the rising bubbles and this improves mass transfer of the bioactive compounds to the top phase (Lee et al., 2016). Studies using ATPF have shown increased partitioning behavior and extraction efficiency (Lee et al., 2016; Padilha et al., 2017) when compared to the ATPE process without bubbles.

Along with the demand for more sustainable manufacturing and extraction processes, consumers have shown a preference for more sustainable products made from renewable resources, due to their reduced environmental impact (North & Halden, 2013) and lower risk to human health (Halden, 2010). Bio-based films are an example of a more sustainable alternative to plastic packaging (Jiménez et al., 2012; Singh et al., 2019; Vieira et al., 2011),

and they are typically made of biopolymers such as proteins (Salgado et al., 2010; Talens & Krochta, 2005) and starches (Lumdubwong, 2019; Nouri & Mohammadi Nafchi, 2014) instead of petroleum-derived compounds. Films developed from pea proteins are a potentially sustainable solution for creating value-added materials, enhancing pulse utilization and creating new market opportunities (Acquah et al., 2020; Choi & Han, 2001). This is especially important for Canada, which is the largest producer and leading exporter of dry peas (Abdel-Aal et al., 2018; Chan et al., 2019; Pulse Canada, 2019), producing 3,580,700 tonnes of dry peas in 2018 (Food and Agriculture Organization of the United Nations, 2018).

Various bio-based and edible films can be made into functional films by incorporating extracts from natural products into the formulations (Marcos et al., 2014; Wang et al., 2012b). Functional films with bioactive extracts may have added antioxidant (Han et al., 2018; Medina Jaramillo et al., 2015) and antimicrobial (Kanmani & Rhim, 2014; Sivarooban et al., 2008) properties which could make them suitable as active packaging for food products. Functional films have been formed using aqueous and alcoholic extracts (Bonilla & Sobral, 2016; Musso et al., 2019; Wang et al., 2012a); however, there have been no studies incorporating bioactive extracts from ATPE or ATPF into films. Researchers have shown that having salt in the film may affect its mechanical properties (Frohberg et al., 2010; Stolte et al., 2012) and overall hygroscopicity (Sängerlaub et al., 2013). Therefore, incorporating bioactive extracts with ATPS components from alcohol/salt systems may have an effect on the film properties and functionality.

Thus, the overall goal of this project was to develop a sustainable approach for producing pea protein-based functional films using haskap leaves as an underutilized, renewable resource, where ATPE and ATPF would be investigated as environmentally friendly extraction methods. It was hypothesized that the haskap leaf extracts obtained from ATPE and ATPF could be incorporated into the pea protein films and would result in added functional properties. The specific research objectives were to:

- i) Investigate ATPE for the extraction of bioactive compounds from haskap leaves using GRAS components (salt/ethanol and sugar/propanol);

- ii) Evaluate the feasibility of recycling the ATPE phase-forming components;
- iii) Investigate ATPF for the bubble-assisted extraction of bioactive compounds from haskap leaves;
- iv) Develop novel pea protein functional films by incorporating haskap leaf extracts from ATPE and ATPF, and to characterize the resultant film properties.

The thesis is outlined in the following paragraphs. In Chapters 3 to 6 which follow a manuscript style, the background of each study is presented, followed by the experimental work, research results, conclusions, and recommendations.

Chapter 2 is a literature review of haskap leaves, explaining their origins and cultivars in Nova Scotia, the bioactive compounds present in berry leaves and haskap leaves, extraction methods of the bioactive compounds, concepts of ATPE and ATPF, factors affecting partitioning, recycling strategies, formation of functional pea protein films, and some commonly assessed properties of films.

Chapter 3 compares the performance of salt/ethanol and sugar/propanol ATPE for the extraction and concentration of bioactive compounds from haskap leaves.

In **Chapter 4**, recycling is evaluated based on the performance of food-compatible ATPE systems (i.e. salt/ethanol and sugar/1-propanol ATPE systems) for the extraction and concentration of bioactive compounds from haskap leaves, as a means of increasing sustainability.

Chapter 5 compares the performance of ATPF in two salt/ethanol systems, namely ammonium sulfate $(\text{NH}_4)_2\text{SO}_4$ /ethanol and sodium dihydrogen phosphate NaH_2PO_4 /ethanol, for the extraction and concentration of bioactive compounds from haskap leaves.

Chapter 6 presents the development of pea protein functional films using haskap leaf extracts from ATPE and ATPF, and characterization of the resultant films.

Chapter 7 then concludes by providing an overall summary of this work with recommendations for future research.

Chapter 2 : Literature Review

2.1 Haskap Plants

Haskap plants (*Lonicera caerulea*) are native to Japan, North Eastern Asia, and Siberia (Naugžemys et al., 2007). There are various names for haskap such as blue honeysuckle, honeyberry, and haskappu. The Japanese indigenous Ainu community uses ‘haskappu’ which translates to ‘little things on top of the branches’ where haskap products have been associated with traditional remedies for eternal youth and longevity (Lefol, 2007). Haskap plants are deciduous shrubs and can grow to 2 meters or more in height (Hummer et al., 2012). They require bees for cross-pollination to produce pale yellow flowers which eventually develop into haskap berries. Appearing as a cross between blueberries and grapes, the colour of these berries ranges from dark blue to purple and they appear oval or long and thin. The leaves have an oval to elongated shape and are about 3 to 5 cm in length. This berry crop has gained commercial interest in North America in the past decade as the haskap plant can withstand severe cold climates, undergoes early fruiting and ripening, and suitable for mechanized harvesting (Hummer et al., 2012). Breeding strategies by inter-crossing different haskap varieties led to increased plant vigour, resistance to mildew, and improved berry flavor (Bors, 2009). Indigo Gem, Berry Blue, and Tundra are common varieties grown in Nova Scotia, Canada (Iheshiulo, 2018).

Similar to most berries, haskap berries can be eaten fresh or processed into dried berries, fruit powders, jams, juices, syrups, and wine. The berries can also be used to develop new food products such as ice cream, pastries, and puffed snacks (Liu et al., 2009). Haskap berries have higher ascorbic acid and anthocyanin content than other berries such as blueberries (Celli et al., 2014). Anthocyanins are categorized as flavonoids and they provide the berries with pigments (Khoo et al., 2017); moreover, flavonoids are known to have anti-inflammatory (Maleki et al., 2019), anticancer (Raffa et al., 2017), and antioxidant properties (Pietta, 2000). These perennial shrubs shed their leaves every autumn, resulting in an abundance of leaves. The leaves are presently not used for any

specific purpose and are an agricultural residue, left under the plants as mulch (C. Swinimer, personal communication, May 4, 2018).

2.2 Bioactive Compounds in Berry Leaves

Studies have shown that bioactive compounds are present in the leaves of many berry plants, and that some berry leaves have significantly higher levels of bioactive compounds in comparison to the fruits (Bonarska-Kujawa et al., 2014; Oszmiański et al., 2011). For example, highbush blueberry leaves (*Vaccinium corymbosum* L.) were reported to have an average of 490 μmol of Trolox equivalents (TE)/g fresh weight (FW) and phenolic content of 45 mg gallic acid equivalents (GAE)/g FW, whereas the berries had 15.9 μmol TE/g FW and 4.2 mg GAE/g FW (Ehlenfeldt & Prior, 2001). Additionally, murta leaves (*Ugni molinae* Turcz.) had 110 to 130 mg GAE/g, resulting in approximately four times higher phenolic content than the fruits with 23 to 34 mg GAE/g dry fruit (López de Dicastillo et al., 2017). The complementary antioxidant assays that were performed, such as oxygen radical absorption capacity (ORAC), ferric reducing antioxidant power (FRAP), 2,2-diphenyl-1-picrylhydrazyl (DPPH), and Trolox equivalent antioxidant capacity (TEAC), supported the results that the leaves showed higher antioxidant activity than the fruits. In cranberry plants (*Vaccinium macrocarpon* L.), 24 and 39 phenolic compounds were identified in the leaves and fruits, respectively. It was reported that flavonols were the main phenolic group in leaves, whereas anthocyanins were abundant in the fruits, and that the total polyphenol content in cranberry leaves averaged 320 mg/g dry matter compared to 117 mg/g dry matter for the fruit (Oszmiański et al., 2016). Haskap leaves have on average 7 times higher chlorogenic acid (CGA), 6.5 times higher total quercetin, and 15 times higher total iridoid concentrations in leaves at the end of the season than in the berries sampled at harvest maturity (Dawson, 2017). It was shown that these concentrations varied throughout the growing season according to the physiological needs of the plants, as these compounds aid in resisting pathogens, deterring herbivores, producing lignin, and protecting against ultraviolet light.

In haskap leaves, the bioactive compounds that are commonly present include flavonoids such as quercetin and phenolic acids such as CGA and gallic acid (Bonarska-Kujawa et al., 2014; Dawson, 2017; Oszmiański et al., 2011). The core structure of a flavonoid is a carbon skeleton consisting of 15 carbon atoms arranged in three rings, C₆-C₃-C₆ (Pietta, 2000). There are many classes of flavonoids such as flavones, flavanones, isoflavones, flavonols, flavanonols, flavan-3-ols, and anthocyanidins. Figure 2.1 shows the chemical structure of a representative flavonoid, quercetin-3-rutinoside. It is also commonly known as rutin. Flavonoids have various ecological roles in plants, and they contribute to shades of blue, scarlet, and orange which attract pollinating insects (Khoo et al., 2017). Some astringent flavanols also function as a defense system against insects and their UV-absorbing properties protect plants from UV radiation of the sun (Agati et al., 2011). Additionally, flavonoids have antioxidant (Wu et al., 2015), anti-inflammatory (Maleki et al., 2019), anti-cancer (Ren et al., 2003) properties.

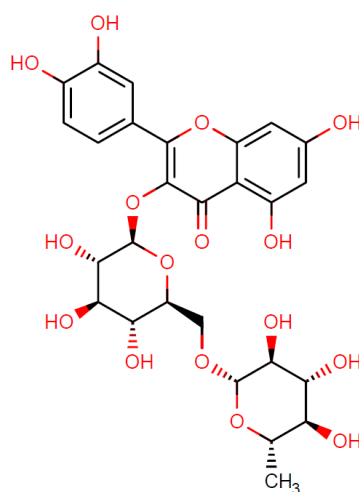


Figure 2.1 Chemical structure of quercetin-3-rutinoside (ChemAxon, 2019)

Chlorogenic acid (CGA) is a phenolic acid commonly found in coffee and tea. Figure 2.2 shows the chemical structure of chlorogenic acid. There are a few isomeric forms of CGA such as 3-CQA (caffeoyl quinic acid), 4-CQA, and 5-CQA (Naveed et al., 2018). CGA as

one of the most common dietary polyphenolic compounds has been associated with anti-diabetic, anti-obesity, antioxidant, anti-inflammatory, anti-hypertension, and antimicrobial properties (Naveed et al., 2018). Its health benefits have encouraged the manufacturing of CGA health supplements. CGA has anti-obesity and antidiabetic properties which are linked to lipid and glucose metabolism (Meng et al., 2013). CGA also demonstrates antioxidant properties in *in vitro* and *in vivo* experiments (Sato et al., 2011). Green coffee extracts containing 28 weight% of CGA exhibited anti-hypertensive properties when it was administered orally to rats (Suzuki et al., 2002). Chlorogenic acid also showed antimicrobial properties on gram-positive and gram-negative bacteria by permeating the cell membrane (Lou et al., 2011).

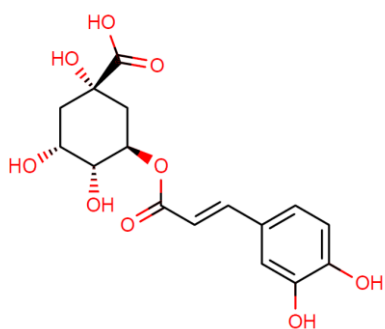


Figure 2.2 Chemical structure of chlorogenic acid (ChemAxon, 2019)

Gallic acid or 3,4,5-trihydroxybenzoic acid is an abundant phenolic acid found in plants. Figure 2.3 shows the chemical structure of gallic acid. Gallic acid has shown antimicrobial activity, anticancer activity, and offers protection from gastrointestinal diseases, cardiovascular diseases, metabolic diseases, and neuropsychological diseases (Kahkeshani et al., 2019). It is commonly used as a standard for the total phenolic content in the Folin-Ciocalteu assay (Singleton et al., 1999). Gallic acid was suggested to protect the mitochondria by reducing oxidative stress (Dutta & Paul, 2019). Mitochondria are known as the powerhouses of the cell, generating chemical energy needed to power biochemical reactions in the cell. Gallic acid from radix *Sanguisorbae* extracts has also shown anti-inflammatory properties in murine macrophage cell line (Seo et al., 2016).

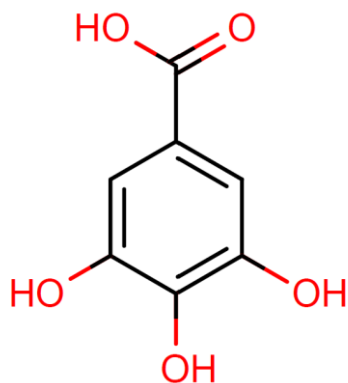


Figure 2.3 Chemical structure of gallic acid (ChemAxon, 2019)

The following Table 2.1 shows the average concentration of bioactive compound in haskap leaves and other berry leaves. Apart from the compounds in Table 2.1, studies have shown that cuticular waxes on haskap leaves of variety *kamtschatica* contain triterpenoids (Becker et al., 2017). The triterpenoid content of leaves and fruits were 219.75 $\mu\text{g}/\text{mg}$ and 62.51 $\mu\text{g}/\text{mg}$ of wax extract mass, respectively. The main triterpenoid in the leaves is 24-methylenecycloartanol which accounted for 126.27 $\mu\text{g}/\text{mg}$ of wax extract and triterpenoids can potentially protect the plant against biotic stresses (Lara et al., 2014). Triterpenoids exhibited strong antiproliferative activities against tumor cells and had 20 to 70 times higher antioxidant activity than ascorbic acid (Qiao et al., 2015). Additionally, iridoid glucosides namely loganin, secologanin, secologanin dimethyl acetal, sweroside, caeruleoside A, and caeruleoside B were identified in haskap leaves of variety *emphyllocalyx* Nakai (Machida et al., 1995).

Table 2.1 Average concentration of chlorogenic acid, flavonoids, and total phenolic content in berry leaves

Leaves	Chlorogenic acid (mg/g DW)	Flavonoids (mg/g DW)	Total phenolic content (mg GAE/g DW)	Reference
Haskap (<i>Lonicera caerulea</i>)	20.5 ^a	113.6 ^a	N/A	Dawson (2017)
Haskap (<i>Lonicera kamtschatica</i> Zielona)	67.1	146.3	N/A	Oszmiański et al. (2011)
Cranberry (<i>Vaccinium macrocarpon</i> L.)	6.1	233.4	319.3	Oszmiański et al. (2016)
Murta (<i>Ugni molinae</i> Turcz.)	N/A	N/A	111.7	López de Dicastillo et al. (2017)
Black currant (<i>Ribes nigrum</i> Titania)	11.5	120.8	N/A	Oszmiański et al. (2011)
Black currant (<i>Ribes nigrum</i> L.)	14.9	31.3	N/A	Raudsepp et al. (2010)
Raspberry (<i>Rubus ideaus</i>)	6.4	108.1	N/A	Oszmiański et al. (2011)
Raspberry	N/A	6.9	22.8	Tian et al. (2018)
Bilberry (<i>Vaccinium myrtillus</i>)	350.6	37.0	N/A	Oszmiański et al. (2011)
Bilberry	N/A	3.09	20.2	Tian et al. (2018)
Bilberry	276.0	665.0	N/A	Hokkanen et al. (2009)
Lingonberry (<i>Vaccinium vitis-idaea</i> L.)	38.7	683.0	N/A	Hokkanen et al. (2009)
Strawberry (<i>Fragaria × ananassa</i> Duch.)	N/A	94.2	N/A	Oszmiański et al. (2011)

^a leaves harvested at end of season

2.3 Extraction of Bioactive Compounds

Some of the conventional solid-liquid extraction methods used to extract bioactive compounds from natural products are maceration, percolation, and reflux (Chanda & Kaneria, 2012; Vongsak et al., 2013). There are several drawbacks associated with these methods including the use of toxic and hazardous solvents such as hexane, petroleum ether, and methanol, long extraction times, low yields, large amount of solvents, and the need for several post-extraction steps (Luque de Castro & Priego-Capote, 2010). With modern technologies, assisted-extraction methods can be introduced to improve the classical methods by integrating technologies such as the application of microwaves (Olalere et al., 2019), ultrasound (Contreras et al., 2020), high pressure (Xi et al., 2009), pulsed electric fields (Zderic & Zondervan, 2016), or enzymes (Boulila et al., 2015). These methods can enhance extraction performance; however, they often require sophisticated equipment. Following the Principles of Green Engineering (Anastas & Zimmerman, 2003), it is important to investigate other sustainable extraction techniques. Extraction methods based on aqueous two phase systems (ATPS) have shown promise as a more sustainable alternative to conventional solid-liquid extraction techniques and have simple equipment requirements (Đorđević & Antov, 2017; Liu et al., 2013). In the following sections, the concept of ATPS will be described, followed by aqueous two phase extraction (ATPE) and aqueous two phase flotation (ATPF).

2.3.1 Aqueous Two-Phase Systems (ATPS)

Aqueous two-phase systems (ATPS) or aqueous biphasic systems are formed with two aqueous components such as polymer/polymer, polymer/salt, ionic liquid/salt, or alcohol/salt (Hatti-Kaul, 2000). Early records show that the first liquid-liquid polymer ATPS was formed by Per-Åke Albertsson through serendipity by mixing potassium phosphate buffer and polyethylene glycol when trying to purify chloroplasts (Albertsson, 1985). Two incompatible aqueous components will partition into two distinct phases after the system achieves equilibrium. Ethanol/salt-based ATPS use the salting-out phenomena, where the solubility of the nonelectrolyte substance, in this case ethanol, decreases in water

with increasing salt concentration (Hyde et al., 2017). The use of sugar in an ATPS is known as sugaring-out. For example, when sugars are introduced in a solution of aqueous acetonitrile, the acetonitrile separates from water and forms an immiscible top phase (Wang et al., 2008).

The first step in an ATPS study is to obtain liquid-liquid equilibrium (LLE) data for the components of interest. There are many LLE data which have been reported covering a wide range of components and temperatures (Cheluget et al., 1994; Hu et al., 2003; Wang et al., 2010). Alternatively, an ATPS phase diagram can be constructed to determine the concentration of phase-forming components required to form two phases. For alcohol/salt or alcohol/sugar ATPS, alcohol is added dropwise to aqueous salt or sugar solutions with known concentrations under constant stirring until the first sign of permanent turbidity is observed (Hatti-Kaul, 2000). After recording the mass of the second component, an ATPS phase diagram, such as in Figure 2.4, can be constructed with the known concentration of both components.

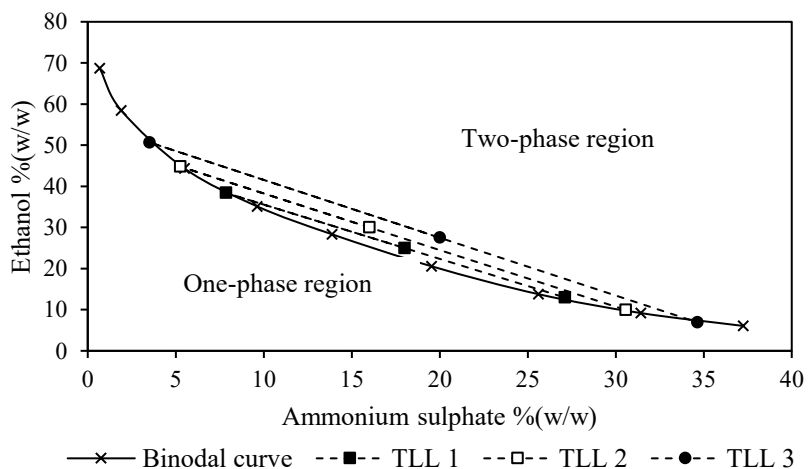


Figure 2.4 ATPS phase diagram of ethanol and ammonium sulphate at 25 °C (Chong et al., 2020)

In Figure 2.4, the concentrations below the binodal curve will form a homogenous solution while the concentrations above the binodal line will form two phases. The points on the

end of the tie line indicate the final concentration of phase components in the top and bottom phases. Moving along the same tie line, all the points on the tie line will have identical compositions in the top and bottom phases (Ruiz-Ruiz et al., 2017). With this, different compositions can also be represented by different tie line lengths (TLL) as shown in Figure 2.4. The difference between points on the same tie line is the volume of the two phases.

Aqueous two-phase extraction (ATPE) occurs when target compounds selectively partition to either phase in an ATPS. This technique integrates equilibration, phase separation, and concentration of solutes in a single step (Hatti-Kaul, 2000). In comparison to conventional extraction methods, ATPE is environmentally friendly as users can select from less toxic phase-forming components such as alcohol, polyethylene glycol, and salt (Leong, Ooi, Law, Julkifle, & Show, 2018; Navapara et al., 2011). Moreover, components can be selected from compounds that are generally recognized as safe (GRAS) (U.S. Food and Drug Administration, 2020).

ATPS has been commonly used for proteins (Huddleston et al., 1991), plasmid deoxyribonucleic acid (pDNA) (Gomes et al., 2009), cells (Frampton et al., 2011), antibodies (Frampton et al., 2014), enzymes (Ling et al., 2010; Ooi et al., 2009) and viruses (Joshi et al., 2019). As a further example, a biotechnology corporation, Genentech, investigated ATPE to separate and purify insulin-like growth factor (IGF-1) with fermentation broth and *Escherichia coli* cells (Hart et al., 1994). In recent work, the use of ATPS for non-proteinaceous compounds, is not as common but demonstrates that this technique is versatile. For example, ATPS have been used to extract bioactive compounds such as phenolic compounds (Reis et al., 2015; Sánchez-Rangel et al., 2016), anthocyanins (Liu et al., 2013), and alkaloids (Zhang et al., 2015). ATPS have also been used to extract contaminants such as acidic drugs (Vieira et al., 2019) and phenols (Rodrigues et al., 2010) from wastewater. Some examples of ATPS studies that extracted non-proteinaceous, low molecular weight compounds from natural products are shown in Table 2.2.

Table 2.2 Applications of aqueous two-phase systems (ATPS) to recover non-proteinaceous compounds using ATPE

Compound of interest	Type of ATPS	ATPS component	Reference
Betacyanin from red-purple pitaya (<i>Hylocereus polyrhizus</i>)	Alcohol/salt	Ethanol Dipotassium hydrogen phosphate	Leong, Ooi, Law, Julkifle, & Show (2018)
Flavonoids from lotus leaves (<i>Folium nelumbinis</i>)	Alcohol/salt	Ethanol Dipotassium hydrogen phosphate	Hou et al. (2018)
Flavonoids, specifically genistein and apigenin from pigeon pea roots (<i>Cajanus cajan</i>)	Alcohol/salt	Ethanol Dipotassium hydrogen phosphate	Zhang et al. (2013)
Flavones from honeysuckle	Alcohol/salt	Ethanol Sodium dihydrogen phosphate	Liu et al. (2013)
<i>Para</i> -coumaric acid from agriculture residues	Acetonitrile/sugar	Acetonitrile Sugars: Glucose, xylose, sucrose	Dhamole et al. (2016)
Anthocyanin from red cabbage (<i>Brassica oleracea</i> L.)	Polymer/salt	Polyethylene glycol, magnesium sulfate	Jampani & Raghavarao (2015)
Anthocyanin from mulberry (<i>Morus atropurpurea</i> Roxb.)	Alcohol/salt	Ethanol Ammonium sulfate	Wu et al. (2011)
Anthocyanin from purple sweet potato (<i>Ipomoea batatas</i> Lam.)	Alcohol/salt	Ethanol Ammonium sulfate	Liu et al. (2013)
Quercitrin, hyperoside, rutin, and afzelin from pepper leaves (<i>Zanthoxylum bungeanum</i> Maxim)	Alcohol/salt	Ethanol Salts: Sodium dihydrogen phosphate and dipotassium hydrogen phosphate	He et al. (2016)
Chlorogenic acid from carrot (<i>Daucus carota</i>)	Alcohol/salt Ionic liquid/salt	Alcohols: Ethanol, butanol Salts: Ammonium sulfate, potassium phosphate	Sánchez-Rangel et al. (2016)

Compound of interest	Type of ATPS	ATPS component	Reference
Chlorogenic acid from ramie leaves (<i>Boehmeria nivea</i> L. Gaud)	Alcohol/salt	Ethanol Ammonium sulfate	Tan et al. (2014)
Chlorogenic acid from blueberry leaves (<i>Vaccinium ericaceae</i>)	Deep eutectic solvent (DES)/salt with negative pressure cavitation	DES Dipotassium hydrogen phosphate	Wang et al. (2017)
Saponin namely ginsenosides from ginseng root (<i>Panax ginseng</i> C. A. Mey)	Ionic liquid/salt	Ionic liquids: <i>n</i> -alkyl-tropinium, <i>n</i> -alkyl-quinolinium bromide Salts: Tripotassium phosphate, potassium carbonate, dipotassium hydrogen phosphate, potassium citrate, sodium dihydrogen phosphate, and sodium citrate	He et al. (2018)
Polyphenols from tea leaves (<i>Camellia sinensis</i> var. <i>assamica</i>)	Polymer/salt	Ethylene oxide–propylene oxide (EPO) Salts: dipotassium phosphate, tri-sodium citrate, and a sulphate salt	Ng et al. (2017)
Polyphenols and lutein from marigold (<i>Tagetes erecta</i> L.)	Alcohol/salt	Ethanol Ammonium sulfate	Fu et al. (2019)

Researchers have investigated methods to improve the extraction efficiency and partitioning of solutes in ATPS-based extraction. For example, the integration of flotation to form the aqueous two-phase flotation (ATPF) technique (Bi, Dong, & Yuan, 2010; Leong, Ooi, Law, Julkifle, Ling, et al., 2018). This bubble-assisted technique allows biomolecules to adsorb onto the surface of the rising bubbles and concentrate in the top phase over time (Bi et al., 2013; Pakhale et al., 2013). Table 2.3 shows example applications of studies involving the extraction of non-proteinaceous low molecular weight compounds from natural products using ATPF.

Table 2.3 Applications of aqueous two-phase systems (ATPS) to recover non-proteinaceous compounds using ATPF

Compound of interest	Type of ATPS	ATPS components	Air flow rate	Flotation time	Column geometry	Reference
Astaxanthin from microalgae (<i>Haematococcus pluvialis</i>)	Alcohol/salt	Alcohols: Ethanol, 2-propanol Salts: Ammonium sulphate, di-potassium hydrogen phosphate, sodium carbonate, magnesium sulphate, sodium citrate	N/A	5 to 25 minutes	50-mL column of diameter 2 cm, height 20 cm	Khoo et al. (2019)
Baicalin from <i>Scutellaria baica lensis</i> plant	Polymer/salt	Polyethylene glycol (PEG) Ammonium sulfate	10 to 60 mL/min	10 to 60 min	400 mL column of diameter 4.5 cm	Bi et al. (2013)
Betacyanin from red-purple pitaya (<i>Hylocereus polyrhizus</i>)	Alcohol/salt	Alcohols: Ethanol, methanol, 1-propanol, 2-propanol Salts: Dipotassium hydrogen phosphate, ammonium sulphate, magnesium sulphate, sodium carbonate, tri-sodium citrate	20 to 30 mL/min	15 min	Column of diameter 2 cm and height 20 cm	Leong, Ooi, Law, Julkifle, Ling, et al. (2018)
Isoflavone namely puerarin from <i>Puerariae</i> root	Polymer/salt	Polyethylene glycol Ammonium sulphate	10 to 60 mL/min	0 to 120 min	400 mL column of diameter 4.5 cm	Bi, Dong, & Yuan (2010)

Compound of interest	Type of ATPS	ATPS components	Air flow rate	Flotation time	Column geometry	Reference
Liquiritin and glycyrrhizic acid from licorice (<i>Glycyrrhiza uralensis</i>)	Polymer/salt Alcohol/salt	Polymers: PEG1000, PEG2000, PEG4000 Alcohols: <i>Iso</i> -propanol, <i>n</i> -propanol, <i>n</i> -butanol Ammonium sulphate	10 to 60 mL/min	0 to 60 min	400 mL column of diameter 4.5 cm	Chang et al. (2014)
Ovalbumin from salted egg white	Polymer/salt	Polyethylene glycol 1000 Ammonium sulfate	25 to 35 mL/min	20 to 40 min	N/A	Jiang et al. (2019)
Polyphenols from camu-camu (<i>Myrciaria dubia</i>)	Polymer/salt	Polyethylene glycol 400 Ammonium sulfate	12.5 to 50 mL/min	0 to 120 min	Column of diameter 2.64 cm and height 30 cm and scale-up column of diameter 8 cm and 60 cm height	de Araújo Padilha et al. (2018)
Sodium chlorophyllin from bamboo leaves	Alcohol/salt	Ethanol Salts: Tripotassium phosphate, potassium carbonate, dipotassium phosphate, tripotassium citrate	10 to 30 mL/min	5 to 35 min	50-mL and a 500-mL scale-up column	Xia et al. (2016)

Other assisting technologies that have been integrated with ATPS have included electricity (Koyande et al., 2019; Leong, Chang, et al., 2019; Leong, Ooi, et al., 2019), microwaves (Cheng et al., 2017; Ma et al., 2013; Zhang et al., 2015), ultrasound waves (Đorđević & Antov, 2017; Sankaran, Manickam, et al., 2018), and enzymes (Fu et al., 2019); these result in improved extraction efficiency as the external forces and enzymatic activity help to disrupt rigid cell walls and membranes.

2.3.2 Aqueous Two-Phase Extraction (ATPE)

ATPE is a simple technique as it only requires a vessel and two phase-forming components to extract compounds of interest Figure 2.5 illustrates the concept of ATPE. Along with the separation from one homogenous phase to two phases, the target compound selectively partitions into either the top or the bottom phase at the end of equilibration time. The partitioning behaviour can be expressed by the partition coefficient, k (Cienfuegos et al., 2017) and it is defined in Equation 2.1.

$$k = \frac{C_T}{C_B} \quad (2.1)$$

Here, C_T is the concentration of the target compound in the top phase and C_B is the concentration of the target compound in the bottom phase. In a salt or sugar-based ATPS, the top phase is an alcohol-rich phase consisting of mainly alcohol, water, and residual salt or sugar. The bottom phase is the salt or sugar-rich phase with some water and residual alcohol. ATPE integrates feed clarification, biomolecule concentration, and partial purification (Soares et al., 2015), where the target compounds can simultaneously partition to one phase and the contaminants to another (Liu et al., 2013).

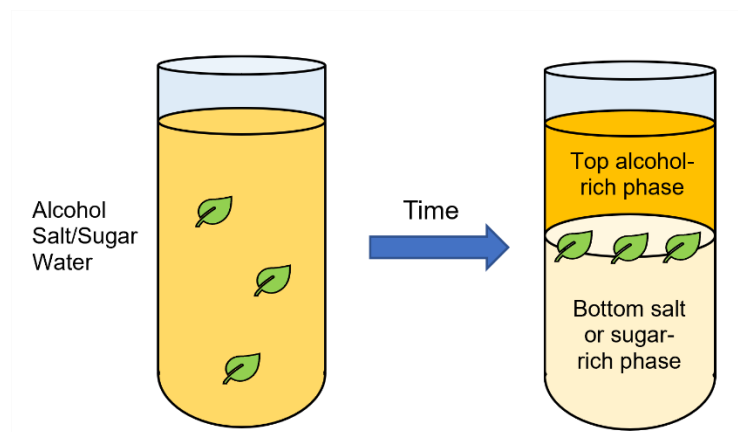


Figure 2.5 Concept of aqueous two-phase extraction with an alcohol and salt/sugar combination with leaves as the raw material (Chong et al., 2020)

ATPE can be easily scaled up, as the time needed for the equilibration of the two phases can be much faster in a vessel with a large cross-sectional area (Solano-Castillo & Rito-Palomares, 2000) and studies have shown that the extraction efficiency can be maintained for 10- and 100-fold experiments (He et al., 2016; Wu et al., 2014). However, the partitioning behaviour of target compounds is still not well understood and process development of ATPE has been mainly based on empirical optimization, although molecular dynamics simulations have contributed to more accurate partitioning models (Dismer et al., 2013; Oelmeier et al., 2012). In the context of alcohol/salt ATPE, there are various factors affecting partitioning of biomolecules in ATPE such as type of salt, alcohol and salt concentrations, temperature, pH and sample loading.

2.3.2.1 Effect of Type of Salt

The effect of the type of salt in ATPS-based extraction has been attributed to the Hofmeister series which was originally based on protein precipitation in aqueous solution (Hyde et al., 2017). According to a hydration theory (Grover & Ryall, 2005), when an electrolyte (salt) is added to a solution of nonelectrolyte (aqueous alcohol), they compete for solvent molecules (water). The salt ionizes and it binds more strongly to the water molecules, decreasing the hydration and solubility of the nonelectrolyte causing phase separation. In an ATPS, the alcohol rises to form a top layer due to its lower density. The Hofmeister series is based on protein partitioning because when proteins are present in the

salting-out process, they can be precipitated. Low-molecular weight bioactive compounds would partition selectively to either phase (Simental-Martínez et al., 2014). The salting-out ability is influenced much more by the anion than the cation and generally follows this sequence from the most partitioning to least partitioning anion: $\text{CO}_3^{2-} > \text{SO}_4^{2-} > \text{S}_2\text{O}_3^{2-} > \text{H}_2\text{PO}_4^- > \text{F}^- > \text{Cl}^- > \text{Br}^- \approx \text{NO}_3^- > \text{I}^- > \text{ClO}_4^- > \text{SCN}^-$ (Hyde et al., 2017). Similarly, cations have a partitioning sequence: $(\text{CH}_3)_4\text{N}^+ > \text{Cs}^+ > \text{Rb}^+ > \text{NH}_4^+ > \text{K}^+ > \text{Na}^+ > \text{Li}^+ > \text{Mg}^{2+} > \text{Ca}^{2+}$ (Hyde et al., 2017). As an example, ammonium sulphate, $(\text{NH}_4)_2\text{SO}_4$ is expected to have higher salting-out ability than sodium dihydrogen phosphate, NaH_2PO_4 . The order of the salting-out ability is influenced by the ease of a salt to ionize and this involves the intramolecular forces within a molecule, specifically ionic bonding. The order also depends on how easily the ionized salt could form a strong bond with the water molecules. A highly electronegative atom such as fluorine is able to attract shared electrons to itself. A salt which easily ionizes and contain strong electronegative forces result in more effective salting-out. The salting effect also depends on other properties such as size, structure, charge density, polarizability, hydration number of the salt (Grover & Ryall, 2005).

2.3.2.2 Effect of ATPS Composition

As mentioned in Section 2.3.1, the ATPS composition is represented on the phase diagram by tie line lengths (TLLs). ATPS composition can influence the partitioning of target molecules. For example, the partition coefficient of polyphenols from black tea leaves was found to increase when the TLL increased from 33.7% (w/w) to 41.4% (w/w) using an ethylene oxide-propylene oxide/salt ATPS (Ng et al., 2017). Other ATPS studies have also observed increased recoveries with increasing TLL for proteins using polyethylene glycol/salt (Santhi et al., 2020) and polyethylene glycol/polyacrylic acid systems (Saravanan et al., 2008), anthocyanins using ethanol/salt systems (Caldeira et al., 2019) and polyphenols using ethanol/salt systems (Xavier et al., 2017), although increasing TLL had no effect on the partition behavior of proteins from soybean extract from polyethylene glycol/salt ATPS (Aguilar & Rito-Palomares, 2008). In general, the increasing TLL and increasing salt concentration results in higher salting-out ability as water content decreases; with less water to hydrate the ions completely, the cation-anion interactions begin to

dominate (He et al., 2018). This would cause greater hydrophobicity differences between the top phase and bottom phase and enhance the partitioning of the target compounds to one of the phases (Asenjo & Andrews, 2011).

2.3.2.3 Effect of pH

The partitioning of a target compound in an ATPS depends on the acid dissociation constant of the compound, K_a . This property is often expressed as pK_a , which is the negative base-10 logarithm of K_a . For organic molecules, the isoelectric point, pI , is at the pH where the molecules have no net electrical charge (Novák & Havlíček, 2016). In a solution where the pH is above the pI or pK_a , the surface of the compound is predominantly negatively charged, and will attract positively charged molecules. When the pH of a solution is below the pI or pK_a , the surface of the compounds will be positively charged. As an example, chlorogenic acid (CGA) with pK_a 3.33 (ChemAxon, 2019) in a solution or environment with higher pH will exist mainly as ions and tend to bond with the water molecules, resulting in partial partitioning of CGA to the hydrophilic bottom phase. When the solution is more acidic, that is having lower pH than the pK_a of CGA, it forms a stable environment for CGA. ATPE of bioactive compounds such as CGA (Wang et al., 2017) and gallic acid (Cláudio et al., 2012; Xavier et al., 2017) have shown that pH near or below the pK_a resulted in high recovery yields as the molecules preferentially partitioned to the top phase. This was also observed in ATPE of wastewater contaminants such as acetylsalicylic acid and salicylic acid where their partition coefficients increased when pH 3 was used (Vieira et al., 2019). However, contrasting partitioning behavior was observed with caffeine and codeine and this phenomenon was attributed to the inherent ability of ATPE for selective separation (Ebrahimi & Sadeghi, 2018).

2.3.2.4 Effect of Temperature

When temperature increases, the two-phase region in the ATPS phase diagram expands (Sadeghi & Jamehbozorg, 2008). Taking an ethanol/salt system as an example, at higher temperatures, the salt solubility in water increases and less salt is required to form a two-phase system. This means that alcohol will separate much more easily to the top phase. An increase in temperature likewise influences the extraction mechanism. For example, the

partition coefficient and total recovery of lignans increased when the temperature was increased to 40 °C, however temperatures higher than that showed little difference (Cheng et al., 2016). Zhang et al. (2013) also reported that at higher temperature, ATPS solubility increased and resulted in more compounds being solved into the ATPS. However, for the extraction of thermolabile bioactive compounds, high temperature may cause degradation (Luque de Castro & Priego-Capote, 2010). Therefore, moderate temperatures are recommended.

2.3.2.5 Effect of Sample Loading

The amount of the solid sample used for ATPE can affect the partitioning of the target compound by changing the volume ratio of the system. The volume ratio is defined as the ratio of the volume of the top phase and volume of bottom phase. Studies have shown that an increase in sample loading until 20 % (w/w) resulted in a corresponding increase in the partition coefficient and yield of cytochrome *c* (Ng et al., 2020), while a loading of 0.3 % (w/w) tea leaves resulted in peak partition coefficient and yield of polyphenols (Ng et al., 2017). Further increases in sample loading decreased the partitioning to the top phase due to the volume exclusion effect (Ng et al., 2017). This occurs when the space available for the biomolecule in the top phase is reduced, causing the biomolecules to partition to the bottom phase instead (Pakhale et al., 2013). Additionally, large sample loadings have a tendency to overload the ATPS. For example, Leong, Ooi, Law, Julkifle, & Show (2018) reported that 10 % (w/w) dried pitaya crude extracts caused the formation of a gel-like mixture due to the large amount of pectin present in the system, and the alcohol in the ATPS was insufficient to break down the pectin.

2.3.2.6 Recycling ATPS Phase-Forming Components

Some disadvantages of the ATPE process is that the high salt concentrations may cause corrosion to metal pumps, lines, and other equipment (Rosa et al., 2009). Post-handling and disposal of these components will also increase the overall costs and may be a hurdle for scaled-up operations (Soares et al., 2015). To ensure the sustainability of the ATPE process, studies have investigated the feasibility of recycling phase-forming components. In an alcohol/salt system, alcohol is usually recovered by evaporation (Sankaran, Show, et

al., 2018) while the salt can be precipitated by addition of alcohol and/or chilling at 4°C (Tan et al., 2014). Some authors chose to partially recycle the components by recycling one phase and preparing the other phase using fresh components (Show et al., 2013). Recycling was shown to have positive effects in a study where the extraction efficiency of chlorogenic acid (CGA) from ramie leaf was maintained after recycling three times (Tan et al., 2014). Wu et al. (2011) has also observed consistent recoveries with anthocyanin extraction using ethanol/ammonium sulphate ATPE for two recycling stages. Similarly, extraction of lignans from *Schisandra chinensis* fruits using ethanol/ammonium sulphate ATPE had stable recoveries and partition coefficients throughout five recycling stages (Cheng et al., 2016). Recycling strategies for lipase extraction using ATPE have also been studied (Sankaran, Show, et al., 2018; Show et al., 2013). The extraction performance may decrease in some studies where contaminants were saturated in the bottom phase (Show et al., 2013).

2.3.3 Aqueous Two-Phase Extraction with Flotation (ATPF)

Aqueous two-phase flotation (ATPF) is the process of extraction when ATPE occurs in the presence of bubbles. Bubbles are created by passing air through porous frits made of glass or stainless steel to minimize corrosion. Figure 2.6 illustrates an experimental set-up of ATPF (Chong et al., 2020b). When a gas stream is introduced at the bottom of a flotation column, biomolecules may adsorb onto the surface of the ascending gas bubbles and will collect in the top phase after some time. Biomolecules that are amphiphilic will aggregate at the interface of the bubble, so that their hydrophilic end will interact with the aqueous salt-rich phase and their hydrophobic end remains inside the bubble, favouring the gas phase (Lee et al., 2016). The factors affecting ATPF are similar to those outlined for ATPE in Section 2.3.2, with the addition of air flow rate and flotation time.

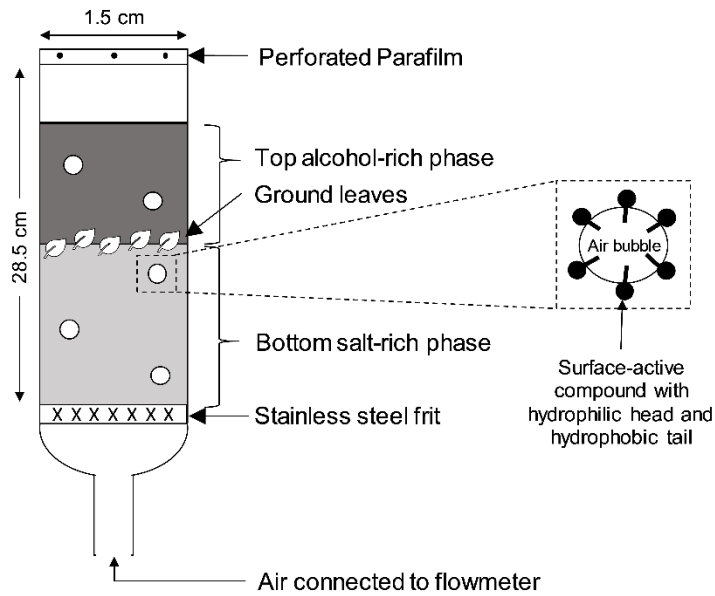


Figure 2.6 Experimental set-up of aqueous two-phase flotation (ATPF) (Chong et al., 2020b)

2.3.3.1 Effect of Air Flow Rate

Since the gas-liquid interfacial area is the site where biomolecules are adsorbed, an increase of air flow rate can improve extraction as the number of bubbles and mass transfer rate of biomolecules will also increase (Lee et al., 2016). For example, when a range of gas or air flow rates were investigated, high recoveries of liquiritin and glycyrrhizic acid were achieved at flow rates of 40 to 60 mL/min (Chang et al., 2014), ovalbumin at 30 mL/min (Jiang et al., 2019), polyphenols at 37.5 mL/min (de Araújo Padilha et al., 2018), bromelain at 80 mL/min (Pakhale et al., 2013), and phenolic compounds at 100 mL/min (Chia et al., 2020). However, further increases in gas or air flow rate decreased the recoveries as there were foam accumulation on the top of the column (Chang et al., 2014) and turbulent mixing that disrupted the interface between the liquid-liquid phases (Chia et al., 2020; Jiang et al., 2019; Pakhale et al., 2013). As flotation columns have different diameters, the superficial gas velocity which is the volumetric flow rate divided by the cross-sectional area, needs to be specified. In ATPF experiments, a homogenous flow regime is desired as there is no coalescence and breakup of bubbles in this regime. This can be achieved at superficial gas velocity of less than 5 cm/second (Prakash et al., 2018). Beyond this flow regime, the gas-

liquid system enters the heterogenous churn-turbulent flow regime which is disordered and causes liquid recirculation or mixing of the two phases (Prakash et al., 2018).

2.3.3.2 Effect of Flotation Time

Extraction efficiency increases with an increase in flotation time due to higher contact duration between the biomolecules and the air bubbles (Xia et al., 2016). For example, for a range of extraction times, protein extraction was maximum at 10 minutes (Sankaran, Manickam, et al., 2018) flotation time, protein at 15 minutes (Koyande et al., 2019), phenolic compounds at 8 minutes (Chia et al., 2020), betacyanins at 15 minutes (Leong, Ooi, Law, Julkifle, Ling, et al., 2018), baicalin at 30 minutes (Bi et al., 2013), ovalbumin at 30 minutes (Jiang et al., 2019), bromelain at 40 minutes (Pakhale et al., 2013), polyphenols at 60 minutes (de Araújo Padilha et al., 2018), puerarin at 100 minutes (Bi, Dong, & Yuan, 2010), and *ortho*-phenylphenol at 120 minutes (Padilha et al., 2017). Prolonged flotation time decreased the efficiency and recovery, and this may be due to the system already achieving equilibrium (Bi, Dong, & Yuan, 2010; Chia et al., 2020; Koyande et al., 2019).

2.4 Bio-Based Films

2.4.1 Introduction

Plastic polymers are widely used as packaging material as they are lightweight, strong, durable, and low cost (Hopewell et al., 2009). Examples of plastic polymers are low density polyethylene (LDPE), high density polyethylene (HDPE), polypropylene (PP), polystyrene (PS), and polyvinyl chloride (PVC) (Halden, 2010). Most plastics are derived from non-renewable fossil resources such as oil, natural gas, and coal (Gironi & Piemonte, 2011). There are concerns about the environmental impact of plastics since littering is rampant and nondegradable plastics accumulate over time (Schwarz et al., 2019). For example it has been reported that 86% of the 34 million tons of plastic disposed in the United States of America were landfilled and only 6% were recycled (North & Halden, 2013). Plastics also have impact on human health due to the release of hazardous chemicals during

manufacturing and use (Hahladakis et al., 2018). For example, bisphenol A and phthalates are common compounds that leach and risk human health due to their endocrine-disrupting properties (Halden, 2010). Therefore, there has been a shift towards bio-based packaging films that are made of renewable plant or animal-based biopolymers such as gelatin (Musso et al., 2019), chitosan (Bonilla & Sobral, 2016), soy protein (Maryam Adilah et al., 2018), whey protein (Ribeiro-Santos et al., 2018), and zein, a protein found in corn (Arcan & Yemenicioğlu, 2011).

Peas (*Pisum sativum* L.) have been commonly grown in the Canadian prairie region almost exclusively for the dry seed market (Chemining'wa & Vessey, 2006). As Canada is the largest producer and leading exporter of dry peas (Roy et al., 2010), there is growing interest in using pea protein as the main component in biobased films. Since peas are grown in large quantities, it is an economical raw material to produce protein concentrates and isolates (Cheng et al., 2019; Sá et al., 2020). Peas are not labelled as allergen, unlike products that contain peanut, milk, shellfish, tree nut, egg, fin fish, strawberry, wheat, and soy (Gupta et al., 2011). There are various studies on pea protein films, nanofibre mats, and bioplastics as shown in Table 2.4. Nanofibre mats are created by an electrospinning method where a biopolymer solution is emitted from a syringe pump and high voltage is used to attract the charged threads, accumulating fibres on the collector's surface (Maftoonazad et al., 2019). Bioplastics are harder and stronger as compared to films as they are produced at higher temperature and pressure (Carvajal-Piñero et al., 2019).

Pea protein consists of 65 to 80% of globulin protein (Sirtori et al., 2012), which can be classified into legumin (11S), vicilin (7S), and convicilin. Pea legumin has a molecular weight of 320 to 380 kDa (Barac et al., 2010), vicilin consists of 150–180 kDa subunits (Lam et al., 2018), and convicilin in its native form has a molecular weight of 290 kDa (Barac et al., 2010). The protein content can range from 24.4 to 26.3% of pea flour (Chung & Liu, 2012), 48.26% of pea protein concentrate (Reinkensmeier et al., 2015), and 91.4% of pea protein isolate (dry basis) (Shevkani & Singh, 2015).

Table 2.4 Films, nanofibre mats, and bioplastics containing pea protein

Main components	Method of formation	Reference
Films		
<ul style="list-style-type: none"> • Pea protein isolate • Plasticizers: Ethylene glycol, diethylene glycol, triethylene glycol, 1,2-propanediol, 1,3-propanediol, glycerol • Monoglycerides of heptanoic, undecanoic, oleic, linoleic, linolenic, and erucic acid 	Bench casting	Viroben et al. (2000)
<ul style="list-style-type: none"> • Pea protein isolate • Glycerol 	Bench casting	Shevkani & Singh (2015)
<ul style="list-style-type: none"> • Pea protein concentrate • Glycerol 	Bench casting	Choi & Han (2001)
<ul style="list-style-type: none"> • Pea protein isolate • Glycerol 	Bench casting	Choi & Han (2002)
<ul style="list-style-type: none"> • Pea protein concentrate or pea protein isolate 	Bench casting	Acquah et al. (2020)
<ul style="list-style-type: none"> • Pea protein isolate • Plasticizers: Glycerol or sorbitol 	Bench casting	Kowalczyk & Baraniak (2011)
<ul style="list-style-type: none"> • Pea protein isolate • Glycerol • Lysozyme 	Bench casting	Fabra et al. (2014)
<ul style="list-style-type: none"> • Pea protein isolate • Sorbitol • Lipids: anhydrous milk fat, candelilla wax, lecithin, oleic acid 	Bench casting	Kowalczyk et al. (2016)
<ul style="list-style-type: none"> • Pea protein isolate • Glycerol • Lactic acid bacteria 	Bench casting	Sánchez-González et al. (2013)
<ul style="list-style-type: none"> • Blend of acetylated cassava starch and pea protein isolate • Glycerol 	Blown film extrusion	Huntrakul et al. (2020)
Nanofibre mats		
<ul style="list-style-type: none"> • Polyvinyl alcohol • Pea protein isolate • Cinnamaldehyde 	Electrospinning	Maftoonazad et al. (2019)
<ul style="list-style-type: none"> • Pullulan • Pea protein isolate 	Electrospinning	Jia et al. (2020)
<ul style="list-style-type: none"> • Pullulan • Pea protein isolate • Tween 80 	Electrospinning	Aguilar-Vázquez et al. (2018)
Bioplastics		
<ul style="list-style-type: none"> • Pea protein isolate • Glycerol 	Injection moulding	Perez et al. (2016)
<ul style="list-style-type: none"> • Pea protein isolate • Glycerol 	Injection moulding	Carvajal-Piñero et al. (2019)

2.4.2 Formulating Biobased Films

Biobased films consist of several components such as binding agents, plasticizers, cross-linkers, fillers, and other additives (Otoni et al., 2017). Binding agents or biopolymers such as starch (Jiménez et al., 2012) and protein (Shi & Dumont, 2014a) form the core of the biobased films. Plasticizers are added to improve the flexibility of the films (Kowalczyk & Baraniak, 2011) while the addition of cross-linkers results in stronger and less permeable films by linking the biopolymer chains (Otoni et al., 2017; Sharma et al., 2018).

2.4.2.1 Binding Agents

Hydrocolloids are hydrophilic polymers which function as important binding agents to improve the physical properties of the films such as increasing film cohesiveness, mechanical strength, and barrier properties. Hydrocolloids such as polysaccharides (Cerqueira et al., 2012), proteins (Shevkani & Singh, 2015), and lipids (Morillon et al., 2002) are used in forming bio-based films. Protein and polysaccharide films are good gas barriers but poor moisture barriers. In contrast, pure lipids films are poor gas barriers but good moisture barriers (Sason & Nussinovitch, 2021). Plant-derived hydrocolloids include starch (Nouri & Mohammadi Nafchi, 2014), alginate (Benavides et al., 2012), pectin (Jo et al., 2005), carrageenan (Briones et al., 2004), and proteins such as zein (Arcan & Yemenicioğlu, 2011), soy (Mir et al., 2018), pea (Choi & Han, 2001), and gluten (Roy et al., 2000). Table 2.5 shows the gross chemical composition of pea flour, pea protein concentrate (PPC), and pea protein isolate (PPI). Pea protein is highly soluble at alkaline pH and moderately soluble in acidic media (Tömösközi et al., 2001). PPI had minimal solubility of 210 mg bovine serum albumin equivalents/g protein at the isoelectric point of pH 4.5 (Ladjal-Ettoumi et al., 2016).

Table 2.5 Chemical composition of pea products (Tömösközi et al., 2001)

	Pea flour	Pea protein concentrate	Pea protein isolate
Protein (%)	26.0	48.5	89.6
Lipid (%)	1.4	0.9	1.6
Ash (%)	3.0	3.0	2.6
Moisture (%)	13.0	8.6	5.3

2.4.2.2 Plasticizers

Plasticizers are added to reduce brittleness and stiffness of films by increasing flexibility, elongation, and ductility (Díaz et al., 2019). Most films are too brittle due to extensive intermolecular forces that hold polymer chains together (Wang et al., 2011). Plasticizers occupy intermolecular spaces between polymer chains, thus reducing secondary forces among them and separate adjacent polymer chains apart (Vieira et al., 2011). Plasticizers also reduce the energy required for molecular motion and formation of hydrogen bonds between the chains, resulting in increased molecular mobility (Vieira et al., 2011). However, the addition of plasticizer increases free volume and molecular mobility and this leads to more water diffusion through the film (Cuq et al., 1997). A concentration of plasticizers that is too high will weaken the cohesion of the polymer chain and the number of plasticizer-plasticizer bonds will increase. This in turn causes phase separation between plasticizer-enriched zones and polymer-plasticizer zones (Jiménez et al., 2012).

Some common plasticizers are glycerol (Medina Jaramillo et al., 2016), sorbitol (Kowalczyk & Baraniak, 2011), sugar (Ghanbarzadeh et al., 2007), propylene glycol (Jagadeesh et al., 2013), oil (Ghanbarzadeh & Oromiehi, 2009), and wax (Talens & Krochta, 2005). Water as a universal solvent also functions as a plasticizer to a certain extent where the elasticity of films improves during initial hydration. When more water is used, film elasticity and cohesiveness decreases due to more water-polymer interactions as compared to polymer-polymer interactions (Cheng et al., 2006). The type of plasticizer was reported to affect water vapor permeability (WVP) of the film. WVP of PPI films increased when glycerol concentration was increased, however WVP was not affected by changes in sorbitol concentration (Kowalczyk & Baraniak, 2011). The authors attributed this to glycerol demonstrating higher hydrophilicity and having lower molecular weight as compared to sorbitol, resulting in the attraction of more water and easier penetration into the protein chains. As shown in Table 2.4, glycerol and sorbitol are the common plasticizers used in pea protein films.

2.4.2.3 Cross-linkers

Modification of the polymer network through cross-linking improves the film functionality. Cross-linkers join adjacent chains together by covalent bonds (Hosseini & Nabid, 2020), resulting in stronger and less permeable films. Physical crosslinking methods such as using gamma irradiation (Lacroix et al., 2002) and ultraviolet (UV) irradiation (Fathi et al., 2018) induce the formation of a tridimensional network. When double bonds and aromatic rings absorb UV radiation, free radicals are formed in amino acids and this leads to the formation of intermolecular covalent bonds (Wihodo & Moraru, 2013). Thermal cross-linking happens when proteins are exposed to high temperatures. The heat disrupts hydrogen bonds and non-polar hydrophobic groups in proteins and this leads to exposure of the amino acid groups to the surrounding solvent and produces a more open structure (Wihodo & Moraru, 2013). The degree of protein cross-linking is consequently affected by the degree of protein unfolding (Perez-gago & Krochta, 2001). Chemical crosslinking occurs with the addition of crosslinking agents such as carboxylic acid (Sharma et al., 2018), glutaraldehyde (Marquié, 2001), and enzymes (Jiang et al., 2007). Past studies have investigated natural crosslinkers particularly phenolic compounds such as tannic acid, caffeic acid, and ferulic acid (Araghi et al., 2015; Picchio et al., 2018). Several cross-linking mechanisms between proteins and carboxylic acids have been proposed (Reddy et al., 2009; Xu et al., 2015) and the degree of cross-linking can be verified with an increase in molecular weight (Xu et al., 2015). Cross-linked protein films are less flexible due to the reduced mobility of protein molecules (Sharma et al., 2018).

The properties of the film also depend on various interactions with other components in the film-forming solution. As an example, citric acid demonstrated dual functionality in corn starch films (Ghanbarzadeh et al., 2011), where citric acid up to 10 weight% increased the strength and reduced the elongation of films, demonstrating a cross-linking effect; at higher concentrations of citric acid, it reduced the strength of the film and increased its elongation, demonstrating a plasticizing effect. Some drawbacks of using carboxylic acid are its poor stability in water and some concentrations may cause irritation (Sato et al., 1996). Enzymatic cross-linking, in most cases using food-grade transglutaminase (Benbettaïeb et al., 2016) are bio-based environmentally-friendly crosslinkers, however

they are specific and sensitive to heat (Garavand et al., 2017). These aspects should be considered when selecting cross-linkers. There are limited studies on the effects of cross-linking in pea protein films. One study used lysozyme with pea protein isolate films, however the focus was on the antimicrobial properties of the enzyme rather than the cross-linking effects (Fabra et al., 2014).

2.4.3 Functional Biobased Films

Functional films are produced when additional components are intentionally included into film formulations to improve the performance of the packaged product while maintaining the sensory, safety, and quality aspects (Day, 2008; Robertson, 2016). Food processing wastes or residues have been used as sources of bioactive compounds as these wastes are underutilized and they have low market value. For example, whole fruit and vegetable residues sourced from isotonic drink processing were used to develop edible films (Andrade et al., 2016). Byproducts from the mango processing industry such as mango peel which is rich in polysaccharides (Torres-León et al., 2018) and mango seed kernel which has antioxidants (Maryam Adilah et al., 2018) have been used in film formulations. Studies have also used extracts from leaves such as green tea extract (Siripatrawan & Harte, 2010) and olive leaf extract (Marcos et al., 2014). Other additives such as essential oils (do Evangelho et al., 2019) can also be added to improve the sensory, nutritional, and microbiological characteristics of the film. However, these functional additives may emit strong and distinct flavor or aroma especially in films containing cinnamon and oregano oils. Film manufacturers would need to consider possible allergic reactions as some consumers are allergic to cinnamon (Calapai et al., 2014). An interesting approach would be to use the films containing the functional additive to pack the same product (McHugh & Senesi, 2000; Otoni et al., 2017).

Studies investigating functional protein films typically use natural extracts that are diluted with either water, aqueous alcohol, or alcohol. Table 2.6 shows some extracts used for biobased films, where films involving the use of lipids and waxes as plasticizers have been excluded from the table. As shown in Table 2.6, the extracts were in the form of a paste, or dissolved in water or aqueous ethanolic solutions. A few studies intentionally introduced

salt as an additive to biopolymer films to improve their functional properties. For example, potassium nitrate crystals were added to sodium caseinate films as the salt provides a fertilizing effect for agricultural purposes (Frohberg et al., 2010; Stolte et al., 2012). Sangerlaub et al. (2013) also incorporated sodium chloride particles into polypropylene films as a potential humidity-regulating filler.

Table 2.6 Extracts incorporated into protein films

Type of protein film	Extract	Final solvent composition of extract	Reference
Gelatin	Red cabbage extract	Water or ethanol	Musso et al. (2019)
Gelatin	Murta leaf extract	Water	G3mez-Guill3n et al. (2007)
Gelatin	Cinnamon, clove, star anise extract	25% ethanol in concentration of 0.5% (w/v)	Hoque et al. (2011)
Soy protein isolate	Red raspberry extract	Powder dissolved in solution of ethanol/water/85% lactic acid in a volumetric ratio of 80:19:1, 85% lactic acid/water in ratio of 1:99, and ethanol/water in ratio of 80:20	Wang et al. (2012)
Soy protein isolate	Grape seed extract	Powder with water extraction solvent. Ratio was not specified	Sivarooban et al. (2008)
Soy protein isolate	Licorice residue extract	Paste dissolved in ethanol at concentration of 43.6 g/L	Han et al. (2018)
Soy protein isolate	Mango kernel extract	Paste, as supernatant was evaporated	Maryam Adilah et al. (2018)
Whey protein concentrate	Cinnamon and rosemary extract	Essential oils obtained by distillation method	Ribeiro-Santos et al. (2018)
Whey protein concentrate	Green tea and rosemary extract	Paste, as supernatant was evaporated	Castro et al. (2019)
Whey protein isolate	Rambutan peel and cinnamon extract	Rambutan peel extract paste as supernatant was evaporated, cinnamon oil	Chollakup et al. (2020)
Zein	Pomegranate peel extract	Water	Mushtaq et al. (2018)
Zein	Paran pine seed coat extract	Ethanol and 80% (v/v) aqueous ethanol	De Freitas et al. (2018)

2.4.4.1 Degassing

Prior to film formation, degassing of the film-forming solution is needed to remove air microbubbles. If the bubbles are left suspended, they tend to remain entrapped in the dried film, causing structural defects and mechanical failure (Otoni et al., 2017). Some methods of degassing are vacuum degassing (Kowalczyk & Baraniak, 2011), ultrasonic degassing (Tonyali et al., 2018), centrifugation (Viroben et al., 2000), or resting the solution for a few hours (Lorevice et al., 2012)

2.4.4.2 Casting

Casting is the most common method to produce films at laboratory and pilot scales where the two types of casting are bench casting and continuous casting (Siemann, 2005). Bench casting is performed by pouring a film-forming solution into a predefined mold, plates, or petri dishes. Film thickness can be controlled by the amount of suspension poured. The solvent will then evaporate, leaving the macromolecules to assemble into a cohesive layer. Drying can be performed at room temperature or mild temperatures such as 30 to 40 °C for 12 to 48 hours. The effect of different drying conditions on the properties of films has been studied by many researchers (Fernández-Pan et al., 2010; Tapia-Blácido et al., 2013). The drying time can be shortened when the temperature is increased (Sothornvit & Pitak, 2007), however high temperatures may cause degradation of the functional additives. Bench casting is a simple method as it does not require specialized equipment. Casting also leads to a better particle-particle interaction resulting in a more homogenous packaging with less defects (Yang et al., 2011). A drawback of this technique is the long drying time which makes it impractical for commercial production. Furthermore, the bench casting technique itself is difficult to scale-up (de Moraes et al., 2013). The films are restricted to simple sheets and there is a potential of toxic solvent being trapped in the films (Suhag et al., 2020). As shown in Table 2.4, pea protein films are mainly produced by bench casting.

Continuous casting utilizes belt conveyors. Using a tape casting machine, a suspension is placed in a reservoir with a blade, whose height can be varied with micrometric screws. A thin layer of suspension is cast on a support which is the moving tape. The formed film is dried by heat conduction, circulation of hot air, and infrared (de Moraes et al., 2013). The

thickness of the films can also be regulated by a coating knife which disperses the film-forming solution at a set rate (Mendes et al., 2019). Continuous casting uses less space and labor, hence making it more suitable for scaling-up. Nevertheless, the high temperatures used for film drying may reduce the retention of functional additives (Du et al., 2008).

2.4.4.3 Dipping

A thin layer of film can be applied to products as a barrier by dipping them in coating solutions. The excess coating can be drained as it dries and solidifies. Dipping is commonly used for fruits, vegetables, and meat products to completely coat surfaces. It ensures uniformity even with rough and irregular products. Banana slices (Bico et al., 2009), pineapple cubes (Yousuf & Srivastava, 2019), and cut apples (Alves et al., 2017) were coated using the dipping technique. With the coating layer, the produce in the studies mentioned above showed reduced weight loss and retention of phenolic compounds. The coating thickness is mainly influenced by the viscosity, concentration, density, and draining time of the coating solution (Cisneros-Zevallos & Krochta, 2003) and surface tension of coated products (Andrade et al., 2012). During the dipping process, products must be completely dry to prevent dilution of the coating solution.

2.4.4.4 Spraying

The spraying technique is suitable when a specific side needs to be coated. It is also useful when two applications are required for cross-linking (Catanzano et al., 2015). After spraying, heated air can be applied to speed up drying and improve uniform distribution on the surfaces. In this technique, the main component is the spray nozzle as the nozzle shape can influence spraying efficiency. Additionally, pressure, fluid viscosity, temperature, and surface tension of the coating liquid are variables which affect the efficiency (Werner et al., 2007). For example, studies were conducted where chitosan was sprayed onto strawberries (Jiang et al., 2020) and xanthan gum-based coatings were sprayed on lotus roots slices (Lara et al., 2020).

2.4.4.5 Extrusion

Extrusion is a common plastic processing method. From the chemical reactor to the finished product, most plastic materials pass through two or more extruders (Robertson, 2016). An extruder barrel can be subdivided into 3 processing zones namely (1) the feeding zone, where the raw material is introduced into the barrel and undergoes slight compression by expelling air, (2) the kneading zone with more compression, a higher degree of fill, increasing pressure, temperature, and material density, and lastly (3) the heating zone where the highest shear rates, temperature, and pressure are achieved along with the final product texture, colour, density, and functional properties (Hernandez-Izquierdo & Krochta, 2008). Bioplastics from wheat gluten (Jiménez-Rosado et al., 2019) and casein/wax edible films (Chevalier et al., 2018) have been developed using extrusion. This technique is flexible at large scale due to the broad range of processing conditions, such as pressure range from 0 to 500 atm, temperature range from 70 to 500 °C, and the ability to regulate residence time and degree of mixing (Liu et al., 2009).

2.4.5 Assessment of Biobased Film Properties

Biobased films can be assessed for their physical, optical, mechanical, barrier, thermal, and antioxidant properties. Physical properties include thickness, moisture content, and microstructure while optical properties are evaluated by light transmission, film transparency, and colour. As barrier properties such as oxygen permeability and water permeability are essential in preserving fresh products (Nouri & Mohammadi Nafchi, 2014), they are commonly evaluated. Additionally, thermal properties such as glass transition temperature and denaturation temperature indicate the stability of the films towards varying temperatures (Ghanbarzadeh & Oromiehi, 2009) while films having antioxidant properties may reduce oxidation, improve nutritional quality, and prolong the shelf life of the packaged product (López-de-Dicastillo et al., 2012).

2.4.5.1 Film Thickness

Film thickness affects permeability as a thicker film increases the resistance to mass transfer across it (McHugh et al., 1993). The thickness of films can be measured with a micrometer at random points of the film (Viroben et al., 2000). Various studies on plant-

based films report film thicknesses ranging from 22.00 to 49.12 μm (Phan et al., 2005), 33.02 to 77.89 μm (Sivaroban et al., 2008), and 56 to 66 μm (Maryam Adilah et al., 2018). According to Maryam Adilah et al. (2018), thickness was affected by the type of proteins used. The authors observed that incorporation of mango kernel extracts into soy protein isolate films had minimal increase in thickness due to soy protein having globular and disordered protein that allowed the extracts to fill the gaps. In the same work, fish gelatin films with extracts were 39% thicker compared to control films without extract. This was attributed to the linear and more ordered structure of fish gelatin, thus expanding the volume and thickness of the fish gelatin film. Addition of internal cross-linkers also increased the film thickness significantly and it was found to be concentration-dependent (Benavides et al., 2012). Thickness was likewise reduced by using lower protein concentrations in whey protein isolate films (Gounga et al., 2007; Longares et al., 2004). Since the degree of protein cross-linking is affected by the degree of protein unfolding (Perez-gago & Krochta, 2001), the films may have been thinner due to fewer amino acid groups being available for cross-linking.

2.4.5.2 Moisture Content

The moisture content of films can affect film properties such as water vapour permeability. High moisture content increases the permeability in hydrophilic films due to swelling and plasticization of the polymer network (Morillon et al., 2002). To measure moisture content, films are first conditioned at a specific relative humidity and temperature. The films are then oven-dried at 105°C for 24 hours and the moisture content is defined as percentage of initial film weight lost during drying (Kowalczyk & Baraniak, 2011).

The moisture content of films with extracts was reported between 10.1 to 12.5% for starch films containing 4% (w/w) sago starch, 40% (w/w) plasticizer with sorbitol:glycerol at 3:1 ratio, and 0 to 30% (w/w) betel leave extract (Nouri & Mohammadi Nafchi, 2014). Kowalczyk and Baraniak (2011) reported moisture content of 17 to 37% with 10% (w/w) aqueous pea protein isolate, 3 to 7% (w/w) glycerol or 4 to 8% (w/w) sorbitol. Protein films containing 10% soy protein isolate, 0.5% glycerol, and 0.5% of either water, raspberry ethanolic extract, or lactic acid solution had moisture content between 16.19 to 17.21%

(Wang et al., 2012). The presence of more hydroxyl groups in the film, whether from the extracts or from other film components, were shown to increase the moisture content of the films as these groups attract more water molecules (Nouri & Mohammadi Nafchi, 2014). Hydrophobic extracts such as essential oils up to a concentration of 2% (w/w) reduced the moisture content of whey protein films (Ribeiro-Santos et al., 2018). Moisture content then increased with higher essential oil concentration and this was attributed to the film network breaking up which caused more water molecules to fit between the protein chains.

2.4.5.3 Light Transmission and Film Transparency

Film transparency allows consumers to view the product before purchasing (Simmonds & Spence, 2017) while protecting the product from light effects, especially ultraviolet (UV) radiation (Ahmed & Ikram, 2016). UV and visible light barrier properties are determined by measuring the light transmission at selected wavelengths from 200 to 800 nm using a UV spectrophotometer (Ramos et al., 2013). The UV region spans along the wavelength of 100 to 400 nm (Calvo et al., 2012) while the rest represents visible light. Opacity is calculated by Equation 2.2 (Shevkani & Singh, 2015):

$$\text{Opacity value} = \frac{A_{600}}{x} \quad (2.2)$$

where A_{600} is the absorbance at 600 nm and x is the film thickness (mm). A higher opacity value indicates lower transparency. Some opacity values for films made of plant-based protein isolates are from 7.1 to 11.3 A_{600}/mm (Shevkani & Singh, 2015) and 0.86 to 1.52 A_{600}/mm (Kowalczyk & Baraniak, 2011). Pea protein films have shown high absorbance at ultraviolet wavelengths and this property is linked to the presence of UV-absorbing chromophore in proteins, particularly aromatic amino acids, namely tyrosine and tryptophan (Kowalczyk & Baraniak, 2011). Potato starch films have also shown UV-protective ability as coffee silverskin concentrations were increased due to the presence of caffeine, chlorogenic acid, and lignin in the silverskin (Oliveira et al., 2020). Similarly, it was suggested that films containing higher concentration of phenolic compounds have the tendency to form protein aggregates which could lead to more opaque films (Salgado et al., 2010).

2.4.5.4 Film Colour

Colour is an important aspect of consumer acceptance. Researchers mostly compare color changes with the original formulation when incorporating an additive or designing a new formulation for films (Ribeiro-Santos et al., 2018). A colorimeter is used to assess film color and the measurements are expressed in CIELAB color system where L^* values are from 0 to 100 (black to white), a^* is from positive to negative (red to green), and b^* is from positive to negative (yellow to blue). Color values from some films have L^* values ranging from 77.47 to 95.37 (Sivarooban et al., 2008), 76.74 (Wang et al., 2012a), and 87.08 to 99.55 (Nouri & Mohammadi Nafchi, 2014), a^* values ranging from -0.40 to 10 (Sivarooban et al., 2008), -1.93 to 2.98 (Wang et al., 2012), and -5.65 to 0.11 (Nouri & Mohammadi Nafchi, 2014), and b^* values ranging from 4.68 to 29.06 (Sivarooban et al., 2008), 22.65 to 39.96 (Wang et al., 2012), and -0.40 to 47.32 (Nouri & Mohammadi Nafchi, 2014).

The colour variations in films may be due to the different types and concentrations of pigments in the raw material (Shevkani & Singh, 2015). Additionally, protein-polyphenol interaction may affect the film colour where it was observed that sunflower proteins produced green pigmentation upon reacting with oxidized chlorogenic acid (Wildermuth et al., 2016). The type and concentration of individual components in the films has been shown to influence film color, as evidenced by positive a^* values indicating redness in soy protein isolate films incorporated with raspberry extract (Wang et al., 2012). Similarly, films with mango kernel extracts had yellowish-orange colour (Maryam Adilah et al., 2018) and films made from pea protein were reported to be slightly yellowish (Choi & Han, 2001). When pea protein isolate concentration was increased, more yellowish films were produced due to protein browning caused by increased Maillard reaction rates at high temperature (Huntrakul et al., 2020).

2.4.5.5 Morphology

Films can be evaluated by observing surface evenness, cracks, and porosity from micrographs (Fang et al., 2002). A scanning electron microscope can be used to examine

the morphology of the film, indicating the porosity and integrity of the film. For instance, films from pea protein isolate have rough and uneven surfaces, covered by round granules with characteristic depressions (Kowalczyk & Baraniak, 2011). Chitosan film was described as smooth, while gelatin film had a fibrous structure which is a feature of the collagen fibrils (BenBettaïeb et al., 2015). Similar observations also showed that soy protein isolate film had a rough surface and cross section due to the unorganized structure of globular protein while fish gelatin film had a smooth surface and cross-section as the structure was more linear and organized (Maryam Adilah et al., 2018). The microstructural properties also provide more insight for films containing lipid mixtures where structural discontinuities can result from the lack of miscibility of the components (Fabra et al., 2009). Surface topography can also be analyzed by atomic force microscopy (Villalobos et al., 2005).

The incorporation of extracts also influenced the film morphology. As an example, the cross-section of soy protein isolate films with raspberry extract were found to be more compact and more ductile compared to the control film without extracts (Wang et al., 2012). This may have been due to the entanglement and intermolecular interactions between the extracts and proteins. In another study, the incorporation of potassium nitrate in sodium caseinate films produced brittle columnar sprawling crystals, and crystalline agglomerates were observed to coexist with adjacent areas of the salt (Frohberg et al., 2010). Increasing the salt concentration was found to result in macroscopic acicular crystalline network after the solvent was evaporated.

2.4.5.6 Tensile Strength and Elongation at Break

Mechanical integrity functions to protect the films against resistance (Briassoulis & Giannoulis, 2018) where flexible and strong films are desirable as poor flexibility and strength may lead to film failure or cracking during handling and storage (Mangaraj et al., 2009). Depending on the film application, films can be strong and yet flexible (Arcan & Yemenicioğlu, 2011). Alternatively, films can be designed to dissolve quickly for drug delivery applications (Cilurzo et al., 2008) and for food pouches containing premeasured ingredients (Janjarasskul et al., 2020). Films can be tested for tensile strength, elastic

modulus, elongation at break, puncture resistance, and tear resistance with texture analyzers or Instron Universal Testing Machines.

Tensile strength is used to gauge resistance of the film against tension. The maximum tensile strength is the ratio between the maximum load and the smallest cross-sectional area of the film prior to testing (Anderson & Simsek, 2019; ASTM International, 2018b). Elongation at break (EAB) is a measure of the stretching capacity or flexibility of the film before breaking (Mir et al., 2018). Puncture resistance is used to evaluate the film's resistance to perforations as films must withstand large forces over small areas (ASTM International, 2018a). Tear resistance is used to assess tear initiation and resistance against tear propagation (ASTM International, 2013).

From studies in the literature, films made of soy protein isolate and mango kernel extract had tensile strength from 1.82 to 3.06 MPa and elongation at break from 49.92 to 148.92 % (Maryam Adilah et al., 2018). Starch films with betel leaf extract had tensile strength of 3 to 7 MPa and EAB from 1.8 to 7.0% (Nouri & Mohammadi Nafchi, 2014) while agar and starch films had tensile strength of 8.51 to 42.11 MPa and EAB from 0.72 to 6.51% (Phan et al., 2005). With regards to protein content, pea protein isolate which has higher protein content yielded films with higher tensile strength and lower EAB as compared to pea protein concentrate films (Choi & Han, 2002).

The addition of extracts which are rich in phenolic compounds generally results in stronger and stiffer films due to the cross-linking of the hydroxyl group from the polyphenol to the hydrogen acceptor of protein molecules via hydrogen bonding (Prodpran et al., 2012). However, it was reported that the globular nature of soy protein isolate could have been a barrier for these cross-linking interactions and resulted in a lower tensile strength compared to the fish gelatin films with more linear structure (Maryam Adilah et al., 2018). Additionally, the addition of potassium nitrate into sodium caseinate films decreased the tensile strength and increased the EAB (Frohberg et al., 2010). These findings were attributed to the formation of very large crystalline structure which damaged the

macromolecular texture, causing weak spots along the film leading to lower tensile strength and weak intermolecular bonds leading to increasing elongation.

2.4.5.7 Water Vapor Permeability

Some products require protection from extreme humidity differences during transportation and storage to prevent spoilage. For instance, fresh fruits and vegetables are perishable as they produce water vapour through transpiration (Salas-Méndez et al., 2019). Films can regulate humidity so that they do not lose water too quickly to prevent shriveled produce, and can simultaneously remove excess condensation to prevent microbial spoilage (Mahajan et al., 2008). In contrast, bakery products require packaging with low water vapor permeability to maintain their textural properties (Melini & Melini, 2018).

Modified ASTM96-92 (ASTM International, 2016) is a gravimetric method where a test film is used to seal a cup partially filled with water, saturated salt solution, or desiccant. The test cup is then placed in a desiccator with controlled temperature and relative humidity. The cup is weighed periodically after steady-state is achieved to determine water vapor flux through the film (McHugh et al., 1993). Alternatively, anhydrous silica can be placed in the cup to maintain 0% relative humidity and a salt solution in the desiccator at a desired humidity (Musso et al., 2019).

Studies have shown that in general, the addition of extracts can alter the WVP of biobased films. For example, raspberry extract decreased the WVP of soy protein isolate films (Wang et al., 2012) and this was associated with the increased intermolecular attractions between the extract and the proteins leading to reduced interchain spaces, and subsequently lowering the mobility of water molecules. The decrease in WVP could be also caused the increased hydrophilicity and attraction of more water molecules in the matrix, leading to limited permeation of water through the water-saturated films (Wang et al., 2012). Similarly, Han et al. (2018) observed a decrease in WVP in soy protein isolate films when hydrophobic licorice residue extract was incorporated. In contrast, red cabbage extracts did not cause significant WVP difference in gelatin films as compared to films without extracts

(Musso et al., 2019). The authors also found that WVP increased with thicker films, indicating the nature of hydrophilic films (McHugh et al., 1993).

2.4.5.8 Thermal Properties

The glass transition temperature, T_g , is the temperature at which the sample undergoes a structural transition from brittle glassy state to rubbery or highly viscous state (Ghanbarzadeh & Oromiehi, 2009). Above T_g , the films exist in a soft, rubbery state which increases gas and water vapor permeability. Below T_g , the films are glassy with low permeability. The addition of plasticizer lowers the T_g of the film (Medina Jaramillo et al., 2015; Perez et al., 2016), thus films will be more flexible. T_g is determined by using a differential scanning calorimeter and the change in the heat capacity of the sample is observed with varying temperature. The film is first ground into powder under liquid nitrogen and conditioned for a period in a desiccator to remove moisture thoroughly. The film powders are then weighed in aluminium pans and sealed. Cooling and heating scans are performed at controlled rates and T_g is obtained from the inflexion point of the thermograms in the second scan (Tulamandi et al., 2016). Thermograms also indicate if the plasticizers and polymers remain homogenous throughout the cooling and heating cycles; for example, phase separation is evident in the film when there are separate glass transition temperatures corresponding to the two pure phases (Ghanbarzadeh & Oromiehi, 2009).

In the literature, pea proteins films that had a singular T_g value indicated that the protein solutions had reacted with the plasticizer to form a co-polymer (Acquah et al., 2020). Whey protein isolate films which had significantly higher melting enthalpy (ΔH_m) than pea protein films also showed that the former films were more resilient to heating (Acquah et al., 2020). In starch films, addition of yerba mate extract decreased the melting temperature, T_m , due to the antioxidants in the extract decreasing intermolecular bonding in the polymer chain (Medina Jaramillo et al., 2016). The same study also observed a decrease in ΔH_m when extracts were included, and this indicates a less stable crystalline structure which required less energy to melt the films. Sharma et al. (2018) found that cross-linking sesame protein films with carboxylic acids increased T_m ; this was associated with the cross-linking effect which stabilized the proteins. However, ΔH_m decreased with an increase in cross-

linker concentration, where this decrease may be due to the formation of more rigid protein chains with more cross-links as the plasticizer concentration was kept constant. According to a study on glucomannan films, an increase in ΔH_m was observed due to the plasticizing effect of water molecules (Cheng et al., 2006).

2.4.5.9 Antioxidant Properties

As plant extracts can be potent antioxidant sources, packaging films incorporating those extracts could be used to inhibit or reduce oxidative degradation of packaged products (Mir et al., 2018). As examples, gelatin films with red cabbage extracts (Musso et al., 2019) and mango peel films with mango seed extracts (Torres-León et al., 2018) have shown higher antioxidant activity than films without extract. Migration or transfer of the bioactive compounds, such as compounds contributing to the total phenolic content (Han et al., 2018; López-de-Dicastillo et al., 2012; Souza et al., 2018) to the packaged product, can be assessed by their release speed. Food simulants are used as substitutes for food to simplify chemical analysis. For instance, 10% ethanol represents alcoholic food, while 95% ethanol is an alternative for fatty food simulants (Rodríguez-Martínez et al., 2016). A piece of film with known weight is immersed completely in each simulant for a specified time and the simulant will then be analyzed for the desired compounds.

An assay that is commonly used to assess the antioxidant properties of a film is the radical scavenging activity (RSA) which is determined by using 1,1-diphenyl-2-picrylhydrazyl (DPPH) as a free radical (Brand-Williams et al., 1995; Medina Jaramillo et al., 2015). Film samples are reacted with alcoholic DPPH solution and incubated for 30-45 minutes and the absorbance is measured at 517 nm using a spectrophotometer. The diffusion of bioactive compounds into the packaged products can be viewed as a gradual preservation technique. From another perspective, if polyphenols are retained in the films, the compounds may improve barrier properties of the films (Souza et al., 2018). The final purpose of the films can be intentionally designed with results from these tests.

2.5 Summary

Research has shown that haskap berry leaves have various bioactive compounds in them, thus there is potential in valorizing this underutilized resource. It could also diversify the source of income for haskap growers if the leaves have a wider range of applications. Extraction methods such as conventional extraction and assisted extraction technologies for plant materials have achieved high yields of bioactive compounds. However, some challenges prevail with the use of highly toxic solvents which may cause health concerns, high temperatures which may degrade the thermolabile bioactive compounds, and lengthy extraction times. ATPS-based extraction has potential as an environmentally friendly technique to recover biomolecules. While there are many ATPS studies on protein extraction, literature has shown an increasing interest in ATPE as an extraction method to recover biomolecules. The ATPS phase-forming components can be selected to be GRAS to ensure that the end applications of the extracts pose minimal health risks. Additionally, recycling strategies may be applied to the phase-forming components to improve the sustainability and economics of the process. The bubble-assisted ATPF process may further improve extraction performance when biomolecules adsorb onto the surface of rising gas bubbles. ATPS-based haskap extracts could potentially be incorporated into functional films for packaging purposes. In the process of developing functional films from ATPS extracts, it is important to consider the presence of ATPS components such as salt in these extracts as there will be interactions with other film components such as the binding agents and plasticizers. Various means of evaluating the functional films will provide an insight on how these components react and whether it is beneficial to include haskap leaf extracts from ATPS-based extraction into the formulation.

Connecting Statement 1

As described in Chapter 2, ATPS-based extraction methods have been used to extract biomolecules from biological samples and that these are a more sustainable option than conventional extraction methods. There are many factors which influence the partitioning behaviour of target molecules in different ATPS. As such, it is important to study how those factors affect the recovery of bioactive compounds from haskap leaves.

Chapter 3 presents the investigation of ATPE using salt/ethanol and sugar/propanol systems to recover bioactive compounds from haskap leaves. In view of potentially using the extracts in food packaging, phase-forming components that are generally recognized as safe (GRAS) were selected. Two types of ATPS were compared: salt/ethanol and sugar/propanol systems. In the study, the effects of extraction time, sample loading, and tie line length on extraction efficiency and partitioning were evaluated. The chapter also compared ATPE with conventional Soxhlet extraction in terms of bioactive yields.

Chapter 3 is based on an article reproduced from *Separation and Purification Technology* with permission from Elsevier. The details of the article are as follows:

Chong, K. Y., Stefanova, R., Zhang, J., & Brooks, M. S.-L. (2020). Aqueous two-phase extraction of bioactive compounds from haskap leaves (*Lonicera caerulea*): Comparison of salt/ethanol and sugar/propanol systems. *Separation and Purification Technology*, 252, 117399.

Chapter 3 : Aqueous Two-Phase Extraction of Bioactive Compounds from Haskap Leaves (*Lonicera caerulea*): Comparison of Salt/Ethanol and Sugar/Propanol Systems

3.1 Abstract

Aqueous two-phase extraction (ATPE) was used to extract bioactive compounds from haskap leaves (*Lonicera caerulea*) using salt/ethanol and sugar/propanol-based systems. The systems consisted of components that are generally recognized as safe (GRAS): ammonium sulphate/ethanol, sodium dihydrogen phosphate/ethanol, glucose/1-propanol, and maltose/1-propanol. The factors investigated were extraction time (5, 62.5, 120 minutes), sample loading (0.1, 0.55, 1 wt.%), and tie line length (TLL) (low, medium, high) to represent different aqueous two-phase system (ATPS) compositions of salt or sugar and alcohol. Multi-response optimization was conducted to maximize the yield of chlorogenic acid, flavonoids, and total phenolic content. The results show that salt/ethanol ATPE systems had higher extraction efficiency than sugar/propanol ATPE. Among these four systems, sodium dihydrogen phosphate (NaH_2PO_4)/ethanol ATPE had the maximum extraction efficiency of 93.9% for chlorogenic acid, 96.8% for flavonoids, and 97.8% for total phenolic content. The corresponding partition coefficients were 1.73 for chlorogenic acid, 3.50 for flavonoids, and 6.59 for total phenolic content. Further analysis using high-performance liquid chromatography (HPLC) revealed that the extracts from ATPE were more refined in comparison to conventional solvent extracts. Additionally, nuclear magnetic resonance (NMR) spectra showed preliminary qualitative profiling of the extracts. This work demonstrates that ATPE using GRAS components is a green alternative to conventional extraction with organic solvents for the recovery of high-value bioactive compounds from haskap leaves.

3.2 Introduction

The haskap plant (*Lonicera caerulea*), also known as blue honeysuckle, honeyberry, and haskappu (Khattab et al., 2016), has many species that are native to Japan, North Eastern Asia, and Siberia (Naugžemys et al., 2007). Haskap plants are relatively new in Canada as cross cultivation only began in 2002 (Bors, 2009). Since then, haskap berry production has increased in North America due to their positive health benefits and growing popularity with consumers (Frier et al., 2016). Haskap berries are well-known for their high antioxidant activity due to numerous bioactive compounds such as anthocyanins and ascorbic acid (Celli et al., 2014). However, there are relatively fewer studies on haskap leaves. Studies have shown that leaves from berry plants such as raspberry, strawberry, and honeysuckle possess numerous high-value compounds such as polyphenols and iridoids and they exhibit important health promoting properties such as neuroprotective (Dawson, 2017), anti-inflammatory (Oszmiański et al., 2011), antioxidant (Buricova et al., 2011), and antimicrobial activities (Panizzi et al., 2002). For instance, chlorogenic acid (CGA) has anti-inflammatory, antioxidant, and anti-hypertension properties (Naveed et al., 2018) and quercetin, a type of flavonoid, is associated with anti-inflammatory, antioxidant, and angioprotective properties (D'Andrea, 2015). In addition, the total phenolic content (TPC) is often used as an overall measure of the phenolic compounds that may be present in some plant materials, and is frequently associated with antioxidant activity (Singleton et al., 1999; Tian et al., 2018). Haskap plants are perennials and shed their leaves after berry harvesting in preparation for winter. Haskap leaves are commonly used as mulch for the plants, however, there is an opportunity to extract and recover bioactive compounds from this underutilized resource. These extracts can be used to develop value-added products for the functional foods and natural health products sector.

Extraction methods such as maceration (Nastić et al., 2018) and reflux (Rodrigues et al., 2018) have some disadvantages when used with conventional organic solvents. These include long extraction times at high temperatures, the toxicity of the solvents, and the need for several steps to facilitate contaminant removal, product isolation and final purification (Luque de Castro & Priego-Capote, 2010; Vongsak et al., 2013). As an alternative, aqueous

two-phase extraction (ATPE) is a simple separation technique that involves equilibration, phase separation, and concentration of solutes in a single step (Hatti-Kaul, 2000), where the extraction of solutes from a solid or liquid material is based on selective partitioning in the aqueous two phase system (ATPS). ATPSs can be formed with polymer/polymer, polymer/salt, ionic liquid/salt, or alcohol/salt aqueous solutions (Yau et al., 2015), where the incompatibility of the two aqueous components causes partitioning into two distinct phases. In comparison to conventional extraction, which generally uses organic solvents such as hexane, ethyl acetate methanol, or acetone (Bampouli et al., 2014; Routray, 2014), ATPE is considered more environmentally friendly as users can select phase-forming components such as alcohols, polyethylene glycol, and salts. Moreover, ATPS components may be selected so that they are generally recognized as safe (GRAS) (U.S. Food and Drug Administration, 2020) and the extracts are compatible in food and consumer personal care products. For example, ATPS comprising of a suitable alcohol with a salt (e.g. ammonium sulphate, $(\text{NH}_4)_2\text{SO}_4$, or sodium dihydrogen phosphate, NaH_2PO_4) or sugar (e.g. glucose or maltose) are considered GRAS. While ammonium sulphate/ethanol and sodium dihydrogen phosphate/ethanol ATPS are popular choices for ATPE with many studies reported in the literature, there are fewer studies using sugar-based ATPS systems that are GRAS. Indeed, acetonitrile (Chia, Chew, et al., 2019; De Brito Cardoso et al., 2013; Dhamole et al., 2016; Koyande et al., 2019; Sankaran, Manickam, et al., 2018; Tu et al., 2018; Wang et al., 2008), ionic liquids (Freire et al., 2011; Sun et al., 2018), and propylene glycol (Tubtimdee & Shotipruk, 2011) have been used for sugar-based ATPS; however, acetonitrile can metabolize in the liver to produce acutely toxic cyanide (Mateus et al., 2005) and many ionic liquids exhibit cytotoxic properties (Gal et al., 2012). Sugar-based ATPS have been investigated with GRAS substances such as ethanol (Tubtimdee & Shotipruk, 2011), however in some cases ethanol has been found to result in unstable ATPS and 1-propanol has been used as a suitable GRAS alternative (Ebrahimi & Sadeghi, 2018). Past studies have used ATPE to extract and purify various high-value compounds such as gallic acid from guava (Reis et al., 2015), CGA from carrots (Sánchez-Rangel et al., 2016), and flavonoids from pigeon pea roots (Zhang et al., 2013). These studies have focused on a single component such as anthocyanins (Wu et al., 2014) or lipase (Ooi et al., 2009), while other studies have also analyzed extracts for two components such as flavones and

sugars (Liu et al., 2013), ascorbic acid and vanillin (Veloso et al., 2020), as well as various flavonoid compounds (He et al., 2016).

Thus, the aim of this research was to compare the performance of salt/ethanol and sugar/propanol ATPE for the extraction and concentration of bioactive compounds from haskap leaves. Three different UV spectrophotometer assays were used to monitor bioactive content, based on CGA, flavonoids, and TPC. CGA and flavonoids were selected for measurement as the main bioactive compounds in haskap leaves (Oszmiański et al., 2011). Although CGA and flavonoids belong to the total phenolics group, TPC was measured to account for other potential bioactive compounds in this group. Extraction time, sample loading, and tie line length (TLL) were optimized based on extraction yields from the UV spectrophotometry measurements using response surface methodology. The optimized extracts were then analyzed using high-performance liquid chromatography (HPLC) to identify and quantify the bioactive compounds. Nuclear magnetic resonance spectroscopy (NMR) was used for preliminary qualitative profiling of the bioactive compounds. The novelty of the present work is that it is the first study to investigate the feasibility of ATPE of bioactive compounds from under-utilized haskap leaves using GRAS components.

3.3 Materials and Methods

3.3.1 Materials

Ethyl alcohol (95%) was obtained from Greenfield Specialty Alcohols Inc. (Toronto, Ontario, Canada). Methanol ($\geq 99.9\%$) was supplied by VWR Analytical (Mississauga, Ontario, Canada). Sodium dihydrogen phosphate (96%) and diosmin were purchased from Alfa Aesar (Ward Hill, Massachusetts, USA). 1-propanol ($\geq 99\%$, food grade), ammonium sulphate (ACS, $\geq 99\%$); sodium nitrite ($\geq 97\%$, ACS), aluminum nitrate nonahydrate (ACS, $\geq 97\%$), sodium carbonate (ACS, 99.95-100.05% dry basis), Folin & Ciocalteu's phenol reagent (2N), gallic acid monohydrate (ACS, $\geq 98\%$), chlorogenic acid ($\geq 95\%$, titration), rutin hydrate ($\geq 94\%$, HPLC grade), and D-(+)-maltose monohydrate (95%, grade II) were purchased from Sigma-Aldrich (Oakville, Ontario, Canada). D-(+)-glucose monohydrate (extra pure) was purchased from Acros Organics (Morris Plains, New Jersey, USA).

Luteolin-7-*O*-glucoside (95.1%) was purchased from ChromaDex. Deionized water from a Milli-Q water purification system (Millipore, Bedford, Massachusetts, USA) was used.

Fresh haskap leaves of the Aurora variety were collected in July 2018 from a haskap farm in Nova Scotia, Canada. The haskap plants were in their first growth year. The fully-developed leaves were picked after the haskap berries were harvested. There was visible leaf browning as the leaves were in the process of natural senescence (Dawson, 2017). The leaves were thoroughly washed with tap water, kept frozen at $-20\text{ }^{\circ}\text{C}$, and then freeze-dried in a Labconco FreeZone 2.5 Plus freeze dryer (Labconco, Kansas City, MO, USA). The dried samples were then sealed in vacuum pouches and stored at $-20\text{ }^{\circ}\text{C}$ in the dark. Prior to experiments, the samples were ground and sieved through a $500\text{ }\mu\text{m}$ mesh sieve. Due to experimental constraints, two batches of leaves were used in this study (Batch A and Batch B). These were selected at random from the same pool of harvested leaves and also serve to demonstrate the robustness of the optimization model.

3.3.2 Methods

3.3.2.1 Aqueous Two-Phase Extraction (ATPE) and Conventional Extraction

Phase diagrams were constructed to determine suitable biphasic working regions. Aqueous solutions of $(\text{NH}_4)_2\text{SO}_4$, NaH_2PO_4 , glucose, and maltose were prepared at specific concentrations. Using cloud point titration (Ooi et al., 2009), the alcohol (either ethanol or propanol), was added drop by drop to the salt or sugar solution until the first sign of permanent turbidity was observed. The weight of alcohol added was recorded using a balance with precision of 0.1 mg (S-64, Denver Instrument, Denver, CO, USA) and a binodal curve was plotted. A minimum of seven points were used to plot each binodal curve. The binodal curves were fitted using either Equation 3.1 (De Brito Cardoso et al., 2013) or Equation 3.2 (Regupathi et al., 2009):

$$Y = A_1 \times \exp(B_1 X^{0.5} - C_1 X^3) \quad (3.1)$$

$$Y = A_2 + B_2 X^{0.5} + C_2 X \quad (3.2)$$

where Y and X are the alcohol and salt/sugar weight percentages, respectively, and $A_1, B_1, C_1, A_2, B_2,$ and C_2 are fitting parameters obtained by least squares regression. The $(\text{NH}_4)_2\text{SO}_4$ /ethanol binodal curve had a better fit using Equation 3.1 while the other three ATPS binodal curves were fitted using Equation 3.2. The tie lines were determined gravimetrically where a point in the two-phase region was selected (Merchuk et al., 1998). The ATPS was prepared, thoroughly mixed, and allowed to equilibrate overnight at 25 °C. The top and bottom phases were then weighed. The mass balance equations (Equations 3.3 to 3.6) were solved using MATLAB R2019a (MathWorks, Natick, MA, USA).

$$Y_T = f(X_T) \quad (3.3)$$

$$Y_B = f(X_B) \quad (3.4)$$

$$Y_T = \left(\frac{Y_M}{\alpha}\right) - \left(\frac{1-\alpha}{\alpha}\right) Y_B \quad (3.5)$$

$$X_T = \left(\frac{X_M}{\alpha}\right) - \left(\frac{1-\alpha}{\alpha}\right) X_B \quad (3.6)$$

In Equations 3.3 to 3.6, X_T is the weight fraction of salt or sugar at the top phase, X_B is the weight fraction of salt or sugar at the bottom phase, X_M is the weight fraction of salt or sugar of the mixture, Y_T is the weight fraction of alcohol at the top phase, Y_B is the weight fraction of alcohol at the bottom phase, and Y_M is the weight fraction of alcohol of the mixture.

$f(X)$ is the function representing the binodal curve and α is defined as the following ratio in Equation 3.7:

$$\alpha = \frac{\text{Weight of top phase}}{\text{Weight of mixture}} \quad (3.7)$$

After obtaining $X_T, X_B, Y_T,$ and Y_B , TLL was determined by Equation 3.8.

$$\text{Tie line length (TLL)} = \sqrt{(X_T - X_B)^2 + (Y_T - Y_B)^2} \quad (3.8)$$

The reliability of the tie line calculation was evaluated using the Othmer-Tobias (Equation 3.9) and Bancroft (Equation 3.10) correlations (Cienfuegos et al., 2017; Wang et al., 2010; Zafarani-Moattar et al., 2005).

$$\frac{1-w_1^T}{w_1^T} = k_1 \left(\frac{1-w_2^B}{w_2^B} \right)^n \quad (3.9)$$

$$\frac{w_3^B}{w_2^B} = k_2 \left(\frac{w_3^T}{w_1^T} \right)^r \quad (3.10)$$

Here, w_1^T , w_2^B , w_3^T , w_3^B represent the equilibrium compositions in weight fractions of alcohol (1), salt/sugar (2), and water (3) in the top T and bottom B phases, respectively, and k_1 , k_2 , n , and r are fitting parameters.

For each ATPS of 10 g, three TLLs (Low, Medium, and High), were selected to represent different ATPS compositions of salt or sugar and alcohol, as all points on the same tie line had the same final concentration of phase components in their respective top and bottom phases (Hatti-Kaul, 2000). Table 3.1 shows the concentration of the phase-forming components for each TLL selected in this study.

For ATPE, the weighed ground leaves (Batch A) were thoroughly vortexed for 15 seconds with the selected ATPS in 15-mL centrifuge tubes, each with a diameter of 1.5 cm and occupied height of 8 cm. The tubes were incubated for the required extraction time at 25 °C. The tubes were then centrifuged at 1500 g (Sorvall T1 centrifuge, Thermo Scientific, USA) for 5 minutes to achieve complete phase separation. The top and bottom liquid phases were carefully removed with a syringe, ensuring that the leaves at the interphase remained in the tube. The top and bottom phase volumes were recorded, and the top phase was analyzed using UV spectroscopy as outlined in Section 3.3.2.2. The bottom phase was purified on Hypersep SPE 500 mg/2.8 mL C18 solid phase extraction cartridges (Thermo Scientific, Rockwood, Tennessee, USA) prior to analysis. Briefly, the aqueous extracts (bottom phase) were loaded onto the cartridges which were preconditioned and equilibrated with water. The cartridges were then washed with acidified water (0.1% v/v formic acid) to remove the salt and sugar components. The organic fractions were then eluted with

75% (v/v) ethanol and 100% (v/v) ethanol. Two concentrations of ethanol were used as 100% (v/v) ethanol was to elute very non-polar compounds while 75% (v/v) ethanol eluted compounds with other polarities. The fractions were dried and dissolved in 80% methanol prior to analysis using UV spectroscopy. The pH values for both the top and bottom phases for all ATPS were recorded using a benchtop pH meter (UB-10, Denver Instrument, Denver, CO, USA). Conventional exhaustive extraction was performed by Soxhlet extraction, where 75 mg of ground leaves were extracted with 150 mL of 80% (v/v) methanol for 24 hours.

Table 3.1 Tie line length and their respective compositions

ATPS	Tie line length (TLL)	Composition
(NH ₄) ₂ SO ₄ /ethanol	Low (31.90)	18 wt% (NH ₄) ₂ SO ₄ , 25 wt% ethanol, 57 wt% water
	Medium (43.05)	16 wt% (NH ₄) ₂ SO ₄ , 30 wt% ethanol, 54% wt% water
	High (53.70)	20 wt% (NH ₄) ₂ SO ₄ , 27.5 wt% ethanol, 52.5 wt% water
NaH ₂ PO ₄ /ethanol	Low (33.60)	10 wt% NaH ₂ PO ₄ , 37 wt% ethanol, 53 wt% water
	Medium (44.15)	10 wt% NaH ₂ PO ₄ , 37.5 wt% ethanol, 52.5 wt% water
	High (47.92)	10 wt% NaH ₂ PO ₄ , 40 wt% ethanol, 50 wt% water
Glucose/1-propanol	Low (30.00)	20 wt% glucose, 38 wt% 1-propanol, 42 wt% water
	Medium (39.90)	20 wt% glucose, 40 wt% 1-propanol, 40 wt% water
	High (45.05)	20 wt% glucose, 42 wt% 1-propanol, 38 wt% water
Maltose/1-propanol	Low (27.47)	25 wt% maltose, 28 wt% 1-propanol, 47 wt% water
	Medium (40.08)	25 wt% maltose, 30 wt% 1-propanol, 45 wt% water
	High (42.65)	25 wt% maltose, 35 wt% 1-propanol, 40 wt% water

3.3.2.2 UV-Vis Spectrophotometric Analysis of Bioactive Compounds

For the following CGA, flavonoids, and TPC assays, individual standard calibration curves, corresponding to a different ATPS composition for each TLL, were plotted to minimize interference from salt and sugar (Golunski et al., 2016). Samples were diluted when necessary, using the corresponding ATPS top phases to ensure that the measurements were in the range of the calibration curve. The wavelength of maximum absorption, λ_{max} , was determined spectrophotometrically by wavelength scanning (Genesys 10S UV/Visible spectrophotometer, Thermo Scientific, USA).

Chlorogenic Acid

The extract was diluted with its corresponding ATPS top phase when necessary. The absorbance of the solution was then measured at 328 nm (Tan et al., 2014) and a standard curve was constructed using chlorogenic acid to determine its concentration.

Flavonoid Content

This was determined by the formation of an aluminium complex (Hou et al., 2018). Here, 450 μL of the extract was combined with 75 μL of 5% (w/v) sodium nitrite solution and 75 μL of 10% (w/w) aluminium nitrate solution with thorough mixing and an incubation time of 6 minutes in between those steps. Then 750 μL of 4% (w/w) sodium hydroxide solution was added, mixed well, and incubated for 15 minutes. The solution was centrifuged at 1500 g for 1 minute, and then the absorbance of the supernatant was measured at 510 nm and compared against the standard curve. Rutin hydrate was used as the standard and results were expressed in terms of rutin equivalents (RE).

Total Phenolic Content (TPC)

This was determined by the Folin-Ciocalteu method (Singleton et al., 1999) in which 100 μL of the extract was mixed with 200 μL Folin-Ciocalteu reagent (diluted with water at a ratio of 1:10 by volume). After 5 minutes of incubation, 800 μL of 7.5% (w/v) aqueous sodium carbonate solution was added. The solution was vortexed and incubated for 2 hours in the dark at room temperature. The mixture was then centrifuged at 1500 g for 1 minute. Its absorbance was determined at the wavelength of maximum absorption (665 nm for all ATPS) and compared against a standard curve. For extracts obtained by conventional extraction, TPC was determined at the wavelength of maximum absorption which was 765 nm. Gallic acid monohydrate was used as the standard and results were expressed in terms of gallic acid equivalents (GAE).

3.3.2.3 Performance Indicators

To evaluate the effectiveness of the ATPS in this study, the performance indicators were yield, partition coefficient, k , and extraction efficiency, EE . The yield, which was used as

the response variable for optimizing the extraction conditions, was calculated using Equation 3.11 (Fu et al., 2019; Zhang et al., 2015).

$$Yield = \frac{C_T \times V_T}{\text{Dry weight of leaves}} \quad (3.11)$$

Here, C_T and V_T are the concentration of the target compounds and volume of the top phase, respectively.

The partition coefficient was calculated using Equation 2.1 as the ratio of concentration of bioactive compounds at the top phase to the concentration of bioactive compounds at the bottom phase. The extraction efficiency was calculated for extracts from the optimized conditions using Equations 3.12 and 3.13.

$$\text{Volume ratio, } R_V = \frac{V_T}{V_B} \quad (3.12)$$

$$\text{Extraction efficiency, } EE (\%) = \left(\frac{kR_V}{1+kR_V} \right) \times 100 = \left(\frac{M_{top}}{M_{total}} \right) \times 100 \quad (3.13)$$

Here, k is the partition coefficient; V_T and V_B are the top and bottom phase volumes at equilibrium; M_{top} is the mass of target compounds in the top phase and M_{total} is the total mass of target compound in both phases.

3.3.2.4 Design of Experiment, Optimization, and Statistical Analysis

Table 3.2 shows the face-centered central composite design used with the following factors and corresponding levels in parentheses: extraction time (5, 62.5, and 120 minutes), sample loading (0.1%, 0.55%, and 1% (w/w)) and TLL (Low, Medium, and High). As each experiment used 10 g of ATPS, the corresponding sample loading can also be expressed as 10 mg, 55 mg, and 100 mg. A maximum extraction time of 120 minutes was selected as a representative value, similar to that used in other ATPE studies (Hou et al., 2018; Wu et al., 2014). Since it was difficult to distinguish between top and bottom phases at high sample loadings, the maximum sample loading was set at 1% (w/w). The categorical TLLs

were determined from preliminary experiments where the levels were selected to include ATPS composition near the binodal curve and furthest from it without having any crystallization. The experiments were performed once in randomized order. Chlorogenic acid, flavonoids, and total phenolic content measurements were obtained from triplicate analyses and results were expressed as mean values. Analysis of variance (ANOVA) and response surface optimization were performed using Minitab statistical software (Version 18, Minitab Inc. USA). As TLL is a categorical factor, separate models were generated for each TLL. Multi-response optimization was used to maximize the yield of the CGA, flavonoids and total phenolic content. The model was validated using both batches of harvested leaves (Batch A and Batch B).

Table 3.2 Design of experiment in uncoded units

Run#	Extraction time (min), A	Sample loading % (w/w), B	Tie line length, C
1	5	0.10	Low
2	5	0.10	Medium
3	5	0.10	High
4	5	0.55	Low
5	5	0.55	Medium
6	5	0.55	High
7	5	1.00	Low
8	5	1.00	Medium
9	5	1.00	High
10	62.5	0.10	Low
11	62.5	0.10	Medium
12	62.5	0.10	High
13	62.5	0.55	Low
14	62.5	0.55	Low
15	62.5	0.55	Low
16	62.5	0.55	Low
17	62.5	0.55	Low
18	62.5	0.55	Medium
19	62.5	0.55	Medium
20	62.5	0.55	Medium
21	62.5	0.55	Medium
22	62.5	0.55	Medium
23	62.5	0.55	High
24	62.5	0.55	High
25	62.5	0.55	High
26	62.5	0.55	High
27	62.5	0.55	High
28	62.5	1.00	Low
29	62.5	1.00	Medium
30	62.5	1.00	High
31	120	0.10	Low
32	120	0.10	Medium
33	120	0.10	High
34	120	0.55	Low
35	120	0.55	Medium
36	120	0.55	High
37	120	1.00	Low
38	120	1.00	Medium
39	120	1.00	High

Runs were performed in random order

3.3.2.5 High Performance Liquid Chromatography (HPLC) and Nuclear Magnetic Resonance (NMR) Analysis for Optimized Conditions

For HPLC and NMR analysis, Batch A leaves were used. The desired bioactive compounds were retained and impurities were removed from the leaf extracts using C18 SPE 500 mg/2.8 mL solid phase extraction cartridges (Thermo Scientific, Rockwood, Tennessee, USA) prior to analysis. Extracts dissolved in water were loaded onto C18 cartridges which were preconditioned and equilibrated with water. The cartridges were then washed with acidified water, 0.1% (v/v) formic acid, to remove inorganics and subsequently eluted with 75% (v/v) ethanol and 100% ethanol. The organic fractions were combined and dried under nitrogen.

For NMR profiling, the organic fractions from conventional extract and optimized extracts were prepared with concentration of 10 mg/mL in deuterated dimethyl sulfoxide, DMSO- d_6 , then transferred to 5 mm NMR tubes. All spectra were obtained with a Bruker Avance III 700 MHz spectrometer (Bruker Biospin, Karlsruhe, Baden-Württemberg, Germany) equipped with cooled probe operating at 16 K.

The organic fractions were then analyzed by HPLC, using an Agilent 1200 HPLC system (Agilent, Waldbronn, Germany) equipped with a quaternary pump (Agilent G1311A), an autosampler (G1329A), a column compartment with temperature controller (G1316A), and a diode array detector (G1315B). The column (Zorbax SB-C18, 1.8 μ m, 4.6 mm \times 50 mm, Agilent, U.S.A.) was eluted with a mobile phase consisting of (A) 0.1% formic acid in Milli-Q water and (B) 0.1% formic acid in acetonitrile using a gradient of 1% to 99% B in 25 minutes at a flow rate of 0.3 mL/min. Elution was monitored at 320 and 250 nm on the diode array detector and by MS detector. The injection volume was 1 μ L and the column temperature was maintained at 40°C. Quantification of chlorogenic acid, rutin, luteolin-7-*O*-glucoside, and diosmin was performed using five-point calibration curves that were prepared for each standard to obtain linear regression equations for the compounds.

3.4 Results and Discussion

3.4.1 Phase Diagram

The ATPS phase diagrams for $(\text{NH}_4)_2\text{SO}_4$ /ethanol, NaH_2PO_4 /ethanol, glucose/1-propanol/, and maltose/1-propanol at 25 °C were plotted in Figure 3.1 and the binodal curves are similar to other studies (Wang et al., 2010). For sugar-based ATPS, the maltose/1-propanol binodal curve was slightly closer to the origin in comparison to glucose/1-propanol curve. This indicates that maltose formed two phases with 1-propanol more easily than with glucose, as less sugar was required (Ebrahimi & Sadeghi, 2018).

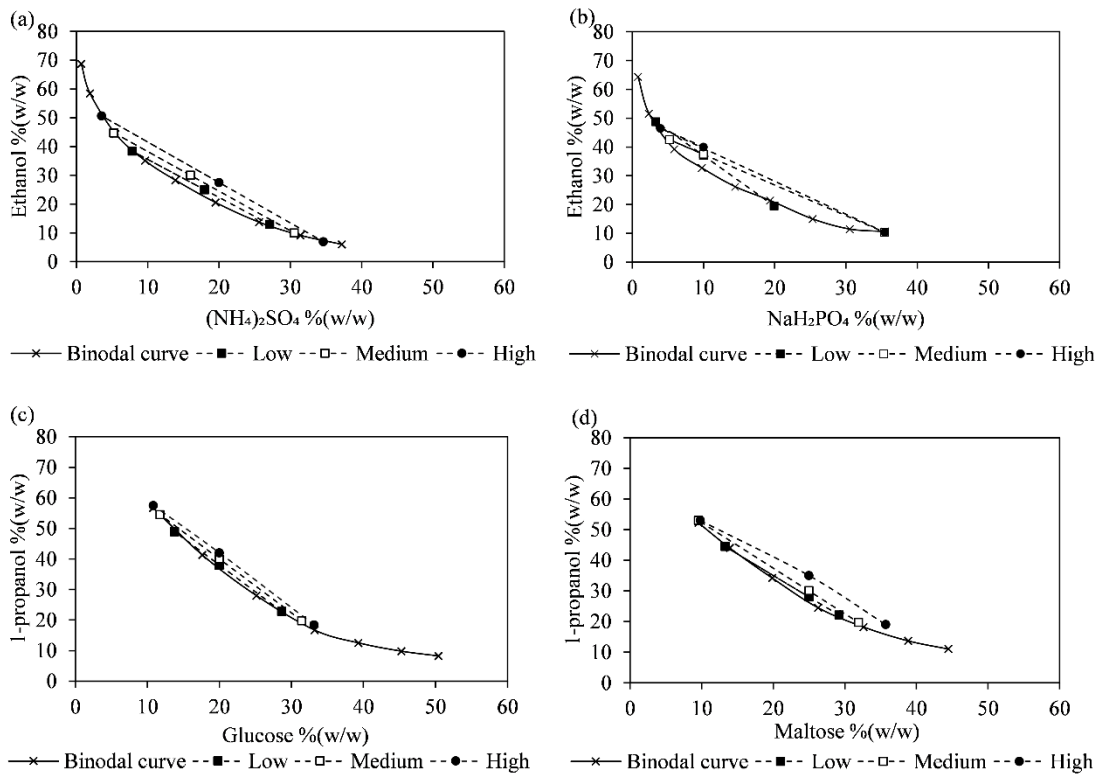


Figure 3.1 ATPS phase diagrams for (a) $(\text{NH}_4)_2\text{SO}_4$ /ethanol, (b) NaH_2PO_4 /ethanol, (c) glucose/1-propanol/, and (d) maltose/1-propanol at 25 °C

The Othmer-Tobias and Bancroft correlation had R^2 values that were close to 1 for the $(\text{NH}_4)_2\text{SO}_4$ /ethanol and glucose/1-propanol tie lines, and a linear dependence of the logarithmic-transformed function indicated good fitting properties (Wang et al., 2010). In comparison, the correlation values for NaH_2PO_4 /ethanol and maltose/1-propanol systems

averaged 0.62. The pH values for the different ATPS and their respective TLL are listed in Table 3.3 for later discussion.

Table 3.3 pH values of different ATPS studied

ATPS	Tie line length	Top phase pH	Bottom phase pH
(NH ₄) ₂ SO ₄ /ethanol	Low	5.58	5.54
	Medium	5.47	5.47
	High	5.54	5.56
NaH ₂ PO ₄ /ethanol	Low	3.81	4.09
	Medium	4.02	4.09
	High	3.99	4.01
Glucose/1-propanol	Low	5.32	5.80
	Medium	5.31	5.12
	High	5.39	4.89
Maltose/1-propanol	Low	5.51	4.48
	Medium	5.73	4.65
	High	5.81	4.62

3.4.2 Response Surface Regression

For all ATPEs, analyses were performed using the yield for either CGA, flavonoids or TPC as the response variable. The effects of TLL on extraction yield were varied depending on the bioactive compounds measured and ATPS used. For ATPE using (NH₄)₂SO₄/ethanol, maximum CGA, flavonoids, and TPC yields were obtained at Medium, High, and High TLL, respectively. High TLL was selected as the optimized point, which was similarly observed in another study extracting polyphenols using (NH₄)₂SO₄/ethanol, where the authors also reported the highest partition coefficient was attained at the highest TLL (Xavier et al., 2017). This was likewise observed in a different study where bioactive compounds were extracted using potassium phosphate/ethanol and it was attributed to the salting-out effect produced by increasing salt concentration in the bottom phase (Simental-Martínez et al., 2014). For ATPE using NaH₂PO₄/ethanol, maximum CGA, flavonoids, and TPC yields were obtained at Low, Medium, and Low TLL, respectively. The preference for Low TLL in NaH₂PO₄/ethanol systems differs with the findings of He and co-workers who used a fixed salt concentration of 29% and varying ethanol concentrations of 17% to 25% (He et al., 2016). They found that several flavonoids had highest partition coefficient and recoveries at the highest ethanol concentration. This difference may be due to a higher

viscosity in the ATPS as they used a much higher salt concentration compared to the 10% salt concentration in this study. A higher viscosity gradient would be the driving force for compounds to partition upwards. The glucose/1-propanol ATPE had maximum CGA, flavonoids, and TPC yields at High, Medium, and High TLL, respectively and the High TLL was chosen as the optimal point. ATPE using maltose/1-propanol achieved maximum CGA, flavonoids, and TPC yields at Low, Low, and Medium TLL, respectively and the Medium TLL was chosen as the optimal TLL.

The coefficients for response surface equations in Table 3.4 are listed with their *P*-value, where only the selected TLLs corresponding to optimized conditions are shown. For some responses, Box-Cox transformation was performed to normalize the responses, as noted in the table.

All response models were found to be statistically significant at $P < 0.01$ with acceptable R^2 values greater than 0.7 except for the CGA yield from ATPE with glucose/1-propanol. A closer examination of this response showed that only one term, which was the interaction between sample loading and tie line length, was significant at $\alpha = 0.01$. In addition, the R^2 value indicates that this model for CGA yield can only explain 57.34% of the variability of the response around its mean, whereas $R^2 \geq 0.7$ is considered good for sensory, colorimetric, and physicochemical results (Granato et al., 2010). Moreover, there was significant lack-of-fit for some responses in Table 3.4, indicating that the variability between the design point replicates was higher than the variability between different runs, as reported by other ATPS work (Shahbaz Mohammadi et al., 2015).

Table 3.4 Regression coefficients of quadratic polynomial model

Salt/ethanol ATPE						
Coefficient	(NH ₄) ₂ SO ₄ ATPE (High TLL)			NaH ₂ PO ₄ ATPE (Low TLL)		
	CGA Yield	Flavonoids Yield	TPC Yield ^a	CGA Yield	Flavonoids Yield	TPC Yield
β_0	6.33	0.15240	-0.00930	26.43	0.1094	0.13281
β_1	0.0637	0.000079	0.000159	-0.0454	-0.000247	-0.000295
β_2	61.46	-0.05568	-0.00790	53.52	0.1738	-0.1197
β_{11}	-0.00046	-0.000001	-0.000001	0.000317	0.000003	0.000001
β_{22}	-39.17	0.02608	-0.00388	-45.60	0.0567	0.0562
β_{12}	0.0161	0.000064	-0.000049	0.0273	-0.000502	0.00018
R^2	0.9763	0.9056	0.9406	0.9454	0.9386	0.9083
R^2 (adj)	0.9666	0.8672	0.9163	0.9231	0.9135	0.8709
P (model)	0.000*	0.000*	0.000*	0.000*	0.000*	0.000*
P (lack of fit)	0.188 ^{ns}	0.034 ^{ns}	0.003*	0.000*	0.010 ^{ns}	0.699 ^{ns}

Sugar/1-propanol ATPE						
Coefficient	Glucose ATPE (High TLL)			Maltose ATPE (Medium TLL)		
	CGA Yield	Flavonoids Yield	TPC Yield ^b	CGA Yield ^c	Flavonoids Yield	TPC Yield
β_0	25.70	0.08742	-375.0	2.08	0.05912	0.02826
β_1	-0.0383	-0.000196	0.21	0.0073	0.000058	0.000033
β_2	-0.19	-0.01584	-612.0	11.02	0.00466	-0.01497
β_{11}	0.000084	0.000001	0.0049	-0.000121	0	0
β_{22}	-1.34	0.00951	76.0	-7.17	-0.00545	0.00559
β_{12}	-0.0101	0.000003	-2.21	0.0376	0.000045	-0.000013
R^2	0.5734	0.8043	0.82	0.7189	0.7985	0.7830
R^2 (adj)	0.3997	0.7246	0.7467	0.6043	0.7164	0.6947
P (model)	0.006*	0.000*	0.000*	0.000*	0.000*	0.000*
P (lack of fit)	0.033 ^{ns}	0.049 ^{ns}	0.031 ^{ns}	0.007*	0.007*	0.000*

β_0 is the estimated constant regression coefficient.

β_1 and β_2 are the estimated linear regression coefficient of extraction time and sample loading, respectively. β_{11} and β_{22} are the estimated quadratic regression coefficient of extraction time and sample loading, respectively.

β_{12} is the estimated interaction regression coefficient of extraction temperature and sample loading.

* P -value is significant at $\alpha=0.01$

^a (NH₄)₂SO₄/ethanol ATPE transformed with response of (TPC Yield⁻⁶)/(-321,451,508.1).

^b Glucose/1-propanol ATPE transformed with response of (-TPC Yield⁻²)

^c Maltose/1-propanol ATPE transformed with response of (CGA Yield²)/(699.3)

Figure 3.2 shows the effects of extraction time and sample loading, where three-dimensional surface plots are plotted using the optimized levels for TLLs. In general, there were no consistent trends in the interactions at the optimum TLL levels for CGA, flavonoids and TPC yield, nor between the different ATPS. Figure 3.2 (a) indicates that

for ATPE with $(\text{NH}_4)_2\text{SO}_4$ /ethanol, flavonoids and TPC yields were lower than for CGA and that maximum CGA yields were achieved at high sample loadings. For the same ATPE, there was an initial decrease in CGA yield observed with increasing extraction time. The higher CGA yields observed with increased extraction time could be due to the longer contact time between the leaves and the solvent for mass transfer, whereas the decrease in CGA yields with longer extraction times could be attributed to a volume exclusion effect in which the biomolecules tend to partition to the bottom phase due to reduced space being available in the top phase of the ATPS (Babu et al., 2008). In comparison, the results from ATPE with glucose/propanol in Figure 3.2 (c) indicate that a high concentration of bioactive compounds was obtained at low sample loadings.

It is possible that the yields from ATPE may have been affected by pH. For example, chlorogenic acid has a pKa value 3.33 (ChemAxon, 2019) and if the pH of the surrounding environment was at 3.33 there would be equal amounts of protonated and deprotonated CGA molecules. In an ATPS where the pH is higher than 3.33, chlorogenic acid would exist mainly as ions and tend to bond with the water molecules, resulting in partial partitioning to the hydrophilic bottom phase. In this work the NaH_2PO_4 /ethanol ATPS with Low TLL and associated pH of 3.81, had the highest CGA yield among the four ATPE systems although chlorogenic acid would exist in its ionic form under these conditions. However, the overall acidic pH would have provided a stable environment for the phenolic compounds (Friedman & Jürgens, 2000). For ATPE using NaH_2PO_4 /ethanol, CGA yields decreased from 37.5 to 35 $\mu\text{g}/\text{mg}$ leaves with increasing extraction time. This may be attributed to NaH_2PO_4 having lower salting-out ability than $(\text{NH}_4)_2\text{SO}_4$ (Show et al., 2013). Anions have been associated with a greater effect on salting-out ability than cations, and based on Hofmeister series, the H_2PO_4^- ion has lower salting-out ability than the SO_4^{2-} ion (Hyde et al., 2017). With increasing extraction time, the weaker dihydrogen phosphate anion-water bond would allow more time for the hydrophilic bioactive compounds to interact and bond with water in the bottom aqueous phase.

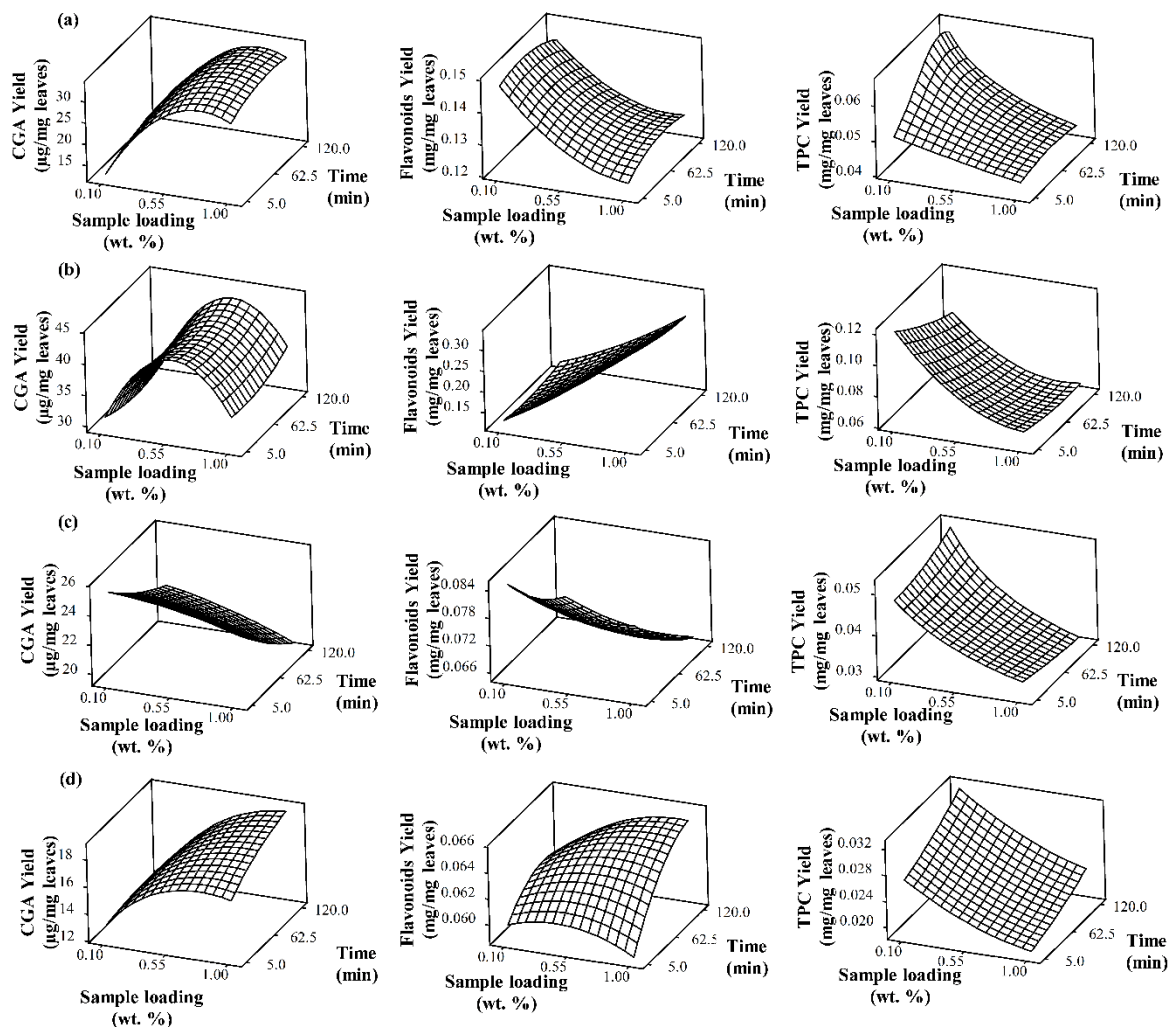


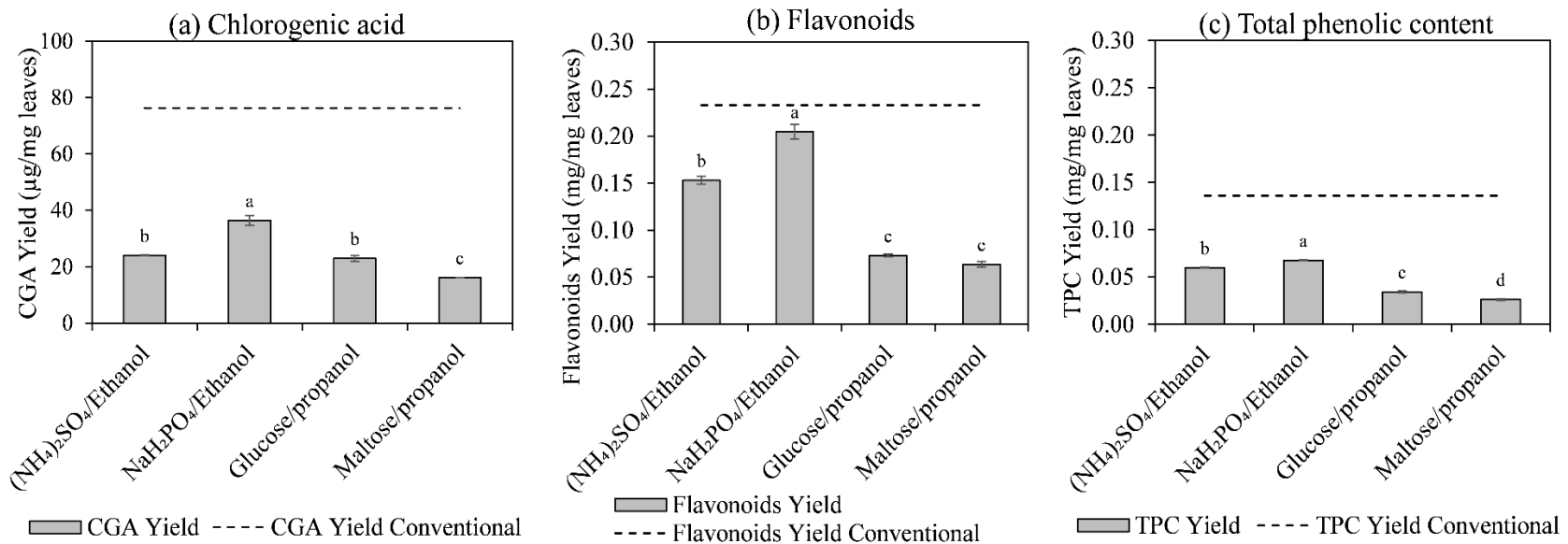
Figure 3.2 Interaction effects of sample loading and time on CGA yield, flavonoid yield, and TPC yield for (a) $(\text{NH}_4)_2\text{SO}_4$ /ethanol ATPE at High TLL, (b) NaH_2PO_4 /ethanol ATPE at Low TLL, (c) glucose/1-propanol ATPE at High TLL, and (d) maltose/1-propanol ATPE at Medium TLL

3.4.3 Optimization of ATPE and Comparison between Systems

Optimum conditions for ATPE were determined by simultaneously maximizing the CGA yield, flavonoids yield, and TPC yield. The weight factor for all the responses was fixed at 1 in Minitab to ensure that they had the same influence on the desirability. Table 3.5 shows four optimized solutions for each ATPE and their individual desirability values. The overall desirability, D is a measure of how well the goals for the three responses were optimized. Desirability has a range from 0 to 1, where 1 represents the ideal situation and 0 shows that

one or more responses are out of their acceptable limits. This desirability scale indicates that the values are considered satisfactory for salt-based ATPE and good for sugar-based ATPE (Lazic, 2006). Extracts from Batch A leaves had 7 out of 12 responses located in the 95% prediction interval, however the results from Batch B leaves were not as close to the predicted value and generally lower.

Figure 3.3 shows a yield comparison between the conventional extract and the optimized ATPE extract using Batch A leaves. From Soxhlet extraction, the CGA yield, flavonoids yield, and TPC yield for Batch A were 76.28 $\mu\text{g}/\text{mg}$ leaves, 0.23 mg/mg leaves, and 0.14 mg/mg leaves, respectively. Batch B had lower yields which were 66.38 $\mu\text{g}/\text{mg}$ leaves, 0.20 mg/mg leaves, and 0.11 mg/mg leaves for CGA, flavonoids, and TPC, respectively. The yields from ATPE were lower than the yields of Soxhlet extraction. It is evident that the ATPE did not recover all the compounds from the leaves, although the extraction time (5 mins to 120 mins) was far shorter than the time for Soxhlet extraction (24 hours), and further extractions with the remaining solids could be considered. From Figure 3.3, $\text{NaH}_2\text{PO}_4/\text{ethanol}$ ATPE resulted in the highest yield for all compounds. This may be due to the lower pH 3.81 in the top phase which provides a favorable environment for phenolic compounds. Salt-based systems also had higher yields compared to sugar-based systems, and this trend is consistent among the two different batches of leaves.



Error bars represent the standard deviation of n=3 repeat measurements. Different letters within each graph correspond to statistically significant differences ($P < 0.05$).

Figure 3.3 Yield comparison of ATPE and conventional Soxhlet extraction using Batch A leaves

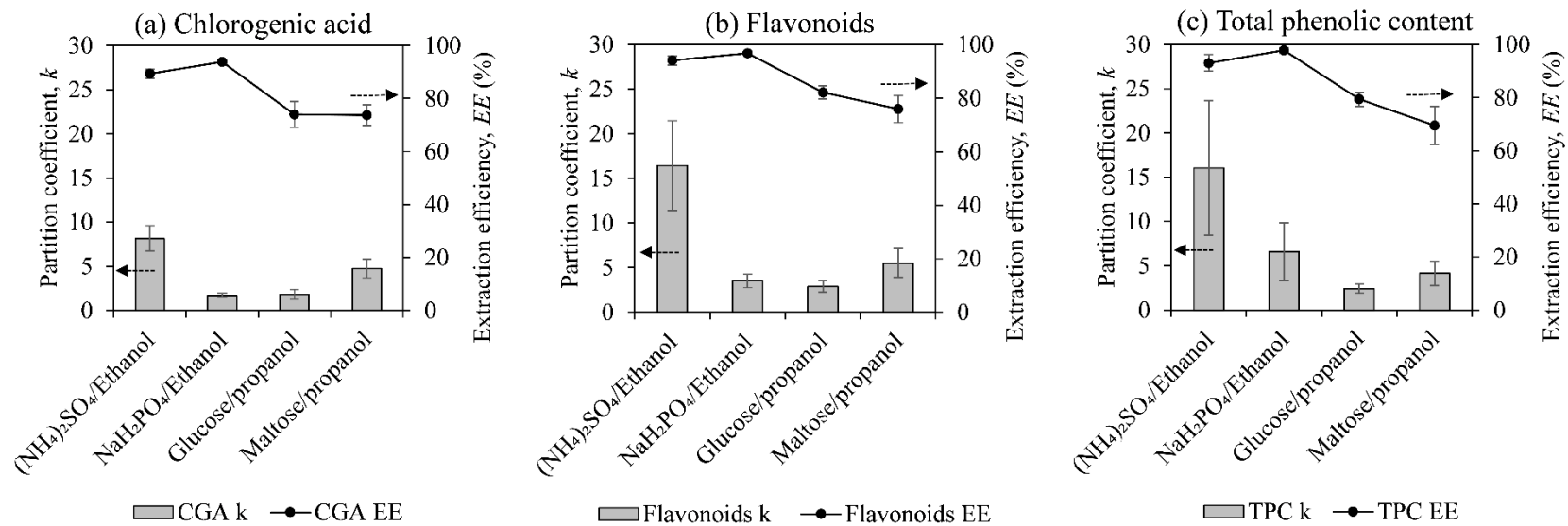
Table 3.5 Optimization of ATPE based on maximum CGA yield ($\mu\text{g}/\text{mg}$), flavonoids yield ($\text{mg RE}/\text{mg}$), and TPC yield ($\text{mg GAE}/\text{mg}$)

Responses	Individual desirability, <i>d</i>	Predicted value	Batch A experimental value	Batch A deviation (%)	Batch B experimental value	Batch B deviation (%)
(NH ₄) ₂ SO ₄ /ethanol: High TLL, 87.5 min, 0.19 weight% leaves. <i>D</i> = 0.62						
CGA yield	0.45	18.93	23.99	26.7	34.65	83.0
Flavonoid yield	0.75	0.144	0.153	6.3	0.132	8.3
TPC yield	0.69	0.061	0.060	1.5*	0.050	18.0
NaH ₂ PO ₄ /ethanol: Low TLL, 5 min, 0.5 weight% leaves. <i>D</i> = 0.60						
CGA yield	1.00	41.63	36.43	12.5*	29.83	28.3
Flavonoid yield	0.48	0.208	0.205	1.5*	0.133	36.0
TPC yield	0.45	0.086	0.068	21.3	0.050	41.9
Glucose/propanol: High TLL, 5 min, 0.1 weight% leaves. <i>D</i> = 0.76						
CGA yield	0.90	25.47	22.92	10.0*	16.54	35.0
Flavonoid yield	0.81	0.085	0.073	14.1	0.051	40.0
TPC yield	0.60	0.048	0.034	28.4	0.024	50.0
Maltose/propanol: Medium TLL, 120 min, 0.427 weight% leaves. <i>D</i> = 0.64						
CGA yield	0.78	16.61	16.07	3.2*	10.39	37.4
Flavonoid yield	0.66	0.064	0.064	0.0*	0.034	46.9
TPC yield	0.51	0.028	0.026	6.7*	0.017	39.3

* in 95% prediction interval

For comparison between the ATPE systems, Figure 3.4 shows the partition coefficient and extraction efficiency of the optimized extracts from Batch B. From Figure 3.4, the CGA, flavonoids, and TPC partitioned to the top phase, since the partition coefficient was higher than 1 for all systems. The partition coefficient for CGA (and their corresponding extraction efficiency in parentheses) for (NH₄)₂SO₄/ethanol, NaH₂PO₄/ethanol, glucose/propanol, and maltose/propanol ATPS were 8.16 (89.3%), 1.73 (93.9%), 1.84 (74.0%), and 4.76 (73.8%), respectively. In comparison, a study extracting CGA from ramie leaves found that the partition coefficient ranged from 2.56 to 32.66 for (NH₄)₂SO₄/ethanol systems and from 3.39 to 38.49 for NaH₂PO₄/ethanol systems (Tan et al., 2014). These higher partition coefficient values may have been affected by the pre-extraction step using ethanol and ultrasonication, thus increasing the partitioning ability as observed by Tan and co-workers. Another study on CGA extraction used potassium phosphate/ethanol ATPS and resulted in partitioning to the top phase (Simental-Martínez et al., 2014). In the present work, the partition coefficients for flavonoids (and their

corresponding extraction efficiency in parentheses) for ATPE using $(\text{NH}_4)_2\text{SO}_4$ /ethanol, NaH_2PO_4 /ethanol, glucose/propanol, and maltose/propanol were 16.44 (94.0%), 3.50 (96.8%), 2.88 (82.1%), and 5.52 (76.0%), respectively. In comparison, partition coefficients in the range of 7 to 10 were obtained using NaH_2PO_4 /ethanol ATPE for extracting rutin from *Zanthoxylum Bungeanum* Maxim leaves (He et al., 2016). The partition coefficients for TPC (and their corresponding extraction efficiency in parentheses) for ATPE using $(\text{NH}_4)_2\text{SO}_4$ /ethanol, NaH_2PO_4 /ethanol, glucose/propanol, and maltose/propanol were 16.05 (93.0%), 6.59 (97.8%), 2.41 (79.4%), and 4.14 (69.5%), respectively. In the literature, polyphenols extracted from eucalyptus wood wastes were found to migrate to the top phase when acidic conditions formed by $(\text{NH}_4)_2\text{SO}_4$ /ethanol ATPE was used (Xavier et al., 2017), while in alkaline and neutral conditions, phenols partitioned to the bottom phase. For all these phenolic components, $(\text{NH}_4)_2\text{SO}_4$ /ethanol extract had higher partition coefficients than for the NaH_2PO_4 /ethanol extracts. This may be due to $(\text{NH}_4)_2\text{SO}_4$ having a better salting-out ability than NaH_2PO_4 according to the Hofmeister series (Hyde et al., 2017). The standard error of mean for the partition coefficient values of flavonoids and total phenolic content in Figure 3.4 were notably higher than those of the extraction efficiencies. This may be due to the loss of some bioactive compounds during the salt removal using SPE. The additional steps involved in the sample preparation for the bottom phase may have contributed to the larger standard error of mean in the partition coefficient.



Note: Error bars represent duplicate measurements

Figure 3.4 Comparison of partition coefficient (k) and extraction efficiency (EE) between four ATPE systems for (a) chlorogenic acid, (b) flavonoids, and (c) total phenolic content using Batch B leaves

The extraction efficiency of all these bioactive components ranged from 89.31 to 97.82% for salt-based ATPE and 69.52 to 82.13% for sugar-based ATPE. Similarly, ionic liquid salting-out systems have demonstrated a strong ability to remove proteins in comparison to sugaring-out systems (Sun et al., 2018). In another study (Tu et al., 2018) extracting the fatty acid 10-hydroxy-2-decenoic acid (10-HDA) with sodium chloride/acetonitrile, magnesium sulphate/acetonitrile, and glucose/acetonitrile ATPE, Tu and co-workers found that magnesium sulphate/acetonitrile produced higher extraction yields compared to the other two systems (Tu et al., 2018). The lower efficiency of sugar-based ATPE may be due to sugars being covalent while salts are ionic compounds. Since intramolecular forces are greater than intermolecular forces due to the transfer and sharing of electrons, they may be more significant to consider. The intramolecular force of ionic compounds is stronger than that of covalent compounds, and thus salt has a greater ability to attract water molecules to itself in comparison to sugars. Although sugars do not have charged groups, they have many hydrophilic hydroxyl groups that contribute to its high solubility in water, making the sugaring-out phenomenon possible.

3.4.4 HPLC and NMR Analysis

Figure 3.5 shows the yield of bioactive compounds obtained from conventional extracts and optimized extracts from ATPE as determined by HPLC. From Figure 3.4, the yields of chlorogenic acid from ATPE with $(\text{NH}_4)_2\text{SO}_4$ /ethanol and glucose/1-propanol were higher than that of the conventional extract. ATPE with glucose/propanol also resulted in higher yields of rutin, luteolin-7-*O*-glucoside, and diosmin.

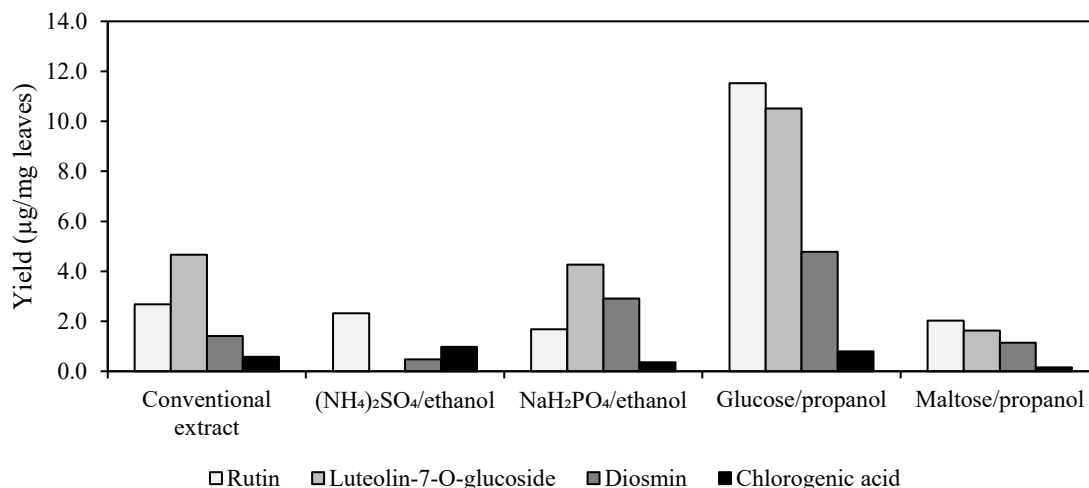


Figure 3.5 Bioactive compounds yield in conventional extract and top phase ATPE extract as determined by HPLC

Figure 3.5 also shows that the extract from NaH₂PO₄/ethanol ATPE had a similar trend in yield to the conventional extract, as luteolin-7-*O*-glucoside had the highest yield, followed by lower yields for rutin and diosmin, and then CGA. ATPE with glucose/propanol had the highest rutin, luteolin-7-*O*-glucoside, and diosmin yield, implying the system might be enriching flavonoid glycosides from haskap leaves.

A comparison of Figure 3.5 with Figure 3.3 indicates that for some bioactives, higher yields were obtained from the UV-vis assays, in relation to comparable yields obtained from HPLC. This would be due to the specificity of HPLC, as the presence of other similar compounds in the haskap leaves would not be quantified using HPLC. For example, the UV-Vis assay (Figure 3.3) detected the highest CGA yields at 36.43 µg/mg using ATPE composed of NaH₂PO₄/ethanol. However, HPLC (Figure 3.5) detected the highest CGA yields at 0.9703 µg/mg using ATPE with (NH₄)₂SO₄/ethanol. This difference may be due to the presence of CGA isomers and other compounds that have similar absorption spectra to CGA at 328 nm in the UV spectrophotometric measurement. Although it has been reported that phenolic acids such as CGA can be detected in the flavonoids assay used in this study (Pękal & Pyrzynska, 2014), Figure 3.5 indicates that the yield of CGA is much lower than the overall yield of measured flavonoids (rutin, luteolin-7-*O*-glucoside, and diosmin), as determined by HPLC.

The models developed by Dawson (2017), which correlated concentration of bioactive compounds and growth stage for haskap leaves from the cultivar 'Tundra', were used to predict the content of various metabolites for this study. The values were then compared to our experimental results. We used 80 days post-fertilization of the flower as the independent variable to represent the closest stage of plant growth where shoot growth would have stopped, terminal buds were formed, and berries were harvested. The model predicted a CGA content of 10.5 $\mu\text{g}/\text{mg}$ dry weight (DW) leaves and rutin content of 7 $\mu\text{g}/\text{mg}$ DW leaves. Another study using haskap leaves from the cultivar 'Zielona' detected CGA of 67.1 $\mu\text{g}/\text{mg}$ DW leaves, rutin of 19.5 $\mu\text{g}/\text{mg}$ DW leaves, and total phenolic compound of 297 $\mu\text{g}/\text{mg}$ DW leaves (Oszmiański et al., 2011). The yield of the bioactive compounds from conventional haskap leaf extracts in this study were lower than that predicted from Dawson (Dawson, 2017) and reported by Oszmiański et al. (2011). These differences may be caused by variety difference, geographical conditions, maturity stage, and environmental factors (Boyarskikh et al., 2015; Dawson, 2017; Senica et al., 2018). The glucose/propanol extract however, yielded 11.52 μg rutin/mg DW leaves. This was a higher value than that predicted from Dawson's model for 'Tundra' leaves (Dawson, 2017).

The HPLC chromatograms for conventional extracts and NaH_2PO_4 /ethanol extract are shown in Figure 3.6 and chromatograms for the other ATPE extracts are included in Appendix A, Figures A.1 to A.3. showed the identified compounds of chlorogenic acid, rutin, luteolin-7-*O*-glucoside, and diosmin. The NaH_2PO_4 /ethanol extract had fewer peaks, which indicated that it is more refined in comparison to the conventional extract. This partial purification may be largely due to impurities such as metallic elements and proteins being partitioned to the bottom phase (He et al., 2016). The corresponding retention times are documented in Appendix B, Table A.3.

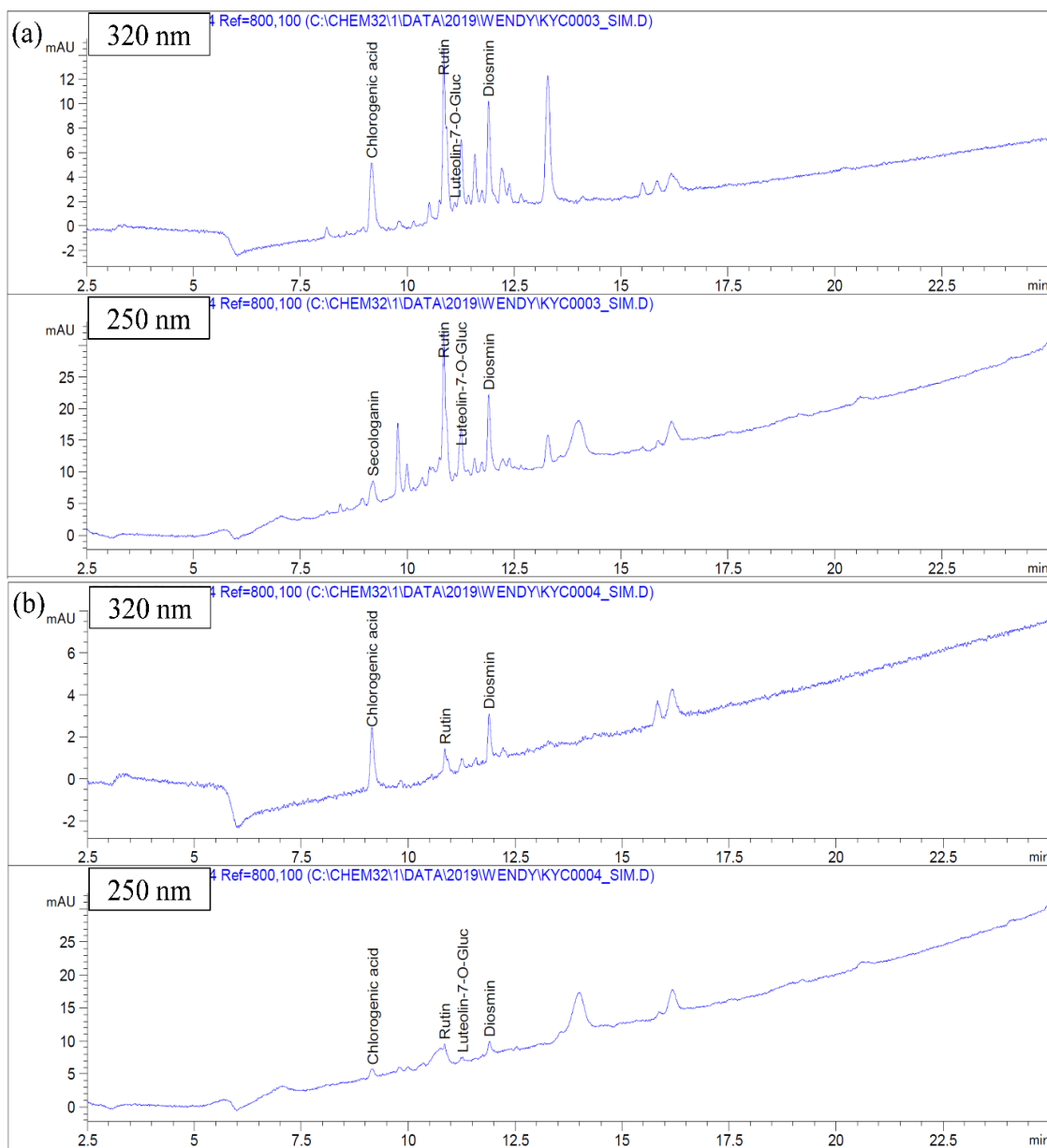


Figure 3.6 HPLC chromatograms of (a) conventional extracts and (b) NaH₂PO₄/ethanol extract using Batch A leaves

NMR was used to assess the general composition profile of the extracts. Figure 3.7 shows the ¹H-NMR spectra of NaH₂PO₄/ethanol extract and conventional extract. Chlorogenic acid standard was included as a comparison. From the 6-8 ppm resonance frequency in Figure 3.7, the signals are typical for protons in aromatic compounds (Ek et al., 2006; Lambert & Mazzola, 2004). The preliminary qualitative profiling shows the possible

presence of chlorogenic acid. Other $^1\text{H-NMR}$ spectra are included in Appendix A, Figure A.4. This qualitative profiling supports the quantitative results obtained by HPLC in Figure 3.5.

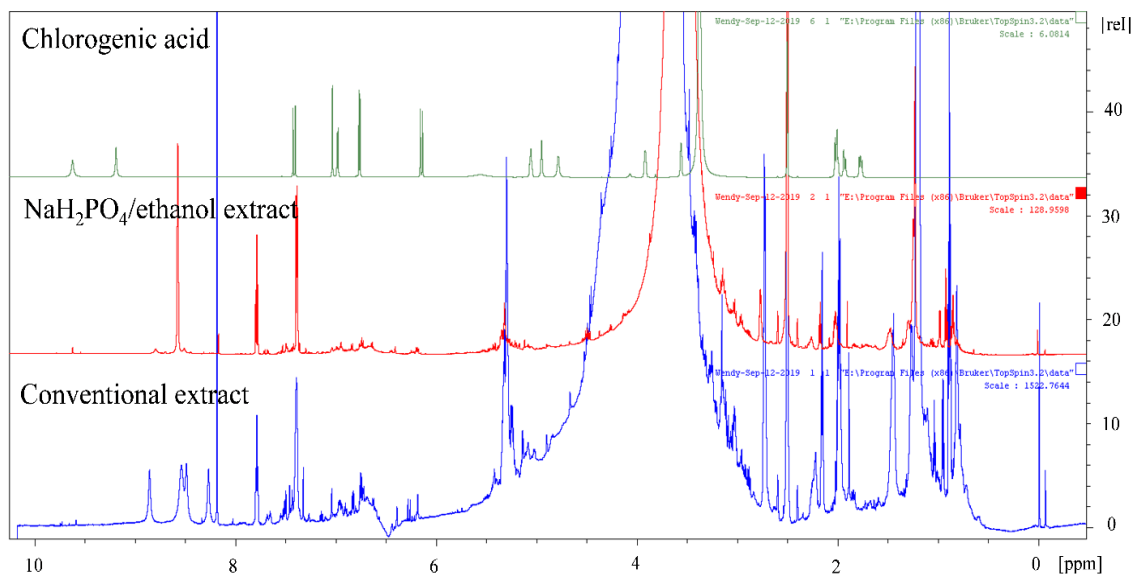


Figure 3.7 $^1\text{H-NMR}$ spectra for NaH_2PO_4 /ethanol extract and conventional extract using Batch A leaves

3.5 Conclusion

Our study confirms that haskap leaves contain high-value bioactive compounds that have been associated with health benefits. The results show that GRAS salt/ethanol ATPE systems had higher extraction efficiency than sugar/propanol ATPE. ATPE using NaH_2PO_4 /ethanol exhibited the highest extraction efficiency of 93.9% for chlorogenic acid, 96.8% for flavonoids, and 97.8% for total phenolic content among the four ATPE systems. Its corresponding partition coefficients were 1.73 for chlorogenic acid, 3.50 for flavonoids, and 6.59 for total phenolic content. In general, the HPLC analysis showed fewer components in the extracts obtained from ATPE than the conventional extract. The partition coefficient values and HPLC chromatograms support the concept that ATPE integrates biomolecule concentration and partial purification. Thus, ATPE is a potential alternative green extraction technique to recover bioactive compounds from haskap leaves as compared to conventional extraction. This work demonstrated that toxic solvents and

long extraction times are not necessary to extract biomolecules. With further studies, haskap leaf extracts may be incorporated into food or pharmaceutical applications in suitable concentrations.

Connecting Statement 2

The potential of aqueous two-phase extraction (ATPE) to recover bioactive compounds from haskap leaves was evidenced in Chapter 3. The results showed that salt/ethanol ATPE had higher extraction efficiency for the target bioactive compounds than sugar/propanol ATPE and that sodium dihydrogen phosphate/ethanol ATPE had the highest extraction efficiency among the four ATPE systems. In large scale operations, ATPE would involve issues such as high salt concentrations from salt-based ATPE which may corrode metal equipment and associated post-disposal processes. To increase the economic and environmental sustainability of ATPE, Chapter 4 investigates the effects of recycling ATPE components from salt/ethanol and sugar/propanol systems on the extraction performance of bioactive compounds from haskap leaves.

Chapter 4 is based on an article reproduced from *Separation and Purification Technology* with permission from Elsevier. The details of the article are as follows:

Chong, K. Y., & Brooks, M. S.-L. (2021). Effects of recycling on the aqueous two-phase extraction of bioactives from haskap leaves. *Separation and Purification Technology*, 255, 117755.

Chapter 4 : Effects of Recycling on the Aqueous Two-Phase Extraction of Bioactives from Haskap Leaves

4.1 Abstract

Aqueous two-phase extraction (ATPE) is an emerging technique that integrates separation, concentration, and partial purification of target compounds from natural resources. One potential issue which may prevent industrial application of ATPE, is the large consumption of phase-forming components such as alcohol, polymers, salt, and sugar. On top of that, post-handling and disposal of these components will increase associated costs. This research evaluated the effects of recycling ATPE components on the extraction of bioactive compounds from haskap (*Lonicera caerulea*) leaves. In this work, the ATPE systems were combinations of ammonium sulphate/ethanol, sodium dihydrogen phosphate/ethanol, glucose/1-propanol, and maltose/1-propanol. Total phenolic content (TPC), flavonoids, and chlorogenic acid were assessed in terms of their partitioning behavior, extraction efficiencies, and yields. The results showed that with two recycling stages, the extraction performance for all four ATPE systems was maintained. The average TPC extraction efficiencies across the first extraction stage and two recycling stages were 91.4% for ammonium sulphate/ethanol, 99.6% for sodium dihydrogen phosphate/ethanol, 85.1% for glucose/1-propanol, and 85.0% for maltose/1-propanol systems. This suggests that recycling could make ATPE a more sustainable technique in recovering high-value compounds from natural resources.

4.2 Introduction

The haskap plant (*Lonicera caerulea*) is a rich source of bioactive compounds, and is mainly cultivated for commercial production of haskap berries, which have high levels of ascorbic acid and anthocyanin content in comparison to other berries (Chen et al., 2013; Harb et al., 2010; Pantelidis et al., 2007). In addition, haskap leaves have been reported to contain various phenolic compounds and triterpenoids (Becker et al., 2017; Dawson, 2017; Machida et al., 1995; Oszmiański et al., 2011), however they are an underutilized resource and comparatively few studies have been reported on the extraction of bioactives from haskap leaves (Bonarska-Kujawa et al., 2014). Functional compounds in plants have been

extracted as the main source for medicine, food, cosmetic, perfumery, dyes, and building materials for many years. Classical methods such as Soxhlet extraction, maceration, percolation (Vongsak et al., 2013), reflux or distillation (Nakamura et al., 2019) are commonly used to extract plant material. However, these methods are time-consuming, require a lot of energy, and generally use toxic organic solvents such as hexane and methanol (Luque de Castro & Priego-Capote, 2010; Ong, 2004). Alternatively, water is a common choice as it is safe, accessible, and economical. However, water requires a lot of energy to vaporize and has limited solubility with non-polar compounds (Chemat et al., 2019). This has caused a shift towards other environmentally friendly or green extraction methods. Emerging technologies such as ultrasound (Eh & Teoh, 2012), microwave (Routray et al., 2014), and high-pressure (Kraujalis et al., 2015) have been used to intensify and assist conventional extraction processes, however, these methods often require sophisticated equipment and parts such as ultrasound transducer, magnetron, and pressure vessel.

Aqueous two-phase systems (ATPSs) have been explored as a simple green liquid-liquid or solid-liquid extraction technique. They are formed by mixing two immiscible aqueous phases such as combinations of alcohol/salt, polymer/salt, polymer/polymer, or ionic liquid/salt solutions. Separation occurs after some time and two distinct phases, a top and a bottom phase, will form. This separation is also known as an aqueous biphasic system as two phases are formed. Aqueous two-phase extraction (ATPE) occurs when solutes from a solid or liquid material selectively partition between the two phases. ATPE integrates separation, concentration, and partial purification in one step (Soares et al., 2015). It is an adaptable process as less hazardous phase-forming components, such as alcohol, salt, and sugars, can be used with mild extraction temperatures. Additionally, ATPS can be designed to enhance selective partitioning of compounds of interest instead of contaminants (Hatti-Kaul, 2000). ATPE has been used to extract anthocyanins from red cabbage (Jampani & Raghavarao, 2015), chlorogenic acid from blueberry leaves (Wang et al., 2017), flavonoids from lotus leaves (Hou et al., 2018), polyphenols from wheat chaff (Đorđević & Antov, 2017), and saponins from ginseng root (He et al., 2018).

Despite the advantages, the relatively high salt concentrations and cost of polymers can be an issue for ATPE. For example, the salt may corrode metal pumps, lines, or other equipment (Rosa et al., 2009). Additionally, post handling and disposal of phase-forming components will increase associated costs and this may be a barrier for large scale applications (Soares et al., 2015). Recycling is a potential method that can be used to reduce the amount of phase-forming components required. Past studies have included recycling attempts for ATPE combinations of potassium phosphate/2-propanol (Show et al., 2013), sodium dihydrogen phosphate/ethanol (Tan et al., 2014), ammonium sulphate/ethanol (Cheng et al., 2016; Wu et al., 2011), and ammonium sulphate/1-propanol (Sankaran, Show, et al., 2018). To the best of our knowledge, this is the first study that investigates the effects of recycling on the recovery of bioactive compounds from haskap leaves.

The aim of this research was to evaluate recycling on the performance of food compatible ATPE systems (i.e. salt/ethanol and sugar/1-propanol ATPE systems), as a means of increasing the economic and environmental sustainability of this technology and potential applicability to the functional food industry. Ammonium sulphate ($(\text{NH}_4)_2\text{SO}_4$) and sodium dihydrogen phosphate (NaH_2PO_4) were used in salt systems while glucose and maltose were used in sugar systems. This work builds upon the investigation by our previous study (Chong et al., 2020a) on the recovery of bioactive compounds from haskap leaves, as it uses the optimized ATPE parameters that were obtained for these salt and sugar-based systems as a basis for recycling studies. The performance of the recycling stages was assessed by examining the partition coefficient, extraction efficiency, and yield of chlorogenic acid (CGA), flavonoids, and total phenolic content (TPC) obtained from haskap leaves. This study is novel as it is the first time that the recycling of food compatible ATPE systems of salt/ethanol and sugar/1-propanol have been investigated for the recovery of bioactive compounds from haskap leaves.

4.3 Materials and Methods

4.3.1 Materials

Ethyl alcohol (95% volume) was obtained from Greenfield Specialty Alcohols Inc. (Toronto, Ontario, Canada) while diosmin and sodium dihydrogen phosphate 96% were

purchased from Alfa Aesar (Ward Hill, Massachusetts, USA). Aluminum nitrate nonahydrate (ACS, $\geq 97\%$), ammonium sulphate (ACS, $\geq 99\%$), chlorogenic acid ($\geq 95\%$, titration), Folin & Ciocalteu's phenol reagent (2N), gallic acid monohydrate (ACS, $\geq 98\%$), D-(+)-maltose monohydrate (95%, grade II), 1-propanol ($\geq 99\%$, food grade), rutin hydrate ($\geq 94\%$, HPLC grade), sodium carbonate (ACS, 99.95-100.05% dry basis), and sodium nitrite ($\geq 97\%$, ACS) were purchased from Sigma-Aldrich (Oakville, Ontario, Canada). D-(+)-glucose monohydrate (extra pure) was purchased from Acros Organics (Morris Plains, New Jersey, USA) and deionized water was obtained from a Milli-Q water purification system (Millipore, Bedford, Massachusetts, USA).

Fresh haskap leaves of Aurora variety were harvested in July 2018 from a haskap farm in Nova Scotia, Canada. The plants were in their first growth year. After the berries were harvested, fully developed leaves were picked. At this stage of natural senescence, leaf browning was visible. The samples were frozen at $-20\text{ }^{\circ}\text{C}$ and subsequently freeze-dried in a Labconco FreeZone 2.5 Plus freeze dryer (Labconco, Kansas City, MO, USA). The dried samples were sealed in vacuum pouches and stored at $-20\text{ }^{\circ}\text{C}$ in the dark. The samples were freshly ground, sieved through a $500\text{ }\mu\text{m}$ mesh opening, stored at $-20\text{ }^{\circ}\text{C}$, and used within 17 days.

4.3.2 Methods

4.3.2.1 Aqueous Two-Phase Extraction (ATPE) and Recycling

ATPE systems of 20 g were prepared according to Table 4.1, where our previous study (Chong et al., 2020a) had determined the optimal parameters for the extraction of phenolic compounds and flavonoids from haskap leaves.

Table 4.1 Aqueous two-phase extraction optimized parameters (Chong et al., 2020)

ATPE systems	Composition	Extraction time	Sample loading
(NH ₄) ₂ SO ₄ /ethanol	20 wt% (NH ₄) ₂ SO ₄ , 27.5 wt% ethanol, 52.5 wt% water	87.5 min	0.190 %(w/w)
NaH ₂ PO ₄ /ethanol	10 wt% NaH ₂ PO ₄ , 37.0 wt% ethanol, 53 wt% water	5 min	0.500 %(w/w)
Glucose/1-propanol	20 wt% glucose, 42.0 wt% 1-propanol, 38 wt% water	5 min	0.100 %(w/w)
Maltose/1-propanol	25 wt% maltose, 30.0 wt% 1-propanol, 45 wt% water	120 min	0.427 %(w/w)

A flowchart of the experimental work for the Extraction as well as Recycling Stages 1 and 2 is shown in Figure 4.1.

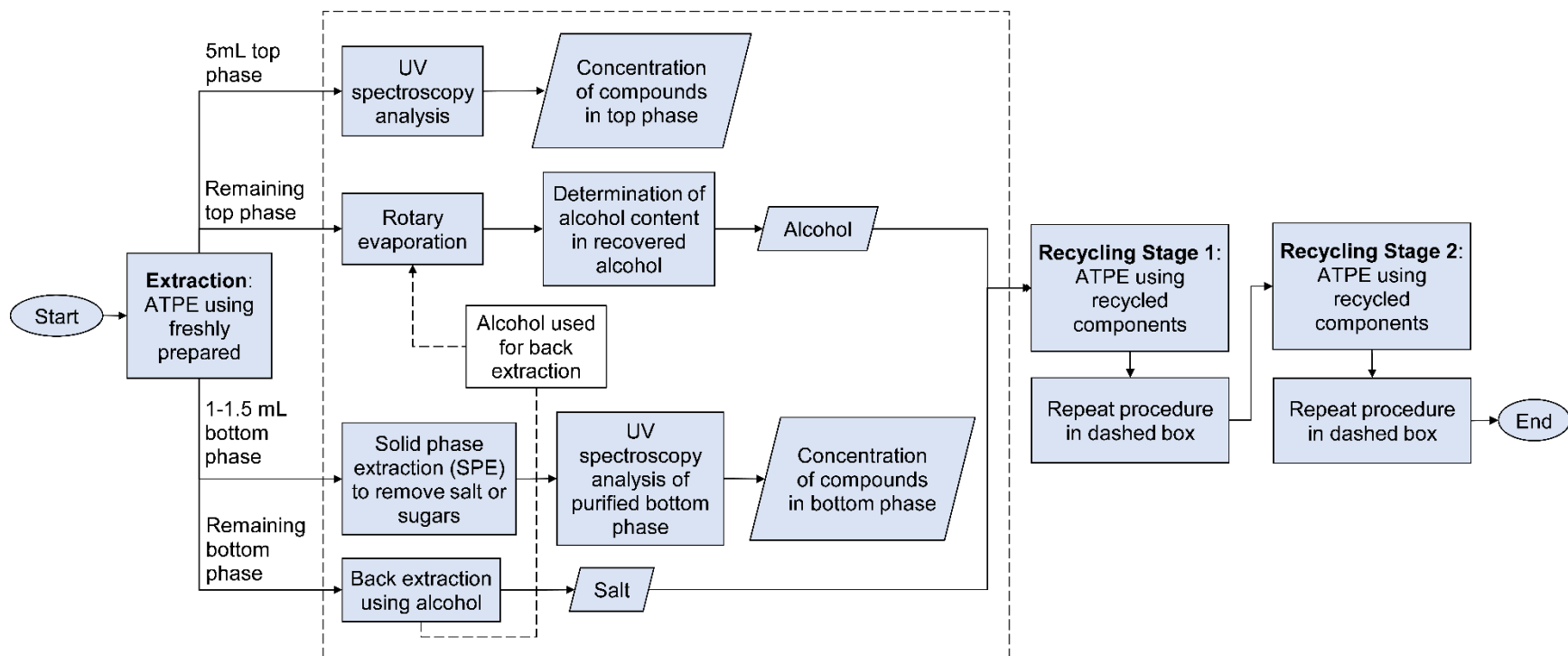


Figure 4.1 F lowchart of experimental work

For the initial extraction of haskap leaves, freshly prepared components were used. Here, the 20 g ATPE systems were prepared in 50 mL centrifuge tubes with internal diameter of 2.8 cm and occupied height of 4.5 cm. The ground leaves were then mixed thoroughly for 15 seconds and incubated at 25 °C for the required extraction time. The tubes were centrifuged at 1500 g (Sorvall T1 centrifuge, Thermo Scientific, USA) for 1 minute to ensure complete phase separation. The volumes of top and bottom phases were recorded, and 5 mL top phase was reserved for UV spectroscopy analysis. The remaining top phase was kept for recycling.

The bottom phase required pre-treatment before analysis due to interference from the salt and sugar (Golunski et al., 2016). About 1 to 1.5 mL bottom phase was purified with solid phase extraction (SPE) using Hypersep SPE 500 mg/2.8 mL C18 solid phase extraction cartridges (Thermo Scientific, Rockwood, Tennessee, USA). Briefly, the bottom phase was loaded onto the cartridges which were preconditioned and equilibrated with water. The cartridges were then washed with acidified water, 0.1% (v/v) formic acid, to remove the salt and sugar components. The organic fractions were then eluted with 75% (v/v) ethanol and 100% (v/v) ethanol. The fractions were dried using rotary evaporator (HiTEC RE-51, Yamato Scientific America, California, USA) set at 50 °C at 200 rpm. They were dissolved in 80% methanol prior to analysis using UV spectroscopy.

The remaining bottom phase was mixed with 3 to 5 mL alcohol to precipitate salt according to the concept of dilution crystallization (Sankaran, Show, et al., 2018; Tan et al., 2014; Wu et al., 2011). The solution was then filtered with Grade 415 qualitative filter paper (VWR International, Pennsylvania, USA) and the salt residue was dried in a vacuum oven (Lindberg/Blue M, Thermo Scientific, USA) at 70 °C to remove any remaining solvent. The recycled salt was added with an appropriate amount of fresh salt to maintain the concentration for two-phase formation (Sankaran, Show, et al., 2018).

The alcohol filtrate was combined with the remaining top phase and it was dried using the rotary evaporator at 50 °C and rotation speed of 200 rpm. The alcohol recovered in the receiving flask was then tested for its alcohol content and density using an EasyDens meter

(Anton-Paar GmbH, Graz, Austria). The recycled alcohol was topped up with fresh alcohol until the desired volume was achieved (Chia, Mak, et al., 2019), where the amount of fresh alcohol required was calculated from Equations 4.1 and 4.2, and the combined solution designated as recycled alcohol.

$$\begin{aligned}
 \text{Correction factor } \left(\frac{kg}{kg}\right) &= \text{Alcohol content of recycled ethanol } \% \left(\frac{m^3}{m^3}\right) \\
 &\times \frac{\text{Theoretical density of alcohol } \frac{kg}{m^3}}{\text{Density of recycled alcohol } \frac{kg}{m^3}}
 \end{aligned}
 \tag{4.1}$$

For Equation 4.1, the theoretical densities of ethanol and 1-propanol used were 789 kg/m³ and 803 kg/m³, respectively. For Equation 4.2, the weight of the 100% alcohol required was calculated based on the ATPE composition in Table 4.1.

$$\text{Weight of alcohol required} = \frac{\text{Weight of 100\% alcohol required}}{\text{Correction factor}}
 \tag{4.2}$$

Sugars were not recovered for ATPE recycling as there were difficulties in the recovery process. From our observations, glucose and maltose were unable to precipitate and formed a slurry when the dilution crystallization technique was applied. Rotary evaporation was then tested as an alternative method. However, the sugars in the evaporating flasks remained as slurry due to their high degree of dissolution (Alves et al., 2007) and only aqueous 1-propanol was evaporated. Although Flood and Srisanga (2012) have described an improved crystallization process with seed crystals for the recovery of glucose monohydrate from aqueous solutions, this was not investigated in the present study.

The recycled ethanol and dried salt were used to form the ATPE system for Recycling Stage 1. The same procedure was repeated and the next ATPE system was used for Recycling Stage 2. Ground leaves were retrieved from the freezer for every stage and the

spent leaves were discarded at the end of each extraction. For sugar-based ATPE, only 1-propanol was recycled. There were two independent experiments for each ATPE.

4.3.2.2 UV-Vis Spectrophotometric Analysis of Bioactive Compounds

The following assays used a UV/Visible spectrophotometer (Genesys 10S, Thermo Scientific, USA) to determine the concentration of bioactive compounds in the extract. The corresponding top phases without samples and methanol were used as blanks for the top phase and bottom phase, respectively. Total phenolic content (TPC), total flavonoid content, and chlorogenic acid were determined according to Section 3.3.2.2.

4.3.2.3 Performance Indicators and Statistical Analysis

Partition coefficient, k , extraction efficiency, EE , and yield were determined according to Section 3.3.2.3.

One-way analysis of variance (ANOVA) and post hoc Tukey's test were performed using Minitab statistical software (Version 18, Minitab Inc. USA) at $P < 0.05$. Values in figures and tables were expressed in average \pm standard error of mean.

4.4 Results and Discussion

4.4.1 Comparison of Partition Coefficients with Previous Optimization Study

The partition coefficients from this study can be compared to those from a previous study, which focused on the optimization of ATPE parameters for the extraction of bioactive compounds from haskap leaves (Chong et al., 2020a), as shown in Table 4.2. Corresponding partition coefficients were assessed in Table 4.2 as partition coefficients from the present study refer to the values from the first extraction using fresh phase-forming components. The values from this study are mostly much higher than that of the previous work. Although some had statistically insignificant difference, the increase in partitioning for the present study may be mostly due to the difference in the height-to-diameter (H/D) ratio of the extraction vessel. In the previous study, 15 mL centrifuge tubes were used for the 10 g ATPE and the H/D ratio was 5.3. The height refers to the height of the solution in the tube. In the present study, 50 mL centrifuge tubes were used for the 20 g

ATPE and the H/D ratio was 1.6. The time needed for phases to separate has been reported to be much faster in batch settlers with large cross-sectional area (Solano-Castillo & Rito-Palomares, 2000) and a H/D ratio of less than one has been recommended. The results in Table 4.2 show that the appropriate selection of the extraction vessel dimensions is critical for partitioning performance.

Table 4.2 Comparison of partition coefficient obtained from previous work and this study

	Previous work ¹	First extraction from this study	Previous work ¹	First extraction from this study
	(NH ₄) ₂ SO ₄ /ethanol		NaH ₂ PO ₄ /ethanol	
<i>k</i> TPC	16.05 ± 7.58 ^a	11.15 ± 2.79 ^a	6.59 ± 3.28 ^a	28.85 ± 15.47 ^a
<i>k</i> flavonoids	16.44 ± 5.02 ^a	16.99 ± 1.69 ^a	3.50 ± 0.74 ^a	28.17 ± 7.14 ^a
<i>k</i> CGA	8.16 ± 1.44 ^a	8.72 ± 0.17 ^a	1.73 ± 0.23 ^a	10.99 ± 2.87 ^a
	Glucose/1-propanol		Maltose/1-propanol	
<i>k</i> TPC	2.41 ± 0.52 ^a	3.91 ± 0.27 ^a	4.14 ± 1.37 ^a	11.03 ± 1.75 ^a
<i>k</i> flavonoids	2.88 ± 0.63 ^a	4.81 ± 0.46 ^a	5.52 ± 1.62 ^a	17.56 ± 2.66 ^a
<i>k</i> CGA	1.84 ± 0.56 ^b	5.08 ± 0.14 ^a	4.76 ± 1.04 ^b	14.94 ± 1.60 ^a

¹ Partition coefficient from previous work (Chong et al., 2020a)

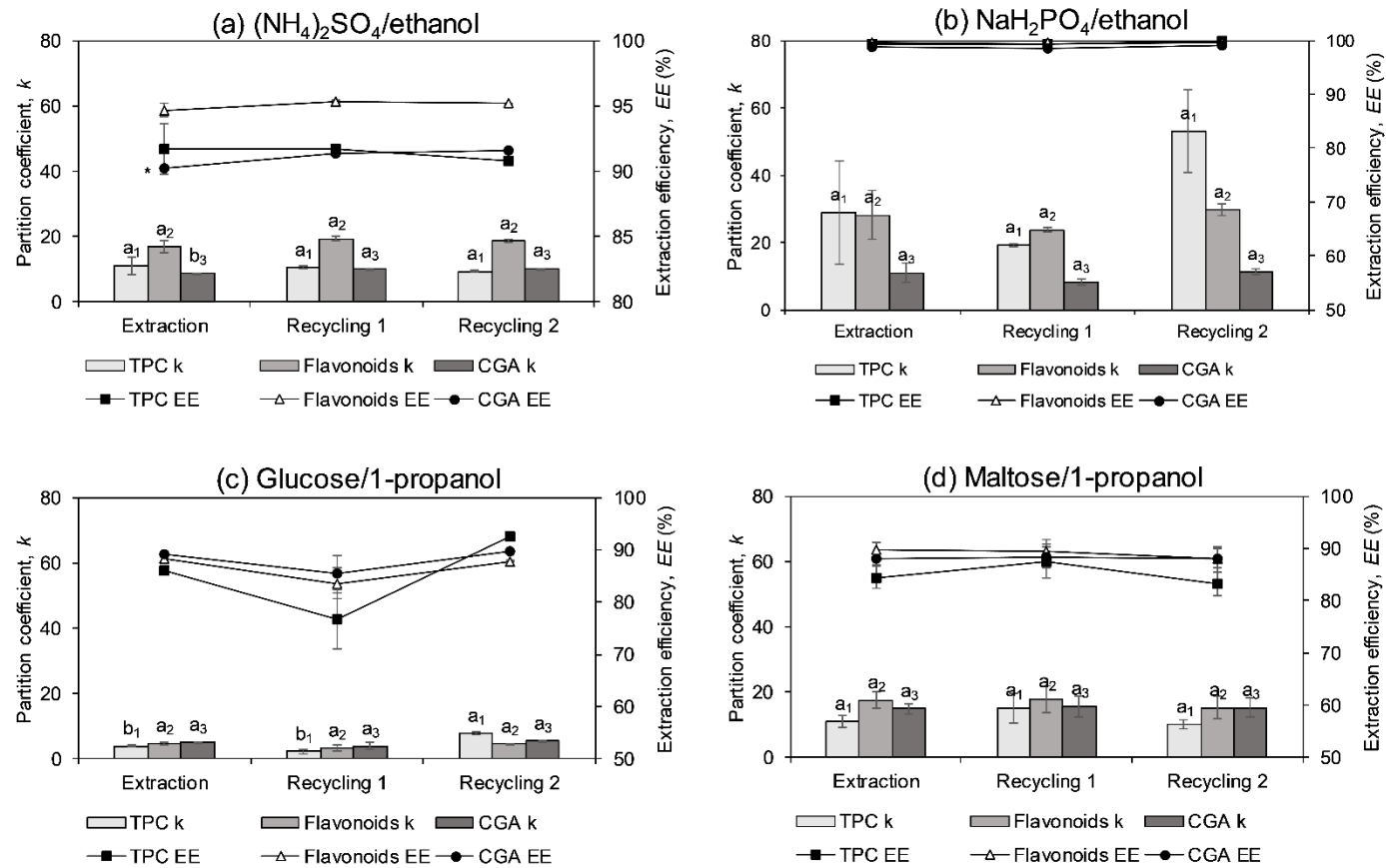
Different superscripts indicate statistically significant difference between the previous study and this study at $P < 0.05$

4.4.2 Effects of Recycling on ATPE Partition Coefficient and Extraction Efficiency

In Figure 4.2 (a), (NH₄)₂SO₄/ethanol ATPE had partition coefficient for TPC of 11.15, 10.51, and 9.37 for the first extraction, first and second recycling stage, respectively. For flavonoids the partition coefficients were 16.99, 19.40, and 18.61. The values were not statistically different. For CGA, the partition coefficients were 8.72, 10.06, and 10.32. There was an increase in partition coefficient from the first extraction. High extraction efficiencies for flavonoids were recorded at about 95% while for TPC and flavonoids, they averaged at about 91%. Wu et al. (2011) investigated multiple extractions of (NH₄)₂SO₄/ethanol ATPE for mulberry anthocyanins. The authors' methodology was different such that most of the top phase from the first extraction was used in the second extraction with fresh bottom phase. The partition coefficient increased from 3.53, 3.36, and lastly 4.50 for the third partitioning step. These partition coefficients from Wu et al. (2011)

for mulberry anthocyanins were lower than the partition coefficients for the TPC of haskap leaves reported in this study. It should be noted that as anthocyanins are a subset of compounds belonging to the diverse group of polyphenolic compounds, the partition coefficients for TPC may be higher than for the anthocyanins, as a broader group of compounds would be detected. The ethanol and salt from Wu's work were recycled although it was unclear how those substances were used after recycling (Wu et al., 2011). In a different study, $(\text{NH}_4)_2\text{SO}_4$ /ethanol ATPE was used to recover lignans (Cheng et al., 2016). Although the partition coefficient values were not reported, the authors stated that the partition coefficient hardly decreased and showed no difference after recycling the ethanol and salt for five times. This indicated that the ethanol and salt were not contaminated by impurities and target compounds. These findings aligned with our results which reported stable partition coefficient and extraction efficiencies between the three stages.

Figure 4.2 (b) shows the performance indicators for NaH_2PO_4 /ethanol ATPE. The partition coefficients for TPC were 28.85, 19.18, and 53.07. Although it seemed that the partition coefficient increased with recycling, the large standard error of mean made the difference statistically insignificant. For flavonoids, the partition coefficients were 28.17, 23.75, and 29.70 while for CGA they were 10.99, 8.21, and 11.20. TPC and flavonoids had more partitioning to the top phase than CGA in NaH_2PO_4 /ethanol ATPE. Extraction efficiencies were nearing 100%. Similarly, Tan et al. (2014) reported that the extraction efficiency of NaH_2PO_4 /ethanol ATPE to recover chlorogenic acid from ramie leaf hardly decreased after recycling the salt for 3 times. This phenomenon was attributed to impurities being transferred to the alcohol used for salt precipitation.



Different letters indicate significant difference between the stages at $P < 0.05$. Subscripts 1, 2, and 3 distinguish bars for TPC, flavonoids, and CGA. An asterisk indicates significant extraction efficiency decrease from the rest of the stages. Unmarked extraction efficiencies indicate no statistical difference.

Figure 4.2 Partition coefficient and extraction efficiency of (a) $(\text{NH}_4)_2\text{SO}_4/\text{ethanol}$, (b) $\text{NaH}_2\text{PO}_4/\text{ethanol}$, (c) glucose/1-propanol, and (d) maltose/1-propanol ATPE for the first extraction and subsequent two recycling stages

For glucose/1-propanol ATPE in Figure 4.2 (c), TPC had a significant increase in partition coefficient of 7.81 in the second recycling stage. This may be due to the accumulation of phenolic content in the 1-propanol from previous cycles (Sankaran, Show, et al., 2018). Flavonoids had partition coefficient of 4.81, 3.31, and 4.53 with the first extraction, first and second recycling stage, respectively. CGA had corresponding partition coefficient of 5.08, 3.90, and 5.44. The extraction efficiencies for flavonoids and CGA averaged at 86.6% and 88.03%. They had no statistically significant difference between the stages. TPC had a decreased extraction efficiency of 76.70% at the first recycling stage.

In Figure 4.2 (d) for maltose/1-propanol ATPE, TPC had partition coefficient of 11.03, 15.19, and 10.11, flavonoids had partition coefficient of 17.56, 17.87, and 15.24, and CGA had partition coefficient of 14.94, 15.64, and 15.27, respectively. The extraction efficiencies for TPC, flavonoids, and CGA averaged at 85.04%, 89.02%, and 88.17%, respectively. All the values had no statistical difference. In general, there are very few studies on the effect of recycling on sugar/1-propanol ATPE. However, Show et al. (2013) used ATPE comprising of potassium phosphate and 2-propanol to recover lipase. One of the performance indicators was concentration coefficient and it was defined as the ratio between concentration of lipase at the top phase at time t and original concentration of lipase in bottom phase. The concentration coefficient decreased from 16.1, 13.4, and to 5.4. Fresh components were used in the first extraction while successive first and second recycling stages used recycled 2-propanol and reused bottom phases. They also observed that separation efficiencies decreased across the stages. However, when both top and bottom phases were recycled, the separation efficiencies were 88.6% and 88.5% for the fourth and fifth stages respectively. This is similar to our findings that the extraction efficiency remained fairly constant without any statistically significant difference.

Among salt-based systems, NaH_2PO_4 /ethanol ATPE had higher partitioning and extraction efficiency of bioactive compounds to the top phase. In contrast, our previous study showed that $(\text{NH}_4)_2\text{SO}_4$ /ethanol ATPE performed better (Chong et al., 2020a). Results from the present study also did not adhere to the Hofmeister series' salting-out ability where the H_2PO_4^- ion is expected to have lower salting-out ability. This may be due to the container

geometry used in this study where a larger surface area will facilitate rapid partitioning to the top phase. Taking NaH_2PO_4 /ethanol ATPE as an example, a container that provides larger interfacial area will reduce the time needed for phase separation as compared to a narrow container (Benavides & Rito-Palomares, 2007) in the span of 5 minutes. The extraction time of 87.5 minutes for $(\text{NH}_4)_2\text{SO}_4$ /ethanol ATPE allowed ample time for biomolecules to partition. In sugar-based systems, maltose/1-propanol ATPE had better extraction performance than glucose. This is consistent with our previous findings (Chong et al., 2020a). The masses of sugar in a 20 g system (and their corresponding number of moles in parentheses) were 4 g glucose (0.022 mole) and 5 g maltose (0.015 mole) (Dhamole et al., 2016). As glucose can form five hydrogen bonds while maltose can form eight hydrogen bonds, the number of hydrogen bonds that can be formed for maltose is higher than that of glucose. Since maltose has a greater capacity to bond with water, more 1-propanol will be pushed to the top phase, resulting in higher partitioning and extraction efficiency. Figure 4.2 shows that the partition coefficient and extraction efficiency were fairly constant with the two recycling stages, indicating that it is feasible to recycle the phase-forming components.

4.4.3 Effects of Recycling on ATPE Extraction Yields

Table 4.3 shows the extraction yields obtained from fresh phase-forming components, first, and second recycling stage. In Table 4.3, the yields had slight variation between the stages and only a few statistically different values were observed, which also supports the feasibility of recycling ATPE components.

For the NaH_2PO_4 /ethanol ATPE, the first recycling stage had a TPC yield that was 12% greater than that obtained from the original extraction. However, the flavonoids yield from the $(\text{NH}_4)_2\text{SO}_4$ /ethanol ATPE was the highest at the first extraction and then decreased with the rest of the stages. It was also observed that salt-based ATPE produced higher yields in comparison to sugar-based ATPE, which is consistent with the results from our previous work (Chong et al., 2020a). Among the salt-based and sugar-based ATPE systems, NaH_2PO_4 /ethanol ATPE and glucose/1-propanol ATPE had higher extraction yields, respectively.

Like the present work, other studies in the literature have shown that the recycling of ATPE components can result in a fairly consistent extraction yield across the recycling stages. For example, Wu et al. (2011) reported that the average anthocyanin yield in the top phase was 84.7% and there was no statistically significant difference across three extractions. It is worth noting that the authors used a different approach from our study, where they reused the top phase instead of recycling so that their second partitioning step comprised of the partitioned top phase from the first step with fresh bottom phase. Similarly, Cheng et al. (2016) reported that the extraction yields of lignans hardly decreased and showed no difference after recycling five times. However, Show et al. (2013) demonstrated that when the top phase was recycled and the bottom aqueous phase reused for the subsequent stages, lipase extraction yields decreased from 99.2%, to 89.9%, then 73.2% for the first extraction and two consecutive recycling stages, respectively. This decrease in yield was attributed to the bottom phase being saturated with contaminants. When both top and bottom phases were recycled, the yields improved to 96.7% and 97.3% for two consecutive stages, indicating better performance when both phases are recycled. In another recycling study by Sankaran et al. (2018), lipase extraction yields were 71.69%, 58.87%, and 79.39% for the first extraction and two consecutive recycling stages where both the top and bottom phases were recycled.

Table 4.3 Effect of extraction and recycling on TPC yield (mg GAE/mg), flavonoids yield (mg RE/mg), and CGA yield (µg CGA/mg)

	Extraction	Recycling 1	Recycling 2	Extraction	Recycling 1	Recycling 2
		(NH ₄) ₂ SO ₄ /ethanol			NaH ₂ PO ₄ /ethanol	
TPC yield	0.050 ± 0.00 ^a	0.049 ± 0.00 ^a	0.051 ± 0.00 ^a	0.067 ± 0.00 ^b	0.075 ± 0.00 ^a	0.067 ± 0.00 ^b
Flavonoids yield	0.146 ± 0.00 ^a	0.141 ± 0.00 ^b	0.142 ± 0.00 ^b	0.248 ± 0.00 ^a	0.247 ± 0.00 ^a	0.247 ± 0.00 ^a
CGA yield	31.75 ± 0.27 ^a	31.85 ± 0.78 ^a	29.60 ± 0.09 ^a	39.75 ± 0.23 ^a	40.67 ± 0.99 ^a	39.10 ± 0.38 ^a
		Glucose/1-propanol			Maltose/1-propanol	
TPC yield	0.033 ± 0.00 ^a	0.036 ± 0.00 ^a	0.036 ± 0.00 ^a	0.025 ± 0.00 ^a	0.022 ± 0.00 ^a	0.022 ± 0.00 ^a
Flavonoids yield	0.062 ± 0.00 ^a	0.075 ± 0.01 ^a	0.080 ± 0.00 ^a	0.055 ± 0.00 ^a	0.054 ± 0.00 ^a	0.054 ± 0.00 ^a
CGA yield	19.62 ± 1.16 ^a	24.54 ± 3.09 ^a	24.52 ± 2.70 ^a	17.37 ± 0.22 ^a	17.13 ± 1.10 ^a	16.76 ± 0.16 ^a

Different superscripts indicate statistically significant difference between extraction, first, and second recycling stages at $P < 0.05$

When determining the feasibility of ATPE for industrial scale processing, it is important to consider the savings that would result from recycling and the reduction in fresh ATPE components needed for the process. In this study, the average amount of salt and ethanol recovered from the $(\text{NH}_4)_2\text{SO}_4$ /ethanol ATPE over the three extraction stages were 36.1% and 73.1%, respectively, where the salt was recovered after drying in the vacuum oven, while the ethanol was recovered after rotary evaporation. In comparison, for the NaH_2PO_4 /ethanol ATPE the average salt recovery was much lower at 8.9%, while the ethanol recovery was 69%. Experiments with glucose/1-propanol ATPE were able to recover 47.7% propanol, while 54% propanol was recovered with the maltose/1-propanol ATPE. In comparison to the average salt recovery of 60.8% and alcohol recovery of 69.9% reported by Show et al. (2013) for potassium phosphate/2-propanol ATPE, lower salt recoveries have been obtained the present work. It is possible that the low salt recoveries from our study could be due to the SPE cartridges used to purify the bottom phase for analysis. In any case, these results indicate that economic benefits would be possible when scaling up to the industrial scale, as small percentage recoveries would be significant at the larger scale.

4.5 Conclusion and Future Work

This study presented the effects of recycling ATPE phase-forming components. Using the recovery of TPC, flavonoids, and CGA from haskap leaves as an applied model, two recycling stages for ammonium sulphate/ethanol, sodium phosphate/ethanol, glucose/1-propanol, and maltose/1-propanol ATPE produced consistent partitioning, extraction efficiencies, and extraction yields. We concluded that recycling has the potential to reduce the amount of materials and post handling costs required for ATPE while maintaining its performance. Further studies may include integration of sugar crystallization with ATPE to enhance its sustainability.

Connecting Statement 3

Chapter 4 has shown that ATPE phase-forming components can be recycled for two stages while maintaining the extraction efficiency. However, the glucose and maltose used in the sugar/propanol ATPE systems could not be separated from the slurries. In view of this and the higher extraction efficiencies shown by salt/ethanol ATPE systems in Chapter 3, two ATPS, namely ammonium sulphate/ethanol and sodium dihydrogen phosphate/ethanol, were selected for the following investigations in Chapter 5.

Chapter 5 evaluates aqueous two-phase flotation (ATPF) which is a bubble-assisted ATPE, for the extraction of bioactives from haskap leaves. In this work, the salt-based ATPS and haskap leaves were placed in a flotation column. Air was passed through a frit at the bottom of the column, producing bubbles which serve as surfaces for the biomolecules to adsorb. The rising bubbles were hypothesized to increase extraction efficiency as it facilitates mass transfer of bioactive compounds to the top phase.

Chapter 5 is based on an article reproduced from *Food and Bioprocess Technology* with permission from Springer Nature. The details of the article are as follows:

Chong, K. Y., Stefanova, R., Zhang, J., & Brooks, M. S. L. (2020). Extraction of Bioactive Compounds from Haskap Leaves (*Lonicera caerulea*) Using Salt/Ethanol Aqueous Two-Phase Flotation. *Food and Bioprocess Technology*, 13, 2131–2144.

Chapter 5 : Extraction of Bioactive Compounds from Haskap Leaves (*Lonicera caerulea*) using Salt/Ethanol Aqueous Two-Phase Flotation

5.1 Abstract

Aqueous two-phase flotation (ATPF) was used for the extraction and partial purification of bioactive compounds from haskap leaves. Two ATPF systems, ammonium sulphate/ethanol and sodium phosphate/ethanol, were compared. A Box-Behnken approach was used to investigate the operating parameters which included sample loading (5.0, 52.5, and 100.0 mg), flotation time (5, 62.5, 120 minutes), and air flow rate (11.4, 20.0, 28.6 mL/min). Response surface optimization was performed to maximize the yields of chlorogenic acid (CGA), flavonoids, and total phenolics (total phenolic content, TPC). At the optimized parameters for the ammonium sulphate/ethanol ATPF system (i.e. 5 mg leaves, 120 min flotation time, and air flow rate of 28.6 mL/min), the extraction efficiencies were 97.1%, 98.7%, and 99.6% for CGA, flavonoids, and TPC, respectively. The corresponding partition coefficients were 29.6 for CGA, 62.4 for flavonoids, and 231.4 for TPC. Quantitation of individual compounds using high-performance liquid chromatography showed that ATPF with ammonium sulphate/ethanol achieved yields of 0.031 mg CGA/mg dry mass leaves, 0.027 mg rutin/mg dry mass leaves, 0.006 mg luteolin-7-*O*-glucoside/mg dry mass leaves, and 0.007 mg diosmin/mg dry mass leaves. Based on the overall extraction performance, ammonium sulphate/ethanol ATPF is the preferred system in comparison to sodium phosphate/ethanol ATPF, for the extraction of bioactive compounds from haskap leaves.

5.2 Introduction

Haskap plants or blue honeysuckle, *Lonicera caerulea*, are known for their berries which are rich in antioxidants due to the presence of various bioactive compounds such as anthocyanins and flavonoids (Celli et al., 2014; Khattab et al., 2016). They have recently gained interest as a commercial crop in North America, particularly Canada, due to their ability to withstand severe cold climates, such as in the northern prairie region (Hummer et al., 2012). These deciduous shrubs shed their leaves annually, resulting in an abundant source of leaves. Studies have shown that haskap leaves contain a range of metabolites

such as chlorogenic acid, flavonoids, loganin, secologanin, and triterpenoids (Becker et al., 2017; Bonarska-Kujawa et al., 2014; Dawson, 2017; Machida et al., 1995; Oszmiański et al., 2011). Chlorogenic acid for instance, can be used to treat inflammation and hypertension (Naveed et al., 2018), and quercetin, which is a major flavonoid in haskap leaves, has demonstrated anticancer properties from *in vitro* studies and prevented cardiovascular diseases (Wang et al., 2016). The polyphenol content in the leaves can also contribute to antioxidative properties which can lower oxidative stress, DNA mutations, and other forms of cell damage (Pisoschi & Pop, 2015). These health-promoting properties make the leaves from haskap plants a valuable by-product stream that could have applications in many industries that produce health supplements, functional foods and consumer products such as cosmetics and personal health products.

Conventional extraction methods such as maceration (Radojković et al., 2016) and distillation (Donelian et al., 2009) have many drawbacks. These methods usually rely on toxic organic solvents in large volumes, have low extraction efficiencies, require multiple steps, and use high temperatures which may cause degradation to thermolabile bioactive compounds. In the recent years, there are emerging extraction technologies such as ultrasound-assisted extraction (Horžić et al. 2012; Jiang et al. 2019), microwave-assisted extraction (Krishnaswamy et al., 2013; Périno-Issartier et al., 2011; Routray & Orsat, 2012), pulsed ohmic heating (El Darra et al., 2013), and supercritical extraction (Bimakr et al., 2012; Leal et al., 2007; Pereira & Meireles, 2010). These techniques require sophisticated equipment such as ultrasound transducer, magnetron, electrodes, and high-pressure pumps, respectively. Aqueous two-phase flotation (ATPF) is explored as an emerging mild extraction technique for recovering biomolecules, and integrates both aqueous two-phase extraction (ATPE) and solvent sublation. ATPE uses an aqueous two phase system (ATPS) comprised of two incompatible aqueous components that partition into two distinct phases (Hatti-Kaul, 2000). ATPE occurs when solutes from a solid or liquid are selectively partitioned in an ATPS. Solvent sublation occurs in the ATPF system when the biomolecules adsorb onto the surface of rising gas bubbles and concentrate in the top phase after some time (Bi, Dong, & Dong, 2010). ATPF promotes both the mass transfer of the biomolecules via solvent sublation and simultaneous selective partitioning between two

aqueous phases. As ATPF can be designed to use less toxic phase-forming components such as alcohols and salts, it is an environmentally friendly technique for separation, concentration, and partial purification of biomolecules. The high water content of an ATPS and its ability to occur at lower temperatures provides a mild extraction environment for the leaves. ATPF has been used to extract baicalin, a flavone glycoside (Bi et al., 2013), betacyanin (Leong, Ooi, Law, Julkifle, Ling, et al., 2018), puerarin, an isoflavone (Bi, Dong, & Yuan, 2010), polyphenols (de Araújo Padilha et al., 2018), bromelain (Pakhale et al., 2013), lincomycin, an antibiotic (Li & Dong, 2010), and various proteins (Lakshmi et al., 2012; Nandini & Rastogi, 2011; Ng et al., 2020; Platis & Labrou, 2006). As ATPF has a simple set-up, requiring only a flotation column and an air source, it is easy to scale-up and much cheaper than emerging extraction technologies, as mentioned previously (Lee et al., 2016). ATPF can be optimized by the classical one factor-at-a-time method or by the design of experiments approach. The former method can be time-consuming and involves numerous experimental runs. With the design of experiments approach, response surface methodology (RSM) allows users to examine the interaction effects between different variables and to minimize the number of experimental runs required. RSM has been successfully applied in other ATPE work (Cheng et al. 2017; Jiang et al. 2019; Ma et al. 2013) and ATPF work (Han et al., 2014; Padilha et al., 2017).

The objective of this research was to compare the performance of ATPF in two salt/ethanol systems, namely ammonium sulphate $(\text{NH}_4)_2\text{SO}_4$ /ethanol and sodium dihydrogen phosphate NaH_2PO_4 /ethanol, for the extraction of bioactive compounds from haskap leaves. Both are categorized as generally recognized as safe (GRAS) substances, where $(\text{NH}_4)_2\text{SO}_4$ is used as a dough strengthener and firming agent while NaH_2PO_4 is used as a thickening agent and emulsifier in animal feed (U.S. Food and Drug Administration, 2020). These ATPS were the focus of this work, as they have shown promising results in a recent ATPE study (Chong et al., 2020a) and the extracts have the benefit of being compatible in food and consumer care products. Three factors, sample loading, flotation time, and air flow rate, were optimized based on bioactive extraction yields using response surface methodology (RSM). Specifically, analyses of chlorogenic acid (CGA), flavonoids, and total phenolic content (TPC) were conducted using UV-Vis spectrophotometric assays. The

optimized extracts were then analyzed using high-performance liquid chromatography (HPLC) and the ATPF technique was compared to ATPE and conventional extraction. The novelty of this work is that it is the first study that investigates and optimizes the extraction of bioactive compounds from haskap leaves using ATPF. This work will explore the feasibility of ATPF as an assisted “green” extraction technology that uses leaves as a sustainable by-product obtained from haskap cultivation and produces natural extracts that will have wide application in food and consumer care products.

5.3 Materials and Methods

5.3.1 Materials

Ethyl alcohol (95% volume) was obtained from Greenfield Specialty Alcohols Inc. (Toronto, Ontario, Canada). Methanol ($\geq 99.9\%$) was supplied by VWR Analytical (Mississauga, Ontario, Canada). Sodium dihydrogen phosphate 96% and diosmin were purchased from Alfa Aesar (Ward Hill, Massachusetts, USA). The following chemicals were purchased from Sigma-Aldrich (Oakville, Ontario, Canada): 1-propanol ($\geq 99\%$, food grade), ammonium sulphate (ACS, $\geq 99\%$), sodium nitrite ($\geq 97\%$, ACS), aluminum nitrate nonahydrate (ACS, $\geq 97\%$), sodium carbonate (ACS, 99.95-100.05% dry basis), Folin & Ciocalteu’s phenol reagent (2N), gallic acid monohydrate (ACS, $\geq 98\%$), chlorogenic acid ($\geq 95\%$, titration), and rutin hydrate ($\geq 94\%$, HPLC grade). In addition, rutin-7-O-glucoside (95.1%) was purchased from ChromaDex and deionized water was obtained from a Milli-Q water purification system (Millipore, Bedford, Massachusetts, USA).

Fresh leaves were harvested in July 2018 from haskap plants of the Aurora variety which were in their first growth year in Nova Scotia, Canada. The geographical coordinates of the harvest location are 44°28'10.8"N, 64°39'25.6"W. The fully developed leaves were picked after the berries had been harvested. At this stage of the plant growth cycle, there were signs of natural senescence (leaf browning) starting to occur on some parts of the plant, however the majority of the leaves on the haskap plants were still green. For this study, leaves that appeared green without any browning were selected for harvesting. The samples were frozen at $-20\text{ }^{\circ}\text{C}$ and subsequently freeze-dried in a Labconco FreeZone 2.5 Plus freeze dryer (Labconco, Kansas City, MO, USA). The dried samples were sealed in

vacuum pouches and stored at $-20\text{ }^{\circ}\text{C}$ in the dark. Before each independent experiment, samples were ground and sieved through a $500\text{ }\mu\text{m}$ mesh opening. Validation studies were performed at the end of the second independent experiment.

5.3.2 Methods

5.3.2.1 Extraction

Conventional Extraction

Conventional extraction was performed using maceration in an incubator shaker (G25 Controlled Environment Incubator Shaker, New Brunswick Scientific, New Jersey, USA) at 200 rpm. Ground leaves were agitated with 80% (v/v) methanol for 24 hours at $25\text{ }^{\circ}\text{C}$ (Safdar et al., 2017). The extract was centrifuged (Sorvall T1 centrifuge, Thermo Scientific, USA) at 1500 g for 1 minute and the supernatant was analyzed using UV-Vis spectroscopy.

Aqueous Two-Phase Flotation (ATPF)

A schematic diagram of the ATPF set-up at $25\text{ }^{\circ}\text{C}$ is shown in Figure 5.1. A glass chromatography column with a length of 28.5 cm from the porous disc to top of the column and internal diameter of 1.5 cm was used as the flotation column. A porous stainless-steel disc with pore size of $10\text{ }\mu\text{m}$ and 1.27 cm diameter was fitted at the bottom end of the column to generate bubbles. A variable-area flowmeter (Cole-Parmer Instruments Co., Chicago, IL) was connected to the column to regulate the air flow rate. The surface-active compounds would then attach to the air bubbles and rise to the top phase.

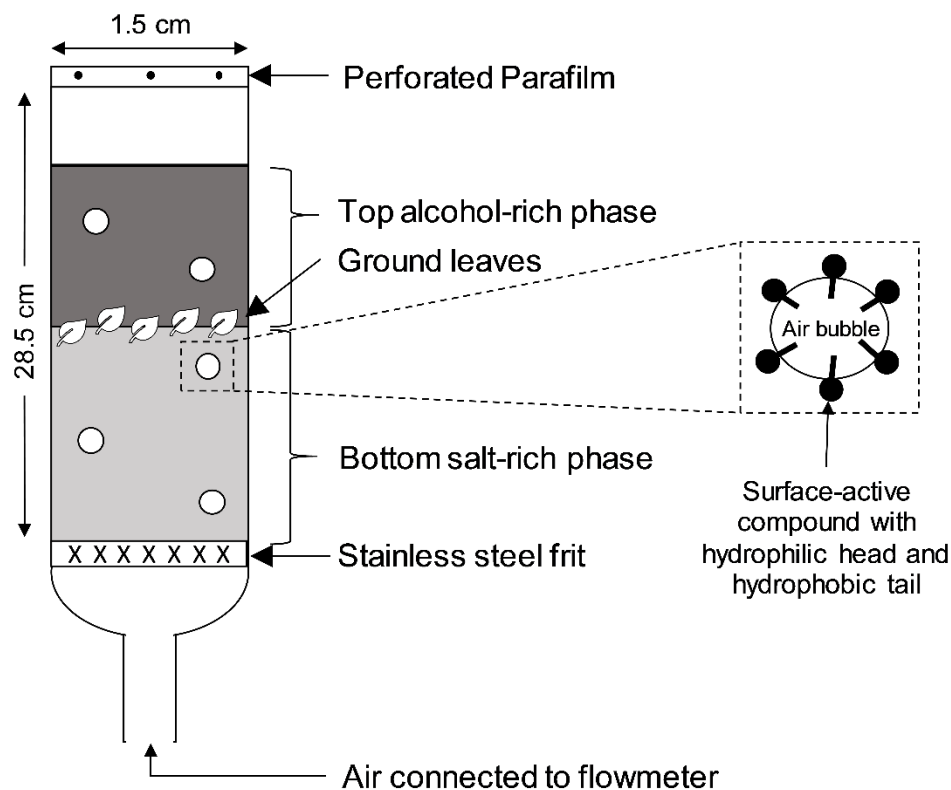


Figure 5.1 Experimental set-up of ATPF

Ammonium sulphate/ethanol and sodium phosphate/ethanol ATPSs were used in this study. Salt/ethanol ATPSs were used as they have been proven to extract high yields of bioactive compounds from an earlier work (Chong et al., 2020a). The ATPS composition was selected based the same earlier work which maximized the yields of bioactive compounds in haskap leaves. The composition for $(\text{NH}_4)_2\text{SO}_4$ /ethanol ATPS was 20 wt% $(\text{NH}_4)_2\text{SO}_4$, 27.5 wt% ethanol, and 52.5 wt% water while the composition for NaH_2PO_4 /ethanol ATPS was 10 wt% NaH_2PO_4 , 37.0 wt% ethanol, and 53 wt% water. The pH of $(\text{NH}_4)_2\text{SO}_4$ /ethanol ATPS top phase was 5.54 while the pH for NaH_2PO_4 /ethanol ATPS top phase was 3.81. The experiments were performed at 25 °C. An ATPS of 20 g was added into the column with ground leaves which were weighed using an analytical balance with a precision of ± 0.1 mg (Denver Instrument PI-314, Bohemia, New York, USA). The solution and ground leaves were mixed vigorously by switching on the air flow at 28.6 mL/min for 30 seconds. The corresponding superficial air velocity was 0.0027 m/s. This mixing step was consistently performed for all ATPF experiments to ensure a homogenous phase prior to

the partitioning mechanism. Then the experiment was conducted according to a specific set of operating parameters, as described in Table 5.1. At the end of the reaction time, the air supply was turned off to equilibrate the system for 1 minute. The top and bottom phases were gently removed from the column, ensuring that the leaves at the interphase remained in the column, and their respective volumes recorded. The top phase from each experiment was then analyzed using the UV-Vis spectrophotometric methods described in Section 3.3.2.2. Solid phase extraction (SPE) was used to purify the bottom phase prior to analysis. Briefly, Hypersep SPE 500 mg/2.8 mL C18 cartridges (Thermo Scientific, Rockwood, Tennessee, USA) were preconditioned and equilibrated with water prior to sample loading. The cartridges were then washed with acidified water, 0.1% (v/v) formic acid, to remove the salt components and the organic fractions were eluted with 75% (v/v) and 100% ethanol. These fractions were dried under nitrogen and dissolved in 80% (v/v) methanol prior to analysis using UV-Vis spectroscopy.

Aqueous Two-Phase Extraction (ATPE)

ATPE was conducted as a comparison by using the same sample loading and extraction time from Table 5.1. Ground leaves were mixed for 30 seconds in the flotation column as described above, however air was not introduced for ATPE. Analysis was conducted as described previously for ATPF extracts.

Water Extraction

For comparison with ATPF, the ground leaves were extracted with water in the flotation column at the optimized operating parameters obtained from ATPF. The same parameters ie. sample loading, flotation time, and air flow rate in Table 5.1 were used. The experiment was also conducted without air (i.e. no flotation) using water at the same operating parameters for comparison with ATPE.

Table 5.1 Box Behnken experimental design matrix and yields (mg/mg leaves) from two independent experiments

Run	Sample loading (mg)	Flotation time (min)	Air flow rate (mL/min)	Ammonium sulphate/ethanol ATPF			Sodium phosphate/ethanol ATPF		
				CGA yield	Flavonoids yield	TPC yield	CGA yield	Flavonoids yield	TPC yield
1 ^a	52.5	62.5	20	0.041 ± 0.001	0.174 ± 0.002	0.061 ± 0.004	0.039 ± 0.006	0.213 ± 0.006	0.090 ± 0.002
2	52.5	120	11.4	0.039 ± 0.003	0.162 ± 0.015	0.058 ± 0.003	0.046 ± 0.001	0.219 ± 0.005	0.090 ± 0.004
3	5	5	20	0.018 ± 0.006	0.195 ± 0.022	0.073 ± 0.011	0.038 ± 0.003	0.227 ± 0.031	0.105 ± 0.008
4 ^a	52.5	62.5	20	0.040 ± 0.001	0.171 ± 0.004	0.060 ± 0.001	0.040 ± 0.05	0.212 ± 0.005	0.086 ± 0.003
5	5	62.5	28.6	0.044 ± 0.001	0.192 ± 0.004	0.074 ± 0.003	0.017 ^b	0.197 ^b	0.099 ^b
6	52.5	120	28.6	0.049 ± 0.001	0.203 ± 0.006	0.070 ± 0.000	0.049 ± 0.002	0.235 ± 0.021	0.091 ± 0.007
7	100	62.5	11.4	0.033 ± 0.001	0.135 ± 0.004	0.047 ± 0.002	0.044 ± 0.000	0.257 ± 0.003	0.079 ± 0.001
8	100	5	20	0.032 ± 0.002	0.149 ± 0.004	0.050 ± 0.001	0.039 ± 0.001	0.223 ± 0.005	0.072 ± 0.002
9	52.5	5	11.4	0.036 ± 0.001	0.158 ± 0.007	0.050 ± 0.000	0.039 ± 0.003	0.178 ± 0.022	0.082 ± 0.002
10	100	120	20	0.041 ± 0.001	0.166 ± 0.005	0.059 ± 0.002	0.047 ± 0.000	0.303 ± 0.016	0.084 ± 0.001
11	5	120	20	0.058 ± 0.072	0.229 ± 0.029	0.083 ± 0.007	0.040 ± 0.002	0.240 ± 0.026	0.107 ± 0.008
12 ^a	52.5	62.5	20	0.038 ± 0.000	0.164 ± 0.000	0.060 ± 0.000	0.048 ± 0.000	0.220 ± 0.001	0.091 ± 0.003
13	52.5	5	28.6	0.036 ± 0.001	0.163 ± 0.006	0.055 ± 0.006	0.041 ± 0.001	0.184 ± 0.013	0.081 ± 0.002
14	100	62.5	28.6	0.043 ± 0.001	0.169 ± 0.007	0.057 ± 0.002	0.048 ± 0.002	0.284 ± 0.020	0.070 ± 0.007
15	5	62.5	11.4	0.029 ± 0.002	0.177 ± 0.005	0.073 ± 0.002	0.062 ± 0.002	0.220 ± 0.006	0.102 ± 0.003

^a denotes center points

^b Run 5 of sodium phosphate/ethanol ATPF was based on one independent experiment due to the column overflowing after several other attempts

5.3.2.2 UV-Vis Spectrophotometric Analysis of Bioactive Compounds

Individual calibration curves were plotted for the two ATPS used to minimize salt interference (Golunski et al., 2016). Samples were diluted when necessary using the corresponding top phase to ensure that the measurements were in the range of the calibration curve. Chlorogenic acid, flavonoid content, and total phenolic content (TPC) were determined according to Section 3.3.2.2.

5.3.2.3 Performance Indicators

Three performance indicators, yield, partition coefficient (k) and extraction efficiency (EE) were used to assess the effectiveness of the ATPF and ATPE experiments. These indicators were determined according to Section 3.3.2.3.

5.3.2.4 Design of Experiment, Optimization, and Statistical Analysis

Table 5.1 shows the RSM design using a Box-Behnken approach with the factors and their levels in parentheses: sample loading (5.0, 52.5, and 100.00 mg), flotation time (5, 62.5, 120 minutes), and air flow rate (11.4, 20.0, 28.6 mL/min). A Box-Behnken design allows efficient estimation of the first and second-order coefficients of mathematical models (Bezerra et al., 2008). Since the total mass of the ATPS was 20 g, the sample loading can be expressed as 0.025%, 0.263%, and 0.5% (w/w) for 5.0, 52.5, and 100.0 mg leaves, respectively. The maximum sample loading of 100 mg was selected so that the top and bottom phases could be identified (Chong et al., 2020a) and the maximum flotation time of 120 minutes was based on other ATPF studies (Bi, Dong, & Yuan, 2010; Lin et al., 2015). Preliminary tests showed that the maximum air flow rate that could be used with the solution and column was 28.6 mL/min, as higher air flow rates resulted in the column overflowing due to increased gas holdup (Besagni & Inzoli, 2017). Two independent experiments comprising of 15 base runs were performed in randomized order for each type of salt/ethanol system and the yields for CGA, flavonoids, and TPC were determined from triplicate analyses. The behavior of the response surface was modelled with a second-order polynomial, as shown by Equation 5.1.

$$Y_i = \beta_0 + \beta_{AA}A + \beta_{BB}B + \beta_{CC}C + \beta_{AAA}A^2 + \beta_{BBB}B^2 + \beta_{CCC}C^2 + \beta_{AB}AB + \beta_{AC}AC + \beta_{BC}BC \quad (5.1)$$

Here, Y_i is the yield and β_0 is the estimated constant coefficient; β_A , β_B , and β_C are the estimated coefficients for linear effect terms; β_{AA} , β_{BB} , and β_{CC} are the estimated coefficients for quadratic terms; and β_{AB} , β_{AC} , and β_{BC} are the estimated coefficients for interaction terms. A , B , and C are the uncoded independent variables for sample loading, flotation time, and air flow rate, respectively. Final models were obtained for each yield by manually removing insignificant variables ($P > 0.01$ for the ammonium sulphate/ethanol ATPF and $P > 0.05$ for the sodium phosphate/ethanol ATPF) while following the hierarchical model convention and retaining all lower order terms for significant interactions.

Analysis of variance (ANOVA) and response surface optimization were performed using Minitab statistical software (Version 18, Minitab Inc. USA). One-way ANOVA was used to test for significant differences between means using Tukey's multiple comparison test, and error bars included in figures and tables represent the standard error of means (SEM). Multi-response optimization was used to predict the conditions that would result in maximized yields for CGA, flavonoids and TPC. The results were then validated experimentally and Equation 5.2 was used to compare the predicted and experimental values.

$$Deviation (\%) = \left| \frac{Experimental\ value - Predicted\ value}{Predicted\ value} \right| \times 100 \quad (5.2)$$

5.3.2.5 High Performance Liquid Chromatography (HPLC) Analysis for Optimized Conditions

Prior to analysis, the top phase from the optimized extraction was dried using a centrifugal evaporator (Genevac EZ-2, SP Scientific, New York, USA) and then dissolved in distilled water. This aqueous solution was loaded onto a 500 mg/2.8 mL C18 solid phase extraction cartridge (Thermo Scientific, Rockwood, Tennessee, USA) which had been preconditioned with methanol and equilibrated with water. The cartridge was then washed with acidified water, 0.1% (v/v) formic acid, to remove the salt. The desired compounds were subsequently eluted with a solution of 75% (v/v) aqueous ethanol with 0.1% (v/v) formic acid, followed by 100% ethanol. These organic

fractions were then dried under nitrogen. Prior to HPLC analysis, the organic fractions were dissolved in 1 mL of 50% (v/v) methanol.

HPLC analysis was conducted using an Agilent 1200 HPLC system (Agilent, Waldbronn, Germany) equipped with a quaternary pump (Agilent G1311A), an autosampler (G1329A), a column compartment with temperature controller (G1316A), and a diode array detector (G1315B). The column (Zorbax SB-C18, 1.8 μm , 4.6 mm \times 50 mm, Agilent, U.S.A.) was eluted with a mobile phase consisting of (A) 0.1% (v/v) formic acid in Milli-Q water and (B) 0.1% (v/v) formic acid in acetonitrile using a gradient of 1% to 99% B in 25 minutes at a flow rate of 0.3 mL/min. The injection volume was 1 μL and the column temperature was maintained at 40 $^{\circ}\text{C}$. Elution was monitored at 320 and 250 nm on the diode array detector. Chlorogenic acid, rutin, luteolin-7-*O*-glucoside, and diosmin were quantified using linear regression equations obtained from five-point calibration curves. These compounds were selected for HPLC analysis as they had been identified and quantified in haskap leaves (Dawson, 2017).

5.4 Results and Discussion

5.4.1 Response Surface Regression

The coefficients for response surface equations are shown in Table 5.2. All the models were statistically significant at $P < 0.01$ for ATPF using ammonium sulphate/ethanol and $P < 0.05$ for ATPF using sodium phosphate/ethanol, except for the CGA yield from ATPF using sodium phosphate/ethanol. Upon detailed examination, only the interaction between sample loading and air flow rate (A*C) was significant with a P value of 0.002. Its R^2 value of 0.3887 shows that this model for CGA yield can only account for 38.87% of the variability of the response around its mean. Our previous study also showed insignificant models for CGA yields obtained from the glucose/1-propanol ATPS (Chong et al., 2020a). In our analysis, blocking was included between the first and second independent experiment to minimize bias and reduce unexplained variability. It was found that the blocks were insignificant except for flavonoids yield using sodium phosphate/ethanol.

Table 5.2 Regression coefficients for yields obtained from ATPF

Coefficient ^a	Ammonium sulphate/ethanol ATPF ^b			Sodium phosphate/ethanol ATPF ^b		
	CGA Yield	Flavonoids Yield	TPC Yield	CGA Yield	Flavonoids Yield	TPC Yield
β_0	0.00988	0.1737	0.059	0.0791	0.20857	0.08818
β_A	0.00018	-0.02188	-0.01125	-0.000506	0.02192	-0.0079
β_B	0.000285	0.01181	0.00537	N/A	0.02319	0.00181
β_C	0.000531	0.01181	0.00337	-0.001954	N/A	-0.00704
β_{AA}	N/A	N/A	0.00562	N/A	0.03626	N/A
β_{BB}	N/A	N/A	N/A	N/A	N/A	N/A
β_{CC}	N/A	N/A	N/A	N/A	N/A	N/A
β_{AB}	-0.000003	N/A	N/A	N/A	0.01688	N/A
β_{AC}	N/A	N/A	N/A	0.000028	N/A	N/A
β_{BC}	N/A	N/A	N/A	N/A	N/A	N/A
R^2	0.7375	0.7084	0.8378	0.3887	0.8308	0.5286
R^2 (adj)	0.6829	0.6617	0.8040	0.2869	0.7940	0.4500
R^2 (pred)	0.5246	0.5603	0.7409	0.00	0.7139	0.3414
P (model) ^c	0.000	0.000	0.000	0.015	0.000	0.001
P (lack of fit) ^c	0.024	0.026	0.089	0.233	0.037	0.228
P (blocks) ^c	0.208	0.031	0.087	0.443	0.002	0.112

^a β_0 is the estimated constant coefficient

β_A , β_B , and β_C are the estimated coefficients for linear effect terms

β_{AA} , β_{BB} , and β_{CC} are the estimated coefficient for quadratic terms

β_{AB} , β_{AC} , and β_{BC} are the estimated coefficient for interaction terms

A , B , and C are the uncoded independent variables for sample loading, flotation time, and air flow rate

^b N/A not applicable; factor was not significant. The equations were averaged over blocks

^c A 99% confidence interval was used for ammonium sulphate/ethanol ATPF while a 95% confidence interval was used for sodium phosphate/ethanol ATPF

The effects of sample loading, flotation time, and air flow rate are illustrated in Figure 5.2, where selected three-dimensional surface plots are shown. As surface plots illustrate interactions between two factors, the third factor was held at the zero level in coded units. Figure 5.2 (a) and (c) show that as sample loading increased from 5 to 100 mg, the yields for CGA and TPC decreased, which may have been due to the larger amount of leaves forming a barrier blocking the bubble flow to the top phase, resulting in lower yields. Similarly, other studies have attributed decreasing yields to an increased viscosity in the bottom phase preventing the bubbles from rising effectively (Koyande et al., 2019). Other studies have reported a volume exclusion effect, which can occur

when there is reduced space in the top phase for the biomolecules to partition (Ng et al., 2020) therefore decreasing the yields.

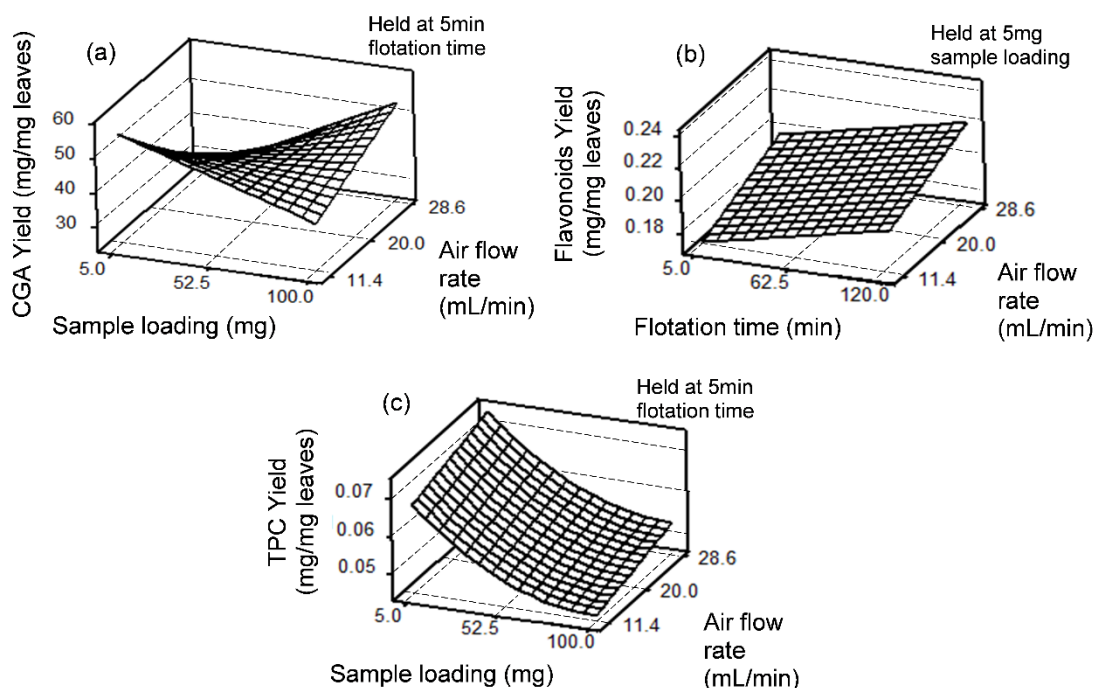


Figure 5.2 Interaction effects on (a) CGA yield from sodium phosphate/ethanol ATPF; and (b) flavonoids yield, and (c) TPC yield from ammonium sulphate/ethanol ATPF

In Figure 5.2, it is evident that as the air flow rate increased from 11.4 to 28.6 mL/min, the yields for CGA and TPC increased. This behaviour has been attributed to the higher air flow rates generating more air bubbles and increasing the surface area for the adsorption of biomolecules (de Araújo Padilha et al., 2018; Koyande et al., 2019); however, there is a limit to the maximum allowable air flow rate to avoid foam accumulation (Bi et al., 2013). Figure 5.2 (b) shows that the flavonoids yield increased with increasing flotation time from 5 to 120 minutes. This can be attributed to an increase in the biomolecules adsorbing onto the bubble surface with the greater flotation time. Other studies reported similar trends with increased recoveries of isoflavone (Bi, Dong, & Yuan, 2010) and proteins (Tham et al., 2019) obtained with increased flotation time.

Figure 5.2 (a) also shows the interaction effects of sample loading and air flow rate. Here, the maximum CGA yield of about 0.052 mg/mg leaves from ATPF with sodium

phosphate/ethanol is shown at a sample loading of 5 mg and air flow rate of 11.4 mL/min. However, high CGA yields of around 0.050 mg/mg leaves are also observed at a sample loading of 100 mg and air flow rate of 28.6 mL/min. The presence of these two scenarios with high CGA yields in the sodium phosphate/ethanol system may be due to a poor regression fit, as shown in Table 5.2. The highest flavonoids yield of about 0.220 mg RE/mg leaves was achieved at 120 min flotation time and 28.6 mL/min air flow rate while the highest TPC yield of 0.077 mg/mg leaves was reached at a low sample loading of 5 mg and high air flow rate of 28.6 mL/min (Figure 5.2 (b) and (c), respectively).

5.4.2 Optimization of ATPF

The operating conditions were optimized for maximum CGA yield, flavonoids yield, and TPC yield from haskap leaves. For all responses, the weight factor was set to 1 to ensure equal importance on the desirability. Table 5.3 shows two optimized solution for each ATPF system, individual desirability values, and validation results. The overall desirability, D is a measure of how well the goals for the three responses were optimized, and ranges from 0 to 1, where 1 represents the ideal situation and 0 indicates that one or more responses are out of their acceptable limits.

Table 5.3 Optimized parameters of ATPF, desirability, and validation results for CGA yield (mg/mg leaves), flavonoids yield (mg RE/mg leaves), and TPC yield (mg GAE/mg leaves)

Responses	Individual desirability, d	Predicted value	Experimental value	Deviation (%)
(NH₄)₂SO₄/ethanol: 5 mg leaves, 120 min flotation time, 28.6 mL/min air flow rate.				
$D = 0.81^a$				
CGA yield	0.88	0.058	0.035	39.7
Flavonoid yield	0.69	0.219	0.307	40.0*
TPC yield	0.86	0.085	0.097	14.6
NaH₂PO₄/ethanol: 5 mg leaves, 120 min flotation time, 11.4 mL/min air flow rate.				
$D = 0.61^a$				
CGA yield	0.61	0.056	0.034	39.3
Flavonoid yield	0.45	0.229	0.193	15.6
TPC yield	0.82	0.105	0.093	11.7

^a D : overall desirability

*value is outside of 99% prediction interval

The optimized parameters for ATPF using ammonium sulphate/ethanol were 5 mg leaves, 120 min flotation time, and 28.6 mL/min for the air flow rate, while the optimized parameters for ATPF using sodium phosphate/ethanol were 5 mg leaves, 120 min flotation time, 11.4 mL/min for the air flow rate. Their composite desirabilities of 0.81 and 0.61 are considered ‘very good’ and ‘satisfactory’ (Lazic, 2006).

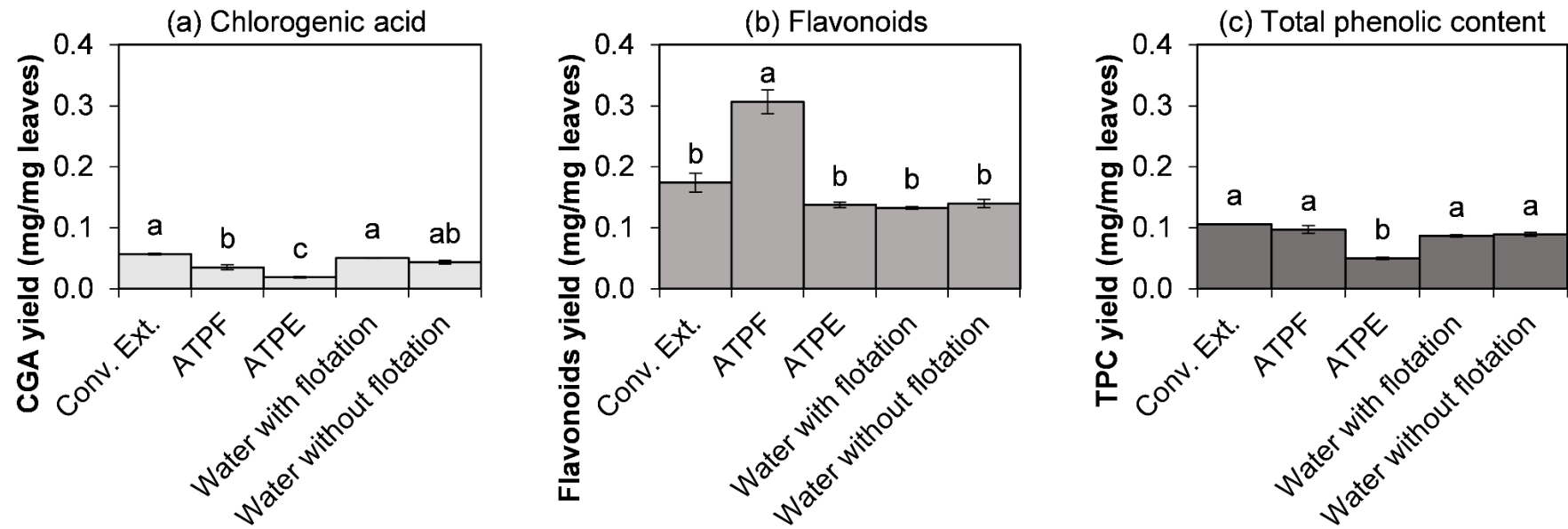
Deviations between the experimental and predicted values were within the 99% prediction interval except for the flavonoids yield from ATPF using ammonium sulphate/ethanol. This is in keeping with the predicted R^2 value of 0.56 for the flavonoids yield in Table 5.2. It is possible that the nine-day period between the completion of the ammonium sulphate/ethanol ATPF experiments and the experimental validation could have contributed to the results outside of the 99% prediction interval. In a separate experiment to investigate the effect of frozen storage time on the bioactive content of the ground leaves, the flavonoids yield was found to increase by 0.027 mg/mg leaves after nine days (data not shown). This was also observed in other produce where transient increases were noted for some bioactive compounds with longer postharvest storage time (Kevers et al., 2007; Piljac-Žegarac & Šamec, 2011; Sanchez-Ballesta et al., 2007).

5.4.3 Comparison of Optimized Parameters with Aqueous Two-Phase Extraction

Figure 5.3 shows the results from different extraction methods for ammonium sulphate/ethanol systems. Using the optimized parameters, ATPF with ammonium sulphate/ethanol yielded 0.035 mg CGA/mg leaves, 0.307 mg RE/mg, and 0.100 mg GAE/mg while ATPE resulted in 0.019 mg CGA/mg, 0.138 mg RE/mg, and 0.050 mg GAE/mg. This significant improvement in yield can be attributed to the role of the bubbles in ATPF, where the biomolecules are adsorbed onto the bubble surface and greater extraction results as the bubbles rise up to the top phase (de Araújo Padilha et al., 2018; Leong, Ooi, Law, Julkifle, Ling, et al., 2018). Conventional extraction which was performed for 24 hours yielded 0.057 mg CGA/mg leaves, 0.174 mg RE/mg, and 0.106 mg GAE/mg. Whereas extractions using water and conducted with and without flotation yielded 0.051 and 0.044 mg CGA/mg leaves, 0.133 and 0.140 mg RE/mg leaves, and 0.087 and 0.089 mg GAE/mg leaves, respectively. Although water extraction achieved yields that were comparable to those from conventional extraction, there are disadvantages associated with using water as the solvent, such as the high

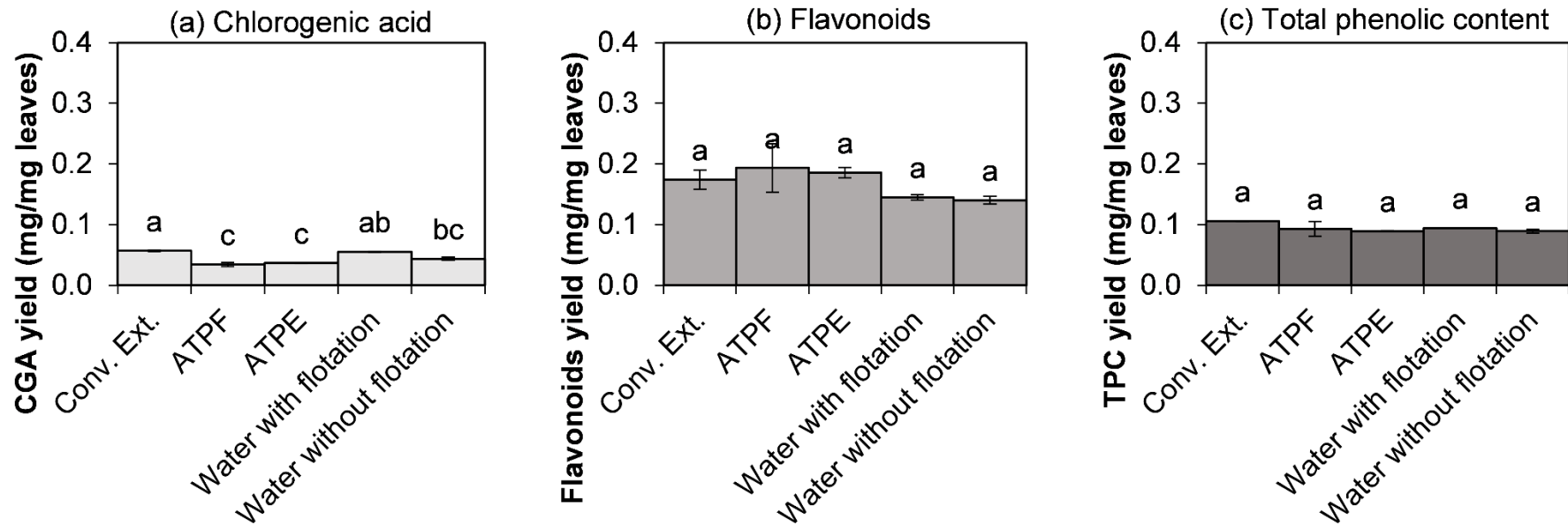
energy requirement for the removal of water (Chemat et al., 2019). Moreover, as water is a polar solvent, non-polar compounds would have limited extractability in this solvent system. Other berry leaves such as blueberry leaves had 0.164 mg GAE/mg leaves (Routray et al., 2014) while Chilean berry leaves ranged from 0.11 to 0.13 mg GAE/mg leaves (López de Dicastillo et al., 2017).

Figure 5.4 shows the yield comparison between different extraction methods for sodium phosphate/ethanol systems. For ATPF using sodium phosphate/ethanol, yields of 0.034 mg CGA/mg, 0.19 mg RE/mg, and 0.09 mg GAE/mg were obtained while ATPE resulted in 0.037 mg CGA/mg, 0.19 mg RE/mg, and 0.09 mg GAE/mg. The results indicate that there was no significant difference between the yields obtained from ATPF and ATPE for sodium phosphate/ethanol systems.



Different letters in each plot indicate significant difference between extraction methods

Figure 5.3 Yield comparison between conventional extraction, ATPF and ATPE using ammonium sulphate/ethanol, water extraction with flotation, and water extraction without flotation



Different letters in each plot indicate significant difference between extraction methods

Figure 5.4 Yield comparison between conventional extraction, ATPF and ATPE using sodium phosphate/ethanol, water extraction with flotation, and water extraction without flotation

Table 5.4 shows the partition coefficient and extraction efficiency of the optimized ATPF parameters with the values obtained by ATPE as a comparison. Here, the partition coefficient of 29.6 from ATPF with the ammonium sulfate/ethanol system indicates that the top phase is 29.6 times more concentrated than the bottom phase. All the partition coefficient values were more than 1 and this implies that partial purification had occurred as the top phase is more concentrated than the bottom phase.

Table 5.4 Comparison of partition coefficient, *k*, and extraction efficiency, EE (%), of ATPF and ATPE for ammonium sulphate/ethanol and sodium phosphate/ethanol systems

Performance indicators (Average ± SEM)	Ammonium sulphate/ethanol		Sodium phosphate/ethanol	
	ATPF	ATPE	ATPF	ATPE
<i>k</i> CGA	29.6 ± 8.6 ^a	9.6 ± 0.5 ^a	11.1 ± 5.3 ^a	10.2 ± 1.2 ^a
EE CGA (%)	97.1 ± 0.8 ^a	92.2 ± 0.3 ^b	98.7 ± 0.6 ^a	98.9 ± 0.1 ^a
<i>k</i> flavonoids	62.4 ± 4.3 ^a	23.1 ± 1.9 ^b	6.7 ± 1.7 ^a	7.9 ± 0.5 ^a
EE flavonoids (%)	98.7 ± 0.1 ^a	96.6 ± 0.3 ^b	98.3 ± 0.4 ^a	98.6 ± 0.1 ^a
<i>k</i> TPC	231.4 ± 16.5 ^a	161.6 ± 123.6 ^a	∞	104.8 ± 97.2
EE TPC (%)	99.6 ± 0.0 ^a	98.8 ± 0.9 ^a	99.6 ± 0.4 ^a	99.2 ± 0.7 ^a

Different superscript letters indicate significant difference between ATPF and ATPE of the same system.

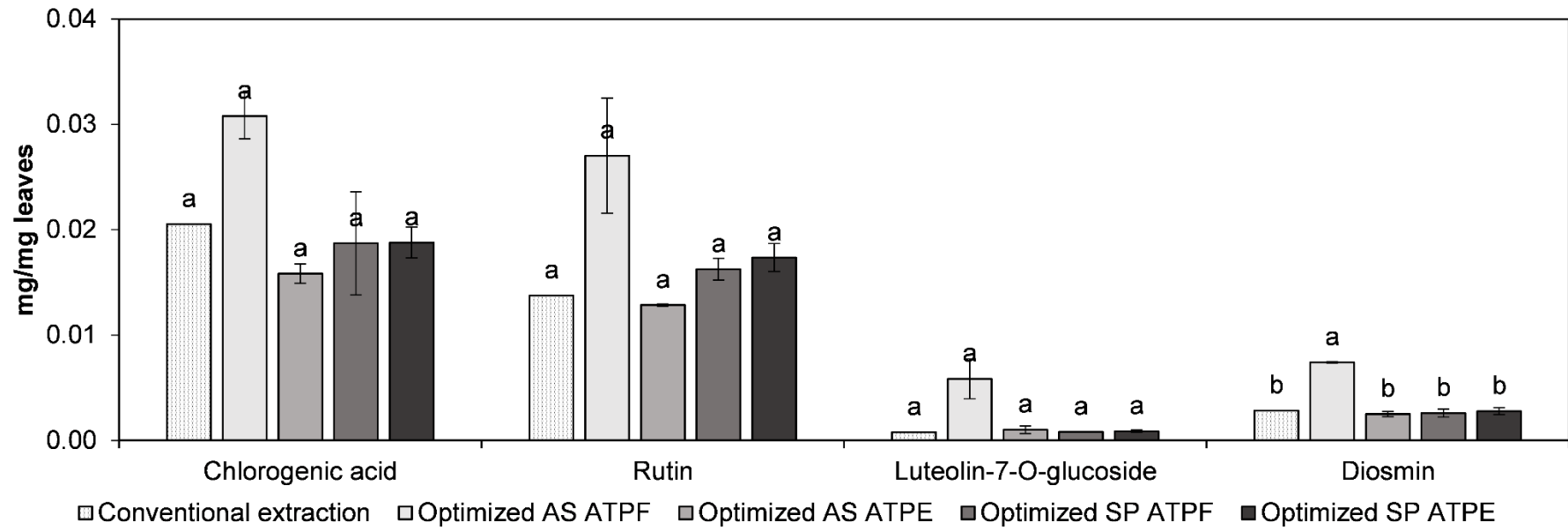
Table 5.4 also shows that ATPF using ammonium sulphate/ethanol had a significant increase in partition coefficient and extraction efficiency when compared to that obtained from ATPE for flavonoids and TPC. Moreover, the partition coefficient for CGA and flavonoids increased by 208% and 170% respectively with ATPF. A similar increase was reported by Bi and co-workers (Bi et al., 2013), where an increase in concentration coefficient from 2.5 to 27 resulted when ATPF was used instead of ATPE to extract baicalin, a flavone glycoside. ATPF also showed a 19.5% improvement of the partition coefficient for the recovery of polyphenols in comparison to that obtained from ATPE (de Araújo Padilha et al., 2018). In our work, there were no significant

differences between the partition coefficients and extraction efficiencies from ATPF and ATPE using the sodium phosphate/ethanol ATPS. However, almost all the TPC obtained by ATPF using sodium phosphate/ethanol partitioned to the top phase, resulting in infinity partitioning.

Based on studies by other researchers (Bi et al., 2013; de Araújo Padilha et al., 2018), it was expected that ATPF would improve yields, however this was not observed in our work for the sodium phosphate/ethanol systems. To investigate this further, a separate experiment was done to investigate the effect of volumetric ratio (i.e. ratio of top phase to the bottom phase volume) on the extraction performance. A volumetric ratio of 1.6 was tested using 19.9 wt% sodium phosphate, 19.5 wt% ethanol, and 60.6 wt% water, which was based on the ATPS phase diagram from previous work (Chong et al., 2020a), as a comparison to the volumetric ratio of 9 otherwise used in this study with sodium phosphate/ethanol. The results also showed that the partition coefficient and extraction efficiency of ATPF and ATPE for CGA and flavonoids did not have a significant difference while infinity partitioning was observed for TPC (data not shown). This strong affinity towards the top phase for TPC was also exhibited by laccase in a polyethylene glycol/phosphate ATPS (Blatkiewicz et al., 2018) and resulted in infinity partitioning. However, the large standard error of mean observed for the TPC partition coefficient in both ammonium sulphate/ethanol and sodium phosphate/ethanol systems of this study suggests that TPC may not be a suitable performance indicator.

5.4.4 HPLC Analysis

While the spectrophotometer provides an economical and rapid method to analyze a broad spectrum of compounds, HPLC analysis offers higher precision when quantifying individual compounds. Figure 5.5 illustrates the yield of four compounds quantified using HPLC for conventional extraction, in comparison to ATPF and ATPE for ammonium sulphate/ethanol and sodium phosphate/ethanol systems.



Different letters for each compound indicate significant differences between extraction methods

AS: Ammonium sulphate/ethanol system

SP: Sodium phosphate/ethanol system

Figure 5.5 Yield comparison of chlorogenic acid, rutin, luteolin-7-O-glucoside, and diosmin as detected by HPLC.

The retention times are included in Table 5.5. For the conventional extracts, the yields obtained by HPLC were 0.021 mg CGA/mg, 0.014 mg rutin/mg, 0.001 mg luteolin-7-*O*-glucoside/mg, and 0.003 mg diosmin/mg leaves. The optimized ATPF extracts using ammonium sulphate/ethanol recorded the largest yield increase of 49.9%, 96.4%, 652.1%, and 160.6% for chlorogenic acid, rutin, luteolin-7-*O*-glucoside, and diosmin respectively when compared to conventional extracts.

Table 5.5 Wavelength, retention time, and content of selected bioactive compounds from HPLC

Compounds	Wavelength (nm)	Retention time (min)	Yield (mg/mg dry weight leaves)
Conventional extract			
CGA	320	9.641	0.021
Rutin	250	11.421	0.014
Luteolin-7- <i>O</i> -glucoside	250	11.834	0.001
Diosmin	250	12.444	0.003
Optimized extract for (NH₄)₂SO₄/ethanol ATPF			
CGA	320	9.651	0.031
Rutin	250	11.449	0.027
Luteolin-7- <i>O</i> -glucoside	250	11.859	0.006
Diosmin	250 nm	12.468	0.007
Optimized extract for (NH₄)₂SO₄/ethanol ATPE			
CGA	320	9.644	0.016
Rutin	250	11.440	0.013
Luteolin-7- <i>O</i> -glucoside	250	11.839	0.001
Diosmin	250	12.464	0.003
Optimized extract for NaH₂PO₄/ethanol ATPF			
CGA	320	9.644	0.019
Rutin	250	11.438	0.016
Luteolin-7- <i>O</i> -glucoside	250	11.852	0.001
Diosmin	250	12.469	0.003
Optimized extract for NaH₂PO₄/ethanol ATPE			
CGA	320	9.629	0.019
Rutin	250	11.438	0.017
Luteolin-7- <i>O</i> -glucoside	250	11.833	0.001
Diosmin	250	12.465	0.003

Retention times and yields reported for ATPF and APTE extracts are an average of two independent experiments

These findings support the significant increase observed in the partition coefficients for CGA and flavonoids from ATPF using ammonium sulphate/ethanol compared with sodium phosphate/ethanol in Table 5.4. The other remaining extraction systems resulted in varying yields. For instance, the optimized ATPF extracts using sodium phosphate/ethanol had 0.019 mg CGA/mg, 0.016 mg rutin/mg, 0.001 mg luteolin-7-*O*-glucoside/mg, and 0.003 mg diosmin/mg leaves while the optimized ATPE extracts using sodium phosphate/ethanol had 0.019 mg CGA/mg, 0.017 mg rutin/mg, 0.001 mg luteolin-7-*O*-glucoside/mg, and 0.003 mg diosmin/mg leaves. The yields were not statistically significant different except for diosmin extracted by ammonium sulphate/ethanol ATPF. In comparison, our previous ATPE work on a different batch of Aurora haskap leaves (Chong et al., 2020a) had a maximum yield of 0.005 mg/mg leaves for the bioactive compounds. The chlorogenic acid and rutin yields are much higher in the present study. This difference could be due to varying environmental conditions such as soil quality, precipitation, and light intensity (Boyarskikh et al., 2015; Senica et al., 2018).

The yields obtained using HPLC and UV-Vis spectrophotometry methods for chlorogenic acid and rutin were compared. The CGA yield obtained from ATPF with ammonium sulphate/ethanol was similar (0.03 to 0.04 mg/mg leaves) when using UV-Vis spectrophotometry (Figure 5.3) and HPLC (Figure 5.5). For conventional extracts, the CGA yield from UV-Vis spectrophotometry (Figure 5.3) was about 2.8 times higher than the CGA yield from HPLC (Figure 5.5). This difference may be caused by the interference of other components such as CGA isomers, as well as solvent-related effects with the ATPS that could have affected the absorption when using the UV-Vis method, while the HPLC measurement was very specific. The remaining chlorogenic acid and rutin yields extracted by ATPE using ammonium sulphate/ethanol, and by ATPF and ATPE using sodium phosphate/ethanol were consistent between both analytical methods. The relationship between the two methods were also statistically examined with Pearson correlation. Chlorogenic acid had a low, positive, and insignificant linear correlation ($r = 0.370$, $n = 9$, $p > 0.05$) while flavonoids had a very strong, positive linear correlation between spectrophotometric method and HPLC method ($r = 0.928$, $n = 9$, $p < 0.05$). Due to the visibly non-monotonic relationship for chlorogenic acid, the Spearman rank correlation could not be applied. In a study comparing spectrophotometric and HPLC methods for the determination of CGA in

coffee beans, the CGA percentage obtained by UV-Vis spectroscopy was slightly higher than those from the HPLC method (Belay & Gholap, 2009). The authors attributed the difference to the minor interference of water-soluble compounds present in the sample. In our study, the different trends for the CGA yields may be due to the sample preparation step using SPE cartridges for HPLC but not for UV-Vis spectroscopy. It is worth noting that although there was a high Pearson correlation for flavonoids, the HPLC method used only a single compound rutin, as the standard, while the UV-Vis spectrophotometric method measured an array of flavonoids.

5.5 Conclusion

This study demonstrated that aqueous two-phase flotation improved the extraction performance of bioactive compounds from haskap leaves. The spectrophotometric assays for ATPF using ammonium sulphate/ethanol increased the partition coefficient by 208% for chlorogenic acid and 170% for flavonoids when compared to ATPE. It was further confirmed by HPLC quantification where ATPF using ammonium sulphate/ethanol increased yields by 49.9%, 96.4%, 652.1%, and 160.6% for chlorogenic acid, rutin, luteolin-7-*O*-glucoside, and diosmin respectively, in comparison to ATPE. However, there was no significant difference between ATPF and ATPE for sodium phosphate/ethanol systems in terms of yield, partition coefficient, nor extraction efficiency. With that, ammonium sulphate/ethanol ATPF is preferred for its enhanced ability to recover bioactive compounds. Potential applications of the ATPF extracts include food and bioproducts and future work may integrate ATPF with mechanical processes such as ultrasound and pulsed electric field to improve its efficiency.

Connecting Statement 4

Chapter 5 demonstrated that the partition coefficient for bioactive compounds extracted from ammonium sulphate/ethanol ATPS was improved by flotation (ATPF) when compared to ATPE without bubbles. The effect of flotation on the sodium dihydrogen phosphate/ethanol system was not significant. Considering this and the results from Chapter 3, these two salt/ethanol systems were used in Chapter 6.

In Chapter 6, sodium dihydrogen phosphate/ethanol ATPE and ammonium sulphate/ethanol ATPF were used to extract bioactive compounds from haskap leaves. These extracts consisting of salt, alcohol, water, and bioactive compounds were incorporated into pea protein films for food packaging applications. Since studies have used aqueous or hydroalcoholic extracts to develop functional films, this study is novel due to the direct incorporation of haskap leaf ATPS extracts, including the ATPS components, into pea protein films. Various properties of the films such as physical, mechanical, thermal, and migration behaviour of the phenolic compounds into food simulants were assessed.

Chapter 6 is based on a manuscript submitted for publication.

Chapter 6 : Development of pea protein films with haskap (*Lonicera caerulea*) leaf extracts from aqueous two-phase systems

6.1 Abstract

Pea protein films were developed using haskap (*Lonicera caerulea*) leaf extracts obtained from aqueous two-phase extraction (ATPE) and aqueous two-phase flotation (ATPF), where the components from the aqueous two-phase systems were incorporated directly into the films. The films were formulated with components that were GRAS (Generally Recognized as Safe): either pea protein isolate (PPI) or pea protein concentrate (PPC), glycerol as plasticizer, carboxylic acids (citric acid or malic acid) as cross-linkers and the haskap leaf extracts comprising of bioactive compounds, ethanol, salt (sodium phosphate or ammonium sulphate), and water. Films were produced by the bench casting method and they were assessed in terms of physical, mechanical, optical, water vapor permeability, thermal, migration and antioxidant properties. Some formulations with the haskap leaf extracts demonstrated better water vapour permeability and flexibility with the presence of salt. The films also exhibited thermal stability as the melting temperatures were higher than 150 °C and ultraviolet absorption properties that would protect products from ultraviolet degradation. Additionally, the films allowed the migration of bioactive compounds into alcoholic and fatty food simulants, which suggests that they could extend the shelf life of perishable food and increase the antioxidant properties of the packaged products. This work also shows that post-extraction steps such as alcohol evaporation and salt precipitation are not necessary with aqueous two-phase systems and could therefore reduce associated processing costs.

6.2 Introduction

Plastic polymers such as polystyrene (PS), polyvinyl chloride (PVC), and low density polyethylene (LDPE) are commonly used as they are strong, lightweight, durable, and economical. Plastics products derived from non-renewable resources such as petroleum, natural gas, and coal have raised environmental concerns due to widespread littering and accumulation of the nondegradable material over time. About 150 million metric tons of plastics produced annually are for disposable applications, or products that are discarded within a year of purchase (North & Halden, 2013). Plastics also pose health

risks by releasing hazardous chemicals during the manufacturing process and usage of the end products. Leaching of bisphenol A and phthalates are detrimental as they can disrupt the endocrine system (Halden, 2010). These issues have driven research on biobased packaging materials as alternatives to plastics (Jiménez et al., 2012; Vieira et al., 2011). Starch (Nouri & Mohammadi Nafchi, 2014), whey protein (Ribeiro-Santos et al., 2018), gelatin (Musso et al., 2019), and chitosan (Souza et al., 2018) have been used to produce functional films which contain plant extracts in the form of aqueous extract, alcoholic extract, or essential oil. Canada being the largest producer and leading exporter of dry peas (Roy et al., 2010) spurs a growing interest in pea protein as the main component in biobased films (Acquah et al., 2020; Choi & Han, 2001; Kowalczyk & Baraniak, 2011). These plant-based films are suitable for vegans especially if they are designed to be edible, and for consumers who prefer plant-based products due to their lower environmental footprint (Sabaté & Soret, 2014).

Haskap (*Lonicera caerulea*) leaves are an agricultural residue from haskap farms and contain various bioactive compounds such as chlorogenic acid, flavonoids, and phenolic compounds (Dawson, 2017; Oszmiański et al., 2011). In comparison to Soxhlet extraction, previous studies reported an improved extraction efficiency for bioactive compounds from haskap leaves with aqueous two-phase extraction (ATPE) and aqueous two-phase flotation (ATPF), where the extraction parameters were optimized to achieve maximum yields of bioactive compounds (Chong et al., 2020a, 2020b). Aqueous two-phase systems (ATPS) integrate separation, concentration, and partial purification of the target bioactive compounds in a single step (Hatti-Kaul, 2000). Previous studies have shown that haskap leaf extracts from ATPE and ATPF using alcohol/salt-based ATPS contain bioactive compounds as well as the ATPS components namely alcohol, salt, and water (Chong et al., 2020a, 2020b).

The aim of this research was to develop functional pea protein films by incorporating haskap leaf extracts obtained from ATPS-based extraction techniques. The films consisted of components that were GRAS (Generally Recognized as Safe): either pea protein isolate (PPI) or pea protein concentrate (PPC), glycerol as plasticizer, carboxylic acids (citric acid or malic acid) as cross-linkers and the haskap leaf extracts comprising of bioactive compounds, ethanol, salt (sodium phosphate or ammonium sulphate), and water. The films were analyzed for physical properties, mechanical

properties, optical properties, water vapor permeability, thermal properties, migration and antioxidant properties. To date, there has been no report of using extracts obtained from ATPS for other applications as ATPS research mainly revolves around optimization of the extraction conditions and integration of technology such as ultrasound (Zhu et al., 2020) and microwave (Zhang et al., 2015) to improve its efficiency. The novelty of this work is the direct incorporation of the ATPE and ATPF haskap leaf extracts which contain bioactive compounds, ethanol, water, and residual salt without further purification or isolation of individual compounds. Although recycling of the ATPS phase-forming components have been investigated (Chong & Brooks, 2021), this additional separation step which involves alcohol evaporation and salt precipitation would increase the overall extraction costs. This work provides an alternative application of the ATPS extracts by incorporating them into pea protein films.

6.3 Materials and Methods

6.3.1 Materials

Pea protein concentrate (Prestige Pea Protein) with $50 \pm 2\%$ protein (manufacturer specifications) was kindly provided by Parrheim Foods and pea protein isolate (PURIST™ Pea 870) with 80% protein (manufacturer specifications) was obtained from PURIST™. Ethyl alcohol (95% volume) was obtained from Greenfield Specialty Alcohols Inc. (Toronto, Ontario, Canada). Sodium dihydrogen phosphate 96% was purchased from Alfa Aesar (Ward Hill, Massachusetts, USA). The following chemicals were purchased from Sigma-Aldrich (Oakville, Ontario, Canada): 2,2-diphenyl-1-picrylhydrazyl (DPPH), ammonium sulphate (ACS, $\geq 99\%$), citric acid (ACS, $\geq 99.5\%$), DL-malic acid $\geq 99\%$, sodium nitrite ($\geq 97\%$, ACS), aluminum nitrate nonahydrate (ACS, $\geq 97\%$), sodium carbonate (ACS, 99.95-100.05% dry basis), Folin & Ciocalteu's phenol reagent (2N), gallic acid monohydrate (ACS, $\geq 98\%$), chlorogenic acid ($\geq 95\%$, titration), and rutin hydrate ($\geq 94\%$, HPLC grade). Glycerol (ACS, $\geq 99.5\%$), calcium chloride (anhydrous pellets), and magnesium chloride hexahydrate (FCC/USP grade) were purchased from Fisher Chemical. Deionized water was obtained from a Milli-Q water purification system (Millipore, Bedford, Massachusetts, USA).

6.3.2 Methods

6.3.2.1 Extraction of Haskap Leaves

Fresh leaves were harvested in July 2018 from haskap plants of the Aurora variety. The harvest location was Lone Tree Farm, Bridgewater in Nova Scotia, Canada with geographical coordinates of 44° 28' 10.8" N, 64° 39' 25.6" W. The plants were in their first growth year and fully developed-leaves were picked after the haskap berries were harvested. The samples were frozen at -20 °C and subsequently freeze-dried in a Labconco FreeZone 2.5 Plus freeze dryer (Labconco, Kansas City, MO, USA). The dried samples were sealed in vacuum pouches and stored at -20 °C in the dark prior to experiments. At the start of the study, samples were ground and sieved through a 500 µm mesh opening. Haskap leaves were extracted using optimized aqueous two-phase extraction (ATPE) parameters (Chong et al., 2020a) where a 20-g sodium phosphate/ethanol ATPE consisted of 10 wt% sodium phosphate, 37 wt% ethanol, 53 wt% water with 0.5 weight% leaves and 5 min extraction time in a 50-mL centrifuge tube. The second extraction method using aqueous two-phase flotation (ATPF) consisted of ammonium sulphate/ethanol ATPS with 20 wt% ammonium sulphate, 27.5 wt% ethanol, and 52.5 wt% water, 0.025 weight% leaves, 120 min flotation time, 11.4 mL/min air flow rate (Chong et al., 2020b). Multiple extractions were performed to ensure that the extracted quantities were sufficient for all the experiments. The extracts are termed as sodium phosphate extracts (SP) and ammonium sulphate extracts (AS) hereafter. The pooled extracts were analyzed for their bioactive compounds concentration specifically chlorogenic acid, total flavonoids, and total phenolic content as described in a previous study (Chong et al., 2020a). The radical scavenging activity (RSA) of the extracts was analyzed according to Section 6.3.2.3.

6.3.2.2 Film Preparation

Pea protein solutions were prepared by dispersing 5 g of either pea protein isolate (PPI) or pea protein concentrate (PPC) with 0.455 g glycerol or 0.90% (w/w) and 40 g deionized water. The PPI solution was stirred at 700 rpm while the PPC solution was stirred at 900 rpm for 30 minutes due to PPC solution being more viscous. The PPI solution was heated at 90 °C while PPC solution was heated at 80 °C for 30 min in 50-mL conical flasks. A shaking water bath (Precision 2870; Thermo Scientific, Waltham, MA, US) was used at 100 rpm for heating and the conical flasks were covered with

parchment paper to minimize evaporation. The solution was then cooled to room temperature and 5 g of haskap leaf extract was added. Control films were formed with 95% ethanol or water instead of the haskap leaf extracts. Citric acid of 1.70 g (3.29 wt%) or malic acid of 1.34 g (2.61 wt%) and 1.70 g (3.29 wt%) were added as a cross-linker. The concentration of cross-linker added was based on another study (Eswaranandam et al., 2004) and preliminary tests. The resulting solution was stirred at 900 rpm for PPI solution and 1100 rpm for PPC solution for 30 min. The PPC solution was degassed by centrifugation at 500 g for 1 minute and left to equilibrate for 25 min. The foam atop the PPC solutions was then collapsed by adding 200 μ L of 95% ethanol. Degassing was not required for the PPI solutions as the PPI solution was less viscous and the bubbles rose easily to the top. For all films, 5 mL of solution was cast on each 15 \times 100 mm polystyrene petri dish. About six to seven films were cast onto those dishes with the degassed solution.

Preliminary experiments showed that two stages of drying were required to form films without cracks. The films were first dried overnight at 19 °C on a leveled surface. They were then transferred to an incubator (G25 Controlled Environment Incubator Shaker, New Brunswick Scientific, NJ, USA) at 25 °C with air circulation until the films were ready to peel. The peeled films were placed between parchment paper and conditioned at 19 °C and 68% relative humidity in a sealed container over magnesium chloride solution for at least 48 hours before further analysis. PPI films could not be formed with ammonium sulphate extracts as severe cracks were observed after several attempts with varying amounts of cross-linkers. Two independent experiments were performed with the film formulations listed in Table 6.1.

6.3.2.3 Analysis of Films

Thickness

The thickness of the films was measured with a micrometer (Schut Geometrical Metrology, Groningen, Netherlands) to the nearest 0.001 mm. Five measurements were taken at different locations and averaged.

Table 6.1 Composition of pea protein films

Films ^a	Sodium phosphate extract (g)	Ammonium sulphate extract (g)	Citric acid (g)	Malic acid (g)	Ethanol (g)	Water (g)
PPI 5SP 1.7CA	5	0	1.70	0.00	0	40
PPI 5SP 1.34MA	5	0	0.00	1.34	0	40
PPI 5SP 1.7MA	5	0	0.00	1.70	0	40
PPI 5EtOH 1.7CA ^b	0	0	1.70	0.00	5	40
PPI 5EtOH 1.7MA	0	0	0.00	1.70	5	40
PPI 5W 1.7CA	0	0	1.70	0.00	0	45
PPI 5W 1.7MA	0	0	0.00	1.70	0	45
PPC 5SP 1.7CA	5	0	1.70	0.00	0	40
PPC 5SP 1.34MA	5	0	0.00	1.34	0	40
PPC 5SP 1.7MA	5	0	0.00	1.70	0	40
PPC 5EtOH 1.7CA	0	0	1.70	0.00	5	40
PPC 5EtOH 1.7MA	0	0	0.00	1.70	5	40
PPC 5W 1.7CA	0	0	1.70	0.00	0	45
PPC 5W 1.7MA	0	0	0.00	1.70	0	45
PPC 5AS 1.7CA	0	5	1.70	0.00	0	40
PPC 5AS 1.34MA	0	5	0.00	1.34	0	40
PPC 5AS 1.7MA	0	5	0.00	1.70	0	40

^a Glycerol was fixed at 0.455 g for all formulations

^b this formulation did not yield a continuous film and was discarded

Moisture Content

Film specimens were weighed using an analytical balance with precision of 0.0001 g (S-64, Denver Instrument, Denver, CO, USA) and dried in an oven (Gravity Oven, Fisher Scientific, MA, USA) at 105 °C for 24 h (Kowalczyk & Baraniak, 2011). The moisture content value was determined as the percentage of initial film weight lost during drying and reported on wet basis. When transferring from oven to scale, films were placed in a container filled with calcium chloride to prevent any reabsorption of moisture.

Mechanical Properties

The tensile strength and elongation at break were assessed using a tensile tester (EZ Test EZ-LX HS, Shimadzu, Japan) with its accompanying software Shimadzu Trapezium X following the procedures outlined in ASTM method D882-18 (ASTM International, 2018b). Briefly, films were cut into the size of 50 × 7.5 mm, the initial grip separation was set at 40 mm and the crosshead speed at 12.5 mm/min. Tensile strength and elongation at break were then determined from the stress-strain curves. Four replications from different films were tested for each formulation.

Optical Properties

Film samples were cut into rectangular strips (20 mm × 4 mm) and carefully inserted onto the inner window of 1.5 mL semi-micro methacrylate cuvettes. An empty cuvette was used as blank. Light transmission was determined from 285 to 750 nm with a UV/Visible spectrophotometer (Genesys 10S, Thermo Scientific, USA). The opacity of the films was calculated by Equation 2.2 (Shevkani & Singh, 2015) which was defined as the ratio of absorbance at 600 nm to the film thickness. Three strips of each pea protein film type were tested.

Water Vapor Permeability (WVP)

Water vapor permeability was tested according to ASTM method E96 (ASTM International, 2016; Musso et al., 2019) with some modifications. Using a permeation cell, each film sample was sealed over a circular opening of 0.00056 m² that was stored at 19 °C in dessicators. Anhydrous calcium chloride (0% RH) was placed inside the cell and 150 mL of water (87 to 99% RH) was used in the dessicators to maintain a relative humidity (RH) gradient across the film. Weight increase was determined at 24 hours and 48 hours. WVP was calculated using Equations 6.1 and 6.2 (Han et al., 2018; Musso et al., 2019):

$$WVTR = \frac{\Delta w}{A\Delta t} \quad (6.1)$$

$$WVP = \left(\frac{WVTR}{P_V^{H_2O} (RH_d - RH_c)} \right) \times d \quad (6.2)$$

Here, $WVTR$ is water vapor transmission rate, $\Delta w/\Delta t$ is the mass change of the cell per time (g s^{-1}), A is the permeation area (m^2), $P_v^{H_2O}$ is the saturation water vapor pressure at test temperature (2199.82 Pa at 19 °C), $RH_d - RH_c$ is the relative humidity gradient across the film expressed as a fraction, and d is the film thickness (m). Each WVP value represents the mean value of two samples taken from different films.

Thermal Properties

The thermal behaviour of pea protein films was evaluated by differential scanning calorimetry (Q1000, TA Instruments, USA). Each sample of about 7 mg was heated on an aluminum hermetic pan from 25 to 300 °C at 10 °C/min under inert atmospheric condition with 25 mL/min of nitrogen gas. An accompanying Universal Analysis software was used to obtain the melting temperature (T_m) and enthalpy of melting (ΔH_m). T_m was taken as the temperature of the endothermic peak while ΔH_m was determined from the area under the endothermic peak. An empty aluminum pan with its lid was used as the reference. For PPI and PPC powder samples, a protein suspension of 15% (w/w) was prepared with water and transferred into the pan (Shevkani & Singh, 2015). It was then hermetically sealed and allowed to stand for 2 hours at room temperature. The scanning rate and temperature range were the same as the films.

Migration and Antioxidant Tests

Using 10% (v/v) ethanol as an alcoholic food simulant and 95% (v/v) ethanol as a fatty food simulant (Han et al., 2018), 30 mg of the film was immersed in 5 mL of each simulant in a centrifuge tube with continuous shaking at 100 rpm and 25 °C (G25 Controlled Environment Incubator Shaker, New Brunswick Scientific, NJ, USA). Multiple tubes were prepared at the same time and the tubes were removed at intervals. The films were immediately removed with a tweezer or filtered with a qualitative filter paper (VWR, Grade 415), depending on whether the films had disintegrated. The migration of total phenolic content (TPC) in 10% (v/v) ethanol and 95% (v/v) ethanol was monitored for 1 hour and 51 hours, respectively (Han et al., 2018). TPC release from the film was assessed using the Folin-Ciocalteu method (Singleton et al., 1999) where 100 μL of the simulant was mixed with 200 μL Folin-Ciocalteu reagent (diluted with water at a ratio of 1:10 by volume). After 5 minutes of incubation, 800 μL of 7.5% (w/v) aqueous sodium carbonate solution was added. The solution was vortexed and incubated for 2 hours in the dark at room temperature. The 10% (v/v) ethanolic mixture

did not require centrifugation while the 95% ethanolic mixture was centrifuged at 1500 g for 1 minute due to interference with the high ethanol content in the final reaction mixture (Cicco et al., 2009). Its absorbance was determined at 765 nm using a UV/Visible spectrophotometer (Genesys 10S, Thermo Scientific, USA). Gallic acid monohydrate was used as the standard and calibration curves were plotted using the corresponding simulants. The results were expressed in terms of mg gallic acid equivalents (GAE)/g film.

To evaluate its antioxidant activity, radical scavenging activity (RSA) was evaluated using the 2,2-diphenyl-1-picrylhydrazyl (DPPH) assay (Brand-Williams et al., 1995). Here, 200 μ L of simulant was mixed with 1.8 mL of 0.1 mM DPPH solution which was prepared with ethanol. The solution was incubated for 30 min in the dark and absorbance was measured at 517 nm. A control was made by using 10% (v/v) or 95% (v/v) ethanol instead of the simulants which was immersed with films. RSA was calculated using Equation 6.3.

$$RSA (\%) = \frac{A_{control} - A_{sample}}{A_{control}} \times 100 \quad (6.3)$$

where $A_{control}$ is the absorbance of the control solution and A_{sample} is the absorbance of the sample. Simulants from each interval were tested twice with the TPC and RSA assay.

Statistical Analysis

One-way analysis of variance (ANOVA) was performed with Minitab statistical software (Version 19, Minitab Inc. USA). This was used to test for significant differences between means using Tukey's multiple comparison test, and error bars included in figures and tables represent the standard error of mean (SEM).

6.4 Results and Discussion

6.4.1 Characterization of Haskap Leaf Extracts from ATPE and ATPF

The concentrations of bioactive compounds in haskap leaf extracts obtained using ATPE and ATPF are shown in Table 6.2. The sodium phosphate/ethanol extracts have higher chlorogenic acid, total flavonoids, total phenolic content, and radical scavenging activity compared to the ammonium sulphate extracts. This is due to the higher amount

of leaves used in the sodium phosphate/ethanol ATPE which is 0.5 wt% while the ATPF process used 0.025 wt% leaves.

Table 6.2 Concentration of bioactive compounds in pooled haskap leaf extracts

Bioactive compounds	Sodium phosphate/ethanol ATPE: 10 wt% NaH₂PO₄, 37 wt% ethanol, 53 wt% water, 0.5 wt% (0.1 g) leaves, 5 min extraction time	Ammonium sulphate/ethanol ATPF: 20 wt% (NH₄)₂SO₄, 27.5 wt% ethanol, 52.5 wt% water, 0.025 wt% (5 mg) leaves, 120 min flotation time, 28.6 mL/min air flow rate
Chlorogenic acid (µg/mL)	182.18 ± 7.86	6.11 ± 0.18
Total flavonoids (mg/mL)	1.17 ± 0.03	0.11 ± 0.01
Total phenolic content (mg GAE/mL) ^a	0.37 ± 0.00	0.03 ± 0.00
Radical scavenging activity, %	74.99 ± 0.53	47.86 ± 3.30

^a GAE: gallic acid equivalents

For extracts obtained from sodium phosphate/ethanol ATPE, a prior study obtained higher concentrations of chlorogenic acid (202.39 µg/mL) however the concentration of total flavonoids (1.14 mg/mL) and TPC (0.38 mg GAE/mL) were similar to that achieved in this study (Chong et al., 2020a). In another study, the ammonium sulphate/ethanol ATPF technique produced extracts with a much lower chlorogenic acid concentration of 0.02 µg/mL, and similar concentrations of total flavonoids and TPC (0.14 mg/mL and 0.05 mg GAE/mL, respectively) (Chong et al., 2020b). Some bioactive concentrations reported in Table 6.2 may differ with previous studies due to factors such as differences in the dimensions of extraction vessel (Solano-Castillo & Rito-Palomares, 2000). The increase in chlorogenic acid may be contributed by the accumulation of sugars which act as substrates for its synthesis (Galani et al., 2017). The variability of these biological samples was also evident in the reported deviations between the predicted and experimental yields (Chong et al., 2020b).

6.4.2 Film Thickness

The thickness of a film affects other properties such as strength and water vapor permeability. It is also important to evaluate thickness as it is a specification for films. Table 6.3 shows the thickness of the pea protein films.

Table 6.3 Thickness of pea protein films

PPI films thickness (mm)				
Cross-linker	Sodium phosphate extract	Ammonium sulphate extract	Water	Ethanol
1.7g citric acid	0.111 ± 0.003 ^a	N/A	0.090 ± 0.008 ^b	Did not form
1.7g malic acid	0.091 ± 0.006 ^b	N/A	0.096 ± 0.006 ^b	0.120 ± 0.007 ^a
1.34g malic acid	0.098 ± 0.003	N/A	N/A	N/A
PPC films thickness (mm)				
	Sodium phosphate extract	Ammonium sulphate extract	Water	Ethanol
1.7g citric acid	0.094 ± 0.005 ^{bc}	0.114 ± 0.005 ^{ab}	0.084 ± 0.004 ^c	0.127 ± 0.009 ^a
1.7g malic acid	0.089 ± 0.003 ^a	0.118 ± 0.009 ^a	0.108 ± 0.016 ^a	0.096 ± 0.004 ^a
1.34g malic acid	0.081 ± 0.003 ^b	0.106 ± 0.005 ^a	N/A	N/A

Means with different letters in the same row are significantly different ($P < 0.05$).

PPI films had thickness ranging from 0.090 to 0.120 mm and PPC films ranged from 0.081 to 0.127 mm. PPI 5EtOH 1.7MA was thicker than other PPI films. This could be due to the decreased solubility of malic acid in ethanol as compared to water (Yuan et al., 2014), leading to some visibly embedded particles. Although citric acid is more soluble in ethanol than in water (Oliveira et al., 2013), PPC 5EtOH 1.7CA was thicker than other PPC films. This may be due to denaturation induced by the ethanol. Authors have found that whey protein isolate solutions prepared with 5% residual ethanol had considerable retention of denaturation (Nikolaidis & Moschakis, 2018). The interaction between ethanol and soybean protein has also shown partial and progressive dehydration which transformed gel-like sediments into opaque flocks or precipitates (Lambrecht et al., 2016). The precipitate may have caused a slight increase in thickness. The addition of both types of extracts did not cause significant difference to the

thickness of the PPC films with 1.7g malic acid. This may be due to the structure of pea protein which consists of 65-80% globular and disordered protein (Sirtori et al., 2012). The extracts may fill the gaps between the disorganized structure, resulting in limited increase in thickness (Maryam Adilah et al., 2018). Other studies have reported that incorporation of grape seed extracts in soy protein films observed an increase of the thickness due to the increased cross-links between the proteins and polyphenols (Sivaroban et al., 2008). In contrast, the average thickness of chitosan films remained statistically the same with the incorporation of plant extracts (Souza et al., 2018). The thickness of PPI films from this study is similar to other reported PPI films from 0.098 to 0.100 mm (Kowalczyk & Baraniak, 2011). According to Choi and Han (2001), PPC films produced were much thicker ranging from 4.45 to 5.83 mm. The differences may be due to the amount of film-forming solution casted onto the dishes where the authors used 5 to 6 g while 5 mL of film-forming solution was used in this study. Viscosity of the film-forming solution also affected the film thickness (Phan et al., 2005). In this study, although the PPC solutions were observed to be slightly more viscous than PPI solutions, the overall thickness of the films remained similar for both formulations. Commercial bio-based food packaging films are thinner and they can range from 0.025 to 0.050 mm (Briassoulis & Giannoulis, 2018). Manufacturers commonly use blown film extrusion to produce the films (Mallegni et al., 2018) as compared to bench-scale casting which leads to precise and uniform thickness.

6.4.3 Moisture Content

Moisture content is related to the total void volume of water molecules in the film microstructure (Goudarzi et al., 2017). Table 6.4 shows that PPI films had moisture content from 17.1 to 24.0% and PPC films had moisture content from 18.8 to 38.9%. Two samples, PPC 5SP 1.7MA and PPC 5EtOH 1.7CA had higher moisture content than other films. This may be caused by a breakup of the film network which draws more water molecules between the polymer chains through hydrogen bonding (Jouki et al., 2014).

Table 6.4 Moisture content of pea protein films

PPI films moisture content (%)				
Cross-linker	Sodium phosphate extract	Ammonium sulphate extract	Water	Ethanol
1.7g citric acid	17.1 ± 2.5 ^a	N/A	22.7 ± 3.5 ^a	Did not form
1.7g malic acid	22.7 ± 3.5 ^a	N/A	24.0 ± 1.3 ^a	23.5 ± 2.4 ^a
1.34g malic acid	19.0 ± 2.0	N/A	N/A	N/A
PPC films moisture content (%)				
	Sodium phosphate extract	Ammonium sulphate extract	Water	Ethanol
1.7g citric acid	18.8 ± 0.3 ^b	19.9 ± 0.7 ^b	22.4 ± 1.4 ^b	38.9 ± 1.2 ^a
1.7g malic acid	34.7 ± 1.9 ^a	21.2 ± 1.4 ^b	22.0 ± 1.2 ^b	23.4 ± 0.8 ^b
1.34g malic acid	19.6 ± 1.0 ^a	19.7 ± 0.5 ^a	N/A	N/A

Means with different letters in the same row are significantly different ($P < 0.05$).

Comparing with other pea protein films, PPI films without extracts had average moisture content of 16.5% with 3wt% glycerol used (Kowalczyk & Baraniak, 2011). Another study reported that the moisture content of 3.21 and 5.69% for PPI and PPC films, respectively (Acquah et al., 2020). These values are lower than the values in this study and it could be due to the lower protein concentration used, which was 4% (w/v) compared to 10% (w/w) in this study. The carboxyl and hydroxyl groups in the protein are hydrophilic, thus leading to an increase in water absorption (Yue et al., 2012). Table 6.4 also shows that the addition of 1.7 g malic acid with extracts resulted in higher moisture content of the films. This could be due to the slightly higher hygroscopicity of malic acid as compared to citric acid (Peng et al., 2001). With regards to addition of extracts, Torres-León et al. (2018) found that the addition of 0.078 g L⁻¹ mango seed extracts in mango peel films did not alter the moisture content significantly. An addition of raspberry extract to soy protein isolate films likewise have recorded similar moisture content compared to soy control films (Wang et al., 2012a). Our findings are in contrast with studies which reported an increase of moisture content with the addition of aqueous extracts in carageenan films (Kanmani & Rhim, 2014) and ethanolic extracts in starch films (Nouri & Mohammadi Nafchi, 2014) due to the increase of more hydroxyl groups attracting more water molecules, and thus increasing the overall hydrophilicity. Both phenolic compounds and the solvents used to dissolve the extracts have hydroxyl groups. The consistent moisture content may be due to the presence of

ammonium sulphate and sodium phosphate salts in the extracts. These salts could have contributed to the overall hygroscopicity of the film as sodium chloride (Sängerlaub et al., 2013) and other salts (Takuno, 1992) have been used to create humidity-regulating films.

6.4.4 Tensile Strength and Elongation at Break

Strong and flexible films are desired for various applications. Tensile strength (TS) is calculated by dividing the maximum force by the original average cross sectional area of the film. Elongation at break (EAB) shows the how much the film had extended until the moment of rupture (ASTM International, 2018b). Table 6.5 shows the TS and EAB for the pea protein films. The tensile strength for PPI films were from 2.5 to 5.2 MPa while the tensile strength for PPC films ranged from 1.1 to 5.3 MPa. The EAB values of PPI films ranged from 8.8 to 65.4% while PPC films had EAB values of 21.5 to 55.7%.

PPI films had an average higher tensile strength than PPC films and all EAB values of PPC films were higher than the corresponding PPI films except for PPC 5SP 1.7MA. Similarly, Choi and Han (2002) found that PPI films were 3 to 3.5 times stronger and had lower EAB values than PPC films. During thermal denaturation, PPI which has higher protein content will form more disulphide bonds between proteins, thus resulting in a rigid protein matrix. In contrast, PPC with lower protein concentration and more impurities such as starch and lipids form weaker films (Banerjee & Chen, 1995). The tensile strength of films incorporated with sodium phosphate extract and ammonium sulphate extract were lower than that of the control films. This may be caused by the presence of residual salt in the extracts. Frohberg et al. (2010) who investigated the addition of potassium nitrate into sodium caseinate films reported a considerable decrease in the mechanical performance when a ratio of $\text{KNO}_3/\text{NaCas}$ of higher than 1:2 was used. This was associated with the formation of relatively very large crystalline structures which damaged the macromolecular textures. It was also observed that the pea protein films in this study had visibly embedded particles in PPI formulations with malic acid. Citric acid and malic acid are non-toxic and economical cross-linkers which were proven to improve the strength of protein films (Sharma et al., 2018). However

the crosslinking mechanism also leads to restricted mobility of protein molecules, resulting in less flexible and lower EAB values.

Table 6.5 Mechanical properties of pea protein films

PPI Films Tensile strength (MPa)				
Cross-linker	Sodium phosphate extract	Ammonium sulphate extract	Water	Ethanol
1.7g citric acid	2.5 ± 0.2 ^b	N/A	5.2 ± 0.6 ^a	Did not form
1.7g malic acid	3.6 ± 0.4 ^a	N/A	4.9 ± 0.6 ^a	3.7 ± 0.3 ^a
1.34g malic acid	4.6 ± 0.1	N/A	N/A	N/A
PPC Films Tensile strength (MPa)				
	Sodium phosphate extract	Ammonium sulphate extract	Water	Ethanol
1.7g citric acid	2.4 ± 0.1 ^{bc}	1.8 ± 0.1 ^c	5.3 ± 0.3 ^a	2.9 ± 0.2 ^b
1.7g malic acid	1.7 ± 0.1 ^a	1.1 ± 0.1 ^b	2.0 ± 0.1 ^a	2.0 ± 0.1 ^a
1.34g malic acid	2.3 ± 0.1 ^a	2.0 ± 0.3 ^a	N/A	N/A
PPI Films Elongation at break (%)				
	Sodium phosphate extract	Ammonium sulphate extract	Water	Ethanol
1.7g citric acid	17.8 ± 3.6 ^a	N/A	8.8 ± 2.2 ^a	Did not form
1.7g malic acid	65.4 ± 8.8 ^a	N/A	29.1 ± 6.4 ^b	25.8 ± 3.4 ^b
1.34g malic acid	24.3 ± 4.5	N/A	N/A	N/A
PPC Films Elongation at break (%)				
	Sodium phosphate extract	Ammonium sulphate extract	Water	Ethanol
1.7g citric acid	43.1 ± 3.6 ^a	25.9 ± 1.5 ^b	21.5 ± 4.5 ^b	25.3 ± 3.2 ^b
1.7g malic acid	52.2 ± 3.8 ^a	22.6 ± 1.6 ^b	46.5 ± 5.8 ^a	55.7 ± 5.1 ^a
1.34g malic acid	40.9 ± 3.9 ^a	31.2 ± 2.4 ^b	N/A	N/A

Means with different letters in the same row are significantly different ($P < 0.05$).

Table 6.5 also shows that for PPI films with sodium phosphate extract, the addition of 1.7 g malic acid produced stronger films than PPI films with 1.7 g citric acid. The tensile strength further increased when a lower amount of malic acid was used. This could be due to the effect of higher molecular weight as citric acid (192.12 g/mol) may have caused a reduction in protein-protein interaction as compared to malic acid (134.09 g/mol) (Eswaranandam et al., 2004). However, the effect of different concentrations of cross-linker on the tensile strength was not evident with PPC films.

Films with differing strength and flexibility can be used for various end uses. PPC films with lower tensile strength and moderate EAB values could be used to package dual-textured food, for example to separate croutons in salad kits.

6.4.5 Transparency and Light Transmission

Optical properties are important packaging features as transparent packaging allows consumers to view the product before purchasing and low light transmission prevents the product from photodegradation, particularly from ultraviolet (UV) rays. The terms opacity and transparency are used interchangeably to describe how well a film transmits light. In this study, opacity is the preferred term (Equation 1) as a higher value translates to a more opaque film. Despite the green coloration from haskap leaf extracts, the films appeared yellow overall due to the pea protein sourced from yellow field peas. Table 6.6 shows that pea protein films are quite opaque as PPI films had opacity values of 1.34 to 3.50 mm⁻¹ while PPC films ranged from 2.79 to 7.54 mm⁻¹.

Table 6.6 Transparency and light transmission of pea protein films

PPI films transparency (A₆₀₀ mm⁻¹)				
Cross-linker	Sodium phosphate extract	Ammonium sulphate extract	Water	Ethanol
1.7g citric acid	3.50 ± 0.27 ^a	N/A	1.30 ± 0.05 ^b	Did not form
1.7g malic acid	1.49 ± 0.12 ^b	N/A	1.95 ± 0.13 ^a	1.34 ± 0.11 ^b
1.34g malic acid	1.54 ± 0.05	N/A	N/A	N/A
PPC films transparency (A₆₀₀ mm⁻¹)				
	Sodium phosphate extract	Ammonium sulphate extract	Water	Ethanol
1.7g citric acid	3.09 ± 0.13 ^b	7.54 ± 1.49 ^a	3.81 ± 0.24 ^b	3.37 ± 0.14 ^b
1.7g malic acid	2.79 ± 0.12 ^a	3.67 ± 0.31 ^a	3.37 ± 0.28 ^a	3.57 ± 0.19 ^a
1.34g malic acid	3.26 ± 0.22 ^b	4.85 ± 0.18 ^a	N/A	N/A

Means with different letters in the same row are significantly different ($P < 0.05$).

PPC films were more opaque than PPI films and this was similar to other studies where PPC and PPI films had opacity values of 1.7 and 1.3, respectively (Acquah et al., 2020). Similarly, Kowalczyk and Baraniak (2011) obtained opacity values of about 1 for PPI films. In contrast, Choi and Han (2002) reported an average opacity of 16.71 mm⁻¹ for

PPI films. Whey protein films incorporated with essential oils had opacity from 1.158 to 2.422 mm^{-1} (Ribeiro-Santos et al., 2018) while gelatin-chitosan blend films with ethanolic plant extracts had lower opacity from 0.233 to 1.230 mm^{-1} (Bonilla & Sobral, 2016). The addition of sodium phosphate and ammonium sulphate extracts increased the opacity of PPI 5SP 1.7CA, PPC 5AS 1.7CA, and PPC 5AS 1.34MA films. Similarly, when potassium nitrate was incorporated into sodium caseinate films, the authors reported an increasing opacity due to salt crystallization during solvent evaporation (Frohberg et al., 2010). As a comparison to synthetic films, low-density polyethylene, polyester, and polyvinylidene chloride films had opacity of 3.05, 1.51, and 4.58 respectively (Shiku et al., 2003).

UV and visible light are deteriorative as they can degrade sensitive bioactive compounds such as vitamins and pigments (Spikes, 1981). Therefore packaging with UV-absorbing properties can prevent UV from being transmitted to the product. To evaluate light transmittance, methacrylate cuvettes were used and they are only accurate at the wavelength 285 to 750 nm according to the manufacturer's specifications. Ultraviolet (UV) region can be classified into UVA (315 to 400 nm), UVB rays (280 to 315 nm), and UVC rays (100 to 280 nm) (Calvo et al., 2012). Figure 6.1 shows that the films were able to absorb UV radiation in the UVB and UVA regions.

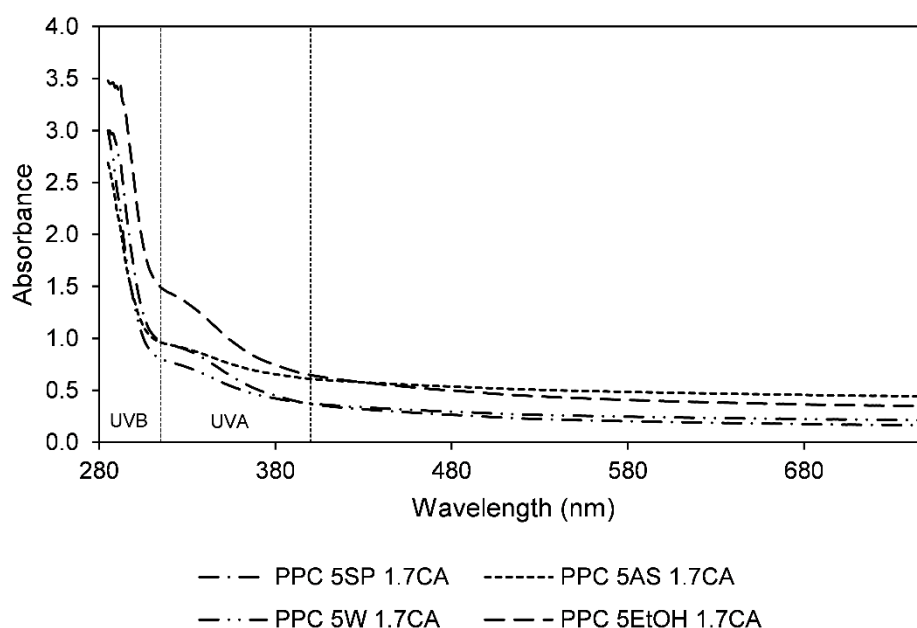


Figure 6.1 Light transmittance of selected films in the UV/visible spectrum

This property is associated with the presence of UV-absorbing chromophore in proteins, particularly aromatic amino acids, namely tyrosine and tryptophan (Kowalczyk & Baraniak, 2011). The addition of sodium phosphate extract in PPI films resulted in higher UV absorption while in PPC films, the ammonium sulphate extract absorbed more UV compared to PPC 5W 1.7CA. PPC 5EtOH 1.7CA had the highest UV absorption at 380 nm and below. The presence of ethanol could have absorbed some UV radiation, as it has been shown to protect yeast and bacteria against UVC irradiation although the protection mechanism is still unclear (Neužilová et al., 2019). Other studies have also shown that the addition of extracts prevented UV transmission in starch films (Nouri & Mohammadi Nafchi, 2014) and soy protein isolate films (Han et al., 2018).

6.4.6 Water Vapor Permeability (WVP)

In the presence of high moisture content, fresh produce are at risk of spoilage caused by microbial growth (Mahajan et al., 2008). Bakery products in contrast undergo staling when moisture is lost from the crumb, causing hardening and loss of freshness (Melini & Melini, 2018). WVP measures the amount of water that can transfer through the films. Table 6.7 shows that the WVP for PPI films ranged from 2.27 to $3.31 \times 10^{-10} \text{ gH}_2\text{O s}^{-1} \text{ m}^{-1} \text{ Pa}^{-1}$ and PPC films ranged from 1.78 to $3.36 \times 10^{-10} \text{ gH}_2\text{O s}^{-1} \text{ m}^{-1} \text{ Pa}^{-1}$. Past studies have reported WVP of about $1.04 \times 10^{-10} \text{ gH}_2\text{O s}^{-1} \text{ m}^{-1} \text{ Pa}^{-1}$ when 3% (w/w) glycerol was used in PPI films (Kowalczyk & Baraniak, 2011) and 1.19 to $2.06 \times 10^{-9} \text{ gH}_2\text{O s}^{-1} \text{ m}^{-1} \text{ Pa}^{-1}$ with PPC films (Choi & Han, 2001). WVP of films are influenced by the storage relative humidity and the amount of plasticizers in the formulations (Choi & Han, 2001). Other factors include the homogeneity and distribution of extract, formation of void or porous channels, temperature, type of plasticizers, and protein structure of the films (Maryam Adilah et al., 2018). In this study, PPI 5SP 1.7CA and PPC 5AS 1.34MA had higher WVP than the rest of the films. Considering that glycerol concentration was the same for all films, the increase in WVP could be due to the film thickness. As shown in Table 6.3 where PPI 5SP 1.7CA and PPC 5AS 1.34MA are thicker, a thicker film could form different structures (McHugh et al., 1993) and create more voids for water to pass through. However this was not evident with PPI 5EtOH 1.7MA where it was the thickest film in comparison to the others but had moderate WVP. Interactions between the cross-linkers and surrounding moisture could also play a role to increase WVP as citric acid and malic acid were shown to absorb and

desorb water continuously and reversibly (Peng et al., 2001). The moisture sorption presumably leads to swelling, resulting in slightly thicker films which facilitates permeation (Banker et al., 1966). From Table 6.7, the visibly embedded particles in pea protein films containing malic acid did not affect WVP as there were increases and decreases in WVP.

Table 6.7 Water vapor permeability (WVP) of pea protein films

PPI films WVP·10¹⁰ (gH₂O s⁻¹ m⁻¹ Pa⁻¹)				
Cross-linker	Sodium phosphate extract	Ammonium sulphate extract	Water	Ethanol
1.7g citric acid	3.31 ± 0.25 ^a	N/A	2.27 ± 0.15 ^b	Did not form
1.7g malic acid	2.89 ± 0.08 ^a	N/A	2.82 ± 0.24 ^a	2.79 ± 0.24 ^a
1.34g malic acid	2.64 ± 0.24	N/A	N/A	N/A
PPC films WVP·10¹⁰ (gH₂O s⁻¹ m⁻¹ Pa⁻¹)				
	Sodium phosphate extract	Ammonium sulphate extract	Water	Ethanol
1.7g citric acid	2.44 ± 0.22 ^{ab}	2.69 ± 0.29 ^a	2.57 ± 0.16 ^{ab}	1.78 ± 0.13 ^b
1.7g malic acid	2.47 ± 0.10 ^{ab}	2.95 ± 0.32 ^a	2.87 ± 0.27 ^a	1.98 ± 0.17 ^b
1.34g malic acid	2.24 ± 0.22 ^b	3.36 ± 0.16 ^a	N/A	N/A

Means with different letters in the same row are significantly different ($P < 0.05$).

6.4.7 Thermal Analysis

Thermally resilient films are important as it is exposed to a wide range of temperature. The presence of intermolecular interaction of proteins, such as hydrogen bonds, ionic interactions, and hydrophobic-hydrophobic interactions which stabilized the film network can influence the thermal stability of films (Hoque et al., 2010). The thermal behaviour of selected films formulated with PPI and PPC are shown in Table 6.8.

Table 6.8 Thermal properties of pea protein flours and films

Sample	Peak denaturation point, T_d (°C)	Enthalpy of denaturation, ΔH_d (J/g)
PPI	104.3	1272
PPC	111.5	1426
	Peak melting point, T_m (°C)	Enthalpy of melting, ΔH_m (J/g)
PPI 5SP 1.7MA	207.9	163.7
PPI 5W 1.7MA	211.6	133.8
PPC 5SP 1.7MA	200.5	172.6
PPC 5AS 1.34MA	172.8	202.5

Glass transition was not observed in all the flours and selected films tested using DSC. In contrast, Acquah et al. (2020) reported glass transition temperatures at 96 °C for PPI and PPC films, while Bora et al. (1994) found that mixed globulins of pea had one thermal transition at 86.2 °C. Glass transition could not be observed and this may be due to the overlapping enthalpy of relaxation and denaturation peaks (Zhou & Labuza, 2007). From 25 to 300 °C, the thermograms in Figure 6.2 showed that all the films had a higher melting temperature than the PPI and PPC flours. The shift of T_m may be caused by the interactions of the citric acid and malic acid with the pea proteins. According to Sharma et al. (2018), cross-linking stabilizes the proteins and increases the overall molecular weight, resulting in an increase in T_m . A notably lower T_m was observed for PPC 5AS 1.34MA when compared to PPC 5SP 1.7MA. Due to the similar tensile strength between these two films as shown in Table 6.5, elongation at break was compared. Elongation at break values for PPC 5AS 1.34MA was lower than that for PPC 5SP 1.7MA. This supports that the weaker cross linking may have caused a lower T_m . Thermogram of the films in Figure 6.2 also shows endothermic reaction from 106 to 129 °C. This may be caused by the presence of residual water in the films. Using thermogravimetric analysis, studies have reported about 10% weight loss of films at 130 °C which was attributed to the loss of water or residual solvent mixture (López-de-Dicastillo et al., 2012; Ramos et al., 2013). Sharma et al. (2018) had also attributed weight loss in sesame protein films from 130 to 170 °C to water loss. PPC 5SP 1.7MA had an endothermic event at about 150 °C instead of 130 °C. This may indicate that this film is more cohesive as a higher temperature was needed to cause an endothermic change.

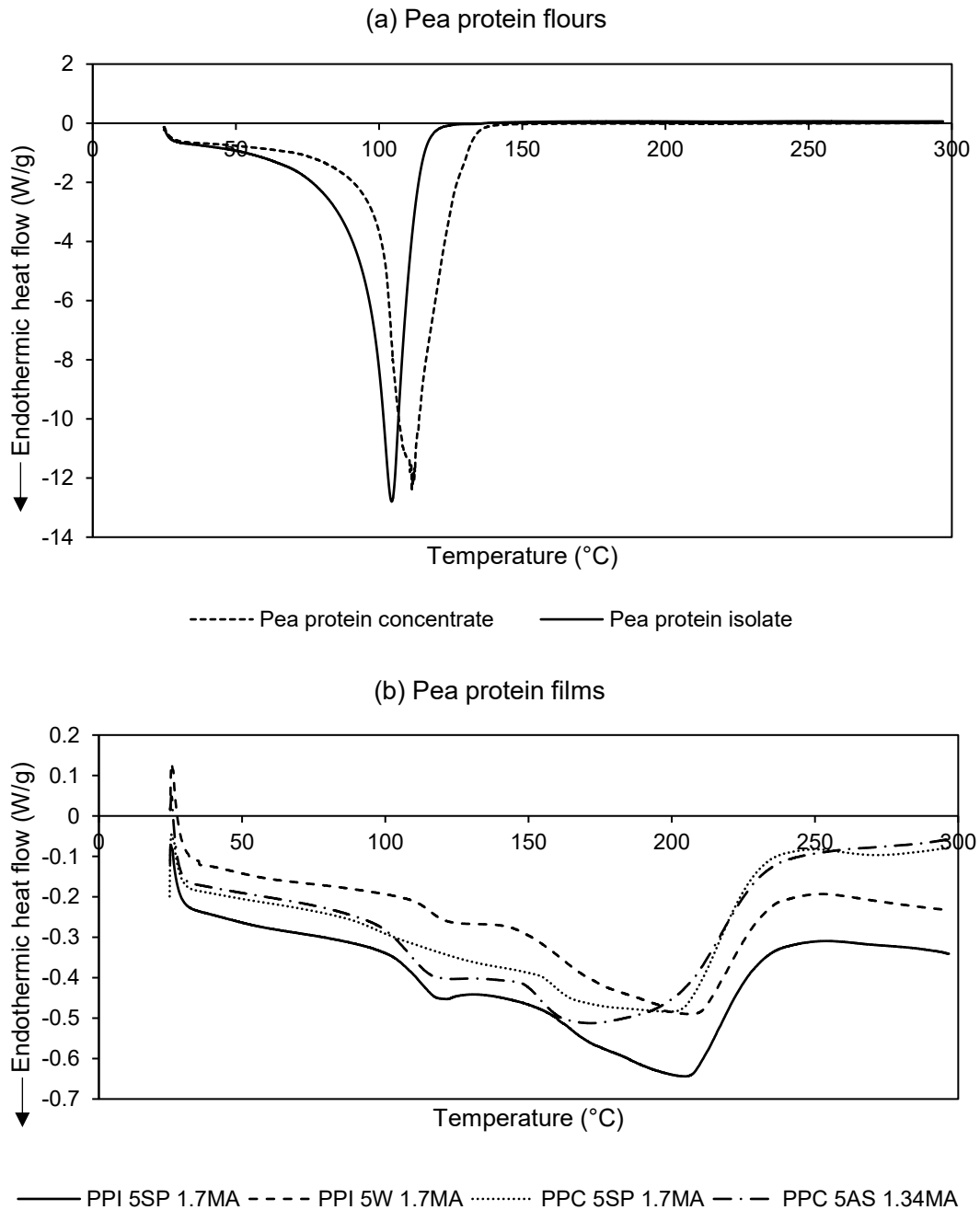


Figure 6.2 Differential scanning calorimetry thermograms for (a) pea protein flours and (b) pea protein films

As shown in Table 6.5, PPC 5SP 1.7MA had a high elongation at break value. The broad peaks observed in Figure 6.2 can be caused by partially crystalline polymers (Mettler Toledo, 2000) and diversity of compounds present (Medina Jaramillo et al., 2016) as compared to the sharp melting peaks of PPI and PPC flours (Figure 6.2 (a)).

As shown in Table 6.8, the enthalpies of denaturation, ΔH_d , of PPI and PPC flours are 1272 J/g and 1426 J/g, respectively. These values are much higher than the values obtained by Shevkani and Singh (2015) where the authors reported an enthalpy of 16.2 J/g for field pea protein isolate suspensions. Grass pea protein isolate had enthalpies from 12.60 to 19.03 J/g (Feyzi et al., 2018) while Sun and Arntfield (2010) reported even lower enthalpy of commercial pea protein isolate at 0.036 J/g protein. The high enthalpies reported in this study may be due to the enthalpy of vapourization of water as the enthalpy of vapourization of pure water is about 2257 J/g (Newsham & Mendez-Lecanda, 1982). In this study, 15% (w/w) pea protein dispersions were used and this translates to a water content of 5.7 g water/g dry matter. In protein and milk dispersions, the heat of fusion increased linearly with an increase in water content within 0 and 25 g water/g dry matter (Le Dean et al., 2001). Table 6.8 also shows ΔH_m for selected films where PPC 5AS 1.34MA had the highest ΔH_m while PPI 5W 1.7MA had the lowest ΔH_m . Although PPC 5AS 1.34MA had a lower T_m than PPI 5W 1.7MA, ΔH_m does not necessarily increase with T_m (Kokoszka et al., 2010) as the chemical structure of polymers greatly affects their properties (Ustunol & Mert, 2004). The decrease in ΔH_m for PPI 5W 1.7MA in comparison to PPI 5SP 1.7MA implies that the thermal stability of the film was reduced (Shi & Dumont, 2014a) when the extracts were not present. In the study by Acquah et al. (2020), PPI and PPC films were reported as having enthalpies of 73.99 and 42.41 J/g, respectively, which are lower than the values for the selected films in this study where malic acid was used as a cross-linker. The increased cross-linkages between proteins and polyphenols in the extracts (Sivarooaban et al., 2008) may cause the ΔH_m to increase as more energy is needed to break the protein network. A higher ΔH_m also indicates higher resilience to heat (Acquah et al., 2020).

6.4.8 Migration and Antioxidant Tests

Functional films which are incorporated with extracts have the added benefits of releasing the bioactive compounds when they are in contact with the packaged product. To simulate alcoholic food and fatty food, 10% (v/v) ethanol and 95% (v/v) ethanol were respectively used (Han et al., 2018; Rodríguez-Martínez et al., 2016). According to the European Union Commission Regulation No 10/2011, 10% (v/v) ethanol represents food that have a hydrophilic character while 95% (v/v) ethanol is a suitable simulant for foods that have a lipophilic character.

Table 6.9 Total phenolic content and radical scavenging activity of PPI and PPC films in 10% ethanol

PPI films total phenolic content release into 10% ethanol at 60 minutes (mg GAE/g film)				
Cross-linker	Sodium phosphate extract	Ammonium sulphate extract	Water	Ethanol
1.7g citric acid	0.670 ± 0.03 ^a	N/A	0.323 ± 0.02 ^b	Did not form
1.7g malic acid	0.454 ± 0.03 ^a	N/A	0.356 ± 0.06 ^a	0.393 ± 0.02 ^a
1.34g malic acid	0.497 ± 0.05	N/A	N/A	N/A
PPC films total phenolic content release into 10% ethanol at 60 minutes (mg GAE/g film)				
	Sodium phosphate extract	Ammonium sulphate extract	Water	Ethanol
1.7g citric acid	2.773 ± 0.12 ^a	2.424 ± 0.09 ^{bc}	2.674 ± 0.04 ^{ab}	2.158 ± 0.03 ^c
1.7g malic acid	2.954 ± 0.36 ^a	2.044 ± 0.22 ^a	2.371 ± 0.04 ^a	2.349 ± 0.13 ^a
1.34g malic acid	2.983 ± 0.13 ^a	2.165 ± 0.11 ^b	N/A	N/A
PPI films radical scavenging activity in 10% ethanol at 60 minutes (%)				
	Sodium phosphate extract	Ammonium sulphate extract	Water	Ethanol
1.7g citric acid	3.7 ± 0.2 ^a	N/A	2.9 ± 0.3 ^a	Did not form
1.7g malic acid	2.6 ± 0.2 ^a	N/A	2.2 ± 0.1 ^a	2.1 ± 0.2 ^a
1.34g malic acid	2.8 ± 0.1	N/A	N/A	N/A
PPC films radical scavenging activity in 10% ethanol at 60 minutes (%)				
	Sodium phosphate extract	Ammonium sulphate extract	Water	Ethanol
1.7g citric acid	3.0 ± 0.6 ^{ab}	2.1 ± 0.3 ^b	4.0 ± 0.3 ^a	3.7 ± 0.3 ^{ab}
1.7g malic acid	3.7 ± 0.3 ^a	2.1 ± 0.2 ^b	3.4 ± 0.1 ^a	3.5 ± 0.1 ^a
1.34g malic acid	3.7 ± 0.2 ^a	2.0 ± 0.2 ^b	N/A	N/A

Means with different letters in the same row are significantly different ($P < 0.05$).

The release of total phenolic content (TPC) and radical scavenging activity (RSA) into 10% ethanol was investigated from 0 to 60 minutes. Table 6.9 shows the TPC and RSA of the films at 60 minutes. The overall release behaviour is shown in Appendix A Figure A.6. PPC films had higher TPC ranging from 2.044 to 2.983 mg GAE/g film compared to PPI films with TPC from 0.323 to 0.670 mg GAE/g film. PPC films were also easily disintegrated in 10% ethanol while PPI films remain intact as whole pieces. With the higher TPC release and disintegration, it is suggested that the PPC films are overall more hydrophilic than PPI films. In a study by Reinkensmeier et al. (2015), PPC flour had higher solubility than PPI flour at pH 7. In the present study, the pH of 10%

ethanol is 6.9 therefore the higher flour solubility may have contributed to the film solubility. The yellow field peas themselves contain phenolic compounds (Agboola et al., 2010) and this could result in the increased release of TPC for films formed with PPC. Reinkensmeier et al. (2015) had also shown that the surface hydrophobicity of PPI flour was higher than PPC at pH 7. This is in contrast with the study by Acquah et al. (2020) who found that PPI films were more hydrophilic than PPC films based on the measurement of surface contact angle with water. The difference could be due to protein types, purity, and amino acid composition of the samples from different studies. Table 6.9 also shows that the addition of ammonium sulphate and sodium phosphate extracts increased the TPC release as compared to the control films. This is due to the presence of haskap leaf extracts as they contain bioactive compounds (Chong et al., 2020a; Oszmiański et al., 2011).

Free radicals are reactive chemical species with unpaired electron and an overproduction will lead to oxidative stress caused by a weakened bodily antioxidant defense system (Mustafa et al., 2010). Radical scavenging compounds such as antioxidants can delay or inhibit the oxidation of lipids and other molecules, therefore a high RSA is desirable as it reflects high antioxidant activity. The RSA of PPI films ranged from 2.1 to 3.7% while PPC films ranged from 2.1 to 4.0% in 10% ethanol. The RSA values were similar for both PPI and PPC films despite the difference in TPC release as discussed. This suggests that there are other secondary metabolites present in haskap leaves such as flavonoids (Dawson, 2017; Oszmiański et al., 2011) that contributed towards the RSA. Some film formulations such as PPI films with sodium phosphate extracts and PPC 5SP 1.7MA showed increased RSA as compared to the control films. Although the cross-linkers citric acid and malic acid are not phenolic compounds as they do not have a phenolic or benzene ring, these carboxylic acids are known to have antioxidant effects. The acids improve the efficiency of phenolic primary antioxidants by chelating metal ions for catalyzing lipid autoxidation (Chahardoli et al., 2020). This was demonstrated by the RSA in the control films that had water and ethanol instead of the leaf extracts. Additionally, the yellow field peas inherently contain phenolic compounds (Agboola et al., 2010) and was detected in control films. In some studies, the Folin-Ciocalteu assay showed low correlation between TPC and antioxidant activity due to its nonspecificity as it reacts with not only

polyphenols but to other substances that could be oxidised by the Folin reagent (Babbar et al., 2011; Fernandes de Oliveira et al., 2012; Singleton et al., 1999).

Using 95% ethanol to simulate fatty foods, TPC release was evaluated from 0 to 51 hours. The PPI and PPC films remained intact at all time intervals. Table A.4 in Appendix B shows TPC release in 95% ethanol which simulates fatty food. PPI films had a TPC release ranging from 1.546 to 2.116 mg GAE/g film while PPC films ranged from 1.781 to 2.565 mg GAE/g film in 95% ethanol. PPI films had improvement of TPC release with sodium phosphate extracts. PPC 5EtOH and PPC 5SP 1.7MA also showed high TPC diffusion into the fatty food simulant. The RSA at the test endpoint of 51 hours indicated that PPI 5SP 1.7CA, PPC 5EtOH 1.7CA, and PPC 5SP 1.7MA had high antioxidant activities.

Figure A.6 and Figure A.7 in Appendix A show that in general, PPC films with and without the extracts released higher TPC in 10% ethanol than in 95% ethanol at equilibrium. In this study, TPC release from both PPI and PPC films mainly occurred in alcoholic food simulant for the first 6 minutes while Han et al. (2018) reported a corresponding duration of 10 minutes. According to Han et al. (2018), protein may be more soluble in 10% ethanol. The authors also attributed the hydrophilic nature of soy protein isolate as the reason for more swelling in 10% ethanol than 95% ethanol. This supports the observation in this work where PPC films disintegrated in 10% ethanol but not in 95% ethanol. Pea protein films are hydrophilic as the water contact angle was less than 90° (Acquah et al., 2020; Blossey, 2003). The disintegration of PPC films in 10% ethanol suggests that they may be utilized in orodispersible films (Hoffmann et al., 2011) or film pouches for premeasured dry foods that dissolve rapidly in aqueous solutions (Janjarasskul et al., 2020). In alcoholic food simulant, Han et al. (2018) observed that the polyphenols released from soy protein isolate films with and without licorice residue extract ranged from 3.5 to 5.5 mg GAE/g film. These values are higher than the results from our study (Table 6.9) which ranged from 0.323 to 2.983 mg GAE/g film. Although the authors did not report the TPC of the initial extract to make corresponding comparisons, the extracts were added in increasing concentrations in the film formulation. In this study, TPC of haskap leaf extracts were 0.03 and 0.37 mg GAE/mL. These concentrations were used without purification to minimize the post-extraction steps. In the fatty food simulant, the TPC values from this study

which were 1.5 to 2 mg GAE/g film are similar to the soy protein isolate films with 10 g licorice residue extract with TPC of 2 mg GAE/g film (Han et al., 2018). The pea protein films in this study which were tested for 51 hours in fatty food simulant had higher TPC release than that of soy protein isolate films with 1 to 5% mango kernel extracts where Maryam Adilah et al. (2018) reported 4.406 to 21.393 μg GAE/g film after 7 days. The results from the TPC release test and RSA assay indicate that some of these films could be used as antioxidative packaging to increase the shelf life of perishable products. However further testing would be necessary to determine the minimum antioxidant levels required in the films for this purpose.

6.5 Conclusion

This work showed that haskap leaf extracts obtained by ATPE and ATPF can be directly incorporated in pea protein films. The physical, mechanical, optical, water barrier, thermal, and antioxidant properties of the films varied depending on the formulation. Among the films with extracts, some formulations such as PPI 5SP 1.34MA and PPI 5SP 1.7MA showed relatively better mechanical properties. These pea protein films also demonstrated UV absorbing properties, which indicates that they could protect packaged products from UV degradation. Films such as PPI 5SP 1.7CA and PPC 5AS 1.34MA had higher WVP than the other films, indicating a possibility of being used as packaging for fresh produce which requires higher moisture transfer. Additionally, the melting point of selected films were well above 150 °C, suggesting that these films are thermally stable. The films have also shown that their antioxidant properties can be transferred to alcoholic and lipid-rich foods. Although PPC films disintegrated in 10% ethanol, more bioactive compounds were released into the simulant as indicated by the higher TPC levels as compared to PPI films, suggesting that PPC films could be used for orodispersible and food pouches for rapid dissolution. Since PPI films had higher average tensile strength and remained intact as whole pieces in 10% ethanol when compared to PPC films, PPI films are recommended as packaging for alcoholic or aqueous food products. Additionally, films with sodium phosphate extract showed higher TPC release compared to other films, suggesting that the presence of haskap leaf extracts obtained by ATPE improved the bioactive content of the films and its subsequent release in alcoholic and aqueous food. Therefore these functional films have the potential to extend the shelf life of perishable products. Since the extracts can be

directly incorporated into pea protein films, evaporation of alcohol and removal of the salts are not necessary. The minimization of post-extraction steps points towards the principles of green engineering where separation operations should be designed to minimize energy consumption. Further investigations are needed to elucidate the efficacy of these pea protein films on model food material.

Chapter 7 : Conclusions

7.1 Summary and Conclusions

This thesis investigated salt/ethanol and sugar/propanol ATPS as an alternative more sustainable extraction medium for the recovery of bioactive compounds from haskap leaves, and demonstrated the feasibility of bubble-assisted configurations for extraction and recycling of ATPS components. Upon further research which showed that the salt/ethanol ATPE had higher extraction efficiency, these ATPE extracts were used in the development of novel pea protein films that may have interesting applications as a sustainable biobased material for food packaging.

In **Chapter 2**, recent literature on haskap plant, ATPS, ATPE, ATPF, recycling techniques, and bio-based films were reviewed. Since there is growing interest of haskap berries in North America, there is an opportunity to recover bioactive compounds from haskap leaves by using environmentally friendly extraction methods. The extracts could also be incorporated into bio-based films as potential food packaging.

In **Chapter 3**, four ATPS namely ammonium sulphate/ethanol, sodium dihydrogen phosphate/ethanol, glucose/1-propanol, and maltose/1-propanol were used and variables namely extraction time, sample loading, and tie line length were investigated. Salt/ethanol ATPE had higher extraction efficiency than sugar/propanol ATPE and more specifically, the sodium dihydrogen phosphate/ethanol ATPE had the highest extraction efficiency of 93.9% for chlorogenic acid, 96.8% for flavonoids, and 97.8% for total phenolic content. Although the bioactive yields obtained by ATPE were lower than that obtained by conventional extraction, Soxhlet extraction required 24 hours to achieve those yields. In addition to extracting at room temperature (25 °C) and a relatively shorter extraction time (maximum 2 hours), the ATPE process is unique as it concentrates the bioactive compounds at the top phase as shown by partition coefficient values greater than one.

To improve the sustainability and economics of ATPE, recycling of the phase-forming components for the four ATPS was investigated in **Chapter 4**. It was shown that ethanol and salts can be recycled by rotary evaporation and dilution crystallization, respectively to be used in two successive ATPE systems. The extraction efficiency maintained throughout two stages, suggesting that recycling is feasible and can

potentially reduce the post-handling costs and the amount of ATPE phase-forming components. However, the sugars could not be separated from the slurries and only 1-propanol was evaporated and recycled.

In **Chapter 5**, the ATPE process was enhanced by the presence of air bubbles that facilitated mass transfer of biomolecules to the top phase. Since sugar/propanol systems had lower extraction efficiency and the sugars could not be recycled, salt/ethanol systems were used in this chapter. Ammonium sulphate/ethanol ATPF increased the partition coefficient by 208% for chlorogenic acid and 170% for flavonoids compared to ATPE using the same system. However, there was no significant difference between ATPF and ATPE for sodium dihydrogen phosphate/ethanol systems.

In **Chapter 6**, sodium dihydrogen phosphate/ethanol ATPE extracts and ammonium sulphate/ethanol ATPF extracts were incorporated directly into pea protein films for the potential application of food packaging. Citric acid and malic acid functioned as cross-linkers while glycerol was added as plasticizer to improve the strength and flexibility of the films. The extracts consisting of bioactive compounds, ethanol, residual salt, and water had shown varying effect on the physical, mechanical, thermal, and antioxidant properties of the films. Some formulations containing haskap leaf extracts and residual salt demonstrated improved water vapour permeability and flexibility. The thermally stable films also absorbed ultraviolet light, suggesting that the films could protect products from ultraviolet degradation.

The specific conclusions relating to the original research objectives are as follows:

- i) Among the four GRAS ATPE systems investigated, sodium dihydrogen phosphate/ethanol ATPE had maximum extraction efficiency of 93.9% for chlorogenic acid, 96.8% for flavonoids, and 97.8% for total phenolic content from haskap leaves with corresponding partition coefficients of 1.73, 3.50, and 6.59.
- ii) Two recycling stages for the four ATPE systems produced consistent partitioning, extraction efficiency, and extraction yields. Both the salts and ethanol in the salt/ethanol ATPE were recycled while only 1-propanol could be recycled in sugar/propanol ATPE.
- iii) Ammonium sulphate/ethanol ATPF was optimized at 5 mg leaves, 120 minutes flotation time, and air flow rate of 28.6 mL/min with extraction efficiencies of

97.1% for chlorogenic acid, 98.7% for flavonoids, and 99.6% for total phenolic content. There was no significant difference between ATPF and ATPE for sodium dihydrogen sulphate/ethanol systems.

iv) Novel pea protein films incorporating haskap leaf extracts obtained from ATPE and ATPF were successfully developed, incorporating not only the bioactive compounds but the ATPS phase components as well. Using citric acid and malic acid as cross-linkers and glycerol as plasticizer, the resultant pea protein films were assessed for their physical properties, mechanical properties, water vapour permeability, thermal properties, and migration behaviour of bioactive compounds into food simulants. Some formulations namely PPI 5SP 1.7CA, PPC 5AS 1.7CA, and PPC 5AS 1.7MA containing haskap leaf extracts and residual salt, demonstrated better water vapour permeability while PPI 5SP 1.7MA, PPC 5SP 1.7CA, and PPC 5SP 1.34MA showed improved flexibility. The peak melting temperature of selected films were above 150 °C, indicating thermal stability. Since PPI films had higher average tensile strength and remained intact as whole pieces in 10% ethanol when compared to PPC films, PPI films are recommended as packaging for alcoholic or aqueous food products. Although PPC films disintegrated in 10% ethanol, more bioactive compounds were released into the simulant as indicated by the higher TPC levels as compared to PPI films. Additionally, films with sodium phosphate extract showed higher TPC release compared to other films.

7.2 Contributions to Knowledge

Commercial products made with haskap berries are becoming well-known since the berries have higher antioxidant activity compared to other berries. With the growing interest of haskap farming for the berries, haskap leaves are generated as an agricultural residue and the amount of this residue is expected to increase. This study provides insights into the valorization of haskap leaves as an alternative and under-utilized source for bioactive compounds. For the first time, haskap leaves were used as a source of bioactive compounds, specifically chlorogenic acid and flavonoids, for the development of packaging films. This study shows that ATPS is an alternative environmentally friendly extraction method to efficiently recover the bioactive compounds. This study also shows that ATPS, which has been used mainly to extract

proteinaceous compounds, can likewise be applied to extract biomolecules from haskap leaves. Additionally, this work has shown that the recycling of phase-forming components for two stages is feasible while maintaining the extraction efficiency. This implies that the amount of materials used and associated post-handling costs can be reduced. The introduction of bubbles in the ATPF process enhanced the extraction efficiency and partitioning behavior of the bioactive compounds particularly in ammonium sulphate/ethanol systems.

For the first time, haskap leaf extracts obtained from ATPE and ATPF were added directly into pea protein formulations to form novel films that incorporated not only the bioactive compounds that were extracted, but the GRAS ATPS components as well. The disintegration of PPC films in 10% ethanol suggests that PPC films can be used in applications that require rapid dissolution and release such as in orodispersible films for the paediatric and geriatric population. PPC films can also be used as film pouches for premeasured dry foods that dissolve rapidly. Both PPI and PPC films with sodium phosphate extracts demonstrated higher TPC release compared to other films, suggesting that the presence of haskap leaf extracts obtained by ATPE improved the bioactive content of the films and its subsequent release in alcoholic and aqueous food. With Canada being the largest producer of dry peas, the development of environmentally friendly bio-based packaging from peas is critical in developing new markets for economic growth as value-added materials. The formulations resulted in varying film properties, suggesting that alcohol evaporation and salt precipitation are not necessary with extracts obtained from ATPS. This reduction in post-processing steps would reduce the associated processing costs and energy. This is in accordance with the Principles of Green Engineering where extraction operations should minimize energy consumption and material use.

7.3 Recommendations for Future Work

Based on the work performed in this thesis, there are some suggestions to advance this area of research:

- a) In addition to benchtop experiments, the partitioning behaviour of biomolecules could be modelled by molecular dynamics simulation software. Many studies using ATPS extraction including ATPE and ATPF have used one-factor-at-a-

time (OFAT) approach and other studies, including this work, have used response surface methodology (RSM) to optimize extraction conditions. Molecular dynamics simulations have been done by other researchers to model protein purification in ATPS containing polyethylene glycol. This will improve understanding of the driving forces and specific properties of the target compounds that influence partitioning.

- b) During the recycling of phase-forming components, fresh components were added to the recycled components to compensate for the diluted alcohol and reduced salt precipitates. Although some alcohol could have been evaporated into the atmosphere, the loss is negligible due to the small amount. However, this loss may be significant when the ATPE process is scaled-up. Therefore, it is recommended to investigate if there are remaining salt in the evaporated alcohol so that further purification can be performed to increase the alcohol concentration and recover more salt. Apart from dilution crystallization which involves adding more alcohol to precipitate the salt, other environmentally friendly and efficient techniques to recover the salt should be assessed.
- c) At the end of the flotation time in the ATPF process, it was not possible to perform centrifugation to promote phase separation. This may be the cause of the insignificant difference in terms of bioactive yields, extraction efficiency, and partition coefficient observed between sodium dihydrogen phosphate/ethanol ATPE and ATPF. Therefore, the ATPF process could be further improved by investigating the design parameters of the flotation column. For batch settlers, a height/diameter ratio of less than one was recommended to improve phase separation. This consideration should be integrated with the partitioning behaviour of different systems for future ATPF work so that the equilibration time can be reduced while achieving desired partitioning.
- d) In addition to bubble-assisted ATPF, ATPE has been integrated with ultrasound, microwave, and electricity to improve the extraction performance. Therefore, these methods should be investigated to enhance the extraction of bioactive compounds from haskap leaves. ATPE and ATPF were scaled-up to 100-folds and 15-folds respectively in past studies, and the systems were shown to provide consistent extraction performance when compared to bench-scale experiments. This shows that scaling-up should be investigated with the ATPE and ATPF of haskap leaves.

e) It has been shown that the pea protein films incorporated with extracts from ATPE and ATPF have varying properties. To evaluate the potential of the films as food packaging, it is recommended to integrate model food systems. As an example, climacteric fruits which can ripen after being picked could be used as model systems as the fruit quality can be assessed as time progresses. In view of this, it may be possible to prolong the shelf life of the fruits by packaging them in pea protein films incorporated with extracts. The required concentration of extracts in the film formulations should also be optimized to achieve the desired shelf life extension. Since sodium chloride has been used to create humidity-regulating trays and film, the incorporation of salt/alcohol ATPS extracts which contains residual salt should be investigated to develop similar packaging solutions.

REFERENCES

- Abdel-Aal, E.-S. M., Ragaei, S., Rabalski, I., Warkentin, T., & Vandenberg, A. (2018). Nutrient content and viscosity of Saskatchewan-grown pulses in relation to their cooking quality. *Canadian Journal of Plant Science*, *99*(1), 67–77. <https://doi.org/10.1139/cjps-2018-0140>
- Acquah, C., Zhang, Y., Dubé, M. A., & Udenigwe, C. C. (2020). Formation and characterization of protein-based films from yellow pea (*Pisum sativum*) protein isolate and concentrate for edible applications. *Current Research in Food Science*, *2*, 61–69. <https://doi.org/10.1016/j.crfs.2019.11.008>
- Agati, G., Biricolti, S., Guidi, L., Ferrini, F., Fini, A., & Tattini, M. (2011). The biosynthesis of flavonoids is enhanced similarly by UV radiation and root zone salinity in *L. vulgare* leaves. *Journal of Plant Physiology*, *168*(3), 204–212. <https://doi.org/10.1016/j.jplph.2010.07.016>
- Agboola, S. O., Mofolasayo, O. A., Watts, B. M., & Aluko, R. E. (2010). Functional properties of yellow field pea (*Pisum sativum* L.) seed flours and the in vitro bioactive properties of their polyphenols. *Food Research International*, *43*(2), 582–588. <https://doi.org/10.1016/j.foodres.2009.07.013>
- Aguilar-Vázquez, G., Loarca-Piña, G., Figueroa-Cárdenas, J. D., & Mendoza, S. (2018). Electrospun fibers from blends of pea (*Pisum sativum*) protein and pullulan. *Food Hydrocolloids*, *83*, 173–181. <https://doi.org/10.1016/j.foodhyd.2018.04.051>
- Aguilar, O., & Rito-Palomares, M. (2008). Processing of soybean (*Glycine max*) extracts in aqueous two-phase systems as a first step for the potential recovery of recombinant proteins. *Journal of Chemical Technology & Biotechnology*, *83*(3), 286–293. <https://doi.org/10.1002/jctb.1805>
- Ahmed, S., & Ikram, S. (2016). Chitosan and gelatin based biodegradable packaging films with UV-light protection. *Journal of Photochemistry and Photobiology B: Biology*, *163*, 115–124. <https://doi.org/10.1016/j.jphotobiol.2016.08.023>
- Albertsson, P.-Å. (1985). *History of Aqueous Polymer Two-Phase Partition* (H. Walter, D. E. Brooks, & D. Fisher (eds.); pp. 1–10). Academic Press. <https://doi.org/10.1016/B978-0-12-733860-6.50008-6>
- Alves, L. A., Almeida e Silva, J. B., & Giuliatti, M. (2007). Solubility of d-Glucose in Water and Ethanol/Water Mixtures. *Journal of Chemical & Engineering Data*, *52*(6), 2166–2170. <https://doi.org/10.1021/je700177n>
- Alves, M. M., Gonçalves, M. P., & Rocha, C. M. R. (2017). Effect of ferulic acid on the performance of soy protein isolate-based edible coatings applied to fresh-cut apples. *LWT*, *80*, 409–415. <https://doi.org/10.1016/j.lwt.2017.03.013>
- Anastas, P. T., & Zimmerman, J. B. (2003). *Design through the 12 principles of green engineering*. ACS Publications. <https://doi.org/10.1021/es032373g>

- Anderson, C., & Simsek, S. (2019). Mechanical profiles and topographical properties of films made from alkaline extracted arabinoxylans from wheat bran, maize bran, or dried distillers grain. *Food Hydrocolloids*, 86, 78–86. <https://doi.org/10.1016/j.foodhyd.2018.02.016>
- Andrade, R. D., Skurtys, O., & Osorio, F. A. (2012). Atomizing Spray Systems for Application of Edible Coatings. *Comprehensive Reviews in Food Science and Food Safety*, 11(3), 323–337. <https://doi.org/10.1111/j.1541-4337.2012.00186.x>
- Andrade, R. M. S., Ferreira, M. S. L., & Gonçalves, É. C. B. A. (2016). Development and Characterization of Edible Films Based on Fruit and Vegetable Residues. *Journal of Food Science*, 81(2), E412–E418. <https://doi.org/10.1111/1750-3841.13192>
- Araghi, M., Moslehi, Z., Mohammadi Nafchi, A., Mostahsan, A., Salamat, N., & Daraei Garmakhany, A. (2015). Cold water fish gelatin modification by a natural phenolic cross-linker (ferulic acid and caffeic acid). *Food Science & Nutrition*, 3(5), 370–375. <https://doi.org/10.1002/fsn3.230>
- Arcan, I., & Yemenicioğlu, A. (2011). Incorporating phenolic compounds opens a new perspective to use zein films as flexible bioactive packaging materials. *Food Research International*, 44(2), 550–556. <https://doi.org/10.1016/j.foodres.2010.11.034>
- Asenjo, J. A., & Andrews, B. A. (2011). Aqueous two-phase systems for protein separation: A perspective. *Journal of Chromatography A*, 1218(49), 8826–8835. <https://doi.org/10.1016/j.chroma.2011.06.051>
- ASTM International. (2013). *ASTM D1004-13 Standard Test Method for Tear Resistance (Graves Tear) of Plastic Film and Sheeting*. <https://doi.org/10.1520/D1004-13>
- ASTM International. (2016). *ASTM E96/E96M-16 Standard Test Methods for Water Vapor Transmission of Materials*. https://doi.org/10.1520/E0096_E0096M-16
- ASTM International. (2018a). *ASTM D7192-18 Standard Test Method for High Speed Puncture Properties of Plastic Films Using Load and Displacement Sensors*. <https://doi.org/10.1520/D7192-18>
- ASTM International. (2018b). *ASTM D882-18 Standard Test Method for Tensile Properties of Thin Plastic Sheeting*. <https://doi.org/10.1520/D0882-18>
- Babbar, N., Oberoi, H. S., Uppal, D. S., & Patil, R. T. (2011). Total phenolic content and antioxidant capacity of extracts obtained from six important fruit residues. *Food Research International*, 44(1), 391–396. <https://doi.org/10.1016/j.foodres.2010.10.001>
- Babu, B. R., Rastogi, N. K., & Raghavarao, K. S. M. S. (2008). Liquid–liquid extraction of bromelain and polyphenol oxidase using aqueous two-phase system. *Chemical Engineering and Processing: Process Intensification*, 47(1), 83–89. <https://doi.org/10.1016/j.cep.2007.08.006>

- Bampouli, A., Kyriakopoulou, K., Papaefstathiou, G., Louli, V., Krokida, M., & Magoulas, K. (2014). Comparison of different extraction methods of *Pistacia lentiscus* var. chia leaves: Yield, antioxidant activity and essential oil chemical composition. *Journal of Applied Research on Medicinal and Aromatic Plants*, *1*(3), 81–91. <https://doi.org/10.1016/j.jarmap.2014.07.001>
- Banerjee, R., & Chen, H. (1995). Functional Properties of Edible Films Using Whey Protein Concentrate. *Journal of Dairy Science*, *78*(8), 1673–1683. [https://doi.org/10.3168/jds.S0022-0302\(95\)76792-3](https://doi.org/10.3168/jds.S0022-0302(95)76792-3)
- Banker, G. S., Gore, A. Y., & Swarbrick, J. (1966). Water vapour transmission properties of free polymer films. *Journal of Pharmacy and Pharmacology*, *18*(7), 457–466. <https://doi.org/10.1111/j.2042-7158.1966.tb07906.x>
- Barac, M., Cabrilo, S., Pesic, M., Stanojevic, S., Zilic, S., Macej, O., & Ristic, N. (2010). Profile and functional properties of seed proteins from six pea (*Pisum sativum*) genotypes. *International Journal of Molecular Sciences*, *11*(12), 4973–4990. <https://doi.org/10.3390/ijms11124973>
- Becker, R., Pączkowski, C., & Szakiel, A. (2017). Triterpenoid profile of fruit and leaf cuticular waxes of edible honeysuckle *Lonicera caerulea* var. kamtschatica. *Acta Societatis Botanicorum Poloniae*, *86*(1). <https://doi.org/10.5586/asbp.3539>
- Belay, A., & Gholap, A. V. (2009). Characterization and determination of chlorogenic acids (CGA) in coffee beans by UV-Vis spectroscopy. *African Journal of Pure and Applied Chemistry*, *3*(11), 34–240.
- Benavides, J., & Rito-Palomares, M. (2007). Practical experiences from the development of aqueous two-phase processes for the recovery of high value biological products. *Journal of Chemical Technology & Biotechnology*, *83*(2), 133–142. <https://doi.org/10.1002/jctb.1844>
- Benavides, S., Villalobos-Carvajal, R., & Reyes, J. E. (2012). Physical, mechanical and antibacterial properties of alginate film: Effect of the crosslinking degree and oregano essential oil concentration. *Journal of Food Engineering*, *110*(2), 232–239. <https://doi.org/10.1016/j.jfoodeng.2011.05.023>
- Benbettaïeb, N., Gay, J.-P., Karbowski, T., & Debeaufort, F. (2016). Tuning the Functional Properties of Polysaccharide–Protein Bio-Based Edible Films by Chemical, Enzymatic, and Physical Cross-Linking. *Comprehensive Reviews in Food Science and Food Safety*, *15*(4), 739–752. <https://doi.org/10.1111/1541-4337.12210>
- BenBettaïeb, N., Karbowski, T., Bornaz, S., & Debeaufort, F. (2015). Spectroscopic analyses of the influence of electron beam irradiation doses on mechanical, transport properties and microstructure of chitosan-fish gelatin blend films. *Food Hydrocolloids*, *46*, 37–51. <https://doi.org/10.1016/j.foodhyd.2014.09.038>

- Besagni, G., & Inzoli, F. (2017). The effect of liquid phase properties on bubble column fluid dynamics: Gas holdup, flow regime transition, bubble size distributions and shapes, interfacial areas and foaming phenomena. *Chemical Engineering Science*, *170*, 270–296. <https://doi.org/10.1016/j.ces.2017.03.043>
- Bezerra, M. A., Santelli, R. E., Oliveira, E. P., Villar, L. S., & Escaleira, L. A. (2008). Response surface methodology (RSM) as a tool for optimization in analytical chemistry. *Talanta*, *76*(5), 965–977. <https://doi.org/10.1016/j.talanta.2008.05.019>
- Bi, P., Chang, L., Mu, Y., Liu, J., Wu, Y., Geng, X., & Wei, Y. (2013). Separation and concentration of baicalin from *Scutellaria Baicalensis* Georgi extract by aqueous two-phase flotation. *Separation and Purification Technology*, *116*, 454–457. <https://doi.org/10.1016/j.seppur.2013.06.024>
- Bi, P., Dong, H., & Dong, J. (2010). The recent progress of solvent sublation. *Journal of Chromatography A*, *1217*(16), 2716–2725. <https://doi.org/10.1016/j.chroma.2009.11.020>
- Bi, P., Dong, H., & Yuan, Y. (2010). Application of aqueous two-phase flotation in the separation and concentration of puerarin from *Puerariae* extract. *Separation and Purification Technology*, *75*(3), 402–406. <https://doi.org/10.1016/j.seppur.2010.09.010>
- Bico, S. L. S., Raposo, M. F. J., Morais, R. M. S. C., & Morais, A. M. M. B. (2009). Combined effects of chemical dip and/or carrageenan coating and/or controlled atmosphere on quality of fresh-cut banana. *Food Control*, *20*(5), 508–514. <https://doi.org/10.1016/j.foodcont.2008.07.017>
- Bimakr, M., Rahman, R. A., Ganjloo, A., Taip, F. S., Salleh, L. M., & Sarker, M. Z. I. (2012). Optimization of Supercritical Carbon Dioxide Extraction of Bioactive Flavonoid Compounds from Spearmint (*Mentha spicata* L.) Leaves by Using Response Surface Methodology. *Food and Bioprocess Technology*, *5*(3), 912–920. <https://doi.org/10.1007/s11947-010-0504-4>
- Blatkiewicz, M., Anteck, A., Boruta, T., Górak, A., & Ledakowicz, S. (2018). Partitioning of laccases derived from *Cerrena unicolor* and *Pleurotus sapidus* in polyethylene glycol – phosphate aqueous two-phase systems. *Process Biochemistry*, *67*, 165–174. <https://doi.org/10.1016/j.procbio.2018.01.011>
- Blossey, R. (2003). Self-cleaning surfaces — virtual realities. *Nature Materials*, *2*(5), 301–306. <https://doi.org/10.1038/nmat856>
- Bonarska-Kujawa, D., Pruchnik, H., Cyboran, S., Żyłka, R., Oszmiański, J., & Kleszczyńska, H. (2014). Biophysical Mechanism of the Protective Effect of Blue Honeysuckle (*Lonicera caerulea* L. var. *kamtschatica* Sevast.) Polyphenols Extracts Against Lipid Peroxidation of Erythrocyte and Lipid Membranes. *The Journal of Membrane Biology*, *247*(7), 611–625. <https://doi.org/10.1007/s00232-014-9677-5>

- Bonilla, J., & Sobral, P. J. A. (2016). Investigation of the physicochemical, antimicrobial and antioxidant properties of gelatin-chitosan edible film mixed with plant ethanolic extracts. *Food Bioscience*, *16*, 17–25. <https://doi.org/10.1016/j.fbio.2016.07.003>
- Bora, P. S., Brekke, C. J., & Powers, J. R. (1994). Heat Induced Gelation of Pea (*Pisum sativum*) Mixed Globulins, Vicilin and Legumin. *Journal of Food Science*, *59*(3), 594–596. <https://doi.org/10.1111/j.1365-2621.1994.tb05570.x>
- Bors, B. (2009). Breeding of *Lonicera caerulea* L. for Saskatchewan and Canada. *Proceedings of the 1st Virtual International Scientific Conference on Lonicera Caerulea L., Saskatoon, SK, Canada*, *23*, 8898.
- Bors, R. H. (2009). *Haskap Breeding & Production: Final Report, January 2009*. Agriculture Development Fund.
- Boulila, A., Hassen, I., Haouari, L., Mejri, F., Amor, I. Ben, Casabianca, H., & Hosni, K. (2015). Enzyme-assisted extraction of bioactive compounds from bay leaves (*Laurus nobilis* L.). *Industrial Crops and Products*, *74*, 485–493. <https://doi.org/10.1016/j.indcrop.2015.05.050>
- Boyarskikh, I. G., Chankina, O. V, Syso, A. I., & Vasiliev, V. G. (2015). Trends in the content of chemical elements in leaves of *Lonicera caerulea* (Caprifoliaceae) in connection with their secondary metabolism in the natural populations of the Altai Mountains. *Bulletin of the Russian Academy of Sciences: Physics*, *79*(1), 94–97. <https://doi.org/10.3103/S1062873815010086>
- Brand-Williams, W., Cuvelier, M. E., & Berset, C. (1995). Use of a free radical method to evaluate antioxidant activity. *LWT - Food Science and Technology*, *28*(1), 25–30. [https://doi.org/10.1016/S0023-6438\(95\)80008-5](https://doi.org/10.1016/S0023-6438(95)80008-5)
- Briassoulis, D., & Giannoulis, A. (2018). Evaluation of the functionality of bio-based food packaging films. *Polymer Testing*, *69*, 39–51. <https://doi.org/10.1016/j.polymertesting.2018.05.003>
- Briones, A. V, Ambal, W. O., Estrella, R. R., Pangilinan, R., De Vera, C. J., Pacis, R. L., Rodriguez, N., & Villanueva, M. A. (2004). Tensile and Tear Strength of Carrageenan Film from Philippine *Eucheuma* Species. *Marine Biotechnology*, *6*(2), 148–151. <https://doi.org/10.1007/s10126-003-0005-9>
- Bujor, O.-C., Tanase, C., & Popa, M. E. (2019). Phenolic Antioxidants in Aerial Parts of Wild *Vaccinium* Species: Towards Pharmaceutical and Biological Properties. In *Antioxidants* (Vol. 8, Issue 12). <https://doi.org/10.3390/antiox8120649>
- Buricova, L., Andjelkovic, M., Cermakova, A., Reblova, Z., Jurcek, O., Kolehmainen, E., Verhe, R., & Kvasnicka, F. (2011). Antioxidant capacities and antioxidants of strawberry, blackberry and raspberry leaves. *Czech Journal of Food Sciences*.
- Calapai, G., Miroddi, M., Mannucci, C., Minciullo, P. L., & Gangemi, S. (2014). Oral adverse reactions due to cinnamon-flavoured chewing gums consumption. *Oral Diseases*, *20*(7), 637–643. <https://doi.org/10.1111/odi.12170>

- Caldeira, A. C. R., Franca, W. F. L. de, Converti, A., Lima, W. J. N., Sampaio, F. C., & Faria, J. T. de. (2019). Liquid-liquid equilibria in aqueous two-phase ethanol/salt systems at different temperatures and their application to anthocyanins extraction. In *Food Science and Technology*. scielo. <https://doi.org/10.1590/fst.32218>
- Calvo, M. E., Castro Smirnov, J. R., & Míguez, H. (2012). Novel approaches to flexible visible transparent hybrid films for ultraviolet protection. *Journal of Polymer Science Part B: Polymer Physics*, 50(14), 945–956. <https://doi.org/10.1002/polb.23087>
- Carvajal-Piñero, J. M., Ramos, M., Jiménez-Rosado, M., Perez-Puyana, V., & Romero, A. (2019). Development of Pea Protein Bioplastics by a Thermomoulding Process: Effect of the Mixing Stage. *Journal of Polymers and the Environment*, 27(5), 968–978. <https://doi.org/10.1007/s10924-019-01404-3>
- Castro, F. V. R., Andrade, M. A., Sanches Silva, A., Vaz, M. F., & Vilarinho, F. (2019). The contribution of a whey protein film incorporated with green tea extract to minimize the lipid oxidation of salmon (*Salmo salar* L.). *Foods*, 8(8), 327. <https://doi.org/10.3390/foods8080327>
- Catanzano, O., Straccia, M. C., Miro, A., Ungaro, F., Romano, I., Mazzarella, G., Santagata, G., Quaglia, F., Laurienzo, P., & Malinconico, M. (2015). Spray-by-spray in situ cross-linking alginate hydrogels delivering a tea tree oil microemulsion. *European Journal of Pharmaceutical Sciences*, 66, 20–28. <https://doi.org/10.1016/j.ejps.2014.09.018>
- Celli, G. B., Ghanem, A., & Brooks, M. S. L. (2014). Haskap Berries (*Lonicera caerulea* L.)—a Critical Review of Antioxidant Capacity and Health-Related Studies for Potential Value-Added Products. *Food and Bioprocess Technology*, 7(6), 1541–1554. <https://doi.org/10.1007/s11947-014-1301-2>
- Cerqueira, M. A., Souza, B. W. S., Teixeira, J. A., & Vicente, A. A. (2012). Effect of glycerol and corn oil on physicochemical properties of polysaccharide films – A comparative study. *Food Hydrocolloids*, 27(1), 175–184. <https://doi.org/10.1016/j.foodhyd.2011.07.007>
- Chahardoli, A., Jalilian, F., Memariani, Z., Farzaei, M. H., & Shokoohinia, Y. (2020). *Chapter 26 - Analysis of organic acids* (A. Sanches Silva, S. F. Nabavi, M. Saeedi, & S. M. B. T.-R. A. in N. P. A. Nabavi (eds.); pp. 767–823). Elsevier. <https://doi.org/10.1016/B978-0-12-816455-6.00026-3>
- Chan, E., Masatcioglu, T. M., & Koxsel, F. (2019). Effects of different blowing agents on physical properties of extruded puffed snacks made from yellow pea and red lentil flours. *Journal of Food Process Engineering*, 42(3), e12989. <https://doi.org/10.1111/jfpe.12989>
- Chanda, S. V., & Kaneria, M. J. (2012). Optimization of Conditions for the Extraction of Antioxidants from Leaves of *Syzygium cumini* L. Using Different Solvents. *Food Analytical Methods*, 5(3), 332–338. <https://doi.org/10.1007/s12161-011-9242-0>

- Chang, L., Wei, Y., Bi, P., & Shao, Q. (2014). Recovery of liquiritin and glycyrrhizic acid from *Glycyrrhiza uralensis* Fisch by aqueous two-phase flotation and multi-stage preparative high performance liquid chromatography. *Separation and Purification Technology*, *134*, 204–209. <https://doi.org/10.1016/j.seppur.2014.07.045>
- Cheluget, E. L., Gelinas, S., Vera, J. H., & Weber, M. E. (1994). Liquid-liquid equilibrium of aqueous mixtures of poly(propylene glycol) with sodium chloride. *Journal of Chemical & Engineering Data*, *39*(1), 127–130. <https://doi.org/10.1021/je00013a036>
- Chemat, F., Abert-Vian, M., Fabiano-Tixier, A. S., Strube, J., Uhlenbrock, L., Gunjevic, V., & Cravotto, G. (2019). Green extraction of natural products. Origins, current status, and future challenges. *TrAC Trends in Analytical Chemistry*, *118*, 248–263. <https://doi.org/10.1016/j.trac.2019.05.037>
- ChemAxon. (2019). *Chemicalize*. <https://chemicalize.com/>
- Chemining'wa, G. N., & Vessey, J. K. (2006). The abundance and efficacy of *Rhizobium leguminosarum* bv. *viciae* in cultivated soils of the eastern Canadian prairie. *Soil Biology and Biochemistry*, *38*(2), 294–302. <https://doi.org/10.1016/j.soilbio.2005.05.007>
- Chen, L., Xin, X., Zhang, H., & Yuan, Q. (2013). Phytochemical properties and antioxidant capacities of commercial raspberry varieties. *Journal of Functional Foods*, *5*(1), 508–515. <https://doi.org/10.1016/j.jff.2012.10.009>
- Cheng, A., Raai, M. N., Zain, N. A. M., Massawe, F., Singh, A., & Wan-Mohtar, W. A. A. Q. I. (2019). In search of alternative proteins: unlocking the potential of underutilized tropical legumes. *Food Security*, *11*(6), 1205–1215. <https://doi.org/10.1007/s12571-019-00977-0>
- Cheng, L. H., Karim, A. A., & Seow, C. C. (2006). Effects of Water-Glycerol and Water-Sorbitol Interactions on the Physical Properties of Konjac Glucomannan Films. *Journal of Food Science*, *71*(2), E62–E67. <https://doi.org/10.1111/j.1365-2621.2006.tb08898.x>
- Cheng, Z., Cheng, L., Song, H., Yu, L., Zhong, F., Shen, Q., & Hu, H. (2016). Aqueous two-phase system for preliminary purification of lignans from fruits of *Schisandra chinensis* Baill. *Separation and Purification Technology*, *166*, 16–25. <https://doi.org/10.1016/j.seppur.2016.04.013>
- Cheng, Z., Song, H., Cao, X., Shen, Q., Han, D., Zhong, F., Hu, H., & Yang, Y. (2017). Simultaneous extraction and purification of polysaccharides from *Gentiana scabra* Bunge by microwave-assisted ethanol-salt aqueous two-phase system. *Industrial Crops and Products*, *102*, 75–87. <https://doi.org/10.1016/j.indcrop.2017.03.029>
- Chevalier, E., Chaabani, A., Assezat, G., Prochazka, F., & Oulahal, N. (2018). Casein/wax blend extrusion for production of edible films as carriers of potassium sorbate—A comparative study of waxes and potassium sorbate effect. *Food Packaging and Shelf Life*, *16*, 41–50. <https://doi.org/10.1016/j.fpsl.2018.01.005>

- Chia, S. R., Chew, K. W., Show, P. L., Sivakumar, M., Ling, T. C., & Tao, Y. (2019). Isolation of protein from *Chlorella sorokiniana* CY1 using liquid biphasic flotation assisted with sonication through sugaring-out effect. *Journal of Oceanology and Limnology*, *37*(3), 898–908. <https://doi.org/10.1007/s00343-019-8246-2>
- Chia, S. R., Foo, S. P., Hew, Y. S., Loh, Y. J., Devadas, V. V., Chew, K. W., & Show, P. L. (2020). Extraction of phenolic compounds from fresh and wilt kesum plant using liquid biphasic flotation. *Separation and Purification Technology*, *242*, 116831. <https://doi.org/https://doi.org/10.1016/j.seppur.2020.116831>
- Chia, S. R., Mak, K. Y., Khaw, Y. J., Suhaidi, N., Chew, K. W., & Show, P. L. (2019). An efficient and rapid method to extract and purify protein – Liquid Triphasic Flotation system. *Bioresource Technology*, *294*, 122158. <https://doi.org/10.1016/j.biortech.2019.122158>
- Choi, W.-S., & Han, J. H. (2001). Physical and Mechanical Properties of Pea-Protein-based Edible Films. *Journal of Food Science*, *66*(2), 319–322. <https://doi.org/10.1111/j.1365-2621.2001.tb11339.x>
- Choi, W. S., & Han, J. H. (2002). Film-forming Mechanism and Heat Denaturation Effects on the Physical and Chemical Properties of Pea-Protein-Isolate Edible Films. *Journal of Food Science*, *67*(4), 1399–1406. <https://doi.org/10.1111/j.1365-2621.2002.tb10297.x>
- Chollakup, R., Pongburoos, S., Boonsong, W., Khanonkon, N., Kongsin, K., Sothornvit, R., Sukyai, P., Sukatta, U., & Harnkarnsujarit, N. (2020). Antioxidant and antibacterial activities of cassava starch and whey protein blend films containing rambutan peel extract and cinnamon oil for active packaging. *LWT*, *130*, 109573. <https://doi.org/10.1016/j.lwt.2020.109573>
- Chong, K. Y., & Brooks, M. S.-L. (2021). Effects of recycling on the aqueous two-phase extraction of bioactives from haskap leaves. *Separation and Purification Technology*, *255*, 117755. <https://doi.org/10.1016/j.seppur.2020.117755>
- Chong, K. Y., Stefanova, R., Zhang, J., & Brooks, M. S.-L. (2020a). Aqueous two-phase extraction of bioactive compounds from haskap leaves (*Lonicera caerulea*): Comparison of salt/ethanol and sugar/propanol systems. *Separation and Purification Technology*, *252*, 117399. <https://doi.org/10.1016/j.seppur.2020.117399>
- Chong, K. Y., Stefanova, R., Zhang, J., & Brooks, M. S. L. (2020b). Extraction of Bioactive Compounds from Haskap Leaves (*Lonicera caerulea*) Using Salt/Ethanol Aqueous Two-Phase Flotation. *Food and Bioprocess Technology*, *13*, 2131–2144. <https://doi.org/10.1007/s11947-020-02553-3>
- Chung, H.-J., & Liu, Q. (2012). Physicochemical properties and in vitro digestibility of flour and starch from pea (*Pisum sativum* L.) cultivars. *International Journal of Biological Macromolecules*, *50*(1), 131–137. <https://doi.org/10.1016/j.ijbiomac.2011.10.004>

- Cicco, N., Lanorte, M. T., Paraggio, M., Viggiano, M., & Lattanzio, V. (2009). A reproducible, rapid and inexpensive Folin-Ciocalteu micro-method in determining phenolics of plant methanol extracts. *Microchemical Journal*, *91*(1), 107–110. <https://doi.org/10.1016/j.microc.2008.08.011>
- Cienfuegos, N. E. C., Santos, P. L., García, A. R., Soares, C. M. F., Lima, A. S., & Souza, R. L. (2017). Integrated process for purification of capsaicin using aqueous two-phase systems based on ethanol. *Food and Bioproducts Processing*, *106*, 1–10. <https://doi.org/10.1016/j.fbp.2017.08.005>
- Cilurzo, F., Cupone, I. E., Minghetti, P., Selmin, F., & Montanari, L. (2008). Fast dissolving films made of maltodextrins. *European Journal of Pharmaceutics and Biopharmaceutics*, *70*(3), 895–900. <https://doi.org/10.1016/j.ejpb.2008.06.032>
- Cisneros-Zevallos, L., & Krochta, J. M. (2003). Dependence of Coating Thickness on Viscosity of Coating Solution Applied to Fruits and Vegetables by Dipping Method. *Journal of Food Science*, *68*(2), 503–510. <https://doi.org/10.1111/j.1365-2621.2003.tb05702.x>
- Cláudio, A. F. M., Ferreira, A. M., Freire, C. S. R., Silvestre, A. J. D., Freire, M. G., & Coutinho, J. A. P. (2012). Optimization of the gallic acid extraction using ionic-liquid-based aqueous two-phase systems. *Separation and Purification Technology*, *97*, 142–149. <https://doi.org/10.1016/j.seppur.2012.02.036>
- Contreras, M. del M., Lama-Muñoz, A., Espínola, F., Moya, M., Romero, I., & Castro, E. (2020). Valorization of olive mill leaves through ultrasound-assisted extraction. *Food Chemistry*, *314*, 126218. <https://doi.org/10.1016/j.foodchem.2020.126218>
- Cuq, B., Gontard, N., Cuq, J.-L., & Guilbert, S. (1997). Selected Functional Properties of Fish Myofibrillar Protein-Based Films As Affected by Hydrophilic Plasticizers. *Journal of Agricultural and Food Chemistry*, *45*(3), 622–626. <https://doi.org/10.1021/jf960352i>
- D'Andrea, G. (2015). Quercetin: A flavonol with multifaceted therapeutic applications? *Fitoterapia*, *106*, 256–271. <https://doi.org/10.1016/j.fitote.2015.09.018>
- Dawson, J. K. (2017). *Concentration and Content of Secondary Metabolites in Fruit and Leaves of Haskap (Lonicera caerulea L.)*.
- Day, B. P. F. (2008). Active packaging of food. *Smart Packaging Technologies for Fast Moving Consumer Goods*, *1*.
- de Araújo Padilha, C. E., Dantas, P. V. F., Nogueira, C. da C., Leitão, A. L. de S., Almeida, H. N., de Santana Souza, D. F., Oliveira, J. A. de, de Macedo, G. R., & dos Santos, E. S. (2018). Enhancing the recovery and concentration of polyphenols from camu-camu (*Myrciaria dubia* H.B.K. McVaugh) by aqueous two-phase flotation and scale-up process. *Separation Science and Technology*, 1–10. <https://doi.org/10.1080/01496395.2018.1442865>

- De Brito Cardoso, G., Mourão, T., Pereira, F. M., Freire, M. G., Fricks, A. T., Soares, C. M. F., & Lima, Á. S. (2013). Aqueous two-phase systems based on acetonitrile and carbohydrates and their application to the extraction of vanillin. *Separation and Purification Technology*, 104, 106–113. <https://doi.org/10.1016/j.seppur.2012.11.001>
- De Freitas, T. B., Santos, C. H. K., da Silva, M. V., Shirai, M. A., Dias, M. I., Barros, L., Barreiro, M. F., Ferreira, I. C. F. R., Gonçalves, O. H., & Leimann, F. V. (2018). Antioxidants extraction from Pinhão (*Araucaria angustifolia* (Bertol.) Kuntze) coats and application to zein films. *Food Packaging and Shelf Life*, 15, 28–34. <https://doi.org/10.1016/j.fpsl.2017.10.006>
- de Moraes, J. O., Scheibe, A. S., Sereno, A., & Laurindo, J. B. (2013). Scale-up of the production of cassava starch based films using tape-casting. *Journal of Food Engineering*, 119(4), 800–808. <https://doi.org/10.1016/j.jfoodeng.2013.07.009>
- Dhamole, P. B., Chavan, S., Patil, R. G., Feng, H., Bule, M., & Kinninge, P. (2016). Extraction of p-coumaric acid from agricultural residues and separation using ‘sugaring out.’ *Korean Journal of Chemical Engineering*, 33(6), 1860–1864. <https://doi.org/10.1007/s11814-016-0020-y>
- Díaz, O., Ferreira, T., Rodríguez-Otero, L. J., & Cobos, Á. (2019). Characterization of Chickpea (*Cicer arietinum* L.) Flour Films: Effects of pH and Plasticizer Concentration. In *International Journal of Molecular Sciences* (Vol. 20, Issue 5). <https://doi.org/10.3390/ijms20051246>
- Dismer, F., Alexander Oelmeier, S., & Hubbuch, J. (2013). Molecular dynamics simulations of aqueous two-phase systems: Understanding phase formation and protein partitioning. *Chemical Engineering Science*, 96, 142–151. <https://doi.org/10.1016/j.ces.2013.03.020>
- do Evangelho, J. A., da Silva Dannenberg, G., Biduski, B., el Halal, S. L. M., Kringel, D. H., Gularte, M. A., Fiorentini, A. M., & da Rosa Zavareze, E. (2019). Antibacterial activity, optical, mechanical, and barrier properties of corn starch films containing orange essential oil. *Carbohydrate Polymers*, 222, 114981. <https://doi.org/10.1016/j.carbpol.2019.114981>
- Donelian, A., Carlson, L. H. C., Lopes, T. J., & Machado, R. A. F. (2009). Comparison of extraction of patchouli (*Pogostemon cablin*) essential oil with supercritical CO₂ and by steam distillation. *The Journal of Supercritical Fluids*, 48(1), 15–20. <https://doi.org/10.1016/j.supflu.2008.09.020>
- Dorđević, T., & Antov, M. (2017). Ultrasound assisted extraction in aqueous two-phase system for the integrated extraction and separation of antioxidants from wheat chaff. *Separation and Purification Technology*, 182, 52–58. <https://doi.org/10.1016/j.seppur.2017.03.025>

- Du, W.-X., Olsen, C. W., Avena-Bustillos, R. J., McHugh, T. H., Levin, C. E., & Friedman, M. (2008). Storage Stability and Antibacterial Activity against *Escherichia coli* O157:H7 of Carvacrol in Edible Apple Films Made by Two Different Casting Methods. *Journal of Agricultural and Food Chemistry*, *56*(9), 3082–3088. <https://doi.org/10.1021/jf703629s>
- Dutta, M., & Paul, G. (2019). Gallic acid protects rat liver mitochondria ex vivo from bisphenol A induced oxidative stress mediated damages. *Toxicology Reports*, *6*, 578–589. <https://doi.org/10.1016/j.toxrep.2019.06.011>
- Ebrahimi, N., & Sadeghi, R. (2018). Propanol – Sugar aqueous biphasic systems as a suitable platform for biomolecules extraction. *Journal of Chromatography A*, *1581–1582*, 156–167. <https://doi.org/10.1016/j.chroma.2018.11.007>
- Eh, A. L.-S., & Teoh, S.-G. (2012). Novel modified ultrasonication technique for the extraction of lycopene from tomatoes. *Ultrasonics Sonochemistry*, *19*(1), 151–159. <https://doi.org/10.1016/j.ultsonch.2011.05.019>
- Ehlenfeldt, M. K., & Prior, R. L. (2001). Oxygen Radical Absorbance Capacity (ORAC) and Phenolic and Anthocyanin Concentrations in Fruit and Leaf Tissues of Highbush Blueberry. *Journal of Agricultural and Food Chemistry*, *49*(5), 2222–2227. <https://doi.org/10.1021/jf0013656>
- Ek, S., Kartimo, H., Mattila, S., & Tolonen, A. (2006). Characterization of Phenolic Compounds from Lingonberry (*Vaccinium vitis-idaea*). *Journal of Agricultural and Food Chemistry*, *54*(26), 9834–9842. <https://doi.org/10.1021/jf0623687>
- El Darra, N., Grimi, N., Vorobiev, E., Louka, N., & Maroun, R. (2013). Extraction of Polyphenols from Red Grape Pomace Assisted by Pulsed Ohmic Heating. *Food and Bioprocess Technology*, *6*(5), 1281–1289. <https://doi.org/10.1007/s11947-012-0869-7>
- Eswaranandam, S., Hettiarachchy, N. S., & Johnson, M. G. (2004). Antimicrobial Activity of Citric, Lactic, Malic, or Tartaric Acids and Nisin-incorporated Soy Protein Film Against *Listeria monocytogenes*, *Escherichia coli* O157:H7, and *Salmonella gaminara*. *Journal of Food Science*, *69*(3), FMS79–FMS84. <https://doi.org/10.1111/j.1365-2621.2004.tb13375.x>
- European Commission. (2011). Commission Regulation (EU) No 10/2011 of 14 January 2011 on plastic materials and articles intended to come into contact with food. *Official Journal of the European Union*, *12*, 1–89. <https://eur-lex.europa.eu/legal-content/EN/ALL/?uri=CELEX%3A32011R0010>
- Fabra, María José, Sánchez-González, L., & Chiralt, A. (2014). Lysozyme release from isolate pea protein and starch based films and their antimicrobial properties. *LWT - Food Science and Technology*, *55*(1), 22–26. <https://doi.org/10.1016/j.lwt.2013.08.001>

- Fabra, Maria José, Talens, P., & Chiralt, A. (2009). Microstructure and optical properties of sodium caseinate films containing oleic acid–beeswax mixtures. *Food Hydrocolloids*, 23(3), 676–683. <https://doi.org/10.1016/j.foodhyd.2008.04.015>
- Fang, Y., Tung, M. A., Britt, I. J., Yada, S., & Dalgleish, D. G. (2002). Tensile and Barrier Properties of Edible Films Made from Whey Proteins. *Journal of Food Science*, 67(1), 188–193. <https://doi.org/10.1111/j.1365-2621.2002.tb11381.x>
- Fathi, N., Almasi, H., & Pirouzifard, M. K. (2018). Effect of ultraviolet radiation on morphological and physicochemical properties of sesame protein isolate based edible films. *Food Hydrocolloids*, 85, 136–143. <https://doi.org/10.1016/j.foodhyd.2018.07.018>
- Ferlemi, A.-V., & Lamari, F. N. (2016). Berry Leaves: An Alternative Source of Bioactive Natural Products of Nutritional and Medicinal Value. *Antioxidants*, 5(2), 17. <https://doi.org/10.3390/antiox5020017>
- Fernandes de Oliveira, A. M., Sousa Pinheiro, L., Souto Pereira, C. K., Neves Matias, W., Albuquerque Gomes, R., Souza Chaves, O., Vanderlei de Souza, M. D. F., Nóbrega de Almeida, R., & Simões de Assis, T. (2012). Total phenolic content and antioxidant activity of some Malvaceae family species. *Antioxidants*, 1(1), 33–43. <https://doi.org/10.3390/antiox1010033>
- Fernández-Pan, I., Ziani, K., Pedroza-Islas, R., & Maté, J. I. (2010). Effect of Drying Conditions on the Mechanical and Barrier Properties of Films Based on Chitosan. *Drying Technology*, 28(12), 1350–1358. <https://doi.org/10.1080/07373937.2010.482692>
- Feyzi, S., Milani, E., & Golimovahhed, Q. A. (2018). Grass Pea (*Lathyrus sativus* L.) Protein Isolate: The Effect of Extraction Optimization and Drying Methods on the Structure and Functional Properties. *Food Hydrocolloids*, 74, 187–196. <https://doi.org/10.1016/j.foodhyd.2017.07.031>
- Flood, A. E., & Srisanga, S. (2012). An improved model of the seeded batch crystallization of glucose monohydrate from aqueous solutions. *Journal of Food Engineering*, 109(2), 209–217. <https://doi.org/10.1016/j.jfoodeng.2011.09.035>
- Food and Agriculture Organization of the United Nations. (2018). *FAOSTAT Database*. <http://www.fao.org/faostat/en/#home>
- Frampton, J. P., Lai, D., Sriram, H., & Takayama, S. (2011). Precisely targeted delivery of cells and biomolecules within microchannels using aqueous two-phase systems. *Biomedical Microdevices*, 13(6), 1043–1051. <https://doi.org/10.1007/s10544-011-9574-y>
- Frampton, J. P., White, J. B., Simon, A. B., Tsuei, M., Paczesny, S., & Takayama, S. (2014). Aqueous two-phase system patterning of detection antibody solutions for cross-reaction-free multiplex ELISA. *Scientific Reports*, 4(1), 4878. <https://doi.org/10.1038/srep04878>

- Freire, M. G., Louros, C. L. S., Rebelo, L. P. N., & Coutinho, J. A. P. (2011). Aqueous biphasic systems composed of a water-stable ionic liquid + carbohydrates and their applications. *Green Chemistry*, 13(6), 1536–1545. <https://doi.org/10.1039/C1GC15110J>
- Friedman, M., & Jürgens, H. S. (2000). Effect of pH on the Stability of Plant Phenolic Compounds. *Journal of Agricultural and Food Chemistry*, 48(6), 2101–2110. <https://doi.org/10.1021/jf990489j>
- Frier, S. D., Somers, C. M., & Sheffield, C. S. (2016). Comparing the performance of native and managed pollinators of Haskap (*Lonicera caerulea*: Caprifoliaceae), an emerging fruit crop. *Agriculture, Ecosystems & Environment*, 219, 42–48. <https://doi.org/10.1016/j.agee.2015.12.011>
- Frohberg, P., Pietzsch, M., & Ulrich, J. (2010). Effect of crystalline substances in biodegradable films. *Chemical Engineering Research and Design*, 88(9), 1148–1152. <https://doi.org/10.1016/j.cherd.2010.01.037>
- Fu, X.-Q., Zhang, G.-L., Deng, L., & Dang, Y.-Y. (2019). Simultaneous extraction and enrichment of polyphenol and lutein from marigold (*Tagetes erecta* L.) flower by an enzyme-assisted ethanol/ammonium sulfate system. *Food & Function*, 10(1), 266–276. <https://doi.org/10.1039/C8FO01865K>
- Gal, N., Malferarri, D., Kolusheva, S., Galletti, P., Tagliavini, E., & Jelinek, R. (2012). Membrane interactions of ionic liquids: Possible determinants for biological activity and toxicity. *Biochimica et Biophysica Acta (BBA) - Biomembranes*, 1818(12), 2967–2974. <https://doi.org/10.1016/j.bbamem.2012.07.025>
- Galani, J. H. Y., Patel, J. S., Patel, N. J., & Talati, J. G. (2017). Storage of Fruits and Vegetables in Refrigerator Increases their Phenolic Acids but Decreases the Total Phenolics, Anthocyanins and Vitamin C with Subsequent Loss of their Antioxidant Capacity. In *Antioxidants* (Vol. 6, Issue 3). <https://doi.org/10.3390/antiox6030059>
- Garavand, F., Rouhi, M., Razavi, S. H., Cacciotti, I., & Mohammadi, R. (2017). Improving the integrity of natural biopolymer films used in food packaging by crosslinking approach: A review. *International Journal of Biological Macromolecules*, 104, 687–707. <https://doi.org/10.1016/j.ijbiomac.2017.06.093>
- Ghanbarzadeh, B., Almasi, H., & Entezami, A. A. (2011). Improving the barrier and mechanical properties of corn starch-based edible films: Effect of citric acid and carboxymethyl cellulose. *Industrial Crops and Products*, 33(1), 229–235. <https://doi.org/10.1016/j.indcrop.2010.10.016>
- Ghanbarzadeh, B., Musavi, M., Oromiehie, A. R., Rezayi, K., Razmi Rad, E., & Milani, J. (2007). Effect of plasticizing sugars on water vapor permeability, surface energy and microstructure properties of zein films. *LWT - Food Science and Technology*, 40(7), 1191–1197. <https://doi.org/10.1016/j.lwt.2006.07.008>

- Ghanbarzadeh, B., & Oromiehi, A. R. (2009). Thermal and mechanical behavior of laminated protein films. *Journal of Food Engineering*, 90(4), 517–524. <https://doi.org/10.1016/j.jfoodeng.2008.07.018>
- Gironi, F., & Piemonte, V. (2011). Bioplastics and Petroleum-based Plastics: Strengths and Weaknesses. *Energy Sources, Part A: Recovery, Utilization, and Environmental Effects*, 33(21), 1949–1959. <https://doi.org/10.1080/15567030903436830>
- Golunski, S. M., Sala, L., Silva, M. F., Dallago, R. M., Mulinari, J., Mossi, A. J., Brandelli, A., Kalil, S. J., Di Luccio, M., & Treichel, H. (2016). Interference of salts used on aqueous two-phase systems on the quantification of total proteins. *International Journal of Biological Macromolecules*, 83, 30–33. <https://doi.org/10.1016/j.ijbiomac.2015.11.056>
- Gomes, G. A., Azevedo, A. M., Aires-Barros, M. R., & Prazeres, D. M. F. (2009). Purification of plasmid DNA with aqueous two phase systems of PEG 600 and sodium citrate/ammonium sulfate. *Separation and Purification Technology*, 65(1), 22–30. <https://doi.org/10.1016/j.seppur.2008.01.026>
- Gómez-Guillén, M. C., Ihl, M., Bifani, V., Silva, A., & Montero, P. (2007). Edible films made from tuna-fish gelatin with antioxidant extracts of two different murta ecotypes leaves (*Ugni molinae* Turcz). *Food Hydrocolloids*, 21(7), 1133–1143. <https://doi.org/10.1016/j.foodhyd.2006.08.006>
- Goudarzi, V., Shahabi-Ghahfarrokhi, I., & Babaei-Ghazvini, A. (2017). Preparation of ecofriendly UV-protective food packaging material by starch/TiO₂ bio-nanocomposite: Characterization. *International Journal of Biological Macromolecules*, 95, 306–313. <https://doi.org/10.1016/j.ijbiomac.2016.11.065>
- Gounga, M. E., Xu, S.-Y., & Wang, Z. (2007). Whey protein isolate-based edible films as affected by protein concentration, glycerol ratio and pullulan addition in film formation. *Journal of Food Engineering*, 83(4), 521–530. <https://doi.org/10.1016/j.jfoodeng.2007.04.008>
- Granato, D., Ribeiro, J. C. B., Castro, I. A., & Masson, M. L. (2010). Sensory evaluation and physicochemical optimisation of soy-based desserts using response surface methodology. *Food Chemistry*, 121(3), 899–906. <https://doi.org/10.1016/j.foodchem.2010.01.014>
- Grilo, A. L., Aires-Barros, M. R., & Azevedo, A. M. (2016). Partitioning in Aqueous Two-Phase Systems: Fundamentals, Applications and Trends. *Separation and Purification Reviews*, 45(1), 68–80. <https://doi.org/10.1080/15422119.2014.983128>
- Grover, P. K., & Ryall, R. L. (2005). Critical Appraisal of Salting-Out and Its Implications for Chemical and Biological Sciences. *Chemical Reviews*, 105(1), 1–10. <https://doi.org/10.1021/cr030454p>

- Gupta, R. S., Springston, E. E., Warriar, M. R., Smith, B., Kumar, R., Pongracic, J., & Holl, J. L. (2011). The Prevalence, Severity, and Distribution of Childhood Food Allergy in the United States. *Pediatrics*, *128*(1), e9 LP-e17. <https://doi.org/10.1542/peds.2011-0204>
- Hahladakis, J. N., Velis, C. A., Weber, R., Iacovidou, E., & Purnell, P. (2018). An overview of chemical additives present in plastics: Migration, release, fate and environmental impact during their use, disposal and recycling. *Journal of Hazardous Materials*, *344*, 179–199. <https://doi.org/10.1016/j.jhazmat.2017.10.014>
- Häkkinen, S., Heinonen, M., Kärenlampi, S., Mykkänen, H., Ruuskanen, J., & Törrönen, R. (1999). Screening of selected flavonoids and phenolic acids in 19 berries. *Food Research International*, *32*(5), 345–353. [https://doi.org/10.1016/S0963-9969\(99\)00095-2](https://doi.org/10.1016/S0963-9969(99)00095-2)
- Halden, R. U. (2010). Plastics and Health Risks. *Annual Review of Public Health*, *31*(1), 179–194. <https://doi.org/10.1146/annurev.publhealth.012809.103714>
- Han, J., Wang, Y., Luo, L., Kang, W., Chen, H., Liu, Y., Li, Y., & Ni, L. (2014). Optimization of separation and determination of chloramphenicol in food using aqueous two-phase flotation coupled with HPLC. *Journal of the Iranian Chemical Society*, *11*(6), 1775–1782. <https://doi.org/10.1007/s13738-014-0463-1>
- Han, Y., Yu, M., & Wang, L. (2018). Preparation and characterization of antioxidant soy protein isolate films incorporating licorice residue extract. *Food Hydrocolloids*, *75*, 13–21. <https://doi.org/10.1016/j.foodhyd.2017.09.020>
- Harb, J., Khraiwesh, B., Streif, J., Reski, R., & Frank, W. (2010). Characterization of blueberry monodehydroascorbate reductase gene and changes in levels of ascorbic acid and the antioxidative capacity of water soluble antioxidants upon storage of fruits under various conditions. *Scientia Horticulturae*, *125*(3), 390–395. <https://doi.org/10.1016/j.scienta.2010.04.031>
- Hart, R. A., Lester, P. M., Reifsnnyder, D. H., Ogez, J. R., & Builder, S. E. (1994). Large Scale, In Situ Isolation of Periplasmic IGF-I from E. coli. *Bio/Technology*, *12*(11), 1113–1117. <https://doi.org/10.1038/nbt1194-1113>
- Hatti-Kaul, R. (2000). *Aqueous Two-Phase Systems: Methods and Protocols* (R. Hatti-Kaul (ed.)). Humana Press. <https://doi.org/10.1385/1-59259-028-4:1>
- He, A., Dong, B., Feng, X., & Yao, S. (2018). Extraction of bioactive ginseng saponins using aqueous two-phase systems of ionic liquids and salts. *Separation and Purification Technology*, *196*, 270–280. <https://doi.org/10.1016/j.seppur.2017.05.041>
- He, F., Li, D., Wang, D., & Deng, M. (2016). Extraction and purification of quercitrin, hyperoside, rutin, and afzelin from *Zanthoxylum Bungeanum* Maxim leaves Using an aqueous two-phase system. *Journal of Food Science*, *81*(7), C1593–C1602. <https://doi.org/10.1111/1750-3841.13331>

- Hernandez-Izquierdo, V. M., & Krochta, J. M. (2008). Thermoplastic Processing of Proteins for Film Formation—A Review. *Journal of Food Science*, 73(2), R30–R39. <https://doi.org/10.1111/j.1750-3841.2007.00636.x>
- Hoffmann, E. M., Breitenbach, A., & Breitzkreutz, J. (2011). Advances in orodispersible films for drug delivery. *Expert Opinion on Drug Delivery*, 8(3), 299–316. <https://doi.org/10.1517/17425247.2011.553217>
- Hokkanen, J., Mattila, S., Jaakola, L., Pirttilä, A. M., & Tolonen, A. (2009). Identification of Phenolic Compounds from Lingonberry (*Vaccinium vitis-idaea* L.), Bilberry (*Vaccinium myrtillus* L.) and Hybrid Bilberry (*Vaccinium x intermedium* Ruthe L.) Leaves. *Journal of Agricultural and Food Chemistry*, 57(20), 9437–9447. <https://doi.org/10.1021/jf9022542>
- Hopewell, J., Dvorak, R., & Kosior, E. (2009). Plastics recycling: challenges and opportunities. *Philosophical Transactions of the Royal Society B: Biological Sciences*, 364(1526), 2115–2126. <https://doi.org/10.1098/rstb.2008.0311>
- Hoque, M. S., Benjakul, S., & Prodpran, T. (2010). Effect of heat treatment of film-forming solution on the properties of film from cuttlefish (*Sepia pharaonis*) skin gelatin. *Journal of Food Engineering*, 96(1), 66–73. <https://doi.org/https://doi.org/10.1016/j.jfoodeng.2009.06.046>
- Hoque, M. S., Benjakul, S., & Prodpran, T. (2011). Properties of film from cuttlefish (*Sepia pharaonis*) skin gelatin incorporated with cinnamon, clove and star anise extracts. *Food Hydrocolloids*, 25(5), 1085–1097. <https://doi.org/10.1016/j.foodhyd.2010.10.005>
- Horžić, D., Jambrak, A. R., Belščak-Cvitanović, A., Komes, D., & Lelas, V. (2012). Comparison of Conventional and Ultrasound Assisted Extraction Techniques of Yellow Tea and Bioactive Composition of Obtained Extracts. *Food and Bioprocess Technology*, 5(7), 2858–2870. <https://doi.org/10.1007/s11947-012-0791-z>
- Hosseini, M. S., & Nabid, M. R. (2020). Synthesis of chemically cross-linked hydrogel films based on basil seed (*Ocimum basilicum* L.) mucilage for wound dressing drug delivery applications. *International Journal of Biological Macromolecules*, 163, 336–347. <https://doi.org/10.1016/j.ijbiomac.2020.06.252>
- Hou, B. J., Wei, Y. Q., Ma, F., Wang, X. N., & Yang, S. Z. (2018). Chelatometric salting-out extraction and characteristics of flavonoids from *Folium nelumbinis* based on an ethanol/K₂HPO₄ system. *Separation Science and Technology (Philadelphia)*, 53(5), 717–724. <https://doi.org/10.1080/01496395.2017.1397023>
- Hu, M., Zhai, Q., Liu, Z., & Xia, S. (2003). Liquid–Liquid and Solid–Liquid Equilibrium of the Ternary System Ethanol + Cesium Sulfate + Water at (10, 30, and 50) °C. *Journal of Chemical & Engineering Data*, 48(6), 1561–1564. <https://doi.org/10.1021/je0301803>

- Huddleston, J., Veide, A., Köhler, K., Flanagan, J., Enfors, S.-O., & Lyddiatt, A. (1991). The molecular basis of partitioning in aqueous two-phase systems. *Trends in Biotechnology*, *9*(1), 381–388. [https://doi.org/10.1016/0167-7799\(91\)90130-A](https://doi.org/10.1016/0167-7799(91)90130-A)
- Hummer, K. E., Pomper, K. W., Postman, J., Graham, C. J., Stover, E., Mercure, E. W., Aradhya, M., Crisosto, C. H., Ferguson, L., Thompson, M. M., Byers, P., & Zee, F. (2012). *Emerging Fruit Crops - Fruit Breeding* (M. L. Badenes & D. H. Byrne (eds.); pp. 97–147). Springer US. https://doi.org/10.1007/978-1-4419-0763-9_4
- Huntrakul, K., Yoksan, R., Sane, A., & Harnkarnsujarit, N. (2020). Effects of pea protein on properties of cassava starch edible films produced by blown-film extrusion for oil packaging. *Food Packaging and Shelf Life*, *24*, 100480. <https://doi.org/10.1016/j.fpsl.2020.100480>
- Hyde, A. M., Zultanski, S. L., Waldman, J. H., Zhong, Y.-L., Shevlin, M., & Peng, F. (2017). General Principles and Strategies for Salting-Out Informed by the Hofmeister Series. *Organic Process Research & Development*, *21*(9), 1355–1370. <https://doi.org/10.1021/acs.oprd.7b00197>
- Iheshiulo, E. M.-A. (2018). *Determination of Soil and Plant Nutrient Sufficiency Levels for Haskap (Lonicera caerulea L.)*.
- Jagadeesh, D., Prem Kumar, B., Sudhakara, P., Venkata Prasad, C., Varada Rajulu, A., & Song, J. I. (2013). Preparation and Properties of Propylene Glycol Plasticized Wheat Protein Isolate Novel Green Films. *Journal of Polymers and the Environment*, *21*(4), 930–936. <https://doi.org/10.1007/s10924-013-0572-4>
- Jampani, C., & Raghavarao, K. S. M. S. (2015). Process integration for purification and concentration of red cabbage (*Brassica oleracea* L.) anthocyanins. *Separation and Purification Technology*, *141*, 10–16. <https://doi.org/10.1016/j.seppur.2014.11.024>
- Janjarasskul, T., Tananuwong, K., Phupoksakul, T., & Thaiphanit, S. (2020). Fast dissolving, hermetically sealable, edible whey protein isolate-based films for instant food and/or dry ingredient pouches. *LWT*, *134*, 110102. <https://doi.org/10.1016/j.lwt.2020.110102>
- Jia, X. wen, Qin, Z. yu, Xu, J. xin, Kong, B. hua, Liu, Q., & Wang, H. (2020). Preparation and characterization of pea protein isolate-pullulan blend electrospun nanofiber films. *International Journal of Biological Macromolecules*, *157*, 641–647. <https://doi.org/10.1016/j.ijbiomac.2019.11.216>
- Jiang, B., Na, J., Wang, L., Li, D., Liu, C., & Feng, Z. (2019). Reutilization of Food Waste: One-Step Extration, Purification and Characterization of Ovalbumin from Salted Egg White by Aqueous Two-Phase Flotation. In *Foods* (Vol. 8, Issue 8). <https://doi.org/10.3390/foods8080286>

- Jiang, L., Belwal, T., Huang, H., Ge, Z., Limwachiranon, J., Zhao, Y., Li, L., Ren, G., & Luo, Z. (2019). Extraction and Characterization of Phenolic Compounds from Bamboo Shoot Shell Under Optimized Ultrasonic-Assisted Conditions: a Potential Source of Nutraceutical Compounds. *Food and Bioprocess Technology*, 12(10), 1741–1755. <https://doi.org/10.1007/s11947-019-02321-y>
- Jiang, Yan, Tang, C.-H., Wen, Q.-B., Li, L., & Yang, X.-Q. (2007). Effect of processing parameters on the properties of transglutaminase-treated soy protein isolate films. *Innovative Food Science & Emerging Technologies*, 8(2), 218–225. <https://doi.org/https://doi.org/10.1016/j.ifset.2006.11.002>
- Jiang, Yongli, Yu, L., Hu, Y., Zhu, Z., Zhuang, C., Zhao, Y., & Zhong, Y. (2020). The preservation performance of chitosan coating with different molecular weight on strawberry using electrostatic spraying technique. *International Journal of Biological Macromolecules*, 151, 278–285. <https://doi.org/10.1016/j.ijbiomac.2020.02.169>
- Jiménez-Rosado, M., Zarate-Ramírez, L. S., Romero, A., Bengoechea, C., Partal, P., & Guerrero, A. (2019). Bioplastics based on wheat gluten processed by extrusion. *Journal of Cleaner Production*, 239, 117994. <https://doi.org/10.1016/j.jclepro.2019.117994>
- Jiménez, A., Fabra, M. J., Talens, P., & Chiralt, A. (2012). Edible and Biodegradable Starch Films: A Review. *Food and Bioprocess Technology*, 5(6), 2058–2076. <https://doi.org/10.1007/s11947-012-0835-4>
- Jo, C., Kang, H., Lee, N. Y., Kwon, J. H., & Byun, M. W. (2005). Pectin- and gelatin-based film: effect of gamma irradiation on the mechanical properties and biodegradation. *Radiation Physics and Chemistry*, 72(6), 745–750. <https://doi.org/10.1016/j.radphyschem.2004.05.045>
- Joshi, P. U., Turpeinen, D. G., Weiss, M., Escalante-Corbin, G., Schroeder, M., & Heldt, C. L. (2019). Tie line framework to optimize non-enveloped virus recovery in aqueous two-phase systems. *Journal of Chromatography B*, 1126–1127, 121744. <https://doi.org/10.1016/j.jchromb.2019.121744>
- Jouki, M., Yazdi, F. T., Mortazavi, S. A., & Koocheki, A. (2014). Quince seed mucilage films incorporated with oregano essential oil: Physical, thermal, barrier, antioxidant and antibacterial properties. *Food Hydrocolloids*, 36, 9–19. <https://doi.org/10.1016/j.foodhyd.2013.08.030>
- Kahkeshani, N., Farzaei, F., Fotouhi, M., Alavi, S. S., Bahramsoltani, R., Naseri, R., Momtaz, S., Abbasabadi, Z., Rahimi, R., Farzaei, M. H., & Bishayee, A. (2019). Pharmacological effects of gallic acid in health and diseases: A mechanistic review. *Iranian Journal of Basic Medical Sciences*, 22(3), 225–237. <https://doi.org/10.22038/ijbms.2019.32806.7897>
- Kanmani, P., & Rhim, J.-W. (2014). Development and characterization of carrageenan/grapefruit seed extract composite films for active packaging. *International Journal of Biological Macromolecules*, 68, 258–266. <https://doi.org/10.1016/j.ijbiomac.2014.05.011>

- Kevers, C., Falkowski, M., Tabart, J., Defraigne, J.-O., Dommès, J., & Pincemail, J. (2007). Evolution of Antioxidant Capacity during Storage of Selected Fruits and Vegetables. *Journal of Agricultural and Food Chemistry*, 55(21), 8596–8603. <https://doi.org/10.1021/jf071736j>
- Khatab, R., Brooks, M. S.-L., & Ghanem, A. (2016). Phenolic Analyses of Haskap Berries (*Lonicera caerulea* L.): Spectrophotometry Versus High Performance Liquid Chromatography. *International Journal of Food Properties*, 19(8), 1708–1725. <https://doi.org/10.1080/10942912.2015.1084316>
- Khoo, H. E., Azlan, A., Tang, S. T., & Lim, S. M. (2017). Anthocyanidins and anthocyanins: colored pigments as food, pharmaceutical ingredients, and the potential health benefits. *Food & Nutrition Research*, 61(1), 1361779. <https://doi.org/10.1080/16546628.2017.1361779>
- Khoo, K. S., Chew, K. W., Ooi, C. W., Ong, H. C., Ling, T. C., & Show, P. L. (2019). Extraction of natural astaxanthin from *Haematococcus pluvialis* using liquid biphasic flotation system. *Bioresource Technology*, 290, 121794. <https://doi.org/10.1016/j.biortech.2019.121794>
- Kobayashi, Y., Miyazawa, M., Kamei, A., Abe, K., & Kojima, T. (2010). Ameliorative Effects of Mulberry (*Morus alba* L.) Leaves on Hyperlipidemia in Rats Fed a High-Fat Diet: Induction of Fatty Acid Oxidation, Inhibition of Lipogenesis, and Suppression of Oxidative Stress. *Bioscience, Biotechnology, and Biochemistry*, 74(12), 2385–2395. <https://doi.org/10.1271/bbb.100392>
- Kokoszka, S., Debeaufort, F., Lenart, A., & Voilley, A. (2010). Water vapour permeability, thermal and wetting properties of whey protein isolate based edible films. *International Dairy Journal*, 20(1), 53–60. <https://doi.org/10.1016/j.idairyj.2009.07.008>
- Kowalczyk, D., & Baraniak, B. (2011). Effects of plasticizers, pH and heating of film-forming solution on the properties of pea protein isolate films. *Journal of Food Engineering*, 105(2), 295–305. <https://doi.org/10.1016/j.jfoodeng.2011.02.037>
- Kowalczyk, D., Gustaw, W., Zięba, E., Lisiecki, S., Stadnik, J., & Baraniak, B. (2016). Microstructure and functional properties of sorbitol-plasticized pea protein isolate emulsion films: Effect of lipid type and concentration. *Food Hydrocolloids*, 60, 353–363. <https://doi.org/10.1016/j.foodhyd.2016.04.006>
- Kowalska, K., & Olejnik, A. (2016). Beneficial effects of cranberry in the prevention of obesity and related complications: Metabolic syndrome and diabetes – A review. *Journal of Functional Foods*, 20, 171–181. <https://doi.org/10.1016/j.jff.2015.11.001>
- Koyande, A. K., Chew, K. W., Lim, J.-W., Lee, S. Y., Lam, M. K., & Show, P.-L. (2019). Optimization of protein extraction from *Chlorella Vulgaris* via novel sugaring-out assisted liquid biphasic electric flotation system. *Engineering in Life Sciences*, 0(0). <https://doi.org/10.1002/elsc.201900068>

- Kraujalis, P., Venskutonis, P. R., Ibáñez, E., & Herrero, M. (2015). Optimization of rutin isolation from *Amaranthus paniculatus* leaves by high pressure extraction and fractionation techniques. *The Journal of Supercritical Fluids*, *104*, 234–242. <https://doi.org/10.1016/j.supflu.2015.06.022>
- Krishnaswamy, K., Orsat, V., Gariépy, Y., & Thangavel, K. (2013). Optimization of Microwave-Assisted Extraction of Phenolic Antioxidants from Grape Seeds (*Vitis vinifera*). *Food and Bioprocess Technology*, *6*(2), 441–455. <https://doi.org/10.1007/s11947-012-0800-2>
- Kucharska, Z. A., Sokół-Łętowska, A., Oszmiański, J., Piórecki, N., & Fecka, I. (2017). Iridoids, Phenolic Compounds and Antioxidant Activity of Edible Honeysuckle Berries (*Lonicera caerulea* var. *kamtschatica* Sevast.). In *Molecules* (Vol. 22, Issue 3). <https://doi.org/10.3390/molecules22030405>
- Lacroix, M., Le, T. C., Ouattara, B., Yu, H., Letendre, M., Sabato, S. F., Mateescu, M. A., & Patterson, G. (2002). Use of γ -irradiation to produce films from whey, casein and soya proteins: structure and functionals characteristics. *Radiation Physics and Chemistry*, *63*(3), 827–832. [https://doi.org/10.1016/S0969-806X\(01\)00574-6](https://doi.org/10.1016/S0969-806X(01)00574-6)
- Ladjal-Ettoumi, Y., Boudries, H., Chibane, M., & Romero, A. (2016). Pea, Chickpea and Lentil Protein Isolates: Physicochemical Characterization and Emulsifying Properties. *Food Biophysics*, *11*(1), 43–51. <https://doi.org/10.1007/s11483-015-9411-6>
- Lakshmi, M. C., Madhusudhan, M. C., & Raghavarao, K. S. M. S. (2012). Extraction and Purification of Lipoxxygenase from Soybean Using Aqueous Two-Phase System. *Food and Bioprocess Technology*, *5*(1), 193–199. <https://doi.org/10.1007/s11947-009-0278-8>
- Lam, A. C. Y., Can Karaca, A., Tyler, R. T., & Nickerson, M. T. (2018). Pea protein isolates: Structure, extraction, and functionality. *Food Reviews International*, *34*(2), 126–147. <https://doi.org/10.1080/87559129.2016.1242135>
- Lambert, J. B., & Mazzola, E. P. (2004). *Nuclear magnetic resonance spectroscopy : an introduction to principles, applications, and experimental methods*. Upper Saddle River, N.J. : Pearson/Prentice Hall.
- Lambrecht, M. A., Rombouts, I., & Delcour, J. A. (2016). Denaturation and covalent network formation of wheat gluten, globular proteins and mixtures thereof in aqueous ethanol and water. *Food Hydrocolloids*, *57*, 122–131. <https://doi.org/10.1016/j.foodhyd.2016.01.018>
- Lara, G., Yakoubi, S., Villacorta, C. M., Uemura, K., Kobayashi, I., Takahashi, C., Nakajima, M., & Neves, M. A. (2020). Spray technology applications of xanthan gum-based edible coatings for fresh-cut lotus root (*Nelumbo nucifera*). *Food Research International*, *137*, 109723. <https://doi.org/10.1016/j.foodres.2020.109723>

- Lara, I., Belge, B., & Goulao, L. F. (2014). The fruit cuticle as a modulator of postharvest quality. *Postharvest Biology and Technology*, *87*, 103–112. <https://doi.org/10.1016/j.postharvbio.2013.08.012>
- Lazic, Z. R. (2006). *Design of experiments in chemical engineering: a practical guide*. John Wiley & Sons.
- Le Dean, A., Mariette, F., Lucas, T., & Marin, M. (2001). Assessment of the State of Water in Reconstituted Milk Protein Dispersions by Nuclear Magnetic Resonance (NMR) and Differential Scanning Calorimetry (DSC). *LWT - Food Science and Technology*, *34*(5), 299–305. <https://doi.org/10.1006/fstl.2001.0765>
- Leal, P. F., Maia, N. B., Carmello, Q. A. C., Catharino, R. R., Eberlin, M. N., & Meireles, M. A. A. (2007). Sweet Basil (*Ocimum basilicum*) Extracts Obtained by Supercritical Fluid Extraction (SFE): Global Yields, Chemical Composition, Antioxidant Activity, and Estimation of the Cost of Manufacturing. *Food and Bioprocess Technology*, *1*(4), 326. <https://doi.org/10.1007/s11947-007-0030-1>
- Lee, S. Y., Khoiroh, I., Ling, T. C., & Show, P. L. (2016). Aqueous Two-Phase Flotation for the Recovery of Biomolecules. *Separation & Purification Reviews*, *45*(1), 81–92. <https://doi.org/10.1080/15422119.2015.1007147>
- Lefol, E. (2007). Haskap market development-the Japanese opportunity. *University of Saskatchewan. MBA Thesis*.
- Leong, H. Y., Chang, Y.-K., Ooi, C. W., Law, C. L., Julkifle, A. L., & Show, P. L. (2019). Liquid Biphasic Electric Partitioning System as a Novel Integration Process for Betacyanins Extraction From Red-Purple Pitaya and Antioxidant Properties Assessment. In *Frontiers in Chemistry* (Vol. 7, p. 201). <https://www.frontiersin.org/article/10.3389/fchem.2019.00201>
- Leong, H. Y., Ooi, C. W., Law, C. L., Julkifle, A. L., Katsuda, T., & Show, P. L. (2019). Integration process for betacyanins extraction from peel and flesh of *Hylocereus polyrhizus* using liquid biphasic electric flotation system and antioxidant activity evaluation. *Separation and Purification Technology*, *209*, 193–201. <https://doi.org/10.1016/j.seppur.2018.07.040>
- Leong, H. Y., Ooi, C. W., Law, C. L., Julkifle, A. L., Ling, T. C., & Show, P. L. (2018). Application of liquid biphasic flotation for betacyanins extraction from peel and flesh of *Hylocereus polyrhizus* and antioxidant activity evaluation. *Separation and Purification Technology*, *201*(May 2018), 156–166. <https://doi.org/10.1016/j.seppur.2018.03.008>
- Leong, H. Y., Ooi, C. W., Law, C. L., Julkifle, A. L., & Show, P. L. (2018). Betacyanins extraction from *Hylocereus polyrhizus* using alcohol/salt-based liquid biphasic partitioning system and antioxidant activity evaluation. *Separation Science and Technology*, *00*(00), 1–12. <https://doi.org/10.1080/01496395.2018.1517795>
- Li, M., & Dong, H. (2010). The investigation on the aqueous two-phase floatation of lincomycin. *Separation and Purification Technology*, *73*(2), 208–212. <https://doi.org/10.1016/j.seppur.2010.04.002>

- Lin, Y. K., Show, P. L., Yap, Y. J., Tan, C. P., Ng, E. P., Ariff, A. B., Mohamad Annuar, M. S. B., & Ling, T. C. (2015). Direct recovery of cyclodextringlycosyltransferase from *Bacillus cereus* using aqueous two-phase flotation. *Journal of Bioscience and Bioengineering*, *120*(6), 684–689. <https://doi.org/10.1016/j.jbiosc.2015.04.013>
- Ling, Y.-Q., Nie, H.-L., Su, S.-N., Branford-White, C., & Zhu, L.-M. (2010). Optimization of affinity partitioning conditions of papain in aqueous two-phase system using response surface methodology. *Separation and Purification Technology*, *73*(3), 343–348. <https://doi.org/10.1016/j.seppur.2010.04.020>
- Liu, C., Xianzhe, Z., Shuhua, J., Ningye, D., & Xiaochen, G. (2009). Comparative Experiment on Hot-Air and Microwave-Vacuum Drying and Puffing of Blue Honeysuckle Snack. *International Journal of Food Engineering*, *5*. <https://doi.org/10.2202/1556-3758.1683>
- Liu, H., Xie, F., Yu, L., Chen, L., & Li, L. (2009). Thermal processing of starch-based polymers. *Progress in Polymer Science*, *34*(12), 1348–1368. <https://doi.org/10.1016/j.progpolymsci.2009.07.001>
- Liu, X., Mu, T., Sun, H., Zhang, M., & Chen, J. (2013). Optimisation of aqueous two-phase extraction of anthocyanins from purple sweet potatoes by response surface methodology. *Food Chemistry*, *141*(3), 3034–3041. <https://doi.org/10.1016/j.foodchem.2013.05.119>
- Liu, Y., Han, J., Wang, Y., Lu, Y., Zhang, G., Sheng, C., & Yan, Y. (2013). Selective separation of flavones and sugars from honeysuckle by alcohol/salt aqueous two-phase system and optimization of extraction process. *Separation and Purification Technology*, *118*, 776–783. <https://doi.org/10.1016/j.seppur.2013.08.018>
- Longares, A., Monahan, F. J., O’Riordan, E. D., & O’Sullivan, M. (2004). Physical properties and sensory evaluation of WPI films of varying thickness. *LWT - Food Science and Technology*, *37*(5), 545–550. <https://doi.org/10.1016/j.lwt.2003.12.005>
- López-de-Dicastillo, C., Gómez-Estaca, J., Catalá, R., Gavara, R., & Hernández-Muñoz, P. (2012). Active antioxidant packaging films: Development and effect on lipid stability of brined sardines. *Food Chemistry*, *131*(4), 1376–1384. <https://doi.org/10.1016/j.foodchem.2011.10.002>
- López de Dicastillo, C., Bustos, F., Valenzuela, X., López-Carballo, G., Vilariño, J. M., & Galotto, M. J. (2017). Chilean berry *Ugni molinae* Turcz. fruit and leaves extracts with interesting antioxidant, antimicrobial and tyrosinase inhibitory properties. *Food Research International*, *102*, 119–128. <https://doi.org/10.1016/j.foodres.2017.09.073>
- Lorevice, M. V, Moura, M. R. de, Aouada, F. A., & Mattoso, L. H. C. (2012). Development of Novel Guava Puree Films Containing Chitosan Nanoparticles. In *Journal of Nanoscience and Nanotechnology* (Vol. 12, Issue 3, pp. 2711–2717). <https://doi.org/10.1166/jnn.2012.5716>

- Lou, Z., Wang, H., Zhu, S., Ma, C., & Wang, Z. (2011). Antibacterial Activity and Mechanism of Action of Chlorogenic Acid. *Journal of Food Science*, 76(6), M398–M403. <https://doi.org/10.1111/j.1750-3841.2011.02213.x>
- Lumdubwong, N. B. T.-R. M. in F. S. (2019). *Applications of Starch-Based Films in Food Packaging*. Elsevier. <https://doi.org/10.1016/B978-0-08-100596-5.22481-5>
- Luque de Castro, M. D., & Priego-Capote, F. (2010). Soxhlet extraction: Past and present panacea. *Journal of Chromatography A*, 1217(16), 2383–2389. <https://doi.org/10.1016/j.chroma.2009.11.027>
- Ma, F.-Y., Gu, C.-B., Li, C.-Y., Luo, M., Wang, W., Zu, Y.-G., Li, J., & Fu, Y.-J. (2013). Microwave-assisted aqueous two-phase extraction of isoflavonoids from *Dalbergia odorifera* T. Chen leaves. *Separation and Purification Technology*, 115, 136–144. <https://doi.org/10.1016/j.seppur.2013.05.003>
- Machida, K., Asano, J., & Kikuchi, M. (1995). Caeruleosides A and B, bis-iridoid glucosides from *Lonicera caerulea*. *Phytochemistry*, 39(1), 111–114. [https://doi.org/10.1016/0031-9422\(94\)00853-L](https://doi.org/10.1016/0031-9422(94)00853-L)
- Maftoonazad, N., Shahmirian, M., John, D., & Ramaswamy, H. (2019). Development and evaluation of antibacterial electrospun pea protein isolate-polyvinyl alcohol nanocomposite mats incorporated with cinnamaldehyde. *Materials Science and Engineering: C*, 94, 393–402. <https://doi.org/10.1016/j.msec.2018.09.033>
- Mahajan, P. V., Oliveira, F. A. R., & Macedo, I. (2008). Effect of temperature and humidity on the transpiration rate of the whole mushrooms. *Journal of Food Engineering*, 84(2), 281–288. <https://doi.org/10.1016/j.jfoodeng.2007.05.021>
- Maleki, S. J., Crespo, J. F., & Cabanillas, B. (2019). Anti-inflammatory effects of flavonoids. *Food Chemistry*, 299, 125124. <https://doi.org/10.1016/j.foodchem.2019.125124>
- Mallegni, N., Phuong, T. V., Coltelli, M.-B., Cinelli, P., & Lazzeri, A. (2018). Poly (lactic acid)(PLA) based tear resistant and biodegradable flexible films by blown film extrusion. *Materials*, 11(1), 148. <https://doi.org/10.3390/ma11010148>
- Mangaraj, S., Goswami, T. K., & Mahajan, P. V. (2009). Applications of Plastic Films for Modified Atmosphere Packaging of Fruits and Vegetables: A Review. *Food Engineering Reviews*, 1(2), 133. <https://doi.org/10.1007/s12393-009-9007-3>
- Marcos, B., Sárraga, C., Castellari, M., Kappen, F., Schennink, G., & Arnau, J. (2014). Development of biodegradable films with antioxidant properties based on polyesters containing α -tocopherol and olive leaf extract for food packaging applications. *Food Packaging and Shelf Life*, 1(2), 140–150. <https://doi.org/10.1016/j.fpsl.2014.04.002>
- Marquié, C. (2001). Chemical Reactions in Cottonseed Protein Cross-Linking by Formaldehyde, Glutaraldehyde, and Glyoxal for the Formation of Protein Films with Enhanced Mechanical Properties. *Journal of Agricultural and Food Chemistry*, 49(10), 4676–4681. <https://doi.org/10.1021/jf0101152>

- Maryam Adilah, Z. A., Jamilah, B., & Nur Hanani, Z. A. (2018). Functional and antioxidant properties of protein-based films incorporated with mango kernel extract for active packaging. *Food Hydrocolloids*, 74, 207–218. <https://doi.org/10.1016/j.foodhyd.2017.08.017>
- Mateus, F. H., Lepera, J. S., & Lanchote, V. L. (2005). Determination of Acetonitrile and Cyanide in Rat Blood: Application to an Experimental Study. *Journal of Analytical Toxicology*, 29(2), 105–109. <https://doi.org/10.1093/jat/29.2.105>
- McHugh, T H, & Senesi, E. (2000). Apple Wraps: A Novel Method to Improve the Quality and Extend the Shelf Life of Fresh-cut Apples. *Journal of Food Science*, 65(3), 480–485. <https://doi.org/10.1111/j.1365-2621.2000.tb16032.x>
- McHugh, T Habig, Avena-Bustillos, R., & Krochta, J. M. (1993). Hydrophilic Edible Films: Modified Procedure for Water Vapor Permeability and Explanation of Thickness Effects. *Journal of Food Science*, 58(4), 899–903. <https://doi.org/10.1111/j.1365-2621.1993.tb09387.x>
- Medina Jaramillo, C., González Seligra, P., Goyanes, S., Bernal, C., & Famá, L. (2015). Biofilms based on cassava starch containing extract of yerba mate as antioxidant and plasticizer. *Starch - Stärke*, 67(9–10), 780–789. <https://doi.org/10.1002/star.201500033>
- Medina Jaramillo, C., Gutiérrez, T. J., Goyanes, S., Bernal, C., & Famá, L. (2016). Biodegradability and plasticizing effect of yerba mate extract on cassava starch edible films. *Carbohydrate Polymers*, 151, 150–159. <https://doi.org/10.1016/j.carbpol.2016.05.025>
- Melini, V., & Melini, F. (2018). Strategies to extend bread and GF bread shelf-Life: From sourdough to antimicrobial active packaging and nanotechnology. *Fermentation*, 4(1), 9. <https://doi.org/10.3390/fermentation4010009>
- Mendes, J. F., Martins, J. T., Manrich, A., Sena Neto, A. R., Pinheiro, A. C. M., Mattoso, L. H. C., & Martins, M. A. (2019). Development and physical-chemical properties of pectin film reinforced with spent coffee grounds by continuous casting. *Carbohydrate Polymers*, 210, 92–99. <https://doi.org/10.1016/j.carbpol.2019.01.058>
- Meng, S., Cao, J., Feng, Q., Peng, J., & Hu, Y. (2013). Roles of Chlorogenic Acid on Regulating Glucose and Lipids Metabolism: A Review. *Evidence-Based Complementary and Alternative Medicine*, 2013, 801457. <https://doi.org/10.1155/2013/801457>
- Merchuk, J. C., Andrews, B. A., & Asenjo, J. A. (1998). Aqueous two-phase systems for protein separation Studies on phase inversion. *J. Chromatogr. B.*, 711, 285.
- Mettler Toledo. (2000). *Interpreting DSC curves Part 1: Dynamic measurements*.
- Mir, S. A., Dar, B. N., Wani, A. A., & Shah, M. A. (2018). Effect of plant extracts on the techno-functional properties of biodegradable packaging films. *Trends in Food Science & Technology*, 80, 141–154. <https://doi.org/10.1016/j.tifs.2018.08.004>

- Morillon, V., Debeaufort, F., Blond, G., Capelle, M., & Voilley, A. (2002). Factors Affecting the Moisture Permeability of Lipid-Based Edible Films: A Review. *Critical Reviews in Food Science and Nutrition*, 42(1), 67–89. <https://doi.org/10.1080/10408690290825466>
- Mushtaq, M., Gani, A., Gani, A., Punoo, H. A., & Masoodi, F. A. (2018). Use of pomegranate peel extract incorporated zein film with improved properties for prolonged shelf life of fresh Himalayan cheese (Kalari/kradi). *Innovative Food Science & Emerging Technologies*, 48, 25–32. <https://doi.org/10.1016/j.ifset.2018.04.020>
- Musso, Y. S., Salgado, P. R., & Mauri, A. N. (2019). Smart gelatin films prepared using red cabbage (*Brassica oleracea* L.) extracts as solvent. *Food Hydrocolloids*, 89(October 2018), 674–681. <https://doi.org/10.1016/j.foodhyd.2018.11.036>
- Mustafa, R. A., Hamid, A. A., Mohamed, S., & Bakar, F. A. (2010). Total Phenolic Compounds, Flavonoids, and Radical Scavenging Activity of 21 Selected Tropical Plants. *Journal of Food Science*, 75(1), C28–C35. <https://doi.org/10.1111/j.1750-3841.2009.01401.x>
- Nakamura, T., Murata, Y., & Nakamura, Y. (2019). Characterization of benzyl isothiocyanate extracted from mashed green papaya by distillation. *Food Chemistry*, 299, 125118. <https://doi.org/10.1016/j.foodchem.2019.125118>
- Nandini, K. E., & Rastogi, N. K. (2011). Liquid–Liquid Extraction of Lipase Using Aqueous Two-Phase System. *Food and Bioprocess Technology*, 4(2), 295–303. <https://doi.org/10.1007/s11947-008-0160-0>
- Nastić, N., Borrás-Linares, I., Lozano-Sánchez, J., Švarc-Gajić, J., & Segura-Carretero, A. (2018). Optimization of the extraction of phytochemicals from black mulberry (*Morus nigra* L.) leaves. *Journal of Industrial and Engineering Chemistry*, 68, 282–292. <https://doi.org/10.1016/j.jiec.2018.07.055>
- Naugžemys, D., Žilinskaitė, S., Denkovskij, J., Patamsytė, J., Literskis, J., & Žvingila, D. (2007). RAPD based study of genetic variation and relationships among *Lonicera* germplasm accessions. *Biologija*, 3.
- Navapara, R. D., Avhad, D. N., & Rathod, V. K. (2011). Application of Response Surface Methodology for Optimization of Bromelain Extraction in Aqueous Two-Phase System. *Separation Science and Technology*, 46(11), 1838–1847. <https://doi.org/10.1080/01496395.2011.578101>
- Naveed, M., Hejazi, V., Abbas, M., Kamboh, A. A., Khan, G. J., Shumzaid, M., Ahmad, F., Babazadeh, D., FangFang, X., Modarresi-Ghazani, F., WenHua, L., & XiaoHui, Z. (2018). Chlorogenic acid (CGA): A pharmacological review and call for further research. *Biomedicine & Pharmacotherapy*, 97, 67–74. <https://doi.org/10.1016/j.biopha.2017.10.064>
- Neužilová, B., Ondrák, L., Čuba, V., & Múčka, V. (2019). Ethanol as a modifier of radiation sensitivity of living cells against UV-C radiation. *Radiation Protection Dosimetry*, 186(2–3), 191–195. <https://doi.org/10.1093/rpd/ncz200>

- Newsham, D. M. T., & Mendez-Lecanda, E. J. (1982). Isobaric enthalpies of vaporization of water, methanol, ethanol, propan-2-ol, and their mixtures. *The Journal of Chemical Thermodynamics*, 14(3), 291–301. [https://doi.org/10.1016/0021-9614\(82\)90020-9](https://doi.org/10.1016/0021-9614(82)90020-9)
- Ng, H. S., Ng, T.-C., Kee, P. E., Tan, J. S., Yim, H. S., & Lan, J. C.-W. (2020). Partition efficiency of cytochrome c with alcohol/salt aqueous biphasic flotation system. *Journal of Bioscience and Bioengineering*, 129(2), 237–241. <https://doi.org/10.1016/j.jbiosc.2019.08.013>
- Ng, H. S., Teoh, A. N., Lim, J. C. W., Tan, J. S., Wan, P. K., Yim, H. S., Show, P. L., & Lan, J. C. W. (2017). Thermo-sensitive aqueous biphasic extraction of polyphenols from *Camellia sinensis* var. *assamica* leaves. *Journal of the Taiwan Institute of Chemical Engineers*, 79, 151–157. <https://doi.org/10.1016/j.jtice.2017.02.018>
- Nikolaidis, A., & Moschakis, T. (2018). On the reversibility of ethanol-induced whey protein denaturation. *Food Hydrocolloids*, 84, 389–395. <https://doi.org/10.1016/j.foodhyd.2018.05.051>
- Nile, S. H., & Park, S. W. (2014). Edible berries: Bioactive components and their effect on human health. *Nutrition*, 30(2), 134–144. <https://doi.org/10.1016/j.nut.2013.04.007>
- North, E. J., & Halden, R. U. (2013). Plastics and environmental health: the road ahead. *Reviews on Environmental Health*, 28(1), 1–8. <https://doi.org/10.1515/reveh-2012-0030>
- Nouri, L., & Mohammadi Nafchi, A. (2014). Antibacterial, mechanical, and barrier properties of sago starch film incorporated with betel leaves extract. *International Journal of Biological Macromolecules*, 66, 254–259. <https://doi.org/10.1016/j.ijbiomac.2014.02.044>
- Novák, P., & Havlíček, V. (2016). 4 - Protein Extraction and Precipitation (P. Ciborowski & J. B. T.-P. P. and A. C. (Second E. Silberring (eds.); pp. 51–62). Elsevier. <https://doi.org/10.1016/B978-0-444-63688-1.00004-5>
- O'Connor, J. (2018). *Better than blueberries? Introducing Canada's new super food — the haskap berry*. National Post. <https://nationalpost.com/news/canada/better-than-blueberries-introducing-canadas-new-super-food-the-haskap-berry>
- Ochmian, I., Grajkowski, J., & Skupień, K. (2008). Field performance, fruit chemical composition and firmness under cold storage and simulated “shelf-life” conditions of three blue honeysuckle cultigens (*Lonicera caerulea*). *Journal of Fruit and Ornamental Plant Research*, 16, 83–91.
- Oelmeier, S. A., Dismer, F., & Hubbuch, J. (2012). Molecular dynamics simulations on aqueous two-phase systems - Single PEG-molecules in solution. *BMC Biophysics*, 5(1), 14. <https://doi.org/10.1186/2046-1682-5-14>

- Olalere, O. A., Abdurahman, H. N., & Gan, C.-Y. (2019). Microwave-enhanced extraction and mass spectrometry fingerprints of polyphenolic constituents in *Sesamum indicum* leaves. *Industrial Crops and Products*, *131*, 151–159. <https://doi.org/10.1016/j.indcrop.2018.12.024>
- Oliveira, G., Gonçalves, I., Barra, A., Nunes, C., Ferreira, P., & Coimbra, M. A. (2020). Coffee silverskin and starch-rich potato washing slurries as raw materials for elastic, antioxidant, and UV-protective biobased films. *Food Research International*, *138*, 109733. <https://doi.org/10.1016/j.foodres.2020.109733>
- Oliveira, M. L. N., Malagoni, R. A., & Franco, M. R. (2013). Solubility of citric acid in water, ethanol, n-propanol and in mixtures of ethanol+water. *Fluid Phase Equilibria*, *352*, 110–113. <https://doi.org/10.1016/j.fluid.2013.05.014>
- Ong, E. S. (2004). Extraction methods and chemical standardization of botanicals and herbal preparations. *Journal of Chromatography B*, *812*(1), 23–33. <https://doi.org/10.1016/j.jchromb.2004.07.041>
- Ooi, C. W., Tey, B. T., Hii, S. L., Kamal, S. M. M., Lan, J. C. W., Ariff, A., & Ling, T. C. (2009). Purification of lipase derived from *Burkholderia pseudomallei* with alcohol/salt-based aqueous two-phase systems. *Process Biochemistry*, *44*(10), 1083–1087. <https://doi.org/10.1016/j.procbio.2009.05.008>
- Oszmiański, J., Wojdyło, A., Gorzelany, J., & Kapusta, I. (2011). Identification and characterization of low molecular weight polyphenols in berry leaf extracts by HPLC-DAD and LC-ESI/MS. *Journal of Agricultural and Food Chemistry*, *59*(24), 12830–12835. <https://doi.org/10.1021/jf203052j>
- Oszmiański, J., Wojdyło, A., Lachowicz, S., Gorzelany, J., & Matłok, N. (2016). Comparison of bioactive potential of cranberry fruit and fruit-based products versus leaves. *Journal of Functional Foods*, *22*, 232–242. <https://doi.org/10.1016/j.jff.2016.01.015>
- Otoni, C. G., Avena-Bustillos, R. J., Azeredo, H. M. C., Lorevice, M. V., Moura, M. R., Mattoso, L. H. C., & McHugh, T. H. (2017). Recent Advances on Edible Films Based on Fruits and Vegetables—A Review. *Comprehensive Reviews in Food Science and Food Safety*, *16*(5), 1151–1169. <https://doi.org/10.1111/1541-4337.12281>
- Padilha, C. E. de A., Dantas, P. V. F., Sousa Júnior, F. C., Oliveira Júnior, S. D., Nogueira, C. da C., Souza, D. F. de S., de Oliveira, J. A., de Macedo, G. R., & dos Santos, E. S. (2017). Recovery and concentration of ortho-phenylphenol from biodesulfurization of 4-methyl dibenzothiophene by aqueous two-phase flotation. *Separation and Purification Technology*, *176*, 306–312. <https://doi.org/10.1016/j.seppur.2016.12.029>
- Pakhale, S. V, Vetel, M. D., & Rathod, V. K. (2013). Separation of Bromelain by Aqueous Two Phase Flotation. *Separation Science and Technology*, *48*(6), 984–989. <https://doi.org/10.1080/01496395.2012.712596>

- Panizzi, L., Caponi, C., Catalano, S., Cioni, P. L., & Morelli, I. (2002). In vitro antimicrobial activity of extracts and isolated constituents of *Rubus ulmifolius*. *Journal of Ethnopharmacology*, *79*(2), 165–168. [https://doi.org/10.1016/S0378-8741\(01\)00363-4](https://doi.org/10.1016/S0378-8741(01)00363-4)
- Pantelidis, G. E., Vasilakakis, M., Manganaris, G. A., & Diamantidis, G. (2007). Antioxidant capacity, phenol, anthocyanin and ascorbic acid contents in raspberries, blackberries, red currants, gooseberries and Cornelian cherries. *Food Chemistry*, *102*(3), 777–783. <https://doi.org/10.1016/j.foodchem.2006.06.021>
- Pękal, A., & Pyrzynska, K. (2014). Evaluation of Aluminium Complexation Reaction for Flavonoid Content Assay. *Food Analytical Methods*, *7*(9), 1776–1782. <https://doi.org/10.1007/s12161-014-9814-x>
- Peng, C., Chan, M. N., & Chan, C. K. (2001). The Hygroscopic Properties of Dicarboxylic and Multifunctional Acids: Measurements and UNIFAC Predictions. *Environmental Science & Technology*, *35*(22), 4495–4501. <https://doi.org/10.1021/es0107531>
- Pereira, C. G., & Meireles, M. A. A. (2010). Supercritical Fluid Extraction of Bioactive Compounds: Fundamentals, Applications and Economic Perspectives. *Food and Bioprocess Technology*, *3*(3), 340–372. <https://doi.org/10.1007/s11947-009-0263-2>
- Pereira, P., Cebola, M.-J., Oliveira, M. C., & Bernardo-Gil, M. G. (2016). Supercritical fluid extraction vs conventional extraction of myrtle leaves and berries: Comparison of antioxidant activity and identification of bioactive compounds. *The Journal of Supercritical Fluids*, *113*, 1–9. <https://doi.org/10.1016/j.supflu.2015.09.006>
- Perez-gago, M. B., & Krochta, J. M. (2001). Denaturation Time and Temperature Effects on Solubility, Tensile Properties, and Oxygen Permeability of Whey Protein Edible Films. *Journal of Food Science*, *66*(5), 705–710. <https://doi.org/10.1111/j.1365-2621.2001.tb04625.x>
- Perez, V., Felix, M., Romero, A., & Guerrero, A. (2016). Characterization of pea protein-based bioplastics processed by injection moulding. *Food and Bioprocess Technology*, *97*, 100–108. <https://doi.org/10.1016/j.fbp.2015.12.004>
- Périno-Issartier, S., Zill-e-Huma, Abert-Vian, M., & Chemat, F. (2011). Solvent Free Microwave-Assisted Extraction of Antioxidants from Sea Buckthorn (*Hippophae rhamnoides*) Food By-Products. *Food and Bioprocess Technology*, *4*(6), 1020–1028. <https://doi.org/10.1007/s11947-010-0438-x>
- Phan, T. D., Debeaufort, F., Luu, D., & Voilley, A. (2005). Functional Properties of Edible Agar-Based and Starch-Based Films for Food Quality Preservation. *Journal of Agricultural and Food Chemistry*, *53*(4), 973–981. <https://doi.org/10.1021/jf040309s>

- Picchio, M. L., Linck, Y. G., Monti, G. A., Gugliotta, L. M., Minari, R. J., & Alvarez Igarzabal, C. I. (2018). Casein films crosslinked by tannic acid for food packaging applications. *Food Hydrocolloids*, *84*, 424–434. <https://doi.org/10.1016/j.foodhyd.2018.06.028>
- Pietta, P.-G. (2000). Flavonoids as Antioxidants. *Journal of Natural Products*, *63*(7), 1035–1042. <https://doi.org/10.1021/np9904509>
- Piljac-Žegarac, J., & Šamec, D. (2011). Antioxidant stability of small fruits in postharvest storage at room and refrigerator temperatures. *Food Research International*, *44*(1), 345–350. <https://doi.org/10.1016/j.foodres.2010.09.039>
- Pimpão, R. C., Dew, T., Oliveira, P. B., Williamson, G., Ferreira, R. B., & Santos, C. N. (2013). Analysis of Phenolic Compounds in Portuguese Wild and Commercial Berries after Multienzyme Hydrolysis. *Journal of Agricultural and Food Chemistry*, *61*(17), 4053–4062. <https://doi.org/10.1021/jf305498j>
- Pisoschi, A. M., & Pop, A. (2015). The role of antioxidants in the chemistry of oxidative stress: A review. *European Journal of Medicinal Chemistry*, *97*, 55–74. <https://doi.org/10.1016/j.ejmech.2015.04.040>
- Platis, D., & Labrou, N. E. (2006). Development of an aqueous two-phase partitioning system for fractionating therapeutic proteins from tobacco extract. *Journal of Chromatography A*, *1128*(1), 114–124. <https://doi.org/10.1016/j.chroma.2006.06.047>
- Prakash, R., Majumder, S. K., & Singh, A. (2018). Flotation technique: Its mechanisms and design parameters. *Chemical Engineering and Processing - Process Intensification*, *127*(March), 249–270. <https://doi.org/10.1016/j.cep.2018.03.029>
- Prodpran, T., Benjakul, S., & Phatcharat, S. (2012). Effect of phenolic compounds on protein cross-linking and properties of film from fish myofibrillar protein. *International Journal of Biological Macromolecules*, *51*(5), 774–782. <https://doi.org/10.1016/j.ijbiomac.2012.07.010>
- Pulse Canada. (2019). *Producers and Industry*. <http://www.pulsecanada.com/producers-industry/>
- Qiao, A., Wang, Y., Xiang, L., Zhang, Z., & He, X. (2015). Novel triterpenoids isolated from hawthorn berries functioned as antioxidant and antiproliferative activities. *Journal of Functional Foods*, *13*, 308–313. <https://doi.org/10.1016/j.jff.2014.12.047>
- Radojković, M., Zeković, Z., Mašković, P., Vidović, S., Mandić, A., Mišan, A., & Đurović, S. (2016). Biological activities and chemical composition of Morus leaves extracts obtained by maceration and supercritical fluid extraction. *The Journal of Supercritical Fluids*, *117*, 50–58. <https://doi.org/10.1016/j.supflu.2016.05.004>
- Raffa, D., Maggio, B., Raimondi, M. V., Plescia, F., & Daidone, G. (2017). Recent discoveries of anticancer flavonoids. *European Journal of Medicinal Chemistry*, *142*, 213–228. <https://doi.org/10.1016/j.ejmech.2017.07.034>

- Ramos, Ó. L., Reinas, I., Silva, S. I., Fernandes, J. C., Cerqueira, M. A., Pereira, R. N., Vicente, A. A., Poças, M. F., Pintado, M. E., & Malcata, F. X. (2013). Effect of whey protein purity and glycerol content upon physical properties of edible films manufactured therefrom. *Food Hydrocolloids*, *30*(1), 110–122. <https://doi.org/10.1016/j.foodhyd.2012.05.001>
- Raudsepp, P., Kaldmäe, H., Kikas, A., Libek, A.-V., & Püssa, T. (2010). Nutritional quality of berries and bioactive compounds in the leaves of black currant (*Ribes nigrum* L.) cultivars evaluated in Estonia. *Journal of Berry Research*, *1*, 53–59. <https://doi.org/10.3233/BR-2010-006>
- Reddy, N., Li, Y., & Yang, Y. (2009). Alkali-catalyzed low temperature wet crosslinking of plant proteins using carboxylic acids. *Biotechnology Progress*, *25*(1), 139–146. <https://doi.org/10.1002/btpr.86>
- Regupathi, I., Murugesan, S., Govindarajan, R., Amaresh, S. P., & Thanapalan, M. (2009). Liquid-liquid equilibrium of poly(ethylene glycol) 6000 + triammonium citrate + water systems at different temperatures. *Journal of Chemical and Engineering Data*, *54*(3), 1094–1097. <https://doi.org/10.1021/jc8008478>
- Reinkensmeier, A., Bußler, S., Schlüter, O., Rohn, S., & Rawel, H. M. (2015). Characterization of individual proteins in pea protein isolates and air classified samples. *Food Research International*, *76*, 160–167. <https://doi.org/10.1016/j.foodres.2015.05.009>
- Reis, I. A. O., Campos, A. F., Santos, P. H. S., Santos, S. B., Soares, C. M. F., & Lima, Á. S. (2015). Potassium Phosphate Salts-Based Aqueous Two-Phase Systems Applied in the Extraction of Gallic Acid from Guava. *Separation Science and Technology*, *50*(4), 520–528. <https://doi.org/10.1080/01496395.2014.956180>
- Ren, W., Qiao, Z., Wang, H., Zhu, L., & Zhang, L. (2003). Flavonoids: Promising anticancer agents. *Medicinal Research Reviews*, *23*(4), 519–534. <https://doi.org/10.1002/med.10033>
- Ribeiro-Santos, R., de Melo, N. R., Andrade, M., Azevedo, G., Machado, A. V., Carvalho-Costa, D., & Sanches-Silva, A. (2018). Whey protein active films incorporated with a blend of essential oils: Characterization and effectiveness. *Packaging Technology and Science*, *31*(1), 27–40. <https://doi.org/10.1002/pts.2352>
- Robertson, G. L. (2016). *Food packaging: principles and practice*. CRC Press.
- Rodrigues, G. D., de Lemos, L. R., da Silva, L. H. M., da Silva, M. do C. H., Minim, L. A., & Coimbra, J. S. dos R. (2010). A green and sensitive method to determine phenols in water and wastewater samples using an aqueous two-phase system. *Talanta*, *80*(3), 1139–1144. <https://doi.org/10.1016/j.talanta.2009.08.039>
- Rodrigues, V. H., de Melo, M. M. R., Portugal, I., & Silva, C. M. (2018). Extraction of Eucalyptus leaves using solvents of distinct polarity. Cluster analysis and extracts characterization. *The Journal of Supercritical Fluids*, *135*, 263–274. <https://doi.org/10.1016/j.supflu.2018.01.010>

- Rodríguez-Martínez, A. V., Sendón, R., Abad, M. J., González-Rodríguez, M. V., Barros-Velázquez, J., Aubourg, S. P., Paseiro-Losada, P., & Rodríguez-Bernaldo de Quirós, A. (2016). Migration kinetics of sorbic acid from polylactic acid and seaweed based films into food simulants. *LWT - Food Science and Technology*, *65*, 630–636. <https://doi.org/10.1016/j.lwt.2015.08.029>
- Rosa, P. A. J., Azevedo, A. M., Sommerfeld, S., Mutter, M., Aires-Barros, M. R., & Bäcker, W. (2009). Application of aqueous two-phase systems to antibody purification: A multi-stage approach. *Journal of Biotechnology*, *139*(4), 306–313. <https://doi.org/10.1016/j.jbiotec.2009.01.001>
- Routray, W. (2014). *Effect of different extraction methods, environmental and post-harvest factors on yield of phenolic compounds from blueberry leaves* [McGill University]. http://digitool.library.mcgill.ca:80/R/-?func=dbin-jump-full&object_id=127090&silolibrary=GEN01
- Routray, W., & Orsat, V. (2012). Microwave-Assisted Extraction of Flavonoids: A Review. *Food and Bioprocess Technology*, *5*(2), 409–424. <https://doi.org/10.1007/s11947-011-0573-z>
- Routray, W., & Orsat, V. (2014). MAE of phenolic compounds from blueberry leaves and comparison with other extraction methods. *Industrial Crops and Products*, *58*, 36–45. <https://doi.org/10.1016/j.indcrop.2014.03.038>
- Routray, W., Orsat, V., & Garipey, Y. (2014). Effect of Different Drying Methods on the Microwave Extraction of Phenolic Components and Antioxidant Activity of Highbush Blueberry Leaves. *Drying Technology*, *32*(16), 1888–1904. <https://doi.org/10.1080/07373937.2014.919002>
- Roy, F., Boye, J. I., & Simpson, B. K. (2010). Bioactive proteins and peptides in pulse crops: Pea, chickpea and lentil. *Food Research International*, *43*(2), 432–442. <https://doi.org/10.1016/j.foodres.2009.09.002>
- Roy, S., Gennadios, A., Weller, C. L., & Testin, R. F. (2000). Water vapor transport parameters of a cast wheat gluten film. *Industrial Crops and Products*, *11*(1), 43–50. [https://doi.org/10.1016/S0926-6690\(99\)00032-1](https://doi.org/10.1016/S0926-6690(99)00032-1)
- Ruiz-Ruiz, F., Benavides, J., & Rito-Palomares, M. (2017). *Affinity ATPS Strategies for the Selective Fractionation of Biomolecules*. https://doi.org/10.1007/978-3-319-59309-8_6
- Sá, A. G. A., Moreno, Y. M. F., & Carciofi, B. A. M. (2020). Plant proteins as high-quality nutritional source for human diet. *Trends in Food Science & Technology*, *97*, 170–184. <https://doi.org/10.1016/j.tifs.2020.01.011>
- Sabaté, J., & Soret, S. (2014). Sustainability of plant-based diets: back to the future. *The American Journal of Clinical Nutrition*, *100*(suppl_1), 476S–482S. <https://doi.org/10.3945/ajcn.113.071522>

- Sadeghi, R., & Jamehbozorg, B. (2008). Effect of temperature on the salting-out effect and phase separation in aqueous solutions of sodium di-hydrogen phosphate and poly(propylene glycol). *Fluid Phase Equilibria*, 271(1), 13–18. <https://doi.org/10.1016/j.fluid.2008.06.018>
- Safdar, M. N., Kausar, T., Jabbar, S., Mumtaz, A., Ahad, K., & Saddozai, A. A. (2017). Extraction and quantification of polyphenols from kinnow (*Citrus reticulata* L.) peel using ultrasound and maceration techniques. *Journal of Food and Drug Analysis*, 25(3), 488–500. <https://doi.org/10.1016/j.jfda.2016.07.010>
- Salas-Méndez, E. de J., Vicente, A., Pinheiro, A. C., Ballesteros, L. F., Silva, P., Rodríguez-García, R., Hernández-Castillo, F. D., Díaz-Jiménez, M. de L. V., Flores-López, M. L., Villarreal-Quintanilla, J. Á., Peña-Ramos, F. M., Carrillo-Lomelí, D. A., & Jasso de Rodríguez, D. (2019). Application of edible nanolaminate coatings with antimicrobial extract of *Flourensia cernua* to extend the shelf-life of tomato (*Solanum lycopersicum* L.) fruit. *Postharvest Biology and Technology*, 150, 19–27. <https://doi.org/10.1016/j.postharvbio.2018.12.008>
- Salgado, P. R., Molina Ortiz, S. E., Petruccelli, S., & Mauri, A. N. (2010). Biodegradable sunflower protein films naturally activated with antioxidant compounds. *Food Hydrocolloids*, 24(5), 525–533. <https://doi.org/10.1016/j.foodhyd.2009.12.002>
- Sanchez-Ballesta, M. T., Romero, I., Jiménez, J. B., Orea, J. M., González-Ureña, Á., Escribano, M. I., & Merodio, C. (2007). Involvement of the phenylpropanoid pathway in the response of table grapes to low temperature and high CO₂ levels. *Postharvest Biology and Technology*, 46(1), 29–35. <https://doi.org/10.1016/j.postharvbio.2007.04.001>
- Sánchez-González, L., Quintero Saavedra, J. I., & Chiralt, A. (2013). Physical properties and antilisterial activity of bioactive edible films containing *Lactobacillus plantarum*. *Food Hydrocolloids*, 33(1), 92–98. <https://doi.org/10.1016/j.foodhyd.2013.02.011>
- Sánchez-Rangel, J. C., Jacobo-Velázquez, D. A., Cisneros-Zevallos, L., & Benavides, J. (2016). Primary recovery of bioactive compounds from stressed carrot tissue using aqueous two-phase systems strategies. *Journal of Chemical Technology and Biotechnology*, 91(1), 144–154. <https://doi.org/10.1002/jctb.4553>
- Sängerlaub, S., Böhmer, M., & Stramm, C. (2013). Influence of stretching ratio and salt concentration on the porosity of polypropylene films containing sodium chloride particles. *Journal of Applied Polymer Science*, 129(3), 1238–1248. <https://doi.org/10.1002/app.38793>
- Sankaran, R., Manickam, S., Yap, Y. J., Ling, T. C., Chang, J. S., & Show, P. L. (2018). Extraction of proteins from microalgae using integrated method of sugaring-out assisted liquid biphasic flotation (LBF) and ultrasound. *Ultrasonics Sonochemistry*, 48(January), 231–239. <https://doi.org/10.1016/j.ultsonch.2018.06.002>

- Sankaran, R., Show, P. L., Yap, Y. J., Lam, H. L., Ling, T. C., Pan, G.-T., & Yang, T. C.-K. (2018). Sustainable approach in recycling of phase components of large scale aqueous two-phase flotation for lipase recovery. *Journal of Cleaner Production*, *184*, 938–948. <https://doi.org/10.1016/j.jclepro.2018.02.301>
- Santhi, J. V., Tavanandi, H. A., Sharma, R., Prabhakar, G., & Raghavarao, K. S. M. S. (2020). Differential partitioning of coconut whey proteins and fat using aqueous two phase extraction. *Fluid Phase Equilibria*, *503*, 112314. <https://doi.org/10.1016/j.fluid.2019.112314>
- Saravanan, S., Rao, J. R., Nair, B. U., & Ramasami, T. (2008). Aqueous two-phase poly(ethylene glycol)-poly(acrylic acid) system for protein partitioning: Influence of molecular weight, pH and temperature. *Process Biochemistry*, *43*(9), 905–911. <https://doi.org/10.1016/j.procbio.2008.04.011>
- Sason, G., & Nussinovitch, A. (2021). *Chapter 7 - Hydrocolloids for edible films, coatings, and food packaging* (G. O. Phillips & P. A. B. T.-H. of H. (Third E. Williams (eds.); pp. 195–235). Woodhead Publishing. <https://doi.org/10.1016/B978-0-12-820104-6.00023-1>
- Sato, A., Obata, K., Ikeda, K., Ohkoshi, K., Okumura, H., Ozawa, N., Ogawa, T., Katsumura, Y., Kawai, J., Tatsumi, H., Honoki, S., Hiramatsu, I., Hiroyama, H., Okada, T., & Kozuka, T. (1996). Evaluation of human skin irritation by carboxylic acids, alcohols, esters and aldehydes, with nitrocellulose-replica method and closed patch testing. *Contact Dermatitis*, *34*(1), 12–16. <https://doi.org/10.1111/j.1600-0536.1996.tb02104.x>
- Sato, Y., Itagaki, S., Kurokawa, T., Ogura, J., Kobayashi, M., Hirano, T., Sugawara, M., & Iseki, K. (2011). In vitro and in vivo antioxidant properties of chlorogenic acid and caffeic acid. *International Journal of Pharmaceutics*, *403*(1), 136–138. <https://doi.org/10.1016/j.ijpharm.2010.09.035>
- Schwarz, A. E., Ligthart, T. N., Boukris, E., & van Harmelen, T. (2019). Sources, transport, and accumulation of different types of plastic litter in aquatic environments: A review study. *Marine Pollution Bulletin*, *143*, 92–100. <https://doi.org/10.1016/j.marpolbul.2019.04.029>
- Senica, M., Bavec, M., Stampar, F., & Mikulic-Petkovsek, M. (2018). Blue honeysuckle (*Lonicera caerulea* subsp. *edulis* (Turcz. ex Herder) Hultén.) berries and changes in their ingredients across different locations. *Journal of the Science of Food and Agriculture*. <https://doi.org/10.1002/jsfa.8837>
- Seo, C.-S., Jeong, S.-J., Yoo, S.-R., Lee, N.-R., & Shin, H.-K. (2016). Quantitative Analysis and In vitro Anti-inflammatory Effects of Gallic Acid, Ellagic Acid, and Quercetin from *Radix Sanguisorbae*. *Pharmacognosy Magazine*, *12*(46), 104–108. <https://doi.org/10.4103/0973-1296.177908>

- Shahbaz Mohammadi, H., Mostafavi, S. S., Soleimani, S., Bozorgian, S., Pooraskari, M., & Kianmehr, A. (2015). Response surface methodology to optimize partition and purification of two recombinant oxidoreductase enzymes, glucose dehydrogenase and d-galactose dehydrogenase in aqueous two-phase systems. *Protein Expression and Purification*, *108*, 41–47. <https://doi.org/10.1016/j.pep.2015.01.002>
- Sharma, L., Sharma, H. K., & Saini, C. S. (2018). Edible films developed from carboxylic acid cross-linked sesame protein isolate: barrier, mechanical, thermal, crystalline and morphological properties. *Journal of Food Science and Technology*, *55*(2), 532–539. <https://doi.org/10.1007/s13197-017-2962-4>
- Shevkani, K., & Singh, N. (2015). Relationship between protein characteristics and film-forming properties of kidney bean, field pea and amaranth protein isolates. *International Journal of Food Science and Technology*, *50*(4), 1033–1043. <https://doi.org/10.1111/ijfs.12733>
- Shi, M., Loftus, H., McAinch, A. J., & Su, X. Q. (2017). Blueberry as a source of bioactive compounds for the treatment of obesity, type 2 diabetes and chronic inflammation. *Journal of Functional Foods*, *30*, 16–29. <https://doi.org/10.1016/j.jff.2016.12.036>
- Shi, W., & Dumont, M.-J. (2014). Processing and physical properties of canola protein isolate-based films. *Industrial Crops and Products*, *52*, 269–277. <https://doi.org/10.1016/j.indcrop.2013.10.037>
- Shiku, Y., Hamaguchi, P. Y., & Tanaka, M. (2003). Effect of pH on the preparation of edible films based on fish myofibrillar proteins. *Fisheries Science*, *69*(5), 1026–1032. <https://doi.org/10.1046/j.1444-2906.2003.00722.x>
- Show, P. L., Ooi, C. W., Anuar, M. S., Ariff, A., Yusof, Y. A., Chen, S. K., Annuar, M. S. M., & Ling, T. C. (2013). Recovery of lipase derived from *Burkholderia cenocepacia* ST8 using sustainable aqueous two-phase flotation composed of recycling hydrophilic organic solvent and inorganic salt. *Separation and Purification Technology*, *110*, 112–118. <https://doi.org/10.1016/j.seppur.2013.03.018>
- Siemann, U. (2005). Solvent cast technology – a versatile tool for thin film production. In N. Stribeck & B. Smarsly (Eds.), *Scattering Methods and the Properties of Polymer Materials* (pp. 1–14). Springer Berlin Heidelberg. <https://doi.org/10.1007/b107336>
- Simental-Martínez, J., Montalvo-Hernández, B., Rito-Palomares, M., & Benavides, J. (2014). Application of Aqueous Two-Phase Systems for the Recovery of Bioactive Low-Molecular Weight Compounds. *Separation Science and Technology (Philadelphia)*, *49*(12), 1872–1882. <https://doi.org/10.1080/01496395.2014.904878>

- Simmonds, G., & Spence, C. (2017). Thinking inside the box: How seeing products on, or through, the packaging influences consumer perceptions and purchase behaviour. *Food Quality and Preference*, *62*, 340–351. <https://doi.org/10.1016/j.foodqual.2016.11.010>
- Singh, P., Magalhães, S., Alves, L., Antunes, F., Miguel, M., Lindman, B., & Medronho, B. (2019). Cellulose-based edible films for probiotic entrapment. *Food Hydrocolloids*, *88*, 68–74. <https://doi.org/10.1016/j.foodhyd.2018.08.057>
- Singleton, V. L., Orthofer, R., & Lamuela-Raventos, R. M. (1999). Analysis of total phenols and other oxidation substrates and antioxidants by means of Folin-Ciocalteu reagent. *Methods in Enzymology*, *299C*, 152–178.
- Siripatrawan, U., & Harte, B. R. (2010). Physical properties and antioxidant activity of an active film from chitosan incorporated with green tea extract. *Food Hydrocolloids*, *24*(8), 770–775. <https://doi.org/10.1016/j.foodhyd.2010.04.003>
- Sirtori, E., Isak, I., Resta, D., Boschini, G., & Arnoldi, A. (2012). Mechanical and thermal processing effects on protein integrity and peptide fingerprint of pea protein isolate. *Food Chemistry*, *134*(1), 113–121. <https://doi.org/10.1016/j.foodchem.2012.02.073>
- Sivarooaban, T., Hettiarachchy, N. S., & Johnson, M. G. (2008). Physical and antimicrobial properties of grape seed extract, nisin, and EDTA incorporated soy protein edible films. *Food Research International*, *41*(8), 781–785. <https://doi.org/10.1016/j.foodres.2008.04.007>
- Soares, R. R. G., Azevedo, A. M., Van Alstine, J. M., & Aires-Barros, M. R. (2015). Partitioning in aqueous two-phase systems: Analysis of strengths, weaknesses, opportunities and threats. *Biotechnology Journal*, *10*(8), 1158–1169. <https://doi.org/10.1002/biot.201400532>
- Solano-Castillo, C., & Rito-Palomares, M. (2000). Kinetics of phase separation under different process and design parameters in aqueous two-phase systems. *Journal of Chromatography B: Biomedical Sciences and Applications*, *743*(1), 195–201. [https://doi.org/10.1016/S0378-4347\(00\)00060-8](https://doi.org/10.1016/S0378-4347(00)00060-8)
- Sothornvit, R., & Pitak, N. (2007). Oxygen permeability and mechanical properties of banana films. *Food Research International*, *40*(3), 365–370. <https://doi.org/10.1016/j.foodres.2006.10.010>
- Souza, V. G. L., Rodrigues, P. F., Duarte, M. P., & Fernando, A. L. (2018). Antioxidant Migration Studies in Chitosan Films Incorporated with Plant Extracts. In *Journal of Renewable Materials* (Vol. 6, Issue 5). <https://doi.org/10.7569/JRM.2018.634104>
- Spikes, J. D. (1981). Photodegradation of foods and beverages. In *Photochemical and photobiological reviews* (pp. 39–85). Springer. https://doi.org/10.1007/978-1-4684-7003-1_2

- Stolte, I., Frohberg, P., Pietzsch, M., & Ulrich, J. (2012). Crystals in protein films: What are they good for? *Chemical Engineering Science*, 77, 196–200. <https://doi.org/10.1016/j.ces.2012.01.053>
- Suhag, R., Kumar, N., Petkoska, A. T., & Upadhyay, A. (2020). Film formation and deposition methods of edible coating on food products: A review. *Food Research International*, 136, 109582. <https://doi.org/10.1016/j.foodres.2020.109582>
- Sun, Y., Zhang, S., Zhang, X., Zheng, Y., & Xiu, Z. (2018). Ionic liquid-based sugaring-out and salting-out extraction of succinic acid. *Separation and Purification Technology*, 204(2), 133–140. <https://doi.org/10.1016/j.seppur.2018.04.064>
- Suzuki, A., Kagawa, D., Ochiai, R., Tokimitsu, I., & Saito, I. (2002). Green Coffee Bean Extract and Its Metabolites Have a Hypotensive Effect in Spontaneously Hypertensive Rats. *Hypertension Research*, 25(1), 99–107. <https://doi.org/10.1291/hypres.25.99>
- Szakiel, A., Pączkowski, C., Koivuniemi, H., & Huttunen, S. (2012). Comparison of the Triterpenoid Content of Berries and Leaves of Lingonberry *Vaccinium vitis-idaea* from Finland and Poland. *Journal of Agricultural and Food Chemistry*, 60(19), 4994–5002. <https://doi.org/10.1021/jf300375b>
- Tabera, J., Guinda, Á., Ruiz-Rodríguez, A., Señoráns, F. J., Ibáñez, E., Albi, T., & Reglero, G. (2004). Countercurrent Supercritical Fluid Extraction and Fractionation of High-Added-Value Compounds from a Hexane Extract of Olive Leaves. *Journal of Agricultural and Food Chemistry*, 52(15), 4774–4779. <https://doi.org/10.1021/jf049881%2B>
- Takuno, M. (1992). *Highly hygroscopic laminate*. Google Patents. <https://patents.google.com/patent/US5143773A/en>
- Talens, P., & Krochta, J. M. (2005). Plasticizing Effects of Beeswax and Carnauba Wax on Tensile and Water Vapor Permeability Properties of Whey Protein Films. *Journal of Food Science*, 70(3), E239–E243. <https://doi.org/10.1111/j.1365-2621.2005.tb07141.x>
- Tan, Z., Wang, C., Yi, Y., Wang, H., Li, M., Zhou, W., Tan, S., & Li, F. (2014). Extraction and purification of chlorogenic acid from ramie (*Boehmeria nivea* L. Gaud) leaf using an ethanol/salt aqueous two-phase system. *Separation and Purification Technology*, 132, 396–400. <https://doi.org/10.1016/j.seppur.2014.05.048>
- Tang, S. L. Y., Smith, R. L., & Poliakoff, M. (2005). Principles of green chemistry: PRODUCTIVELY. *Green Chemistry*, 7(11), 761–762. <https://doi.org/10.1039/B513020B>
- Tapia-Blácido, D. R., Sobral, P. J. do A., & Menegalli, F. C. (2013). Effect of drying conditions and plasticizer type on some physical and mechanical properties of amaranth flour films. *LWT - Food Science and Technology*, 50(2), 392–400. <https://doi.org/10.1016/j.lwt.2012.09.008>

- Tham, P. E., Ng, Y. J., Sankaran, R., Khoo, K. S., Chew, K. W., Yap, Y. J., Malahubban, M., Aziz Zakry, F. A., & Show, P. L. (2019). Recovery of Protein from Dairy Milk Waste Product Using Alcohol-Salt Liquid Biphasic Flotation. In *Processes* (Vol. 7, Issue 12). <https://doi.org/10.3390/pr7120875>
- Tian, Y., Pугanen, A., Alakomi, H.-L., Uusitupa, A., Saarela, M., & Yang, B. (2018). Antioxidative and antibacterial activities of aqueous ethanol extracts of berries, leaves, and branches of berry plants. *Food Research International*, *106*, 291–303. <https://doi.org/10.1016/j.foodres.2017.12.071>
- Tömösközi, S., Lásztity, R., Haraszi, R., & Baticz, O. (2001). Isolation and study of the functional properties of pea proteins. *Food / Nahrung*, *45*(6), 399–401. [https://doi.org/10.1002/1521-3803\(20011001\)45:6<399::AID-FOOD399>3.0.CO;2-0](https://doi.org/10.1002/1521-3803(20011001)45:6<399::AID-FOOD399>3.0.CO;2-0)
- Tonyali, B., Cikrikci, S., & Oztop, M. H. (2018). Physicochemical and microstructural characterization of gum tragacanth added whey protein based films. *Food Research International*, *105*, 1–9. <https://doi.org/10.1016/j.foodres.2017.10.071>
- Torres-León, C., Vicente, A. A., Flores-López, M. L., Rojas, R., Serna-Cock, L., Alvarez-Pérez, O. B., & Aguilar, C. N. (2018). Edible films and coatings based on mango (var. Ataulfo) by-products to improve gas transfer rate of peach. *LWT*, *97*, 624–631. <https://doi.org/10.1016/j.lwt.2018.07.057>
- Tu, X., Sun, F., Wu, S., Liu, W., Gao, Z., Huang, S., & Chen, W. (2018). Comparison of salting-out and sugaring-out liquid–liquid extraction methods for the partition of 10-hydroxy-2-decenoic acid in royal jelly and their co-extracted protein content. *Journal of Chromatography B*, *1073*, 90–95. <https://doi.org/10.1016/j.jchromb.2017.12.020>
- Tubtimdee, C., & Shotipruk, A. (2011). Extraction of phenolics from Terminalia chebula Retz with water–ethanol and water–propylene glycol and sugaring-out concentration of extracts. *Separation and Purification Technology*, *77*(3), 339–346. <https://doi.org/10.1016/j.seppur.2011.01.002>
- Tulamandi, S., Rangarajan, V., Rizvi, S. S. H., Singhal, R. S., Chattopadhyay, S. K., & Saha, N. C. (2016). A biodegradable and edible packaging film based on papaya puree, gelatin, and defatted soy protein. *Food Packaging and Shelf Life*, *10*, 60–71. <https://doi.org/10.1016/j.fpsl.2016.10.007>
- U.S. Food and Drug Administration. (2020). *CFR - Code of Federal Regulations Title 21*. https://www.ecfr.gov/cgi-bin/text-idx?SID=56ecf6cbc894976e144848106d4104e8&mc=true&tpl=/ecfrbrowse/Title21/21cfr582_main_02.tpl
- Ustunol, Z., & Mert, B. (2004). Water Solubility, Mechanical, Barrier, and Thermal Properties of Cross-linked Whey Protein Isolate-based Films. *Journal of Food Science*, *69*(3), FEP129–FEP133. <https://doi.org/10.1111/j.1365-2621.2004.tb13365.x>

- Veloso, A. V., Silva, B. C., Bomfim, S. A., de Souza, R. L., Soares, C. M. F., & Lima, Á. S. (2020). Selective and continuous recovery of ascorbic acid and vanillin from commercial diet pudding waste using an aqueous two-phase system. *Food and Bioproducts Processing*, 119, 268–276. <https://doi.org/10.1016/j.fbp.2019.11.011>
- Vieira, A. W., Molina, G., Mageste, A. B., Rodrigues, G. D., & de Lemos, L. R. (2019). Partitioning of salicylic and acetylsalicylic acids by aqueous two-phase systems: Mechanism aspects and optimization study. *Journal of Molecular Liquids*, 296, 111775. <https://doi.org/10.1016/j.molliq.2019.111775>
- Vieira, M. G. A., da Silva, M. A., dos Santos, L. O., & Beppu, M. M. (2011). Natural-based plasticizers and biopolymer films: A review. *European Polymer Journal*, 47(3), 254–263. <https://doi.org/10.1016/j.eurpolymj.2010.12.011>
- Villalobos, R., Chanona, J., Hernández, P., Gutiérrez, G., & Chiralt, A. (2005). Gloss and transparency of hydroxypropyl methylcellulose films containing surfactants as affected by their microstructure. *Food Hydrocolloids*, 19(1), 53–61. <https://doi.org/10.1016/j.foodhyd.2004.04.014>
- Viroben, G., Barbot, J., Mouloungui, Z., & Guéguen, J. (2000). Preparation and characterization of films from pea protein. *Journal of Agricultural and Food Chemistry*, 48(4), 1064–1069. <https://doi.org/10.1021/jf9813891>
- Vongsak, B., Sithisarn, P., Mangmool, S., Thongpraditchote, S., Wongkrajang, Y., & Gritsanapan, W. (2013). Maximizing total phenolics, total flavonoids contents and antioxidant activity of Moringa oleifera leaf extract by the appropriate extraction method. *Industrial Crops and Products*, 44, 566–571. <https://doi.org/10.1016/j.indcrop.2012.09.021>
- Wang, B., Ezejias, T., Feng, H., & Blaschek, H. (2008). Sugaring-out: A novel phase separation and extraction system. *Chemical Engineering Science*, 63(9), 2595–2600. <https://doi.org/10.1016/j.ces.2008.02.004>
- Wang, S., Marcone, M., Barbut, S., & Lim, L.-T. (2012a). The Impact of Anthocyanin-Rich Red Raspberry Extract (ARRE) on the Properties of Edible Soy Protein Isolate (SPI) Films. *Journal of Food Science*, 77(4), C497–C505. <https://doi.org/10.1111/j.1750-3841.2012.02655.x>
- Wang, S., Marcone, M. F., Barbut, S., & Lim, L.-T. (2012b). Fortification of dietary biopolymers-based packaging material with bioactive plant extracts. *Food Research International*, 49(1), 80–91. <https://doi.org/10.1016/j.foodres.2012.07.023>
- Wang, T., Xu, W.-J., Wang, S.-X., Kou, P., Wang, P., Wang, X.-Q., & Fu, Y.-J. (2017). Integrated and sustainable separation of chlorogenic acid from blueberry leaves by deep eutectic solvents coupled with aqueous two-phase system. *Food and Bioproducts Processing*, 105, 205–214. <https://doi.org/10.1016/j.fbp.2017.07.010>

- Wang, W., Sun, C., Mao, L., Ma, P., Liu, F., Yang, J., & Gao, Y. (2016). The biological activities, chemical stability, metabolism and delivery systems of quercetin: A review. *Trends in Food Science & Technology*, 56, 21–38. <https://doi.org/10.1016/j.tifs.2016.07.004>
- Wang, X., Sun, X., Liu, H., Li, M., & Ma, Z. (2011). Barrier and mechanical properties of carrot puree films. *Food and Bioprocess Processing*, 89(2), 149–156. <https://doi.org/10.1016/j.fbp.2010.03.012>
- Wang, Y., Mao, Y., Han, J., Liu, Y., & Yan, Y. (2010). Liquid–liquid equilibrium of potassium phosphate/potassium citrate/sodium citrate + ethanol aqueous two-phase systems at (298.15 and 313.15) K and correlation. *J. Chem. Eng. Data*, 55, 5621.
- Wang, Yun, Yan, Y., Hu, S., Han, J., & Xu, X. (2010). Phase Diagrams of Ammonium Sulfate + Ethanol/1-Propanol/2-Propanol + Water Aqueous Two-Phase Systems at 298.15 K and Correlation. *Journal of Chemical & Engineering Data*, 55(2), 876–881. <https://doi.org/10.1021/jc900504e>
- Werner, S. R. L., Jones, J. R., Paterson, A. H. J., Archer, R. H., & Pearce, D. L. (2007). Air-suspension particle coating in the food industry: Part I — state of the art. *Powder Technology*, 171(1), 25–33. <https://doi.org/10.1016/j.powtec.2006.08.014>
- Wihodo, M., & Moraru, C. I. (2013). Physical and chemical methods used to enhance the structure and mechanical properties of protein films: A review. *Journal of Food Engineering*, 114(3), 292–302. <https://doi.org/10.1016/j.jfoodeng.2012.08.021>
- Wildermuth, S. R., Young, E. E., & Were, L. M. (2016). Chlorogenic Acid Oxidation and Its Reaction with Sunflower Proteins to Form Green-Colored Complexes. *Comprehensive Reviews in Food Science and Food Safety*, 15(5), 829–843. <https://doi.org/10.1111/1541-4337.12213>
- Wilson, R. D., & Islam, M. S. (2015). Effects of white mulberry (*Morus alba*) leaf tea investigated in a type 2 diabetes model of rats. *Acta Poloniae Pharmaceutica*, 72(1), 153–160.
- Wu, P., Ma, G., Li, N., Deng, Q., Yin, Y., & Huang, R. (2015). Investigation of in vitro and in vivo antioxidant activities of flavonoids rich extract from the berries of *Rhodomyrtus tomentosa*(Ait.) Hassk. *Food Chemistry*, 173, 194–202. <https://doi.org/10.1016/j.foodchem.2014.10.023>
- Wu, X., Liang, L., Zou, Y., Zhao, T., Zhao, J., Li, F., & Yang, L. (2011). Aqueous two-phase extraction, identification and antioxidant activity of anthocyanins from mulberry (*Morus atropurpurea* Roxb.). *Food Chemistry*, 129(2), 443–453. <https://doi.org/10.1016/j.foodchem.2011.04.097>
- Wu, Y., Wang, Y., Zhang, W., Han, J., Liu, Y., Hu, Y., & Ni, L. (2014). Extraction and preliminary purification of anthocyanins from grape juice in aqueous two-phase system. *Separation and Purification Technology*, 124, 170–178. <https://doi.org/10.1016/j.seppur.2014.01.025>

- Xavier, L., Freire, M. S., Vidal-Tato, I., & González-Álvarez, J. (2017). Recovery of phenolic compounds from Eucalyptus wood wastes using ethanol-salt-based aqueous two-phase systems. *Maderas. Ciencia y Tecnología*, *19*(1), 3–14.
- Xi, J., Shen, D., Zhao, S., Lu, B., Li, Y., & Zhang, R. (2009). Characterization of polyphenols from green tea leaves using a high hydrostatic pressure extraction. *International Journal of Pharmaceutics*, *382*(1), 139–143. <https://doi.org/10.1016/j.ijpharm.2009.08.023>
- Xia, J., Ni, L., Han, J., Wang, Y., Li, Y., Li, Y., & Tian, Y. (2016). Simultaneous aqueous two-phase flotation of sodium chlorophyllin and removal of sugars from saponified solution of bamboo leaves. *Chemical Engineering and Processing: Process Intensification*, *101*, 41–49. <https://doi.org/10.1016/j.cep.2015.12.014>
- Xu, H., Shen, L., Xu, L., & Yang, Y. (2015). Low-temperature crosslinking of proteins using non-toxic citric acid in neutral aqueous medium: Mechanism and kinetic study. *Industrial Crops and Products*, *74*, 234–240. <https://doi.org/10.1016/j.indcrop.2015.05.010>
- Yang, J., Yu, J., & Huang, Y. (2011). Recent developments in gelcasting of ceramics. *Journal of the European Ceramic Society*, *31*(14), 2569–2591. <https://doi.org/10.1016/j.jeurceramsoc.2010.12.035>
- Yau, Y. K., Ooi, C. W., Ng, E.-P., Lan, J. C.-W., Ling, T. C., & Show, P. L. (2015). Current applications of different type of aqueous two-phase systems. *Bioresources and Bioprocessing*, *2*(1), 49. <https://doi.org/10.1186/s40643-015-0078-0>
- Yousuf, B., & Srivastava, A. K. (2019). Impact of honey treatments and soy protein isolate-based coating on fresh-cut pineapple during storage at 4 °C. *Food Packaging and Shelf Life*, *21*, 100361. <https://doi.org/10.1016/j.fpsl.2019.100361>
- Yuan, Y., Leng, Y., Shao, H., Huang, C., & Shan, K. (2014). Solubility of dl-malic acid in water, ethanol and in mixtures of ethanol+water. *Fluid Phase Equilibria*, *377*, 27–32. <https://doi.org/10.1016/j.fluid.2014.06.017>
- Yue, H.-B., Cui, Y.-D., Shuttleworth, P. S., & Clark, J. H. (2012). Preparation and characterisation of bioplastics made from cottonseed protein. *Green Chemistry*, *14*(7), 2009–2016. <https://doi.org/10.1039/C2GC35509D>
- Zafarani-Moattar, M. T., Banisaeid, S., & Shamsi Beirami, M. A. (2005). Phase Diagrams of Some Aliphatic Alcohols + Potassium or Sodium Citrate + Water at 25 °C. *Journal of Chemical & Engineering Data*, *50*(4), 1409–1413. <https://doi.org/10.1021/je050086h>
- Zderic, A., & Zondervan, E. (2016). Polyphenol extraction from fresh tea leaves by pulsed electric field: A study of mechanisms. *Chemical Engineering Research and Design*, *109*, 586–592. <https://doi.org/10.1016/j.cherd.2016.03.010>

- Zhang, D.-Y., Zu, Y.-G., Fu, Y.-J., Wang, W., Zhang, L., Luo, M., Mu, F.-S., Yao, X.-H., & Duan, M.-H. (2013). Aqueous two-phase extraction and enrichment of two main flavonoids from pigeon pea roots and the antioxidant activity. *Separation and Purification Technology*, *102*, 26–33. <https://doi.org/10.1016/j.seppur.2012.09.019>
- Zhang, W., Zhu, D., Fan, H., Liu, X., Wan, Q., Wu, X., Liu, P., & Tang, J. Z. (2015). Simultaneous extraction and purification of alkaloids from *Sophora flavescens* Ait. by microwave-assisted aqueous two-phase extraction with ethanol/ammonia sulfate system. *Separation and Purification Technology*, *141*, 113–123. <https://doi.org/10.1016/j.seppur.2014.11.014>
- Zhou, P., & Labuza, T. P. (2007). Effect of Water Content on Glass Transition and Protein Aggregation of Whey Protein Powders During Short-Term Storage. *Food Biophysics*, *2*(2), 108–116. <https://doi.org/10.1007/s11483-007-9037-4>
- Zhu, Liancai, Liu, X., Tan, J., & Wang, B. (2013). Influence of Harvest Season on Antioxidant Activity and Constituents of Rabbiteye Blueberry (*Vaccinium ashei*) Leaves. *Journal of Agricultural and Food Chemistry*, *61*(47), 11477–11483. <https://doi.org/10.1021/jf4035892>
- Zhu, Lina, Lu, Y., Sun, Z., Han, J., & Tan, Z. (2020). The application of an aqueous two-phase system combined with ultrasonic cell disruption extraction and HPLC in the simultaneous separation and analysis of solanine and Solanum nigrum polysaccharide from Solanum nigrum unripe fruit. *Food Chemistry*, *304*, 125383. <https://doi.org/10.1016/j.foodchem.2019.125383>

APPENDIX A: Supplementary Figures

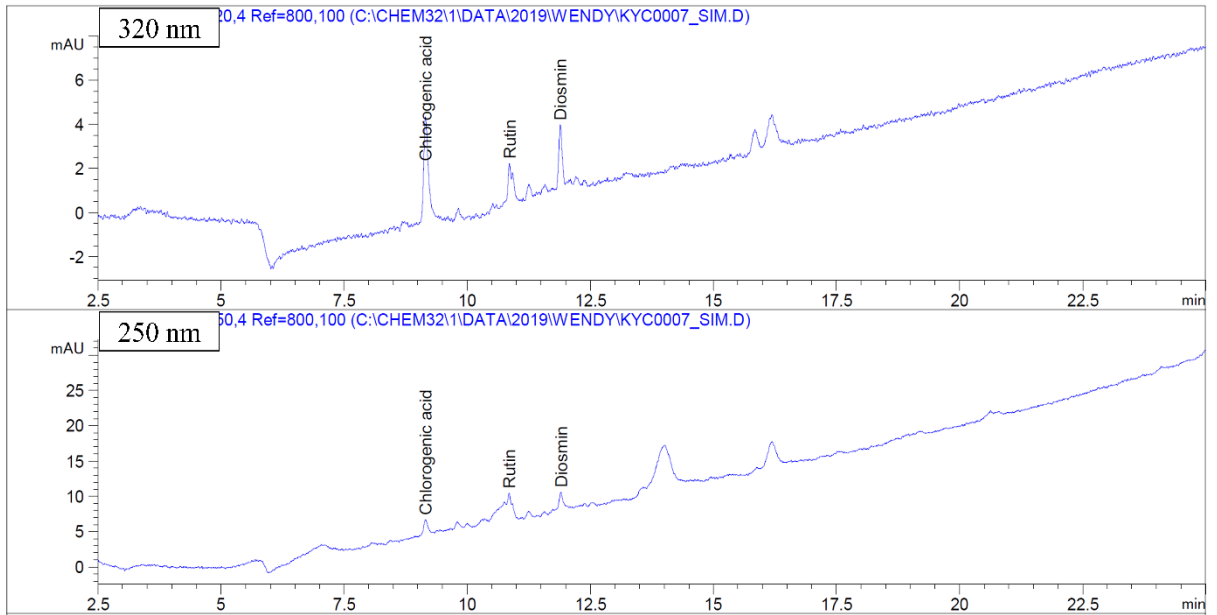


Figure A.1: HPLC chromatogram for ammonium sulphate/ethanol haskap leaf extract

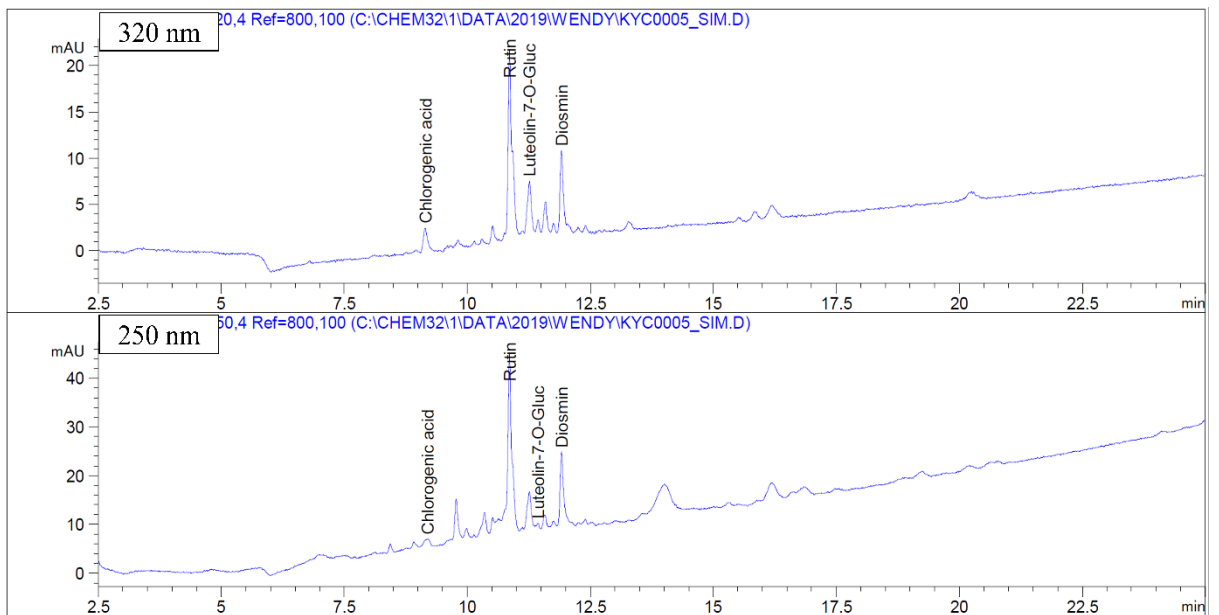


Figure A.2: HPLC chromatogram for glucose/1-propanol haskap leaf extract

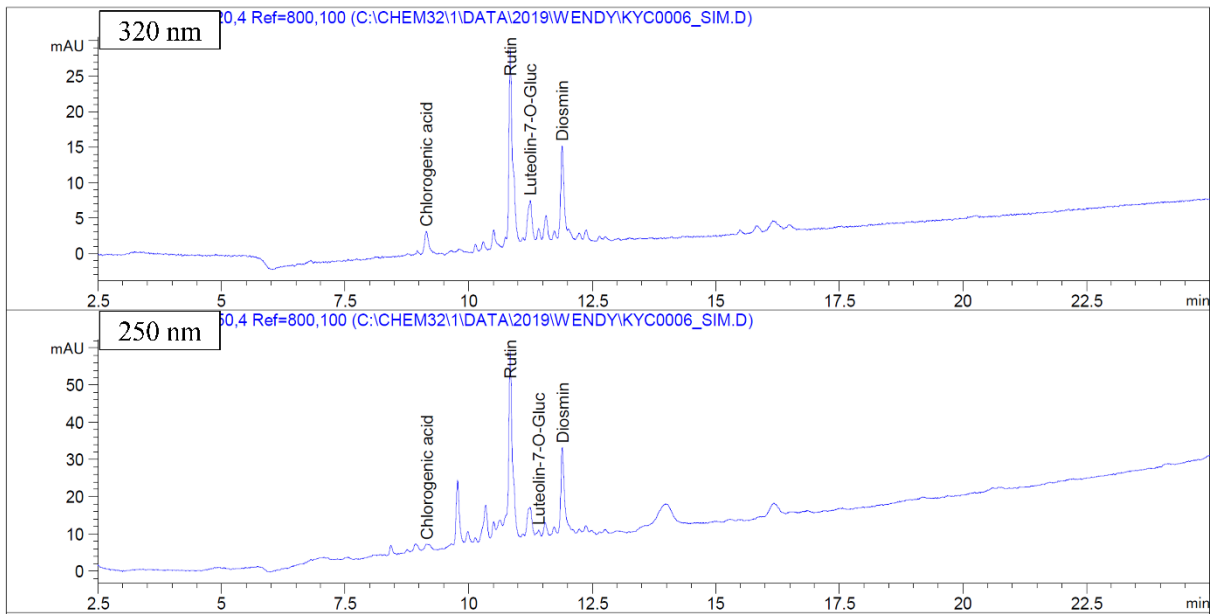


Figure A.3: HPLC chromatogram for maltose/1-propanol haskap leaf extract

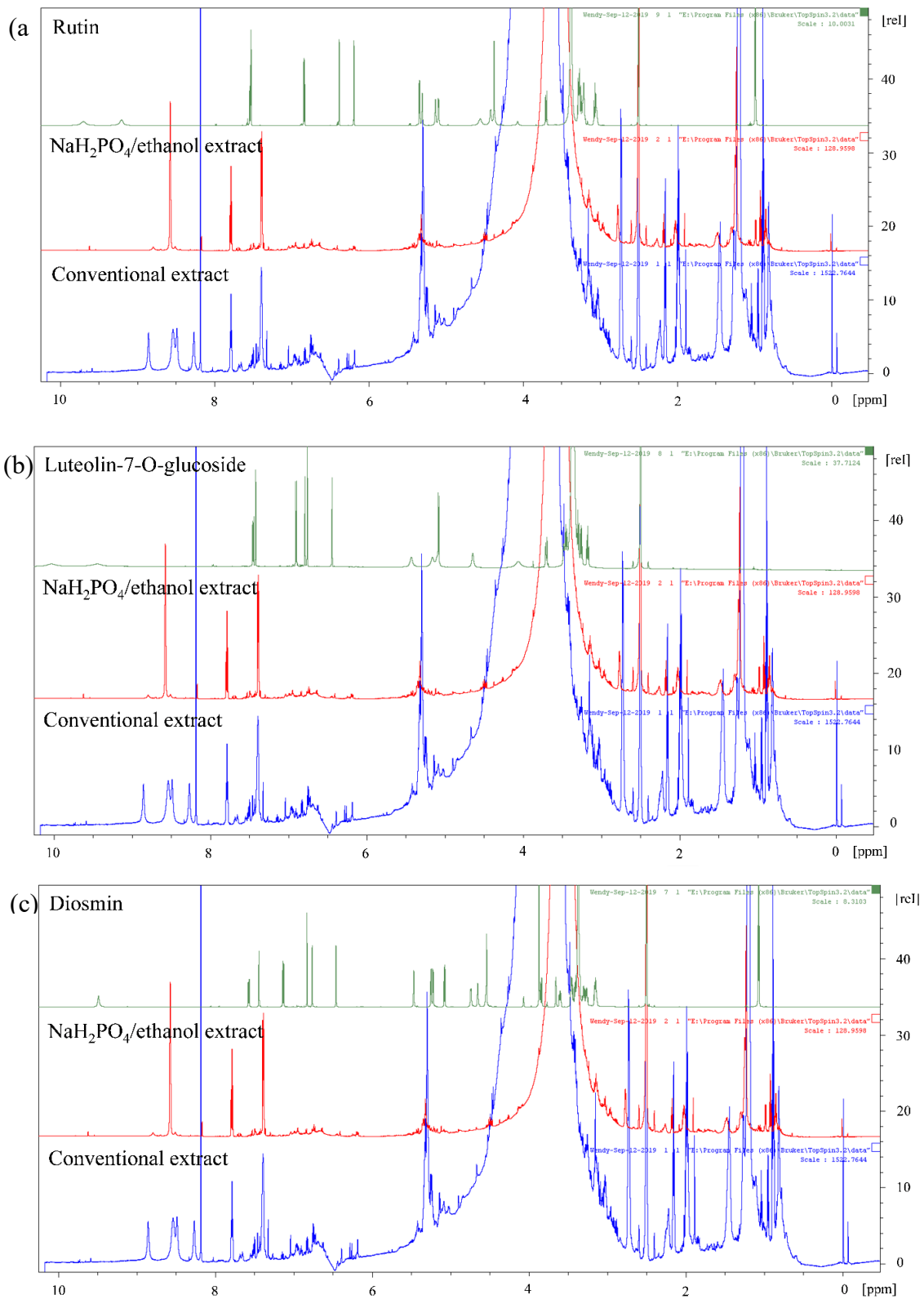


Figure A.4: $^1\text{H-NMR}$ spectra for $\text{NaH}_2\text{PO}_4/\text{ethanol}$ extract and conventional extract with (a) rutin, (b) luteolin-7-O-glucoside, and (c) diosmin as comparison

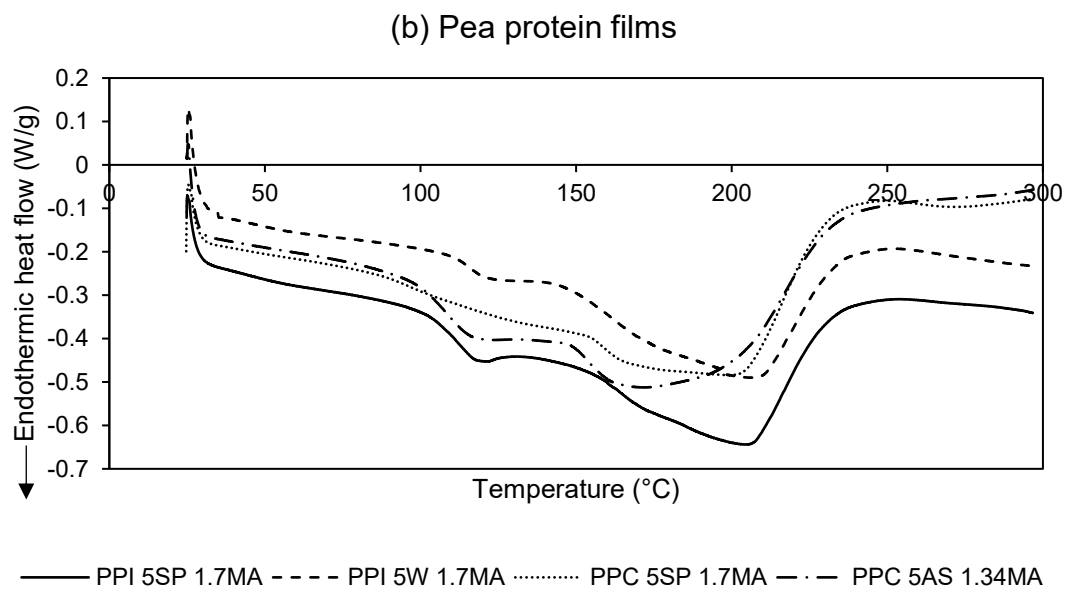
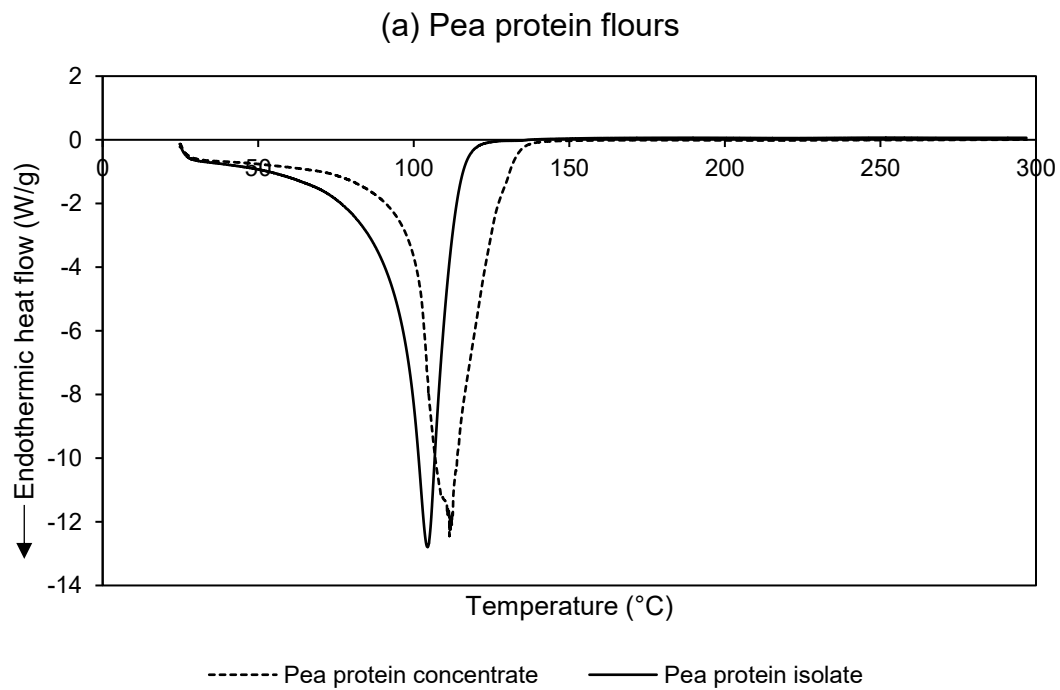


Figure A.5: Differential scanning calorimetry thermograms for (a) pea protein flours and (b) pea protein films

10% ethanol, alcoholic food simulant

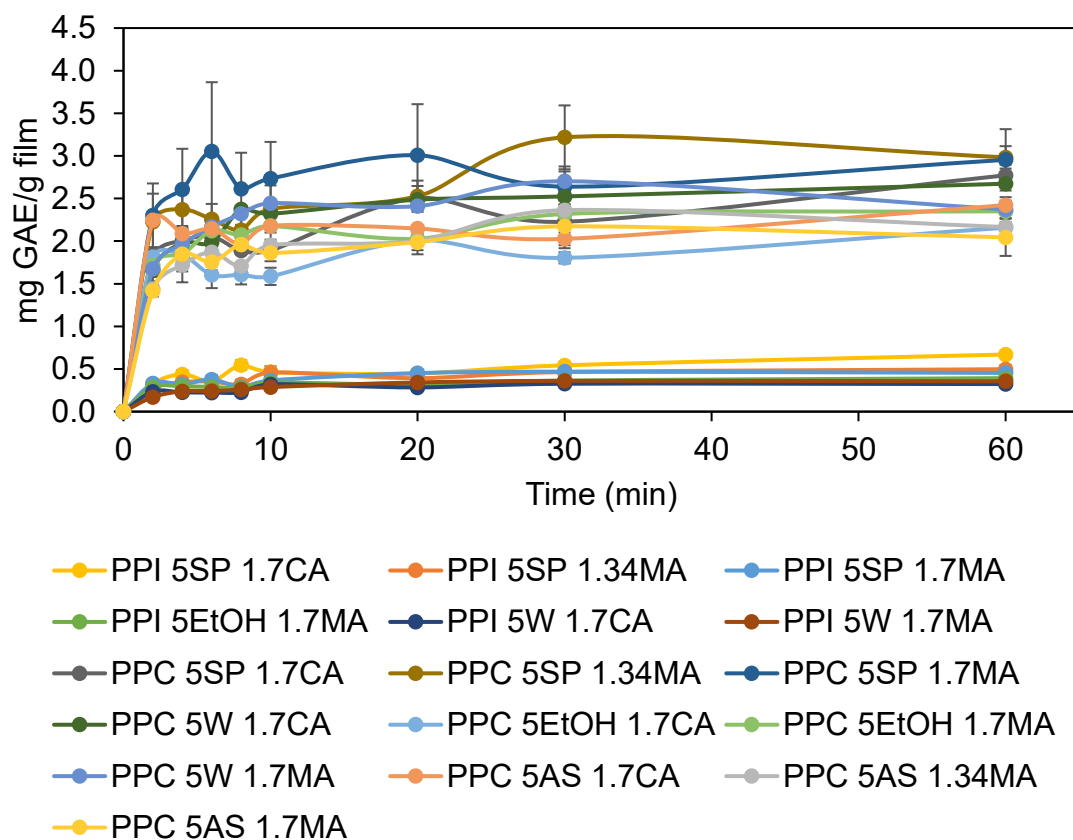


Figure A.6: Total phenolic content release from pea protein films in 10% ethanol

95% ethanol, fatty food simulat

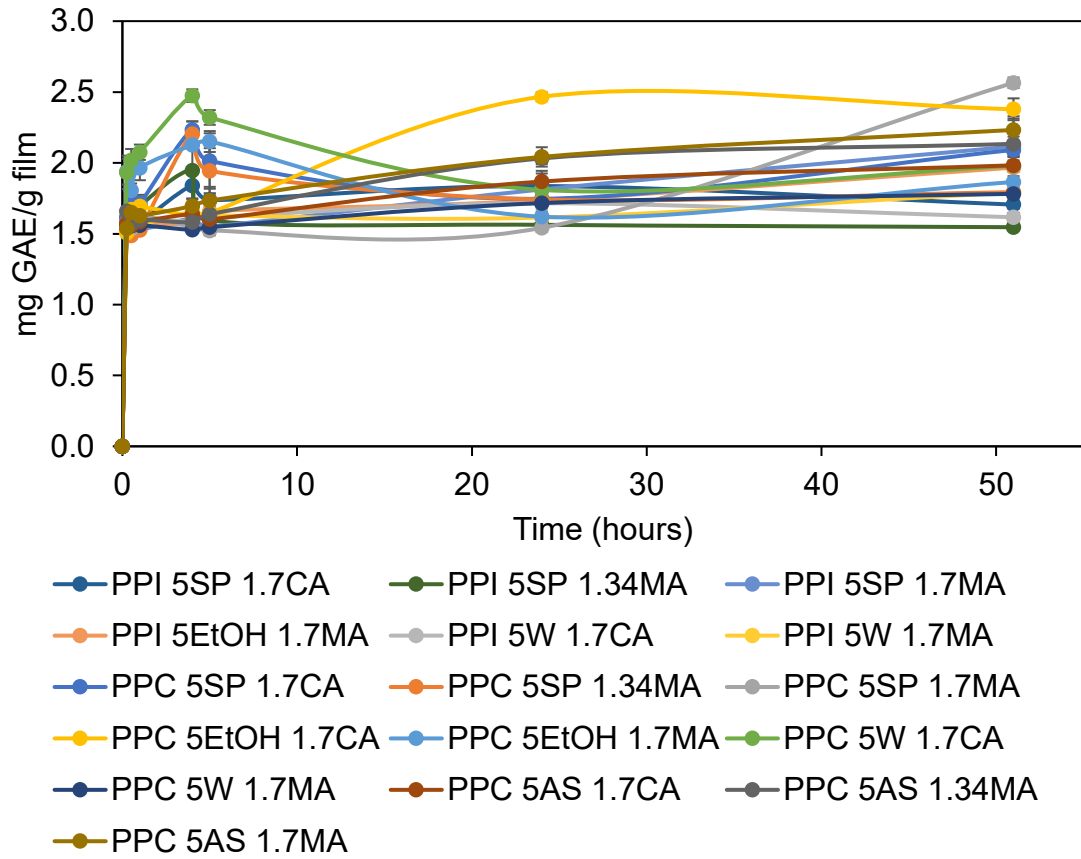


Figure A.7: Total phenolic content release from pea protein films in 95% ethanol

APPENDIX B: Supplementary Tables

Table A.1: Octanol-water partition coefficients (log P) and distribution coefficients (log D) of the phase-forming components (ChemAxon, 2019)

Salt-based systems	Sugar-based systems
Ethanol log P = -0.16	1-propanol log P = 0.36
(NH ₄) ₂ SO ₄ log D = -5.575	Glucose log P = -2.93
NaH ₂ PO ₄ log D = -3.061	Maltose log P = -4.70

Table A.2: Octanol-water distribution coefficients (log D) of the compounds at top phase pH for ATPE systems (ChemAxon, 2019)

Compounds	log D			
	(NH₄)₂SO₄/ethanol High TLL pH 5.5	NaH₂PO₄/ethanol Low TLL pH 3.8	Glucose/propanol High TLL pH 5.4	Maltose/propanol Medium TLL pH 5.7
Chlorogenic acid	-2.419	-0.862	-2.324	-2.608
Rutin	-0.923	-0.87	-0.913	-0.952
Gallic acid	-0.846	0.484	-0.75	-1.039

Table A.3: Wavelength, retention time, and content of selected bioactive compounds from HPLC

Compounds	Wavelength (nm)	Retention time (min)	Content ($\mu\text{g}/\text{mg}$ dry weight leaves) ^a
Conventional extract			
CGA	320	9.167	0.5741
Rutin	250	10.856	2.6790
Luteolin-7-O-glucoside	250	11.262	4.6675
Diosmin	250	11.907	1.4144
Optimized extract for $(\text{NH}_4)_2\text{SO}_4$/ethanol			
CGA	320	9.15	0.9703
Rutin	250	10.854	2.3194
Luteolin-7-O-glucoside	250	N.D.	N.D.
Diosmin	250 nm	11.907	0.4745
Optimized extract for NaH_2PO_4/ethanol			
CGA	320	9.153	0.3659
Rutin	250	10.854	1.6738
Luteolin-7-O-glucoside	250	11.275	4.2622
Diosmin	250	11.904	2.9085
Optimized extract for glucose/propanol			
CGA	320	9.146	0.8005
Rutin	250	10.858	11.5225
Luteolin-7-O-glucoside	250	11.436	10.5078
Diosmin	250	11.919	4.7804
Optimized extract for maltose/propanol			
CGA	320	9.14	0.1539
Rutin	250	10.841	2.0307
Luteolin-7-O-glucoside	250	11.417	1.6329
Diosmin	250	11.895	1.1444

^aN.D. not detected

Note: These results were obtained from a single injection for each sample.



Table A.4: Total phenolic content and radical scavenging activity of PPI and PPC films in 95% ethanol


PPI films total phenolic content release into 95% ethanol at 51 hours (mg GAE/g film)				
Cross linker	Sodium phosphate extract	Ammonium sulphate extract	Water	Ethanol
1.7g citric acid	1.706 ± 0.03 ^a	N/A	1.616 ± 0.03 ^a	Did not form
1.7g malic acid	2.116 ± 0.07 ^a	N/A	1.792 ± 0.15 ^a	1.967 ± 0.14 ^a
1.34g malic acid	1.546 ± 0.02	N/A	N/A	N/A
PPC films total phenolic content release into 95% ethanol at 51 hours (mg GAE/g film)				
	Sodium phosphate extract	Ammonium sulphate extract	Water	Ethanol
1.7g citric acid	2.092 ± 0.05 ^b	1.983 ± 0.03 ^b	1.979 ± 0.07 ^b	2.378 ± 0.08 ^a
1.7g malic acid	2.565 ± 0.04 ^a	2.232 ± 0.08 ^b	1.781 ± 0.03 ^c	1.865 ± 0.09 ^c
1.34g malic acid	1.794 ± 0.02 ^a	2.134 ± 0.20 ^a	N/A	N/A
PPI films radical scavenging activity in 95% ethanol at 51 hours (%)				
	Sodium phosphate extract	Ammonium sulphate extract	Water	Ethanol
1.7g citric acid	4.3 ± 0.2 ^a	N/A	2.9 ± 0.3 ^b	Did not form
1.7g malic acid	3.8 ± 0.0 ^a	N/A	2.9 ± 0.3 ^b	3.0 ± 0.2 ^{ab}
1.34g malic acid	3.6 ± 0.1	N/A	N/A	N/A
PPC films radical scavenging activity in 95% ethanol at 51 hours (%)				
	Sodium phosphate extract	Ammonium sulphate extract	Water	Ethanol
1.7g citric acid	4.0 ± 0.2 ^{ab}	3.5 ± 0.2 ^b	4.6 ± 0.1 ^a	4.4 ± 0.2 ^a
1.7g malic acid	5.0 ± 0.1 ^a	4.2 ± 0.2 ^{ab}	3.5 ± 0.4 ^b	4.2 ± 0.2 ^{ab}
1.34g malic acid	3.7 ± 0.2 ^a	4.0 ± 0.3 ^a	N/A	N/A

Means with different letters in the same row are significantly different ($P < 0.05$).

APPENDIX C: Copyright Permission Letters

Chapter 3

HomeHelpEmail SupportSign inCreate Account



Aqueous two-phase extraction of bioactive compounds from haskap leaves (*Lonicera caerulea*): Comparison of salt/ethanol and sugar/propanol systems

Author: Kar Yeen Chong, Roumiana Stefanova, Junzeng Zhang, Marianne Su-Ling Brooks
Publication: Separation and Purification Technology
Publisher: Elsevier
Date: 1 December 2020

© 2020 Elsevier B.V. All rights reserved.

Journal Author Rights

Please note that, as the author of this Elsevier article, you retain the right to include it in a thesis or dissertation, provided it is not published commercially. Permission is not required, but please ensure that you reference the journal as the original source. For more information on this and on your other retained rights, please visit: <https://www.elsevier.com/about/our-business/policies/copyright#Author-rights>

BACK CLOSE WINDOW

Chapter 4

HomeHelpEmail SupportSign inCreate Account



Effects of recycling on the aqueous two-phase extraction of bioactives from haskap leaves

Author: Kar Yeen Chong, Marianne Su-Ling Brooks
Publication: Separation and Purification Technology
Publisher: Elsevier
Date: 15 January 2021

© 2020 Elsevier B.V. All rights reserved.

Journal Author Rights

Please note that, as the author of this Elsevier article, you retain the right to include it in a thesis or dissertation, provided it is not published commercially. Permission is not required, but please ensure that you reference the journal as the original source. For more information on this and on your other retained rights, please visit: <https://www.elsevier.com/about/our-business/policies/copyright#Author-rights>

BACK CLOSE WINDOW

Chapter 5

SPRINGER NATURE LICENSE
TERMS AND CONDITIONS

Dec 30, 2020

This Agreement between Dalhousie University -- Kar Yeen Chong ("You") and Springer Nature ("Springer Nature") consists of your license details and the terms and conditions provided by Springer Nature and Copyright Clearance Center.

License Number	4979020630359
License date	Dec 30, 2020
Licensed Content Publisher	Springer Nature
Licensed Content Publication	Food and Bioprocess Technology
Licensed Content Title	Extraction of Bioactive Compounds from Haskap Leaves (<i>Lonicera caerulea</i>) Using Salt/Ethanol Aqueous Two-Phase Flotation
Licensed Content Author	Kar Yeen Chong et al
Licensed Content Date	Nov 8, 2020
Type of Use	Thesis/Dissertation
Requestor type	academic/university or research institute
Format	print and electronic
Portion	full article/chapter
Will you be	no

translating?

Circulation/distribution 1 - 29

Author of this Springer Nature content yes

Title Development of Functional Films from Haskap Leaf Extracts using Aqueous Two-Phase Systems

Institution name Dalhousie University

Expected presentation date Apr 2021

Requestor Location Dalhousie University
5273 DaCosta Row, Rm 1117
PO Box 15000
Halifax, NS B3H 4R2
Canada
Attn: Dalhousie University

Total 0.00 CAD

Terms and Conditions

**Springer Nature Customer Service Centre GmbH
Terms and Conditions**

This agreement sets out the terms and conditions of the licence (the **Licence**) between you and **Springer Nature Customer Service Centre GmbH** (the **Licensor**). By clicking 'accept' and completing the transaction for the material (**Licensed Material**), you also confirm your acceptance of these terms and conditions.

1. Grant of License

1. 1. The Licensor grants you a personal, non-exclusive, non-transferable, world-wide licence to reproduce the Licensed Material for the purpose specified in your order only. Licences are granted for the specific use requested in the order and for no other use, subject to the conditions below.

1. 2. The Licensor warrants that it has, to the best of its knowledge, the rights to license reuse of the Licensed Material. However, you should ensure that the material you are requesting is original to the Licensor and does not carry the copyright of

another entity (as credited in the published version).

1. 3. If the credit line on any part of the material you have requested indicates that it was reprinted or adapted with permission from another source, then you should also seek permission from that source to reuse the material.

2. Scope of Licence

2. 1. You may only use the Licensed Content in the manner and to the extent permitted by these Ts&Cs and any applicable laws.

2. 2. A separate licence may be required for any additional use of the Licensed Material, e.g. where a licence has been purchased for print only use, separate permission must be obtained for electronic re-use. Similarly, a licence is only valid in the language selected and does not apply for editions in other languages unless additional translation rights have been granted separately in the licence. Any content owned by third parties are expressly excluded from the licence.

2. 3. Similarly, rights for additional components such as custom editions and derivatives require additional permission and may be subject to an additional fee. Please apply to Journalpermissions@springernature.com/bookpermissions@springernature.com for these rights.

2. 4. Where permission has been granted **free of charge** for material in print, permission may also be granted for any electronic version of that work, provided that the material is incidental to your work as a whole and that the electronic version is essentially equivalent to, or substitutes for, the print version.

2. 5. An alternative scope of licence may apply to signatories of the [STM Permissions Guidelines](#), as amended from time to time.

3. Duration of Licence

3. 1. A licence for is valid from the date of purchase ('Licence Date') at the end of the relevant period in the below table:

Scope of Licence	Duration of Licence
Post on a website	12 months
Presentations	12 months
Books and journals	Lifetime of the edition in the language purchased

4. Acknowledgement

4. 1. The Licensor's permission must be acknowledged next to the Licenced Material in print. In electronic form, this acknowledgement must be visible at the same time as the figures/tables/illustrations or abstract, and must be hyperlinked to the journal/book's homepage. Our required acknowledgement format is in the Appendix below.

5. Restrictions on use

5. 1. Use of the Licensed Material may be permitted for incidental promotional use and minor editing privileges e.g. minor adaptations of single figures, changes of format, colour and/or style where the adaptation is credited as set out in Appendix 1 below. Any other changes including but not limited to, cropping, adapting, omitting material that affect the meaning, intention or moral rights of the author are strictly prohibited.

5. 2. You must not use any Licensed Material as part of any design or trademark.

5. 3. Licensed Material may be used in Open Access Publications (OAP) before publication by Springer Nature, but any Licensed Material must be removed from OAP sites prior to final publication.

6. Ownership of Rights

6. 1. Licensed Material remains the property of either Licensor or the relevant third party and any rights not explicitly granted herein are expressly reserved.

7. Warranty

IN NO EVENT SHALL LICENSOR BE LIABLE TO YOU OR ANY OTHER PARTY OR ANY OTHER PERSON OR FOR ANY SPECIAL, CONSEQUENTIAL, INCIDENTAL OR INDIRECT DAMAGES, HOWEVER CAUSED, ARISING OUT OF OR IN CONNECTION WITH THE DOWNLOADING, VIEWING OR USE OF THE MATERIALS REGARDLESS OF THE FORM OF ACTION, WHETHER FOR BREACH OF CONTRACT, BREACH OF WARRANTY, TORT, NEGLIGENCE, INFRINGEMENT OR OTHERWISE (INCLUDING, WITHOUT LIMITATION, DAMAGES BASED ON LOSS OF PROFITS, DATA, FILES, USE, BUSINESS OPPORTUNITY OR CLAIMS OF THIRD PARTIES), AND WHETHER OR NOT THE PARTY HAS BEEN ADVISED OF THE POSSIBILITY OF SUCH DAMAGES. THIS LIMITATION SHALL APPLY NOTWITHSTANDING ANY FAILURE OF ESSENTIAL PURPOSE OF ANY LIMITED REMEDY PROVIDED HEREIN.

8. Limitations

8. 1. **BOOKS ONLY:** Where 'reuse in a dissertation/thesis' has been selected the following terms apply: Print rights of the final author's accepted manuscript (for clarity, NOT the published version) for up to 100 copies, electronic rights for use only on a personal website or institutional repository as defined by the Sherpa guideline (www.sherpa.ac.uk/romeo/).

8. 2. For content reuse requests that qualify for permission under the [STM Permissions Guidelines](#), which may be updated from time to time, the STM Permissions Guidelines supersede the terms and conditions contained in this licence.

9. Termination and Cancellation

9. 1. Licences will expire after the period shown in Clause 3 (above).

9. 2. Licensee reserves the right to terminate the Licence in the event that payment is not received in full or if there has been a breach of this agreement by you.

Appendix 1 — Acknowledgements:

For Journal Content:

Reprinted by permission from [the Licensor]: [Journal Publisher (e.g. Nature/Springer/Palgrave)] [JOURNAL NAME] [REFERENCE CITATION (Article name, Author(s) Name), [COPYRIGHT] (year of publication)

For Advance Online Publication papers:

Reprinted by permission from [the Licensor]: [Journal Publisher (e.g. Nature/Springer/Palgrave)] [JOURNAL NAME] [REFERENCE CITATION (Article name, Author(s) Name), [COPYRIGHT] (year of publication), advance online publication, day month year (doi: 10.1038/sj.[JOURNAL ACRONYM].)

For Adaptations/Translations:

Adapted/Translated by permission from [the Licensor]: [Journal Publisher (e.g. Nature/Springer/Palgrave)] [JOURNAL NAME] [REFERENCE CITATION (Article name, Author(s) Name), [COPYRIGHT] (year of publication)

Note: For any republication from the British Journal of Cancer, the following credit line style applies:

Reprinted/adapted/translated by permission from [the Licensor]: on behalf of Cancer Research UK: : [Journal Publisher (e.g. Nature/Springer/Palgrave)] [JOURNAL NAME] [REFERENCE CITATION (Article name, Author(s) Name), [COPYRIGHT] (year of publication)

For Advance Online Publication papers:

Reprinted by permission from The [the Licensor]: on behalf of Cancer Research UK: [Journal Publisher (e.g. Nature/Springer/Palgrave)] [JOURNAL NAME] [REFERENCE CITATION (Article name, Author(s) Name), [COPYRIGHT] (year of publication), advance online publication, day month year (doi: 10.1038/sj.[JOURNAL ACRONYM].)

For Book content:

Reprinted/adapted by permission from [the Licensor]: [Book Publisher (e.g. Palgrave Macmillan, Springer etc) [Book Title] by [Book author(s)] [COPYRIGHT] (year of publication)

Other Conditions:

Version 1.3

Questions? customercare@copyright.com or +1-855-239-3415 (toll free in the US) or +1-978-646-2777.